FEDERAL UNIVERSITY OF PERNAMBUCO
CENTER OF TECHNOLOGY AND GEOCIENCES
DEPARTMENT OF CHEMICAL ENGINEERING
GRADUATE PROGRAM IN CHEMICAL ENGINEERING

ALLAN DE ALMEIDA ALBUQUERQUE

REACTIVE SEPARATION PROCESSES APPLIED TO BIODIESEL PRODUCTION:
phase equilibrium, design, optimization and techno-economic assessment

Recife
2019

ALLAN DE ALMEIDA ALBUQUERQUE

REACTIVE SEPARATION PROCESSES APPLIED TO BIODIESEL PRODUCTION:

phase equilibrium, design, optimization and techno-economic assessment

Doctoral Thesis presented to the Graduate Program in Chemical Engineering of the Federal University of Pernambuco in partial fulfillment of the requirements for the degree of Doctor of Science in Chemical Engineering.

Concentration area: Chemical and Biochemical Process Engineering.

Supervisors: Prof. DSc Luiz Stragevitch.
Prof. Dr.-Ing. Leandro Danielski.
Co-supervisor: Prof. PhD Flora Tak Tak Ng.

Recife

2019

Catalogação na fonte
Bibliotecária Margareth Malta, CRB-4 / 1198

A345r Albuquerque, Allan de Almeida.
Reactive separation processes applied to biodiesel production: phase equilibrium, design, optimization and techno-economic assessment / Allan de Almeida Albuquerque. – 2019.
247 folhas, abrev.

Orientador: Prof. Dr. Luiz Stragevitch.
Orientador: Prof. Dr. Leandro Danielski.
Coorientadora: Profa. Dra. Flora Tak Tak Ng.
Tese (Doutorado) – Universidade Federal de Pernambuco. CTG. Programa de Pós-Graduação em Engenharia Química, 2019.
Inclui Referências e Apêndices.
Texto em inglês.

1. Engenharia Química. 2. Biodiesel. 3. Coluna de destilação catalítica. 4. Modelagem do equilíbrio de fases. 5. Coluna de Destilação Reativa. 6. Avaliação técnico-econômica. I. Stragevitch, Luiz. (Orientador). II. Danielski, Leandro. (Orientador). III. Ng, Flora Tak Tak. (Coorientadora). IV. Título.

UFPE

660.2 CDD (22. ed.) BCTG/2019-154

ALLAN DE ALMEIDA ALBUQUERQUE

REACTIVE SEPARATION PROCESSES APPLIED TO BIODIESEL PRODUCTION:

phase equilibrium, design, optimization and techno-economic assessment

Doctoral Thesis presented to the Graduate Program in Chemical Engineering of the Federal University of Pernambuco in partial fulfillment of the requirements for the degree of Doctor of Science in Chemical Engineering.

Approved in: 27/02/2019.

EXAMINING COMMITTEE

_____

Prof. DSc Luiz Stragevitch (Supervisor)
Federal University of Pernambuco

_____

Prof. Dr.-Ing. Leandro Danielski (Supervisor)
Federal University of Pernambuco

_____

Prof. PhD Flora Tak Tak Ng (Co-supervisor)
University of Waterloo

_____

Prof. PhD Warren David Seider (External Examiner)
University of Pennsylvania

_____

Prof. PhD João Paulo Silva Queiroz (External Examiner)
Federal University of São Carlos

_____

Prof. DSc Florival Rodrigues de Carvalho (External Examiner)
Federal University of Pernambuco

_____

Prof. DSc José Geraldo de Andrade Pacheco Filho (Internal Examiner)
Federal University of Pernambuco

_____

Prof. Dr. César Augusto Moraes de Abreu (Internal Examiner)
Federal University of Pernambuco

I dedicate this work to my beloved wife; to my mother, family and relatives; to my supervisors; and to my friends.

ACKNOWLEDGMENTS

There were many people who helped me to complete this work, to all my sincere thanks, among them: to God and to Jesus by ceaseless protection in all moments of my life; to my beloved wife Jéssica Altino for the moments of joy lived, kindness, love and care in the difficult moments; and to my wonderful parents and family, for the aid, trust, the words of encouragement, attention and kindness. Furthermore, I am also grateful to my friends from DEQ and LAC/UFPE, for the companionship in the happy moments that permeated the process of accomplishment of this doctoral thesis; to my friends from Waterloo: Chau Mai, Ruohan Riang, Richard Ackroyd, Marcelo, among others; to my friends of English conversations from Kitchener and Waterloo; to my doctors Felipe Marinho and Wolfgang Aguiar; and to all who contributed directly and indirectly to my health improvement, enabling this work to be done. I am also grateful to Professors DSc Luiz Stragevitch, Dr.-Ing. Leandro Danielski and PhD Flora Ng for accepting to supervise this work with great wisdom and patience; to Professors from graduate program for giving me the chance to acquire enough knowledge through well-planned and committed classes; to all students of the graduate program for the knowledge and exchange of experiences; to the collaborators of the Fuel Laboratory (LAC); to Professor Celmy Barbosa, PRH-28 coordinator; to FINEP and CNPQ for financial support; to CAPES for funding this work with DS and PDSE scholarships; to ANP, PRH 28, FACEPE and LAC for financial support in acquiring the Aspen Plus and Matlab software licenses; and to the Graduate Program in Chemical Engineering (PPGEQ) from UFPE.

Process intensification (PI) is a process design philosophy aimed to improve process flexibility, product quality, speed to market and inherent safety, with a reduced environmental footprint. In the European Union roadmap, PI is defined as a set of innovative principles applied in process and equipment design, which can bring significant benefits in terms of process and chain efficiency, lower capital and operating expenses, higher quality of products, less wastes and improved process safety (KISS, 2014, p. 1).

ABSTRACT

Reactive separation processes (RSP) have been widely studied, since companies have looked for ways to reduce costs, environment impacts and loss of energy. As a result, the keyphrase has been “produce more with less being sustainable”, so that process intensification have received more attention. Among these processes, reactive distillation column (RDC) and catalytic distillation column (CDC) for homogeneous and heterogeneous catalyzed processes have been applied to develop more economical processes as well as increasing performance of equilibrium reactions as found in biodiesel production. For this reason, many studies from RDC and CDC applied to equilibrium-limited esterification and transesterification reactions have been developed. In addition, an alternative process of biodiesel production by free fatty acids (FFA) separation from residual oil and fats (ROF) showed to be more economical feasible than conventional processes. Despite this, there is no economic investigation of RDC in this alternative route. Moreover, few studies evaluated the possibility to produce biodiesel by both reactions simultaneuosly using a solid acid-catalyzed (SAC) route in a CDC. This SAC process can result in cheaper biodiesel since low-cost ROF can be used with less number of equipment and use of alcohol. On the other hand, other cheap feedstock as crude tall oil (CTO) can be used to produce biodiesel from esterification reaction by CDC. In addition, from RDC and CDC studies, absence of a phase equilibrium (PE) modeling for biodiesel reaction systems was detected. Furthermore, few simulation studies of RDC and CDC made comparisons with experiments to validate the results. For all these reasons, this work was proposed in order to investigate innovative RSP applied for biodiesel production from ROF and CTO and to develop a PE modeling for the components involved. Firstly, two processes based on optimized FFA separation from ROF were investigated including a set of reactor/distillation column and a RDC. Both processes presented similar economic results. Secondly, thermophysical properties for acylglycerols were estimated. PE databanks were built and a modeling involving components from biodiesel reactions was proposed using the Non-random two-liquid (NRTL) model. A validation based on simulation of experiments was also carried out. Thirdly, three SAC processes were investigated based on: simultaneous esterification and transterification reactions using a CDC and a catalytic absorption column (CAC); and a hydro-esterification process. CDC and CAC processes were more economical and enviromentally friendly. CDC was the optimal process. A global optimization and a final design for CDC process were proposed. Finally, a SAC process for biodiesel production from CTO was developed. A base

case and an alternative process for CTO purification from three and four distillation columns, respectively, were investigated. The alternative process was the unique techno-economic feasible and was evaluated for biodiesel production by SAC process using a CDC and a catalytic divided-wall column. CDC process was the unique technically feasible. This was globally optimized and flexibilized. Therefore, RSP proved to be useful unit operations to obtain more economical and eco-friendly biodiesel production processes.

Keywords: Biodiesel. Catalytic distillation column. NRTL. Phase equilibrium modeling. Reactive distillation column. Techno-economic assessment.

RESUMO

Processos de reação separação (PRS) têm sido amplamente estudados, visto que as empresas têm buscado reduzir custos, impactos ambientais e perda de energia. Entre esses processos, a coluna de destilação reativa (CDR) e a coluna de destilação catalítica (CDC) para processos com catalisadores homogêneos e heterogêneos têm sido aplicados para desenvolver processos mais econômicos e aumentar o desempenho das reações de equilíbrio encontradas na produção de biodiesel. Como resultado, muitos estudos de CDR e de CDC aplicados a reações de equilíbrio de esterificação e transesterificação foram desenvolvidos. Além disso, um processo alternativo de produção de biodiesel por separação de ácidos graxos livres (AGL) de óleos e gorduras residuais (OGR) mostrou-se mais viável economicamente. Apesar disso, não houve investigação econômica da CDR nessa rota. Ademais, poucos estudos avaliaram a possibilidade de produzir biodiesel por ambas as reações simultaneamente com catalisador sólido ácido (CSA) em uma CDC. Este processo pode resultar em biodiesel mais barato, visto que OGR de baixo custo podem ser usados com menos equipamentos e uso de álcool. Por outro lado, matérias-primas baratas como *tall oil* bruto (TOB) podem ser usadas para produzir biodiesel a partir da reação de esterificação por CDC. Além disso, a partir de estudos de CDR e CDC, ausência de uma modelagem do equilíbrio de fases (EF) para sistemas de reações de biodiesel foi detectada. Adicionalmente, poucos estudos de simulação de CDR e CDC fizeram comparações com experimentos para validar os resultados. Por todas estas razões, este trabalho foi proposto com o objetivo de investigar PRS inovadores aplicados à produção de biodiesel a partir de OGR e TOB e desenvolver uma modelagem do EF para os componentes envolvidos. Primeiramente, dois processos baseados na separação otimizada de AGL dos OGR foram projetados e avaliados, incluindo um conjunto de reator/destilação e uma CDR. Ambos os processos apresentaram resultados econômicos similares. Segundamente, propriedades termofísicas dos acilgliceróis foram estimadas. Bancos de dados de EF foram construídos e uma modelagem envolvendo componentes de reações de biodiesel foi proposta usando o modelo NRTL. Uma validação também foi realizada baseada na simulação de experimentos. Posteriormente, três processos com CSA foram investigados: reações simultâneas de esterificação e transterificação utilizando CDC e coluna de absorção catalítica (CAC); e um processo de hidroesterificação. Os processos por CDC e CAC foram mais economicamente viáveis. O processo por CDC foi o processo ótimo. Uma otimização global e um projeto final para o processo por CDC foram propostos. Finalmente, um processo com CSA para produção

de biodiesel por TOB foi desenvolvido. Um caso base e um processo alternativo para a purificação de TOB a partir de três e quatro colunas de destilação foram investigados. O processo alternativo foi o único com viabilidade técnico-econômica e foi avaliado para produção de biodiesel pelo processo com CSA utilizando uma CDC e uma coluna de parede dividida catalítica. O processo por CDC foi o único tecnicamente viável. Este foi otimizado globalmente e flexibilizado. Portanto, PRS provaram ser operacões unitárias úteis para obter processos de produção de biodiesel mais econômicos e ambientalmente corretos.

Palavras-chave: Biodiesel. Coluna de destilação catalítica. Modelagem do equilíbrio de fases. Coluna de destilação reativa. Avaliação técnico-econômica.

LIST OF ABBREVIATIONS

AFW	Animal fats and wastes
ASTM	American Society for Testing and Materials
CAC	catalytic absorption column
CCD	central composite design
CDC	catalytic distillation column
CDWC	catalytic divided-wall column
CF	constituent Fragments
CnO	canola oil
CTO	crude tall oil
DAG	diacylglycerol
DTO	distilled tall oil
FAAE	fatty acid alkyl ester
FAME	fatty acid methyl ester
FFA	free fatty acids
GC	group Contribution
HAC	homogeneous alkali-catalyzed
HI	heat integration
LLEx	liquid-liquid extraction
MAG	monoacylglycerol
MR	molar ratio of alcohol to oil (or FFA)
MT	mass transfer
NREL	National Renewable Energy Laboratory
NRTL	Non-Random Two Liquid
PE	phase equilibrium
RA	resin acids
RAC	reactive absorption column
RDC	reactive distillation column
REC	reactive extraction column
ROF	residual oil and fats
RSM	response surface methodology

RSP	reactive separation processes
SAC	solid acid-catalyzed
SuO	sunflower oil
TAG	triacylglycerols
TOFA	tall oil fatty acids
TOP	tall oil pitch
TOR	tall oil rosin
USA	United States of America
WCO	waste cooking oil

CONTENTS

1 INTRODUCTION

Biodiesel is a biofuel composed of alkyl esters used in combustion engines and can partially or totally replace diesel oil (BRAZIL, 2005). In recent years, several countries have shown interest in its use, mainly because it is a renewable, biodegradable and non-toxic fuel (MAZUBERT; POUX; AUBIN, 2013). Since the last decade, the Brazilian government has encouraged its production, so that the addition of 2% of biodiesel to diesel became mandatory since 2008 (RAMOS et al., 2011). Subsequently, in 2014 this value change to 7% (B7) and since 2018 a blend composed of 10% (B10) of biodiesel in diesel was stated by law (BRAZIL, 2016). Moreover, a B15 mixture is expected for 2023 in Brazil (BRAZIL, 2018).

Biodiesel can be obtained from direct use and blending, pyrolysis, microemulsions and by transesterification reaction (MA; HANNA, 1999). For this latter, triacylglycerols (TAG) and a short chain alcohol in presence of homogeneous alkali catalyst react to produce glycerol and fatty acid alkyl esters (FAAE) (MEHER; SAGAR; NAIK, 2006). In this reaction, TAG can be obtained from edible oil, non-edible oil, animal fats or residual oil and fats (ROF) (GNANAPRAKASAM et al., 2013).

Among the raw materials used for biodiesel production, the most used are edible oils. However, the use of non-edible oils such as castor, jatropha, cottonseed and tall oil to produce biodiesel is preferable instead of edible oils such as soybean, palm, sunflower and corn oil (AVHAD; MARCHETTI, 2015). This avoids competition with the food industry and reduces environmental problems related to the use of arable land (MOHITE et al., 2015). In addition, noble raw materials can affect up to 85% of the final price of biodiesel produced. As a result, biodiesel is 50% to 200% more expensive than diesel oil (CANAKCI, M; SANLI, 2008).

For instance, tall oil obtained from Kraft pulping process as crude tall oil (CTO) is a pine-derived non-edible oil used for biodiesel production with low price and high value market for products obtained by purification, such as: heads, tall oil pitch (TOP), tall oil rosin (TOR), distilled tall oil (DTO) and tall oil fatty acids (TOFA). Moreover, CTO is composed of 30-53 wt% of free fatty acids (FFA), 30-53 wt.% of resin acids (RA) and 6.5-30 wt% of neutral compounds, so that biodiesel can be produced from TOFA through esterification reaction after RA and neutral compounds removal by CTO purification (ARO; FATEHI, 2017; NOGUEIRA, 1996; NORLIN, 2012; ROHAN, 2016).

On the other hand, the use of ROF to produce biodiesel reduces raw material costs and also avoid waste disposal. Waste cooking oil (WCO) is one of these raw materials with high content of FFA. WCO costs around 40% to 70% less than refined vegetable oils depending on whether is a yellow grease (FFA < 15%) or brown grease (FFA > 15%), since the latter is cheaper than the first one (AVHAD; MARCHETTI, 2015; CAI et al., 2015; REFAAT, 2010).

ROF may also be composed of animal fat wastes (AFW), such as chicken, tallow and lard fats, which also contain high FFA levels (ADEWALE; DUMONT; NGADI, 2015). Therefore, biodiesel production from ROF is a potentially cheaper alternative. In addition, the use of ROF reduces the environmental impacts caused by improper disposal, so that avoid penalties for the companies responsible for generation of these wastes (KULKARNI; DALAI, 2006).

WCO are commonly obtained from a variety of oils, such as derived from sunflower, corn, palm, rapeseed and mainly soybean oil. These have typical FFA contents varying from 10% to 25% (CANAKCI, M; SANLI, 2008; GNANAPRAKASAM et al., 2013). In order to increase the biodiesel yield, ROF are generally subjected to a pretreatment step based on an acid-catalyzed esterification reaction. Subsequently, the pre-treated stream is subjected to a transesterification step using homogeneous alkali catalyst. These two steps compose the conventional process applied industrially in the biodiesel production from raw materials with high FFA levels (CANAKCI, M; VAN GERPEN, 2001a; ZHANG et al., 2003a).

The pretreatment unit is required in order to avoid or at least reduce the occurrence of competitive reactions of FFA saponification and TAG hydrolysis in the transesterification unit (GNANAPRAKASAM et al., 2013). However, the addition of pretreatment has two drawbacks that increase capital and operating costs: the incorporation of additional equipment and the use of glycerol as the washing solvent. As a result, more interesting alternative processes using ROF have been proposed in the literature, such as: application of supercritical conditions, FFA separation from TAG and use of acid catalysts (homogeneous or heterogeneous) to carry out the transesterification and esterification reactions simultaneously (ALBUQUERQUE; DANIELSKI; STRAGEVITCH, 2016; LEE; POSARAC; ELLIS, 2011; WEST; POSARAC; ELLIS, 2008; ZHANG et al., 2003a).

Among those alternatives the solid acid-catalyzed (SAC) process has shown to be the most economically feasible using raw materials with high FFA content as non-edible oils and ROFs, since no pre-treatment step is required. In this way capital and operation costs are

reduced including waste treatment costs since neither glycerol washing nor water washing are required (WEST; POSARAC; ELLIS, 2008). Nowadays, solid acid catalysts have been extensively studied in order to meet some biodiesel industry requirements such as: more active catalysts, high selectivity, high recyclability, easier regeneration, water and FFA insensitivity, operation under moderate conditions, lower reaction times, lower catalyst loading and lower molar ratio (MR) of alcohol to oil (AVHAD; MARCHETTI, 2015; MANSIR et al., 2017; MARDHIAH et al., 2017).

From edible oils, the use of a reactive distillation column (RDC) applied to biodiesel production has been successfully proposed in the literature. This column allows the replacement of the set of reactor/distillation column by only one RDC that carries out the vapor-liquid separation and reaction operations simultaneously on the same equipment. Moreover, other advantages are found, such as: higher production rate; lower investment costs; lower MR of methanol to oil since these are equilibrium reactions and, consequently, with the vaporization of the alcohol at the top reduces its amount fed in the column; less horizontal space required; higher product selectivity and lower costs with piping, pumps and instrumentation (BOON-ANUWAT et al., 2015; PODDAR; JAGANNATH; ALMANSOORI, 2017; SOUZA et al., 2014; STEINIGEWEG; GMEHLING, 2003; TUCHLENSKI et al., 2001).

Furthermore, an alternative process based on FFA separation from ROFs by liquid-liquid extraction (LLEx) using methanol showed to be more economical than conventional process, since no glycerol washing was required in pretreatment unit. Despite to adopt common homogeneous catalysts, this process proved to be feasible in large scale using a set of reactor/distillation column (ALBUQUERQUE; DANIELSKI; STRAGEVITCH, 2016). However, there are no studies in the literature combining FFA separation from ROF to RDC concept. Moreover, FFA separation using methanol was not optimized.

On the other hand, only few studies of design, optimization and techno-economic assessment are available from ROF combining both RDC and SAC route as a catalytic distillation column (CDC) with solid catalyst inside structured packing (GAURAV; NG; REMPEL, 2016). In addition, investigations from new configurations of reactive separation processes (RSP) based on process intensification as catalytic absorption column (CAC) and catalytic divided-wall column (CDWC) have been encouraged (GÓMEZ-CASTRO et al., 2010; 2011; KISS, 2009; 2014; KISS et al., 2012). Furthermore, there is no study about design, optimization and techno-economic feasibility of biodiesel production from tall oil using CDC.

Finally, a lack of a phase equilibrium modeling was identified in commercial simulators to assure more safety in the design and simulation steps of a biodiesel production plant from ROF using CDC.

For all these reasons, this work has been proposed, where the main objective is to investigate innovative RSP applied for biodiesel production as RDC, CDC, CAC and CDWC from ROF and CTO. Moreover, some specific goals have been expected:

- ✓ Optimize the FFA separation from ROF through the alternative process for biodiesel production using LLEx;
- ✓ Design and techno-economic assess the alternative process based on FFA separation from ROF comparing a set of reactor/distillation column to RDC in the transesterification unit;
- ✓ Estimate and evaluate the thermophysical properties from acylglycerols;
- ✓ Development of a vapor-liquid equilibrium (VLE), liquid-liquid equilibrium (LLE) and vapor-liquid-liquid equilibrium (VLLE) databank and a thermodynamic modeling for multicomponent mixtures involved in biodiesel production;
- ✓ Validation of the thermodynamic modelling and kinetic models applied to SAC and homogeneous alkali-catalyzed (HAC) processes for biodiesel production using CDC and RDC, respectively;
- ✓ Design, optimization and techno-economic assessment of innovative RSP for biodiesel production from ROF and CTO by SAC route.

1.1 THESIS STRUCTURE

In this topic a general overview of this thesis is presented besides of objectives, motivation and a step-by-step to be followed in the next chapters.

Chapter 2 presents a literature review beginning from biodiesel including concept and raw materials, recent situation, characteristics, advantages and disadvantages, main production processes and catalysts that has been used. In addition, a review of suitable thermophysical property models for acylglycerols (ACG) and thermodynamic models to predict and correlate components involved in biodiesel mixtures are presented. A review about VLE, LLE and VLLE from gamma-phi approach is also shown including tests of thermodynamic consistency and quality of LLE data. Finally, a brief explanation about RSP and a balance on RDC is given. Moreover, a review of main works about RSP, design and techno-economic assessment of biodiesel production processes is presented.

Chapter 3 contains a study of optimization of FFA separation from ROF by LLEx using methanol by response surface methodology (RSM) based on central composite design (CCD). Furthermore, the objective is to compare this optimized process using a set of reactor/distillation column to a RDC in the transesterification unit. ROF composition was chosen based on a mixture of edible and non-edible oils, thermophysical properties of ROF were estimated and a LLE modeling using Non-Random Two-Liquid (NRTL) model was proposed. Biodiesel production plants were designed and compared related to techno-economic and environment feasibility demonstrating that not always RSP are more economical for biodiesel production.

Chapter 4 shows a phase equilibrium modeling for biodiesel mixtures including transesterification and esterification reactions. Thermophysical properties for triolein were estimated and compared to experimental data. A VLE, a LLE and a VLLE databanks including 5980, 2411 and 41 data, respectively, were built through a survey of papers from Web of Science website between January 2nd, 2017 and December 31st, 2017. A phase equilibrium modeling was proposed using NRTL model including three sets of binary interaction parameters. These were validated to SAC and homogeneous alkali-catalyzed (HAC) processes, so that NRTL1 with some Aspen Plus' fixed parameters showed to be the best to SAC process, while NRTL2 was the best for HAC process. NRTL3 was obtained regressing all parameters involving experimental data. Lowest deviations in pressure and temperature for VLE systems

and composition for LLE systems were found. However, some deviations in biodiesel yield from SAC process demonstrated that NRTL1 is preferable to be used in Aspen Plus.

Chapter 5 shows a study of design, optimization and techno-economic assessment comparing two processes to produce biodiesel from simultaneous esterification and transesterification using ROF by SAC route. The base case process including a CDC was defined from work of Gaurav, Ng and Rempel (2016) and compared to the same route using a CAC. In addition, an industrial SAC hydro-esterification process was also designed and techno-economic assessed including a plug-flow reactor (PFR) and a CDC for hydrolysis and esterification reactions, respectively. All processes were locally optimized based on sensitivity analysis in Aspen Plus and cost estimation was carried out in spreadsheets. Heat integration and a flexibility study from a wide range of FFA composition were also proposed, so that a final design was obtained for raw materials with FFA content between 5 to 25 wt%. Break-even price (BEP) for biodiesel from yellow grease range was very close to reported one and presented a value competitive to diesel price. CDC process was chosen as the best process since it was the most economical, environmentally friendly and simplest before the heat integration. A global optimization for this process through connection between Matlab, Visual Basic for Applications (VBA) from Microsoft Excel and Aspen Plus was also developed obtaining the optimal design specifications.

Finally, Chapter 6 presents a study of design, optimization and techno-economic assessment of biodiesel production from CTO. A base case and an alternative flowsheet were developed using Aspen Plus based on three and four distillation columns in order to separate resin acids (RA) and neutral compounds from tall oil fatty acids (TOFA). The alternative process was the unique technical feasible for biodiesel production and also showed to be more economical. As a result, the alternative process was investigated for biodiesel production by CDC and CDWC using relite CFS as catalyst. CDC process showed to be the unique technical feasible, since temperatures above 300 ^{0}C were found in reactive stages from CDWC. As a consequence, CDC process was optimized based on the same procedure of global optimization from Chapter 5. The best operation point was found varying reflux ratio (RR), TOFA feed temperature, liquid holdup (H_L) in the reactive section (amount of catalyst), number of reactive (N_{RX}), rectification (N_R) and stripping (N_S) stages. Moreover, a flexibility study was carried out including Scandinavian and Canadian CTO, so that the lowest BEP was obtained for the highest FFA and lowest RA content.

2 LITERATURE REVIEW

In this chapter, a literature review about biodiesel; thermophysical properties; thermodynamic models; PE; RSP; design and feasibility of processes are presented.

2.1 BIODIESEL

Biodiesel is defined by the American Society for Testing and Materials (ASTM) as monoalkyl esters derived from lipid raw materials such as vegetable oils or animal fats (MARCHETTI, 2010). According to Avhad and Marchetti (2015) the main raw materials for biodiesel production are edible oils, non-edible oils and residual oil and fats (ROF).

2.1.1 Concept and raw materials

Edible oils are commonly the first choice as raw materials for biodiesel production. These include soybean, sunflower, palm, rapeseed and corn oils. However, competition with food industry has encouraged to use ROF and non-edible oils such as castor, jatropha, cotton and tall oils. This latter has low-cost, a consolidated value-market and can be used as crude tall oil (CTO) or tall oil fatty acids (TOFA), which is obtained after CTO purification, composed of 30–53 wt% and more than 90 wt% of FFA, respectively (ARO; FATEHI, 2017; BABCOCK et al., 2008; DEMIRBAS, 2009; NOGUEIRA, 1996; ROHAN, 2016).

ROF are other cheap raw-materials composed of mixtures of waste cooking oil (WCO), animal fats and wastes (AFW), yellow grease and brown grease. AFW are composed of chicken fat, tallow and lard. Yellow and brown greases are obtained from WCO composing of less than and more than 15 wt% of FFA, respectively. As a result, brown grease is cheaper than yellow grease (AVHAD; MARCHETTI, 2015).

TAG are the main components of vegetable oils and have different compositions of FFA that can influence their physical and chemical properties, as well as the quality of the biodiesel produced. These FFA can have saturated or unsaturated carbon chain. The FFA most commonly found in oils applied for biodiesel production are palmitic (C16:0), stearic (C18:0), oleic (C18:1), linoleic (C18:2) and linolenic (C18:3) acids (AVHAD; MARCHETTI, 2015).

2.1.2 Recent situation

United States of America (USA) and Brazil are still the main biodiesel producers and showed an annual production in 2017 of 6 and 4.3 billion liters according to Figure 2.1 (STATISTA, 2019). Furthermore, an increase of 2% and 13% was obtained from 2016 to 2017 for USA and Brazil, respectively, while an increase of 39% and 24% was found from 2017 to 2018. As a result, biodiesel demand has risen around the world, so that governments have encouraged to intensify studies in biodiesel production (ANP, 2019; EIA, 2019).

Figure 2.1 – Annual biodiesel production for the largest producers around the world

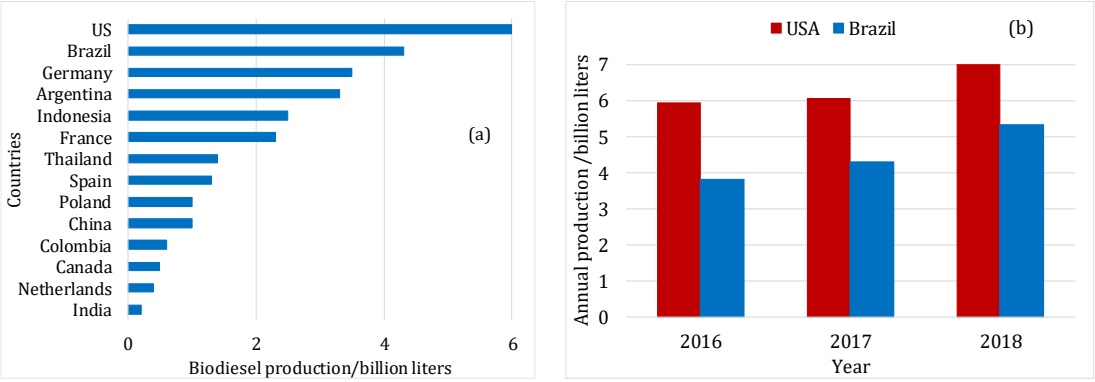

Source: Adapted from ANP (2019), EIA (2019) and Statista (2019)

Related to feedstock, soybean oil is the main used by USA and Brazil, while corn oil and animal fats are the second largest as shown in Figure 2.2. Yellow grease and WCO from ROF showed a low percentage, so that need to be encouraged to decrease waste disposal and biodiesel costs since WCO price is 2 to 3 times cheaper than edible oil (ANP, 2019; EIA, 2019). Moreover, edible oil costs can be responsible to 70–85% of biodiesel costs (SANTANDER, 2010; SOUZA et al., 2014).

Figure 2.2 – Main raw materials used for biodiesel production in 2018 for (a) USA and (b) Brazil

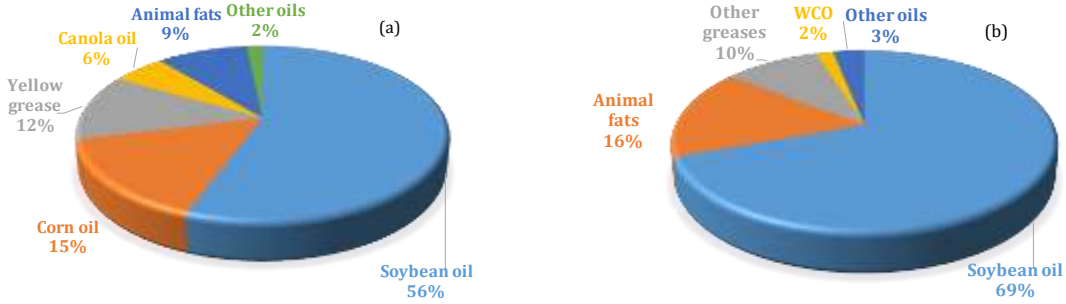

Source: Adapted from ANP (2019) and EIA (2019)

2.1.3 Features and advantages

Table 2.1 summarizes the advantageous characteristics and important properties of biodiesel in relation to petro diesel, so that biodiesel is an interesting alternative and more environmentally friendly fuel. Moreover, from low-cost feedstock and using new production processes, biodiesel can be more economically attractive.

Table 2.1 – Advantages of biodiesel in relation to petro diesel

Features	Advantageous properties
Appropriate chemical characteristics	Sulfur- free and aromatic-free, high cetane number, suitable combustion point, excellent lubricity, non-toxic and biodegradable.
Environmentally beneficial	Level of toxicity compatible with ordinary salt, with dilution as fast as sugar (United States Department of Agriculture).
Less polluting	Biodiesel significantly reduces the emissions of (a) carbon particles (smoke), (b) carbon monoxide, (c) sulfur oxides and (d) polycyclic aromatic hydrocarbons.
Economically competitive	It complements all new diesel technologies with similar performance and without requiring the installation of an infrastructure or training policy.
Reduces global warming	The released carbon dioxide is absorbed by the oilseeds during growth, which balances the negative balance generated by the emission into the atmosphere.
Economically attractive	It allows the valorization of by-products of agro-industry activities, an increase in the regional collection of Tax on the Circulation of Goods and Services (ICMS), reducing rural flight and increasing complementary investments in rural activities.
Regionalization	Small and medium-sized biodiesel production plants can be installed in different regions of the country, taking advantage of the raw material available at each location.

Source: Adapted from Costa Neto *et al.* (2000)

2.1.4 Main biodiesel production method: transesterification

According to Raimundo (2013), manipulations are required to decrease viscosity and to increase the feasibility of vegetable oils as fuel. Among these, some processes can be adopted, such as: pyrolysis, microemulsions, dilution and transesterification reaction. This latter is the reaction between oil or fat with an alcohol to produce fatty acid alkyl esters (FAAE) and glycerol, as shown in Figure 2.3. In this reaction, a catalyst is commonly used to improve the reaction rate and yield, besides of an excess of alcohol since the reaction is reversible and the equilibrium is shifted to produce more products (MA; HANNA, 1999).

Figure 2.3 – Transesterification reaction of vegetable oils, where R and R1 are alkyl groups from TAG and the alcohol used as reaction agents

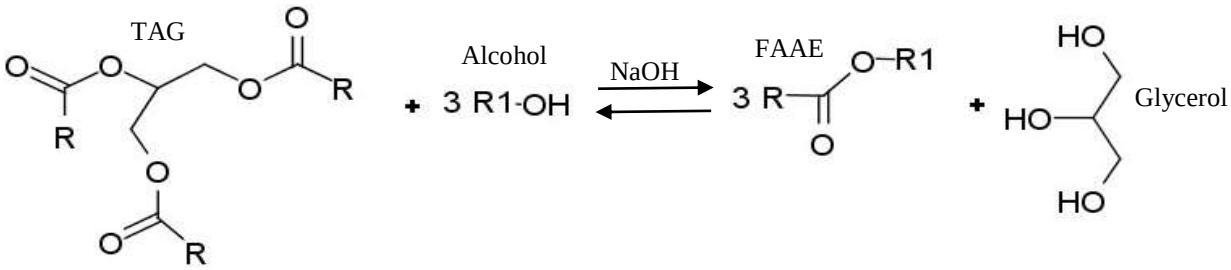

Source: Adapted from Ramos et al. (2011)

Santander (2010) stated that the use of transterification reaction considerably reduces the viscosity of vegetable oils without affecting their calorific value. Therefore, as main product is biodiesel, which has better features, such as combustion, atomization, viscosity and emissions relative to edible oils. By-product glycerol is also produced. Furthermore, the transesterification reaction is developed at ambient pressure or slightly above with a catalyst and close to alcohol boiling point, in order to ensure that the reaction takes place in the liquid phase. Typical catalysts for transesterification reaction are alkali as potassium (KOH) and sodium (NaOH) hydroxide.

According to Camús and Laborda (2006), the catalysts used in this reaction can be:

- ✓ Homogeneous alkali catalysts as KOH and NaOH;
- ✓ Heterogeneous alkali catalyts as MgO and CaO;
- ✓ Homogeneous acid catalysts as H_2SO_4, HCl and H_3PO_4;
- ✓ Heterogeneous solid acid catalysts as resins;
- ✓ Enzyme as lipases from candida, pseudomonas and others.

Camús and Laborda (2006) also stated that among the catalysts used on industrial scale, generally, the homogeneous alkali catalysts are the chosen, since they allow operation in moderate conditions and have higher performance. Freedman, Pryde and Mounts (1984) also claimed that homogeneous alkali catalyst exhibits a catalytic activity in this reaction of up to 4,000 times greater than the homogeneous acid catalysts. Other authors such as Çetinkaya and Karaosmanoğlu (2004) and Souza (2011) also confirmed this point.

According to Figure 2.4 and Figure 2.5, there are alkoxides formation after contact between hydroxyl from the alkali catalyst and methanol (alcohol), besides of the possible mechanism of homogeneous alkali-catalyzed (HAC) transesterification reaction from TAGs. In this reaction, there is a nucleophilic attack to carbonyl carbon of the TAG, obtaining a tetrahedral intermediate that eliminates one molecule of methyl ester and produces another alkoxide ion. Finally, a diacylglycerol and a fatty acid methyl ester (FAME) are produced. After two more repetitions of these steps, two others FAME molecules are obtained and also glycerol (RAMOS et al., 2011).

Figure 2.4 – Production of alcoxides ions

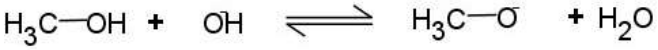

Source: Adapted from Ramos et al. (2011)

Figure 2.5 – Mechanism of alkali-catalyzed transesterification reaction from TAGs

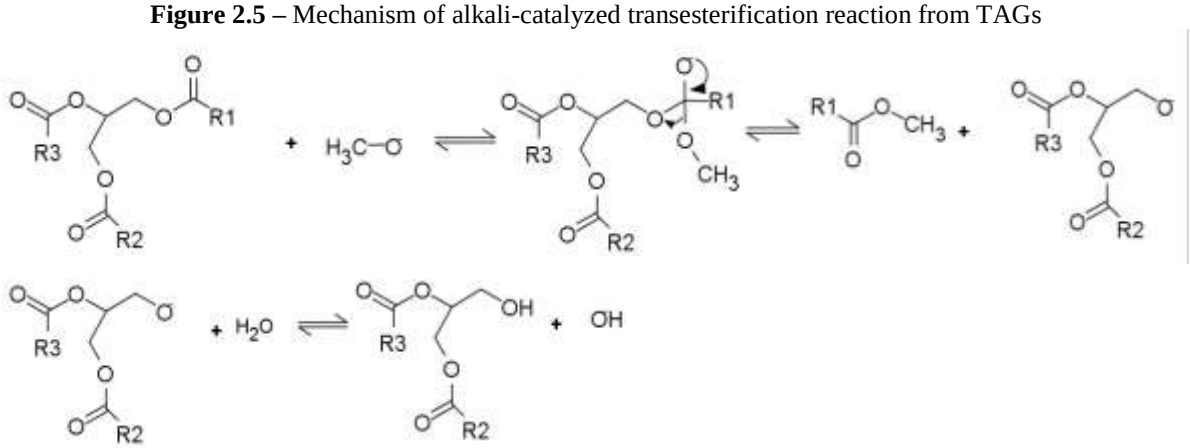

Source: Adapted from Ramos et al. (2011)

2.1.4.1 Parameters from transesterification reaction

The main parameters affecting transesterification reaction are:

1) Water content – Anhydrous oil is generally preferred, despite of water content below 0.06 wt% to be acceptable prior to transesterification reaction. This reduce undesired effects as TAG hydrolysis to FFA and soap formation by consumption of homogeneous alkali catalysts (ATADASHI et al., 2012; MA; CLEMENTS; HANNA, 1998);

2) FFA content – These components are kept below 0.5 wt%, although other authors consider up to 1% and 3%. This depends on the raw material used and other factors. However, for safety reasons, the more conservative value is recommended to reduce soap formation that could decrease biodiesel yield (GNANAPRAKASAM et al., 2013; MA; HANNA, 1999);

3) Type of alcohol – Methanol is the most used alcohol, because of its low cost and physical-chemical advantages (MA; HANNA, 1999). However, other short chain alcohols can be used as ethanol and isopropanol. These have the disadvantage of azeotropic formation between alcohol and water, so that becomes more difficult to recover the alcohol by distillation (GNANAPRAKASAM et al., 2013). Moreover, since they have longer carbon chain than methanol, they have higher solubility in the ester phase, so that makes more difficult to achieve the required ester purity in biodiesel (FOLLEGATTI-ROMERO et al., 2012);

4) Molar ratio (MR) of alcohol to oil – MR of alcohol to oil is an important factor to achieve high biodiesel yields. The stoichiometric ratio of alcohol to oil is 3, despite of a MR of 6 is commonly adopted for HAC process in order to shift the reaction equilibrium to products. Further increases may not significantly improve yield, since alcohol excess can solubilize glycerol in the ester phase. In addition, raw material, type of catalyst, temperature, impurities and other combined factors can also affect MR, so that each case must be evaluated to find optimal condition (GNANAPRAKASAM et al., 2013; PHAN; PHAN, 2008);

5) Type of catalyst – In general, the use of homogeneous alkali catalysts is preferable because of its low cost, high efficiency and fast conversion of oil into biodiesel. However, there are problems to recover these catalysts (NaOH and KOH) and to treat wastestream generated from HAC process. Moreover, water and FFA sensitivity can cause soap formation. As a result, new alternatives as solid alkali catalysts have been studied, since they have advantages as easy reuse and less waste generation. However, some disadvantages can limit their use, such as catalyst

poisoning when exposed to air, FFA sensitivity, leaching of catalyst active sites and others. Enzymes and homogeneous acid catalysts are other options; however, both have a very slow reaction rate and the first have a high cost. Solid acid catalysts can also be used requiring moderate to high temperatures, high MR of alcohol to oil and long reaction times, as well as their synthesis are complicated and they are expensive (LAM; LEE; MOHAMED, 2010). On the other hand, they can lead esterification and transesterification reactions simultaneously. Furthermore, uncatalyzed reaction can be carried out applying high pressures and temperatures in supercritical condition. Despite of the fast conversion, this process still has resistence to be used in large scale (VYAS; VERMA; SUBRAHMANYAM, 2010);

6) Catalyst content – For the most used HAC reaction, when catalyst content is increased, there is a trend for higher yields. However, an excessive increase may decrease yield because of the increase of viscosity in the reaction mixture (GNANAPRAKASAM et al., 2013);

7) Stirring speed – For HAC reactions there is an optimum agitation speed, so that increasing it a decrease in reaction time and an increase in conversion is obtained. Increase of particles collisions and decrease of mass transfer resistance by diffusion can be the main causes, since the beginning of the reaction is biphasic. After this optimum condition, there is no significant increase in yield (GNANAPRAKASAM et al., 2013). For instance, Vicente et al. (2005) found that after 600 rpm there is no significant increase in biodiesel yield for transesterification reaction of sunflower oil with methanol using KOH as catalyst.

8) Temperature – Increasing temperature, in general, decrease stirring time and increase biodiesel yield in HAC reaction. However, temperature must be kept below alcohol bubble point to avoid its vaporization. Furthermore, additional increase after the optimum value may decrease conversion as presented by Phan and Phan (2008). These authors realized that when transesterification reaction of WCO was carried out in presence of 0.75% KOH and MR of methanol to oil of 8, there was a slight drop in conversion by raising the temperature from 60 °C to 70 °C. This can be caused by partial vaporization of methanol at 70 °C;

9) Reaction time – Reaction time must be optimized to decrease costs. HAC process normally requires 1 to 2 hours for complete conversion (GNANAPRAKASAM et al., 2013).

2.1.4.2 Kinetic models for homogeneous alkali-catalyzed transesterification reaction

Kinetic models for transesterification reaction were extensively studied in the literature. Among these, models proposed by Freedman, Butterfield and Pryde (1986) and Noureddini and Zhu (1997) are well-known. The first group studied the kinetics of alkali and acid transesterification of soybean oil in presence of butanol and methanol. Among the alcohols used in HAC reactions, kinetic model for butanol agreed to experimental data suggesting a second order reaction. However, methanol was correlated including a parallel or derivative reaction with simultaneous attacks on TAG molecules by three methoxide ions.

Noureddini and Zhu (1997) studied TAGs methanolysis from soybean oil and correllated a second order model for both forward and backward reactions. The kinetic model also considered formation of diacylglycerols (DAGs) and monoacylglycerols (MAGs) intermediates. However without existence of parallel or derivative step. In addition, they demonstrated that the reaction conversion curve has a sigmoidal characteristic, where three different regimes are found: mass transfer, kinetic and equilibrium.

In the beginning, there is predominance of mass transfer resistance, so that intensive agitation is required in the reactor to solubilize the reaction mixture. Noureddini and Zhu (1997) claimed that after some stirring speed, interfence of this slow step may be negligible. The second step is the kinetic stage, where after the first stage, part of the produced esters aids in the solubilization of oil in the alcohol phase (reactive), so that the reaction occurs faster. In the end of the reaction, equilibrium is achieved, since a lower reaction rate was observed.

Kinetics were also developed using other oils, such as palm oil, sunflower oil, rapeseed oil and others. Darnoko and Cheryan (2000) studied the kinetics of transesterification of palm oil with methanol in the presence of KOH. The authors obtained a pseudo-second order model as found by Noureddini and Zhu (1997). However they did not consider backward steps from equilibrium reactions.

Other well-known kinetic models were developed for sunflower oil (SuO) by Stamenković et al. (2008) for low temperatures (10–30 °C) and by Vicente et al. (2005) for low to moderate temperatures (25–65 °C), respectively. The latter authors defined a second order pseudo-homogeneous kinetic mechanism with respect to forward and backward reactions given by Equations 2.1 to 2.7,

$$\frac{dT}{dt} = -(k_1')[\mathrm{T}][\mathrm{A}] + (k_2')[\mathrm{E}][\mathrm{D}] \quad (2.1)$$

$$\frac{dD}{dt} = (k_1')[\mathrm{T}][\mathrm{A}] - (k_2')[\mathrm{E}][\mathrm{D}] - (k_3')[\mathrm{D}][\mathrm{A}] + (k_4')[\mathrm{E}][\mathrm{M}] \quad (2.2)$$

$$\frac{dM}{dt} = (k_3')[\mathrm{D}][\mathrm{A}] - (k_4')[\mathrm{E}][\mathrm{M}] - (k_5')[\mathrm{M}][\mathrm{A}] + (k_6')[\mathrm{E}][\mathrm{G}] \quad (2.3)$$

$$\frac{dG}{dt} = (k_5')[\mathrm{M}][\mathrm{A}] - (k_6')[\mathrm{E}][\mathrm{G}] \quad (2.4)$$

$$\frac{dE}{dt} = (k_1')[\mathrm{T}][\mathrm{A}] - (k_2')[\mathrm{E}][\mathrm{D}] + (k_3')[\mathrm{D}][\mathrm{A}] - (k_4')[\mathrm{E}][\mathrm{M}] + (k_5')[\mathrm{M}][\mathrm{A}] - (k_6')[\mathrm{E}][\mathrm{G}] \quad (2.5)$$

$$\frac{dA}{dt} = -\frac{dE}{dt} \quad (2.6)$$

$k_{\mathrm{i}}' = k_i C_{cat}$, where i=1,2,…, 6. (2.7)

where T, D, M, G, E and A are relative to the oil (TAGs), DAG, MAG, glycerol, ester and alcohol (methanol), respectively, and the brackets refer to molarity. Forward kinetic constants are k_1', k_3' and k_5' and backward kinetic constants are k_2', k_4' and k_6', where all are in terms of catalyst as an apparent constant. Therefore, kinetic constants without the single quotation mark are relative to the absence of the catalyst and C_{cat} is the catalyst concentration. In addition, the kinetic constant (k_i) is affected by temperature according to Arrhenius law given by Equation 2.8,

$$k_i = k_o e^{-\frac{E_a}{RT}} \quad (2.8)$$

where k_o is the pre-exponential factor, E_a is the activation energy, R is the universal gas constant and T is the temperature (FOGLER, 2016). All parameters for this kinetic model are summarized in Table 2.2, where backward step to recover MAG showed to be not significant.

Table 2.2 – Kinetic parameters for methanolysis of SuO with KOH at MR of methanol to oil of 6

Parameters	TAG → DAG	DAG → TAG	DAG → MAG	MAG → DAG	MAG → G
E_a (J/mol)	31,656.2	31,014.3	41,557.8	41,107.2	5,955.5
k_0	3.4×10^{12}	9.8×10^{12}	2.1×10^{17}	1.2×10^{17}	537.9
R^2	0.9889	0.9817	0.9556	0.9053	0.9608

Source: Vicente et al. (2005).

Vicente et al. (2005) varied amount of catalyst, temperature and stirring speed for methanolysis of SuO with KOH. From these investigations, optimum condition for transesterification reaction was obtained: MR of methanol to oil of 6, 65 °C, KOH concentration of 1 wt% (relative to oil) and stirring speed of 600 rpm. This agitation eliminated mass transfer (MT) interference at the beggining of the reaction, since kinetic model is initially controlled by the MT and then kinetically controlled.

Stamenković et al. (2008) also studied the kinetic of SuO methanolysis at low temperatures and obtained a similar model. However, they considered the model to be composed of two phases, where phase 1 is an irreversible second order reaction controlled by MT and phase 2 is a reversible second order reaction controlled by kinetic regime.

A similar second order pseudo-homogeneous kinetic model was also developed by Mueanmas, Prasertsit e Tongurai (2010) for methanolysis of canola oil (CnO) in a RDC based on experimental results from He, Singh and Thompson (2006). However, only forward reactions were considered since products and methanol excess are continuosly removed in a RDC. Parameters obtained for this kinetic model are shown in Table 2.3.

Table 2.3 – Kinetic parameters for methanolysis of CnO with KOH in a RDC

Parameters	TAG → DAG	DAG → MAG	MAG → G
E_a (J/mol)	141,806.9	124,976.0	81,517.0
k_0	$7{,}46 \times 10^{16}$	$1{,}0 \times 10^{15}$	$6{,}17 \times 10^{8}$

Source: Adapted from Mueanmas, Prasertsit e Tongurai (2010).

2.1.5 Esterification: an alternative for pretreatment and biodiesel production

According to Canakci and Van Gerpen (2001b), when the lipid raw materials have a high FFA content, they should be subjected to a pretreatment step based on acid-catalyzed process to produce FAAE to compose biodiesel. Subsequently, the products obtained with low FFA concentration are fed to a transesterification reactor to increase the biodiesel yield. In this case, Ma and Hanna (1999) highlighted the importance to keep FFA level below 0.5 wt%. Freedman, Pryde and Mounts (1984) stated that disregarding this limit can reduce ester yield.

The initial pretreatment discussed above is known as esterification reaction and helps to reduce saponification reaction, which generates soap when FFA reacts with homogeneous alkali catalyst as shown Figure 2.6 and Figure 2.7. Soap formation increases purification costs and drop biodiesel yield because of the loss of esters to glycerol phase (ZADRA, 2006).

Figure 2.6 – Fatty acid esterification reaction for alkyl groups R and R1

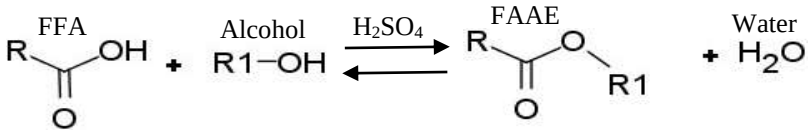

Source: Adapted from Ramos et al. (2011)

Figure 2.7 – Saponification reaction of FFA in presence of alkali catalyst (KOH)

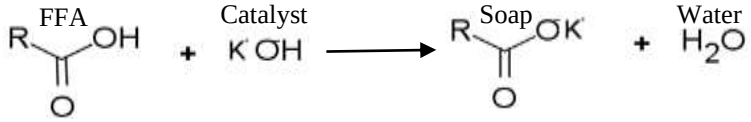

Source: Adapted from Van Gerpen (2005)

Ramos et al. (2011) also presented the mechanism of esterification reaction with homogeneous acid catalysts. Figure 2.8 shows the attack of oxygen to proton, which leads to carbocation formation that undergoes a nucleophilic attack from alcohol generating a tetrahedral intermediate. Finally, ester is obtained, water is removed and catalyst H^+ regenerated.

Figure 2.8 – FFA esterification mechanism, where R_1 and R are FFA and alcohol hydrophobic carbon chains

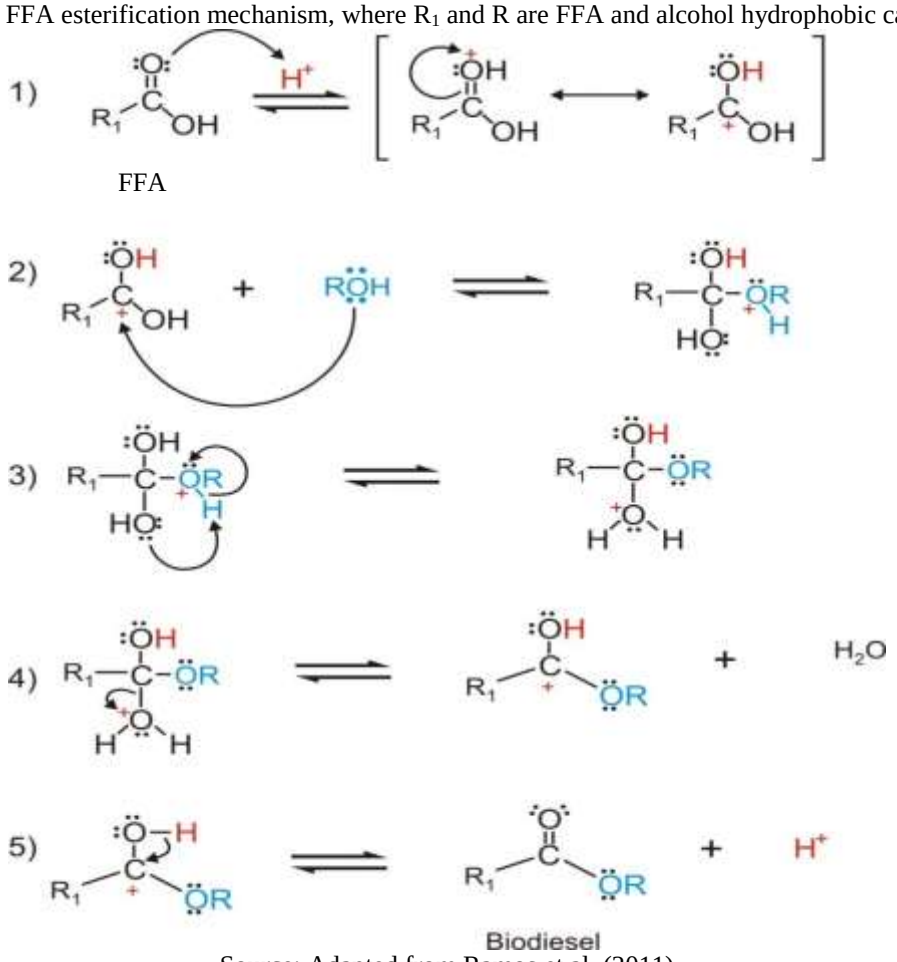

Source: Adapted from Ramos et al. (2011)

2.1.5.1 Parameters from esterification reaction

The main parameters affecting esterification reaction are:

1) Presence of oil and FFA content – The presence of oil affects the esterification reaction, so that requires a higher MR of alcohol to FFA depending on the acidity of the oil. For oils varying the FFA content between 15–25 wt%, a MR of 19.8 is recommended by National Renewable Energy Laboratory (NREL). For concentrations below 15% further optimization studies are required; however, a MR of 40 is generally suggested and the value may be higher or lower depending on the FFA content and type of oil (CHAI et al., 2014). These high values are required because two phases are generated in the beginning, a polar phase (methanol, catalyst and FFA) and another apolar (oil and FFA). Adding excess of methanol, more FFA are transported to polar phase, where the reaction takes place (reactive phase) and, subsequently, occurs migration of esters back into the oil phase. Therefore, methanol behaves as an esterifying

and solvent agent at the same time (DIAZ-FELIX et al., 2009). Canakci and Van Gerpen (2001a) demonstrated this through a diagram showing the solubility of soybean oil, lard, methyl ester of yellow greases, yellow and brown greases. In this study as expected, esters were the most soluble obtaining a single phase at temperatures above 40 °C. In addition, brown greases presented more methanol in the alcohol phase, because of the higher amount of FFAs (33%), followed by yellow grease (9%), soybean oil and lard, where these last two practically showed similar distribution of alcohol in their phases. On the other hand, in absence of oil, FFA are easily esterified with MR of methanol to FFA, more smoothly ranging from 3 to 7 (ARANDA et al., 2008; UNNITHAN; TIWARI, 1987);

2) Water content – In general, anhydrous raw material is preferable to be esterified. However, water content below 5 wt% is acceptable prior to performe esterification reaction with H_2SO_4 if MR of methanol to FFA is above 6. This occurs because of the excess of methanol with H_2SO_4 counterbalances the backward reaction, so that water inhibition decreases. For a solid acid catalyst as Ambelyst-15, greater sensitivity to hydration is observed even in excess of methanol since active sites are poisoned by water (PARK et al., 2010);

3) Type of alcohol – As for transesterification reaction, methanol is the most frequently used alcohol, although other short chain alcohols can be used as ethanol. This has the disadvantage of azeotrope formation. In addition, less decrease in acidity from oil is obtained with ethanol, until same if the reaction rate is higher than in presence of methanol. Higher temperatures (greater than methanol boiling point) and solubility in the apolar (oil and ester) phase can be the causes (CANAKCI; VAN GERPEN, 2001a);

4) MR of alcohol to oil – This is also an important factor in achieving high biodiesel yield for esterification reaction. When increasing MR, there is a trend to improve conversion, mainly from the half to the end of the reaction, as demonstrated by Hassan and Vinjamur (2014). The authors realized from a Taguchi approach that after 75 min of reaction until reaching 180 min, there is a higher influence of MR in comparison to other factors as temperature, amount of catalyst and reaction time (variable independent from the study). This can be caused by the proximity of reaction equilibrium and water formation, requiring excess of alcohol to compensate this inhibition effect. In addition, higher MR values are commonly required in presence of oil as shown previously;

5) Type of catalyst – In general, the use of homogeneous acid catalysts is preferred. Sulphuric acid is the most used because of the high ester yield, low reaction time and low cost. Compared

to HCl, $AlCl_3$, $SnCl_2$·H2O and FeSO4, H_2SO_4 has higher activity and FFA conversion (FARAG; EL-MAGHRABY; TAHA, 2011).

6) Catalyst content – Increasing the concentration of homogeneous acid catalyst, there is a trend to increase FFA conversion (FARAG; EL-MAGHRABY; TAHA, 2011). Hassan and Vinjamur (2014) analyzed the influence of this variable through a Taguchi approach, which showed greater influence in the first 10 min of reaction. Between 10 to 75 min and 75 to 180 min its influence was decreased, although was still considered significant.

7) Stirring speed – Farag, El-Maghraby and Taha (2011) studied the effect of agitation speed on esterification reaction in presence of oil with high FFA content. The authors observed that after 60 min no additional effect on the reaction rate was observed. However, higher conversions were obtained for 40 min at 300 and 600 rpm.

8) Temperature – When temperature rises, generally, reaction time decreases, yield and conversion increase. However, this is generally not kept above the alcohol bubble point in order to avoid alcohol vaporization (Farag; El-Maghriby; Taha, 2011). Despite this, some cases of temperatures above were reported as by Hassan and Vinjamur (2014). They analyzed temperature influence through a Taguchi approach and observed that greatly affects the reaction up to 75 min. After this time the greatest influence changes to MR of methanol to FFA. Therefore, from this study the order of influence from 20 to 75 min was temperature > MR > amount of catalyst > reaction time, while from 75 to 180 min was MR > temperature > reaction time > amount of catalyst, respectively.

2.1.5.2 Kinetic models for homogeneous acid-catalyzed esterification reaction

As for transesterification, kinetic models for esterification reaction have been extensively studied. Some were developed in presence of oil and others in its absence. The ones in presence of oil are more common to be found. Among them, the works of Sendzikiene et al. (2004), Berrios et al. (2007), Thiruvengadaravi et al. (2009), Jansri et al. (2011) and Chai et al. (2014) used rapeseed, sunflower, Pongamia pinnata, palm and cooking oils, respectively.

Sendzikiene et al. (2004) studied the kinetic of esterification reaction from oleic acid in presence of rapeseed oil. The acidity of the oil varied from 10 to 31% and experimental conditions were temperature between 20 and 60 °C, stirring speed of 850 min^{-1} and 1% of

H_2SO_4 (catalyst). In this study, they concluded that reaction rate depends on the amount of catalyst and the acidity of the oil. They also obtained the kinetic parameters as k_0 and E_a defining a kinetic model as pseudo-first order reaction.

Berrios et al. (2007) studied the kinetics of esterification using oleic acid in presence of SuO. The acidity of the oil ranged from 5–7 mg KOH/g oil and the experimental conditions were temperature between 30 and 60 °C, stirring speed between 200 and 600 rpm, MR of methanol to FFA from 10 to 80 in an interval of 10 and also MR of 114.6. Percentage of H_2SO_4 employed varied between 5% and 10 wt% (relative to FFA).

The optimum conditions found were MR of methanol to FFA of 60, 5% of H_2SO_4, stirring speed of 600 rpm and temperature of 60 °C. Therefore, the most conservative limit of 0.5 wt% of FFA in the oil was reached in 120 min, which increased separation efficiency of biodiesel and glycerol phases. They also obtained a first and second order kinetic model with respect to forward and backward reactions, respectively, since methanol was in excess. Equations 2.9 to 2.12 show the results after integration,

$$2\mathrm{k}_2\alpha t = ln\left\{\left[[A_0] + E(\beta - \tfrac{1}{2})\right]/\left[[A_0] - E(\beta + \tfrac{1}{2})\right]\right\} \quad (2.9)$$

$$\alpha = \sqrt{\left({K_{eq}}^2/4\right) + K_{eq}A_0} \quad (2.10)$$

$$\beta = \alpha/K_{eq} \quad (2.11)$$

$$K_{eq} = k_1/k_2 \quad (2.12)$$

where $[A_0]$ is the initial concentration of FFA in mg KOH/g oil (acid value), E is the acidity removed, K_{eq} is the equilibrium reaction constant and k_1 and k_2 are the forward and backward reaction constants, respectively.

Thiruvengadaravi et al. (2009) investigated esterification kinetic from FFA present in Pongamia pinnata oil. Under the conditions studied, the acidity was reduced from 15.96 to 2.42

mg KOH/g oil. In addition, the optimized conditions chosen were MR of 9 and 60 °C. However, amount of H_2SO_4 (0.5–2%) did not significantly affect the conversion. The kinetic model suggested by Berrios et al. (2007) was adopted with some assumptions:

1. The esterification reaction is reversible and heterogeneous, besides the reaction rate under the operating conditions is controlled by chemical reaction (chemical regime);

2. The amount of methanol is considered constant during the reaction because of the excess;

3. In absence of catalyst the reaction does not occur;

4. The reaction occurs in the oil phase.

Jansri et al. (2011) studied the esterification kinetics of FFA present in crude palm oil, besides of the transesterification kinetics for this oil. The initial FFA content varied between 8 and 12 wt% in oil and decreased to 1 wt%. The optimized conditions were MR of methanol to FFA of 10 and 10 wt% of H_2SO_4 in FFA. The kinetic model was second order in relation to both forward and backward reactions. Reaction rate from forward reaction were higher compared to backward for the temperature range (55–65 °C).

Chai et al. (2014) carried out a detailed study comparing esterification practices in the industry and laboratory. The authors investigated the reaction applied for WCO containing 5% of FFA in presence of H_2SO_4. They found that the MR proposed by NREL (MR = 19.8) does not satisfy the FFA content of the raw material studied. Therefore, the optimized condition chosen was MR of methanol to FFA of 40 in order to reach 0.5 wt% of FFA in the oil.

Therefore, Chai et al. (2014) suggested new studies on optimized reaction conditions, which were applied for raw materials with less than 15% (yellow grease). The researchers concluded that the industrial value of MR = 19.8 is suitable only for FFA content ranging from 15–25% (brown grease). Furthermore, a catalyst concentration of 5 wt% of H_2SO_4 is valid in the range of 15–35% of FFA in the oil. As Berrios et al. (2007), Chai et al. (2014) also proposed a first-order kinetic model with respect to forward reaction. However, backward reaction was disregarded because of the excess of methanol (MR = 40 of methanol to oil).

Studies presenting kinetic data for long chain FFA (above 15 carbons) for esterification reaction with methanol and H_2SO_4 in the absence of oil are scarce. Few investigations were carried out by Unnithan and Tiwari (1987) and Aranda et al. (2007). The kinetic model developed by the first group was considered second order with respect to forward and backward reactions, as shown in Equations 2.13 to 2.14.

$$-r_A = -\frac{dC_A}{dt} = k_1\left(C_A C_B - \frac{1}{Keq} C_E C_W\right) \quad (2.13)$$

$$K_{eq} = [C_E C_W / C_A C_B]_{eq} = X_{Aeq}^2 / \left[\left(1 - X_{Aeq}\right)\left(M - X_{Aeq}\right)\right] \quad (2.14)$$

Integrating Equation 2.13 is obtained Equation 2.15,

$$ln[(X_A - A^*)/(X_A - B^*)] = \ln(A^*/B^*) + k_1 C_{A0}(A^* - B^*)t \quad (2.15)$$

where A* and B* are given by Equations 2.16 and 2.17, respectively.

$$A^* = \left[(1 + MR) + \sqrt{(MR-1)^2 + 4k_2 MR}\right] / [2(1 - k_2)] \quad (2.16)$$

$$B^* = \left[(1 + M) - \sqrt{(M-1)^2 + 4k_2 M}\right] / [2(1 - k_2)] \quad (2.17)$$

In these equations C_A, C_B, C_E and C_W are concentrations of FFA, methanol, ester and water, MR is the MR of methanol to FFA and X_{Aeq} is the equilibrium conversion of FFA.

Unnithan and Tiwari (1987) varied temperature from 373.15–403.15K, catalyst load from 0.5–1 wt% of H_2SO_4 on FFA and MR of methanol to FFA from 3–7. In addition, oleic acid and a FFA mixture mainly composed of linoleic and oleic acid were used as raw materials for esterification reaction. Increasing MR, temperature and amount of catalyst was obtained a higher conversion as well as found by Aranda et al. (2007).

Aranda et al. (2007) studied the esterification kinetics for a FFA mixture from palm fatty acids mainly composed of palmitic and oleic acids. The authors used four acid catalysts and the best were the methanesulfonic and sulfuric acids. Furthermore, the use of methanol showed a higher biodiesel yield than using ethanol, since presence of a longer and less polar chain

decreases activity. Moreover, ethanol has a steric hindrance in the reaction and a higher water inhibition, due to the higher phase miscibility and emulsion formation.

The kinetic model developed by Aranda et al. (2007) showed a reaction order of 1 and 0 with respect to FFA mixture and methanol, respectively, for a MR of 3, temperature range from 130 to 160ºC and catalyst concentration from 0 to 1 wt%. However, they did not consider the backward step, which may limit this kinetic model, since esterification is a reversible reaction, mainly, for a small methanol excess.

2.1.6 Catalysts for biodiesel production: efforts to use solid catalysts

Recently, many efforts have been spent to develop catalysts more active, eco-friendly, cheap and applicable for simultaneous esterification and transesterification reactions. As a result, they can be classified in catalysts for isolated and simultaneous biodiesel reactions.

2.1.6.1 Isolated reactions

The catalysts commonly used for biodiesel production in transesterification and esterification reactions are still homogeneous alkali (NaOH and KOH) and acid (H_2SO_4), respectively. These are preferred for industrial purposes because they have low price, high yield and activity. Moreover, they are readily available, operate in moderate conditions and have low reaction time (1–2 h) (TALEBIAN-KIAKALAIEH et al., 2013).

However, there are efforts to change this scenario, since homogeneous catalysts applied for biodiesel production cannot be reused, requiring a washing and a neutralization step that increases waste treatment costs (AVHAD, MARCHETTI, 2015). In addition, the use of cheaper raw materials such as ROF requires prior water removal (<0.06 wt%), incorporation of more equipment and glycerol washing in the FFA pretreatment step to avoid side reactions in transesterification unit (ZHANG et al., 2003a).

In order to overcome the disadvantages of homogeneous catalyzed process, several studies on solid (heterogeneous) basic and acid catalysts have been developed. Solid alkali catalysis has been a interesting alternative to carry out transesterification reaction. Some main

characteristics can be mentioned for this process, such as: reaction time ranging from 1 to 6 h, temperature range from 65 to 190 °C, MR of methanol to oil between 6 and 32, possibility of catalyst reuse and regeneration. However, there are also some disadvantages, such as: possibility of leaching of catalyst active sites and sensitivity to FFA and water. The main catalysts from this class are CaO, MgO and supported alkali or alkaline earth metal oxides (AVHAD; MARCHETTI, 2015; TALEBIAN-KIAKALAIEH et al., 2013).

Kaur and Ali (2011), Rezaei, Mohadesi and Moradi (2013), Rashtizadeh, Farzaneh and Talebpour (2014) and Santiago-Torres, Romero-Ibarra and Pfeiffer (2014) reported high conversions, under moderate conditions and low reaction time for biodiesel production through heterogeneous alkali catalysts. These four researchers groups achieved maximum conversions of ~99%, 94.73%, ~95.7%, and 98.3% with MR of methanol to oil of 6, 9, 25 and 3. In addition, reaction time of 60, 180, 61 and 180 min at 65, 60, 60 and 65°C using Li/CaO, CaO from egg shell, Sr_3AlO_6 and Na_2ZrO_3 catalysts, respectively.

2.1.6.2 Simultaneous reactions

Some studies have been proposed to remove the acid pretreatment step employed to high FFA content raw materials. Among them, the use of homogeneous acid catalysts was proposed, mainly using H_2SO_4, in order to carry out esterification and transesterification reactions simultaneously (CANAKCI, M; VAN GERPEN, 1999; GUAN et al., 2009; ZHANG et al., 2003a). Some advantages are reduction of investment costs (absence of pre-treatment) and insensitivity to high FFA content. However, these catalysts are highly corrosive and have activity in the transesterification reaction up to 4,000 times lower than using homogeneous alkali catalysts (AVHAD; MARCHETTI, 2015; FREEDMAN, B; PRYDE; MOUNTS, 1984).

As a result, more interesting alternative catalysts leading reactions simultaneously have been proposed. Among them, the most promising are heterogeneous solid acid catalysts (HSAC), since some are tolerant to water and FFA presented in oil. Furthermore, other advantages are easy product separation, reduced leaching of activity sites, high possibility of reuse and regeneration depending on their activity (TALEBIAN-KIAKALAIEH et al., 2013). However, in order to meet high conversion requirements and low reaction time for both reactions, HSAC should have moderate acidity, hydrophobicity, porosity to minimize diffusion

drawbacks, high number of acid active sites, less complex preparation method and thermostable characteristics (AVHAD; MARCHETTI, 2015; SANI; DAUD; ABDUL AZIZ, 2014).

Several researchers have focused on the development of new HSAC in order to produce biodiesel from ROF based on an unique step. Abreu et al. (2005), Garcia et al. (2008), Liu and Wang (2009), Yan, Salley and Ng (2009), Li et al. (2010), Dawodu et al. (2014) and Kaur and Ali (2011) reported high yields with optimal reaction time ranging from ~ 1 to 6 h. In addition, kinetic models have been developed, such as those proposed by Shu et al. (2011), Gaurav, Ng and Rempel (2016), Kaur and Ali (2015) and Konwar et al. (2016). However, the last two authors measured the kinetic data (E_a, kinetic constants and k_0) only for transesterification reaction, which demonstrates a gap that must be filled in the next years according to the growing number of publications on these types of catalysts.

HSAC can be divided into some groups such as: zeolites, oxides and inorganic salts, coordination compounds and ionic liquids, ion exchange resins, organic acids and bases and lamellar materials (CORDEIRO et al., 2011). According to Avhad and Marchetti (2015) the most used are mixtures of modified inorganic oxides (silica, sulfated and tungsten zirconia or zeolite), sulphated carbon materials, cation exchange resins and superacid catalysts.

2.2 PURE PROPERTIES OF FATTY COMPOUNDS

Pure properties of long chain fatty compounds are difficult to be measured, mainly, when heating is involved as for vapor pressure and heat of vaporization from acylglycerols (ACG). Some causes are thermal decomposition, wide variety and size (more than 15 carbons) of FFA fragments from oils and greases used for biodiesel production. In this case, estimation methods are commonly adopted to calculate these properties.

Group Contribution (GC) and Constituent Fragments (CF) methods are the most known estimation methods for ACG. These approaches consider a molecule as a combination of functional groups and fragments (glycerol and FFA fragments), respectively, as shown in Figure 2.9 (CERIANI; GANI; LIU, 2013; ZONG; RAMANATHAN; CHEN, 2009; 2010). The first method is more general, since can be applied for a variety of fatty compounds, while CF approaches are commonly used for ACG. Hereafter, some of these methods are detailed for TAG properties based on recommendations of Su et al. (2011).

Figure 2.9 – Constituent fragments and group contribution approaches

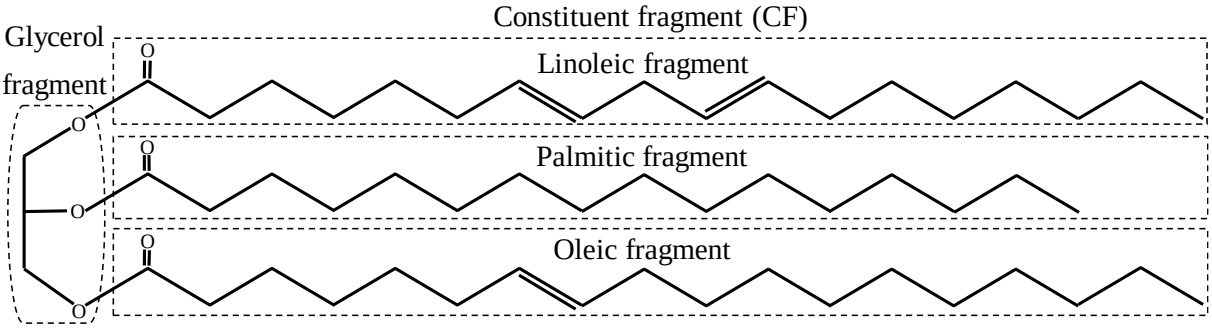

Source: Ceriani, Gani and Liu (2013) and Zong, Ramanathan and Chen (2009, 2010).

2.2.1 Vapor pressure and heat of vaporization

Vapor pressure (P_i^{vap}) of TAG in Pa was estimated based on GC method by

$$\ln \mathrm{P_i^{vap}} = \mathrm{A} + {}^{B}/_{T} + C \cdot ln(T) \tag{2.18}$$

where T is temperature in K; A, B and C are parameters obtained from Equations 2.19–2.21.

$$A = \sum_k N_k \cdot (A_{1k} + MM \cdot A_{2k}) + (s_0 + N_{CS} \cdot s_1) + \alpha \cdot (f_0 + N_{CA} \cdot f_1) \tag{2.19}$$

$$B = \sum_k N_k \cdot (B_{1k} + MM \cdot B_{2k}) + \beta \cdot (f_0 + N_{CA} \cdot f_1) \tag{2.20}$$

$$C = \sum_k N_k \cdot (C_{1k} + MM \cdot C_{2k}) \tag{2.21}$$

In Equations 2.19–2.21, N_k, N_{CA} and N_{CS} are the number of groups k, number of carbons atoms and number of carbons of the alcoholic part of esters (methyl, ethyl, propyl and butyl) in the

molecule, respectively. In addition, MM is the component molecular weight and all the other parameters were obtained by regression of an extensive vapor pressure databank of fatty compounds, alcohols and some hydrocarbons adopting the GC approach (CERIANI; GANI; LIU, 2013).

From the parameters aforementioned and critical temperature T_c in K and pressure P_c in Pa, heat of vaporization (ΔH_i^{vap}) of TAG in J·mol^{-1} can be also estimated according to

$$\Delta H_i^{vap} = 8.3144 \cdot (-B + C \cdot T) \cdot \left(1 - \frac{T}{T_c}\right)^{P_i^{vap}/P_c} \tag{2.22}$$

that was obtained from Clausius–Clapeyron including a correction factor for high temperatures as shown in Equation 2.23 (CERIANI; GANI; LIU, 2013).

$$\frac{dP_i^{vap}}{dT} = \frac{\Delta H_i^{vap}}{T \cdot (V^v - V^l)} \tag{2.23}$$

2.2.2 Liquid heat capacity

Liquid heat capacity (C_p^l) of TAG in J·kmol^{-1}·K^{-1} was estimated from CF approach by

$$C_p^l = \sum_A N_{frag,A} C_{p,A}^l (T) \tag{2.24}$$

where $N_{frag,A}$ means the number of fragments A present in the TAG and $C_{p,A}^l$ represents the contribution of liquid heat capacity from fragment A obtained by Equation 2.25.

$$C_{p,A}^l = A_{1,A} + A_{2,A} T \tag{2.25}$$

In Equation 2.25, $A_{1,A}$ and $A_{2,A}$ are correlation parameters for fragment A obtained by regression of C_p^l experimental data from TAG compounds (ZONG; RAMANATHAN; CHEN, 2009).

2.2.3 Liquid molar volume

Liquid molar volume (V^l) of TAG in $m^3 \cdot kmol^{-1}$ was estimated from CF approach by

$$V^l = \sum_A N_{frag,A} V_A^l\,(T) \tag{2.26}$$

where V_A^l is the contribution of V^l from fragment A calculated by Equation 2.27.

$$V_A^l = \frac{1 + B_{2,A}\,T}{B_{1,A}} \tag{2.27}$$

In Equation 2.27, $B_{1,A}$ and $B_{2,A}$ are correlation parameters for fragment A obtained by regression of V^l experimental data from TAG compounds (ZONG; RAMANATHAN; CHEN, 2009).

2.2.4 Liquid viscosity

Liquid viscosity (η^l) of TAG in Pa·s was estimated from CF approach by

$$\ln \eta^l = \sum_A N_{frag,A} \ln \eta_A^l\,(T) \tag{2.28}$$

where η_A^l is the contribution of viscosity for fragment A obtained by Equation 2.29.

$$\ln \eta_A^l = C_{1,A} + \frac{C_{2,A}}{T} + C_{3,A} \ln T \quad (2.29)$$

In Equation 2.29 $C_{1,A}$, $C_{2,A}$ and $C_{1,A}$ are correlation parameters for fragment A obtained by regression of η^l experimental data from TAG compounds (ZONG; RAMANATHAN; CHEN, 2009).

2.3 THERMODYNAMIC MODELS

The thermodynamic models of activity coefficients are divided into two approaches: molecular and GC models. The former is based on hypothesis of local compositions within a liquid solution, rather than the overall composition of the mixture. These are assumed to be responsible for short-range interactions and non-random orientations caused by differences in molecular size and intermolecular forces (SMITH; VAN NESS; ABBOTT, 2007). GC models are based on the idea of the molecule to be a collection of functional groups, so that a relatively small number of these can represent the properties of several different molecules (SANDLER, 2017).

The molecular and GC models have their adjustable parameters and their interactions referenced, respectively, to the molecules of the species in the mixture and the functional groups with which the molecules are constructed (SANTOS, 1999). Among the models of the first approach, the following stand out: NRTL and Universal Quasi Chemical (UNIQUAC) (ABRAMS; PRAUSNITZ, 1975; RENON; PRAUSNITZ, 1968). Among the models of the second approach the most used is the original Universal Functional-Group Activity Coefficient (UNIFAC) method that presents several extensions such as the UNIFAC Dortmund model (GMEHLING; WEIDLICH, 1986; MAGNUSSEN; RASMUSSEN; FREDENSLUND, 1981; SANDLER, 2017). Hereafter more details are shown for one representative for each approach.

2.3.1 Non-Random Two-Liquid (NRTL)

NRTL is a thermodynamic model that represents well the VLE, LLE and VLLE of non-electrolyte mixtures, containing or not strong-polar compounds, by adjusting the three parameters Δg_{ij}, Δg_{ji} and α_{ij} according to Equations 2.30 to 2.34.

$$\ln \gamma_i = \frac{\sum_j \tau_{ji} G_{ji} x_j}{\sum_k G_{ki} x_k} + \sum_j \frac{x_j G_{ij}}{\sum_k G_{kj} x_k} \left[\tau_{ij} - \frac{\sum_k x_k \tau_{kj} G_{kj}}{\sum_k G_{kj} x_k} \right] \tag{2.30}$$

$$\tau_{ij} = \frac{\Delta g_{ij}}{RT} = \frac{\left(a_{ij} - a_{jj}\right)}{RT} \quad \left(\tau_{ij} \neq \tau_{ji}\right) \tag{2.31}$$

$$G_{ij} = \exp\left(-\alpha_{ij} \tau_{ij}\right) \quad \left(\alpha_{ij} = \alpha_{ji}\right) \tag{2.32}$$

$$\tau_{ij} = \tau_{0ij} + \tau_{1ij}.T \tag{2.33}$$

$$\alpha_{ij} = \alpha_{0ij} + \alpha_{1ij}.T \tag{2.34}$$

The parameters Δg_{ij} and Δg_{ji} in J·mol^{-1} represent characteristic parameters of energy difference of the interactions between the pure components i and j. The parameter α_{ij} is related to the non-randomness of the mixture and in practice varies between 0.20 and 0.47. These can also be represented, respectively, by the binary interaction parameters a_{ij} and a_{ji} in J·mol^{-1}. From these parameters applied on NRTL model is obtained the activity coefficient of component i (γ_i) for a multicomponent mixture, where x_i is the mole fraction of component i. Therefore, this model presents three adjustable parameters for each binary pair $\left(a_{ij}, a_{ji}\ e\ \alpha_{ij}\right)$. However, in some cases are required additional temperature-dependent parameters to be regressed from experimental data (PRAUSNITZ; LICHTENTHALER; AZEVEDO, 1999; RENON; PRAUSNITZ, 1968).

NRTL model has advantages when working with strongly non-ideal systems compared to Van Laar and Wilson models, especially those with limited miscibility. This applies to both binary and multicomponent mixtures (RENON; PRAUSNITZ, 1968).

2.3.2 Universal Functional-Group Activity Coefficient (UNIFAC)

UNIFAC is a predictive model given by the combinatorial part of the Universal Quasi Chemical (UNIQUAC), with a Staverman-Guggenheim correction employed in the form of Flory-Huggins, according to Equation 2.35 for combinatorial activity coefficient of component i (γ_i^C).

$$\ln \gamma_i^C = \ln(\Phi_i/x_i) + 1 - (\Phi_i/x_i) - (z/2)[\ln(\Phi_i/\Theta_i) + 1 - (\Phi_i/\Theta_i)] \tag{2.35}$$

In this equation z is the coordinate number equals to 10. Fractions of surface area (Θ_i) and molecular volume (Φ_i) are given by Equations 2.36–2.37,

$$\theta_i = x_i\, q_i \Big/ \sum_j x_j\, q_j \tag{2.36}$$

$$\phi_i = x_i\, r_i \Big/ \sum_j x_j\, q_j \tag{2.37}$$

where parameters r_i e q_i are calculated by

$$r_i = \sum_k^{NG} v_{ki} R_k \tag{2.38}$$

$$q_i = \sum_k^{NG} v_{ki} Q_k \tag{2.39}$$

applying the parameters of volume (R_k) and area (Q_k) groups given by Hansen et al. (1991) for VLE or Magnussen, Rasmussen and Fredenslund (1981) for LLE. Moreover, v_{ki} and NG are the number of groups of type k in molecule i and in the mixture, respectively.

Residual part from activity coefficient of component i (γ_i^R) is given by the concept of solution by groups,

$$\ln \gamma_i^R = \sum_k^{NG} v_{ki} \left[\ln \Gamma_k - \ln \Gamma_k^i\right] \tag{2.40}$$

where Γ_k and Γ_k^i are the activity coefficients of a group k in the composition of the mixture and in a mixture of groups corresponding to the pure component i, respectively, given by Equation 2.41.

$$\ln \Gamma_k = Q_k \left[1 - \ln \sum_m^{NG} \theta_m \tau_{mk} - \sum_m^{NG} (\theta_m \tau_{km} / \sum_n^{NG} \theta_n \tau_{mn})\right] \tag{2.41}$$

In Equation 2.41, N_c e NG are the number of components and groups in the mixture. While τ_{mn} is the energy interaction parameter between groups m and n calculated by

$$\tau_{mn} = e^{-b_{mn}/T} \tag{2.42}$$

which depends from b_{mn}, group interaction parameter between groups m and n, and temperature (T) (SANDLER, 2017). Furthermore, θ_k and X_k are the area and mole fractions of group k, respectively, given by

$$\theta_k = \left(X_k \frac{z}{2} Q_k\right) \Big/ \left(\sum_m^{NG} X_m \frac{z}{2} Q_m\right) \tag{2.43}$$

$$X_k = \left(\sum_j^{N_c} v_{kj} x_j\right) / \left(\sum_j^{N_c} \sum_m^{NG} v_{mj} x_j\right) \tag{2.44}$$

As for UNIQUAC, by adding up these contributions, the activity coefficient of component i in the mixture (γ_i) is obtained from Equation 2.45.

$$\ln \gamma_i = \ln \gamma_i^C + \ln \gamma_i^R \tag{2.45}$$

Although widely used, UNIFAC model has some limitations that can be stated (SÉ, 2001):

- ✓ Inability to distinguish some types of isomers since is a GC method;
- ✓ Restrictions on pressure values (below the range of 10–15 atm) and temperature (in the range of approximately 290–420 K);
- ✓ Supercritical components and non-condensable gases are not described;
- ✓ Proximity effects are not taken into account;
- ✓ The LLE parameters are different from VLE ones;
- ✓ Polymers and electrolytes are not described.

2.4 PHASE EQUILIBRIUM

In general, industrial processes are designed on the basis of equilibrium conditions. The main chemical processes are mixing, conversion and separation involving gases, liquids and solids. For robust representation of these operations, a rigorous knowledge of the phase equilibrium (PE) involved in these processes is required, such as VLE, LLE, solid-liquid equilibrium and VLLE (WALAS, 1985). In addition, study of chemical equilibrium simultaneously to PE can be done, mainly when the processes involve one or more equilibrium reactions and kinetic data are unavailable.

Therefore, the study of equilibrium conditions is important for a suitable representation and to obtain reliable results from simulation of chemical processes. In this way, definition of thermodynamic model is required to successfully represent PE. Hereafter, some points are clarified about VLE, LLE and VLLE, which are the most common types of PE found in chemical engineering processes.

2.4.1 Vapor-liquid equilibrium (VLE)

VLE is related to equilibrium of amount of molecules that cross the interfaces liquid-vapor and vapor-liquid, in both directions, per unit of time. Therefore, a system under these conditions no longer exhibits macroscopic variations over time.

According to Smith, Van Ness and Abbott (2007), for a closed system at constant temperature (T) and pressure (P) with N_c components, the VLE is represented by

$$P^v = P^l \tag{2.46}$$

$$T^v = T^l \tag{2.47}$$

$$\mu_i^v = \mu_i^l \tag{2.48}$$

where i=1, 2, ..., N_C and μ_i^v, μ_i^l represent the chemical potential of component i in the vapor and liquid phases. However, chemical potentials are very difficult to measure, since they are defined in relation to internal energy and entropy. For this reason, concept of fugacity of component i in the mixture ($\hat{f}_i$) is preferable because it can express the μ for any fluid mixture based on equilibrium condition,

$$\hat{f}_i^v = \hat{f}_i^l \qquad \text{i = 1, 2, ..., } N_c \tag{2.49}$$

where superscripts v and l refer to the vapor and liquid phases, while ^ refers to solution.

The fugacity still suggests the definition of a correction factor in vapor phase relative to standard fluid (ideal gas or ideal solution) as expressed by the fugacity coefficient of component i in the mixture ($\hat{\phi}_i$). For low to moderate pressures, the deviations of idealities of a component i in the liquid phase to ideal solution is represented by γ_i. In this way, Equation 2.49 is defined by

$$y_i \hat{\phi}_i^v P = x_i \gamma_i P_i^{vap} \phi_i^{sat} \exp\left[\frac{V_i^l (P - P_i^{sat})}{RT}\right] \tag{2.50}$$

that is known as the gamma-phi approach, where y_i and x_i are the mole fractions of component i in the vapor and liquid phases. Furthermore, P_i^{vap} is the vapor pressure of component i, R is the universal gas constant and V_i^l is the liquid volume of pure component i. While superscript sat refers to saturation state (SMITH; VAN NESS; ABBOTT, 2007).

Another simplified form is given by

$$y_i \Phi_i P = x_i \gamma_i P_i^{vap} \tag{2.51}$$

$$\Phi_i = \frac{\hat{\phi}_i}{\phi_i^{sat}} \exp\left[-\frac{V_i^l (P - P_i^{vap})}{RT} \right] \tag{2.52}$$

where Φ_i defines the Poynting correction factor (exponential term), which expresses the deviations of the liquid phase relative to the effect of the pressure.

For low to moderate pressures, the Poynting factor is close to unity and can be considered equal to one. In addition, for low pressures Φ_i is also close to unity and Equation 2.51 reduces to modified Raoult's law given by Equation 2.53.

$$y_i P = x_i \gamma_i P_i^{vap} \tag{2.53}$$

After obtained the VLE results, an important issue is to evaluate qualitatively and quantitatively the interaction between mixtures subjected to vapor-liquid contact. For this reason, phase diagrams, as PT, P-x_1-y_1 and/or Tx_1y_1, are commonly generated to better understand those interactions, where subscript 1 is relative to the more volatile component. Those diagrams make easier the analysis of separation possibility via liquid-vapor contact, mainly by searching for existence or absence of azeotropes in a given mixture (SMITH; VAN NESS; ABBOTT, 2007).

2.4.1.1 Tests of thermodynamic consistency

Experimental data measurement is a very important step on science, mainly because some physical-chemical processes cannot be only represented by phenomenological models. However, these data are commonly subjected to some deviations caused by experimental errors, instruments imprecision and inadequate measurement techniques. In this case, an important issue about data quality must be taken in account mainly when using VLE and LLE data to develop a thermodynamic modelling. For this reason, thermodynamic consistency tests are commonly used to evaluate the quality of VLE data based on the following Gibbs-Duhem equation at constant pressure and temperature (HERINGTON, 1947).

$$\sum_i x_i d\ln(\gamma_i) = 0 \tag{2.54}$$

The first thermodynamic consistency test is known as Area test and was developed for isothermal conditions of a binary mixture based on Equation 2.55,

$$RT \int_0^{x_1} \left(ln\beta - ln\frac{p_1^{vap}}{p_2^{vap}} \right) dx_1 = \Delta G_{x_1}^E \tag{2.55}$$

where p_1^{vap} and p_2^{vap} are vapor pressures of components 1 and 2, x_1 is mole fraction of component 1, R is the universal gas constant, β is relative volatility and $\Delta G_{x_1}^E$ is the excess free energy of formation for x_1 (HERINGTON, 1947). Hereafter the development of Area test, many authors proposed improvements as showed by Redlich and Kister (1948) for multicomponent mixtures based on Equation 2.56,

$$E^{free} = \sum_k x_k \log(\gamma_k) \tag{2.56}$$

where E^{free} is a function related to free energy (REDLICH; KISTER, 1948). Despite these methods to be used by many researchers as way to evaluate the quality of VLE data, care must be taken since can be only affirmed that the data satisfy the Gibbs-Duhem equation. Therefore, VLE data that do not satisfy this equation must be probably incorrect; however, even for data that satisfies it cannot be assured they are correct data without a deep evaluation on many variables that causes the uncertainties (PRAUSNITZ; LICHTENTHALER; AZEVEDO, 1999).

2.4.2 Liquid-liquid equilibrium (LLE)

For the case of LLE between two liquid phases, the same equilibrium criteria showed previously according to Equations 2.46 to 2.49 is valid. However, instead of a vapor phase and a liquid phase, two liquid phases I and II are considered. Thus, Equation 2.51 applies to the LLE case changing Φ_i by γ_i^I and P_i^{vap} by the fugacity of pure component i in the liquid phase (f_i), as shown in Equation 2.57 (SMITH; VAN NESS; ABBOTT, 2007).

$$\gamma_i^I x_i^I f_i^I = \gamma_i^{II} x_i^{II} f_i^{II} \tag{2.57}$$

If each pure species can exist in the liquid state at the system temperature, $f_i^I = f_i^{II} = f_i$, then Equation 2.57 becomes,

$$(\gamma_i x_i)^I = (\gamma_i x_i)^{II}, \;\; i = 1,2, \dots, \mathrm{N}_c \tag{2.58}$$

where added to the constrains $\sum_i x_i^I = 1$ e $\sum_i x_i^{II} = 1$, these are the base system of equations for LLE calculation (SMITH; VAN NESS; ABBOTT, 2007).

As in the case of VLE, LLE data analysis is simplified by the use of phase diagrams. The most commonly employed is the ternary diagram which may be of type 1, 2 or 3 depending on the amount of partially miscible pairs. However, separations are generally carried out when the system diagram is from type 1. In this case the solvent has high affinity with the solute and is partially miscible or even substantially immiscible in the diluent component. In addition,

partition coefficients and selectivity must be considered in order to determine the solvent's ability to extract the solute from diluent phase (HENLEY; SEADER, 1981).

2.4.2.1 Quality of LLE data

As well as for VLE data, the quality of LLE data is usually required to be checked. However, for LLE it is difficult to test the thermodynamic consistency, since can be only obtained the ratio of activity coefficients between each phase γ_i^I/γ_i^{II} by Equation 2.58, instead of one γ_i value, as for VLE case obtained by Equation 2.53. For this reason, other methods as Hand (H) and Othmer-Tobias (OT) approaches have been widely applied for this purpose, since they were considered for a long time as reliable approaches (CARNITI; CORI; RAGAINI, 1978; HAND, 1930; OTHMER; TOBIAS, 1942; TREYBAL, 1963). Among these, OT method has been the most used for ternary mixtures and can be summarized by Equation 2.59.

$$log\left(\frac{1-w_2^{II}}{w_2^{II}}\right) = k \cdot \log\left(\frac{1-w_1^{I}}{w_1^{I}}\right) + c \tag{2.59}$$

In Equation 2.59 w_1^I and w_2^{II} are weight fractions of diluent and solvent components in diluent and solvent phases; k and c are slope and linear coefficients from the straight line fitted to obtain the coefficient of determination (R^2). Therefore, for R^2 values close to unity is expected that LLE data are reliable. Notwithstanding, according to Carniti, Cori and Ragaini (1978) despite of H and OT correlations have been used many times as quality checker of LLE data, they showed to be unsuitable for this purpose when these methods were employed for a more variety of LLE systems. In this case, as for VLE data that satisfies some consistency thermodynamic test is not assured that LLE data with R^2 values close to unity, obtained from H or OT plot, are truly reliable.

2.4.3 Vapor-liquid-liquid equilibrium (VLLE)

A more complicated evaluation of phase equilibrium rises when modifications of pressure or temperature on VLE system form a second liquid phase or on LLE system form a

vapor phase. In this case, Equation 2.53 is applied for a multicomponent system containing two liquid phases I and II resulting in

$$x_i^I \gamma_i^I P_i^{vap} = y_i P, \;\; i = 1,2, \dots, N_c \tag{2.60}$$

$$x_i^{II} \gamma_i^{II} P_i^{vap} = y_i P, \;\; i = 1,2, \dots, N_c \tag{2.61}$$

where x_i^I and x_i^{II} are mole fractions of component i in the liquid phases I and II; γ_i^I and γ_i^{II} are the activity coefficients of component i in the liquid phases I and II. Equation 2.58 is also applied together with those to Equations 2.60 to 2.61 respecting the constraints of mole fractions for vapor and liquid phases according to Equations 2.62 to 2.64.

$$\sum_{i=1}^{N_c} x_i^I = 1 \qquad (0 \leq x_i^I \leq 1) \tag{2.62}$$

$$\sum_{i=1}^{N_c} x_i^{II} = 1 \qquad (0 \leq x_i^{II} \leq 1) \tag{2.63}$$

$$\sum_{i=1}^{N_c} y_i = 1 \qquad (0 \leq y_i \leq 1) \tag{2.64}$$

As for VLE and LLE case, VLLE data can be also evaluated more easily using phase diagrams and the most common are Px^Ix^{II}, Tx^Ix^{II} or/and ternary diagrams with one variable between temperature and pressure kept constant and the another varying.

2.5 REACTIVE SEPARATION PROCESSES

Process intensification has been gaining attention in recent years, since it allows to increase efficiency, product quality and process safety as well as decreases waste, investment and operational costs. Among them, reactive separation processes (RSP) have showed to be an interest alternative to reduce wastes, energy usage and costs besides of increase productivity and selectivity. RSP principle are based on simultaneous separation and reaction, so that separation can be improved by a reaction (e.g. when a contaminant is consumed or to overcome

an azeotrope) and/or reaction can be improved by separation (e.g. achieve higher selectivity, overall reaction rate and conversion above equilibrium). An ideal case occurs when both aspects contribute to increase performance of a unit operation. For instance, RDC, CDC, reactive absorption column (RAC), CAC, reactive extraction column (REC), membrane reactors and centrifugal contact separators are some common RSP that has been investigated in the literature (KISS, 2014).

RDC (or CDC) is the most widely studied RSP as shown from more than 1000 papers and 800 patents for more than 200 reaction systems, where almost 40% were applied for equilibrium-limited reactions. As a result, RDC (or CDC) has an important role for biodiesel industry to carry out esterification and transesterification reactions in order to improve productivity and reduce amount of alcohol required and, consequently, costs and environment impacts. However, some aspects must be attended to RDC to be successfully applicable, such as: a match between reaction and separation temperature, reaction in the liquid phase, moderate heat of reaction to avoid changes in vapor and liquid rates in the reactive section, favorable volatilities and reaction rates (KISS, 2014; LUYBEN; YU, 2008).

2.5.1 Balance on reactive distillation column

RDC is a more complex case of distillation column, so that material, equilibrium, summations and heat (MESH) equations are developed including a reaction term for material and/or energy balance. According to Seader, Henley and Roper (2011), a multi-stage RDC problem from Figure 2.10a–b can be solved to obtain desired outputs from process simulation as using commercial simulators. For this reason, MESH equations for a stage j inside a RDC are given by Equations 2.65 to 2.69,

$$M_{i,j} = L_{j-1}x_{i,j-1} - V_{j+1}y_{i,j+1} + F_j z_{i,j} - \left(L_j + U_j\right)x_{i,j} - \left(V_j + W_j\right)y_{i,j} - R_j = 0 \qquad (2.65)$$

$$E_{i,j} = y_{i,j} - \kappa_{i,j}x_{i,j} = 0 \qquad (2.66)$$

$$\left(S_y\right)_j = \sum_{i=1}^{N_c} y_{i,j} - 1 = 0 \tag{2.67}$$

$$\left(S_x\right)_j = \sum_{i=1}^{N_c} x_{i,j} - 1 = 0 \tag{2.68}$$

$$H_{i,j} = L_{j-1}h_{L,j-1} - V_{j+1}h_{V,j+1} + F_j h_{F,j} - \left(L_j + U_j\right)h_{L,j} - \left(V_j + W_j\right)h_{V,j} - Q_j = 0 \tag{2.69}$$

where $M_{i,j}$, $E_{i,j}$, $\left(S_y\right)$ or $\left(S_x\right)$ and $H_{i,j}$ are material, phase equilibrium, mole fraction summations and heat (energy) equations. Moreover, for stage j and countercurrent cascade on multi-stage RDC from Figure 2.10a–b , F, L and V are total mole flow rate of feed, liquid and vapor streams; h_F, h_L and h_V are feed, liquid and vapor enthalpy; U and W are total mole flow of liquid and vapor side streams. Subscripts i and j are related to component i and stage j. Furthermore, Q_j is the heat removed (+) or added (–) to stage j, while $\kappa_{i,j}$ is the equilibrium ratio given by Equation 2.70.

$$\kappa_{i,j} = \frac{\gamma_{i,j}P_i^{sat}}{P} \tag{2.70}$$

For these results some assumptions were considered for the countercurrent cascade: vapor and liquid at each stage are in phase equilibrium; occlusion of vapor and entrainment of liquid are disregarded. As a consequence, the system of equations are represented by $N(2N_c + 3)$ MESH equations, where N and N_c are total number of stages and components, respectively. In addition, almost always depending from input variables, this system of equations is composed of non-linear equations. As a result, for complex cases an iterative method is applied to solve this problem as using Newton-Raphson or inside-out methods, so that Equations 2.67 and 2.68 are multiplied by V_j and L_j to obtain Equations 2.71 to 2.74. These are combined to 2.75 and 2.76 and added to Equation 2.65 to reduce the system to $N(2N_c + 1)$ equations given by Equations 2.71 to 2.80.

Figure 2.10 – General (a) equilibrium stage and (b) countercurrent cascade on multi-stage RDC

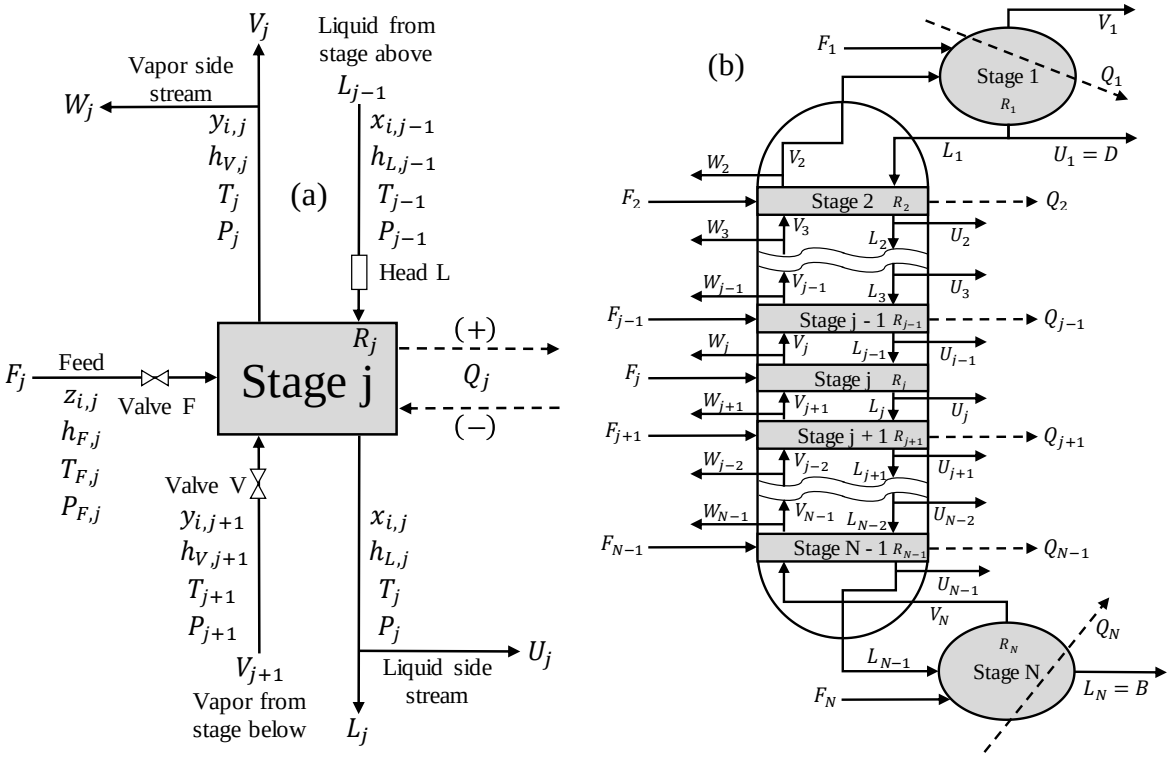

Source: Seader, Henley and Roper (2011).

$$V_j = \sum_{i=1}^{N_c} v_{i,j} \tag{2.71}$$

$$L_j = \sum_{i=1}^{N_c} l_{i,j} \tag{2.72}$$

$$y_{i,j} = \frac{v_{i,j}}{V_j} \tag{2.73}$$

$$x_{i,j} = \frac{l_{i,j}}{L_j} \tag{2.74}$$

$$S_j = \frac{U_j}{L_j} \tag{2.75}$$

$$s_j = \frac{W_j}{V_j} \tag{2.76}$$

$$r_j = \sum_{p=1}^{2} k_{0p}\, exp\left(\frac{-E_{a_p}}{RT_j}\right) \prod_{q=1}^{NRC} C_{j,q}^{m} \tag{2.77}$$

$$M_{i,j} = l_{i,j}(1 + S_j) + v_{i,j}(1 + s_j) - l_{i,j-1} - v_{i,j+1} + f_{i,j} - H_{L,j} \sum_{RX=1}^{NRX} \nu_{i,RX} r_{j,RX} = 0 \tag{2.78}$$

$$E_{i,j} = \kappa_{i,j} l_{i,j} \frac{\sum_{k=1}^{N_c} v_{k,j}}{\sum_{k=1}^{N_c} l_{k,j}} - y_{i,j} = 0 \tag{2.79}$$

$$\begin{aligned} H_{i,j} = {} & h_{L,j}(1 + S_j) \sum_{i=1}^{N_c} l_{i,j} + h_{V,j}(1 + s_j) \sum_{i=1}^{N_c} v_{i,j} - h_{L,j-1} \sum_{i=1}^{N_c} l_{i,j-1} \\ & - h_{V,j+1} \sum_{i=1}^{N_c} v_{i,j+1} - h_{F,j} \sum_{i=1}^{N_c} f_{i,j} - Q_j = 0 \end{aligned} \tag{2.80}$$

For Equations 2.71 to 2.80, f_i, l_i and v_i are component mole flow rate of feed, liquid and vapor streams; S_j and s_j are liquid and vapor dimensionless side stream flows; $H_{L,j}$ is the volumetric liquid holdup on stage j; ν is stoichiometric coefficient; r_j is the reaction rate on stage j; k_0 and E_a are pre-exponential factor and activation energy; C is concentration (molarity) and m is the exponent from C. Moreover, subscripts RX refers to reaction, NRX refers to number of reversible and irreversible reactions, p refers to forward and backward steps with values of 1 and 2, respectively, q refers to component involved in the kinetic expression and NRC refers to number of components in the kinetic expression (SEADER; HENLEY; ROPER, 2011).

Finally, system of equations can be solved using an iterative method programming in softwares elsewhere or using a commercial simulator as Aspen Plus based on Wegstein or Broyden methods. A common approach is to specify N and all $T_{F,j}$, $P_{F,j}$, P_j, S_j, s_j, $f_{i,j}$ and Q_j to solve the system of $N(2N_c + 1)$ non-linear equations. It is worth to mention that more complicated situation is faced when VLLE is considered, so that more equations and specifications are required.

2.6 USE OF REACTIVE SEPARATION PROCESSES FOR BIODIESEL PRODUCTION

Biodiesel production by transesterification and esterification reactions often requires an excess of alcohol above the stoichiometric amount. This excess aims to shift the equilibrium of reactions to higher FAAE yield and shorter reaction time. Alternative processes have been developed to reduce alcohol (solvent) costs and reduce the cost of separation of components that have not been fully converted. In addition, the set of reactor/distillation column has been replaced by a RDC combining chemical reaction and separation in a single operation (SIMASATITKUL et al., 2011; STEINIGEWEG; GMEHLING, 2003).

In this case, high conversions are obtained in the biodiesel production due to continuous removal of products from the reactive zone, which shifts the equilibrium to formation of more products. Therefore, the use of RDC aids to reduce capital and operational costs (lower amount of alcohol and lower energy consumption compared to set of reactor/separator) (HE; SINGH; THOMPSON, 2006). Such advantages have encouraged the development of several studies in this process; however, the most part focuses on isolated transesterification and esterification reactions. In addition, some of these studies were developed by simulation using Aspen® software, so that allows a reliable evaluation of design and operation factors of RDC before its construction (STEINIGEWEG; GMEHLING, 2003).

Among the few studies that showed experimental investigations on RDC applied to the transesterification reaction using short chain alcohols (methanol and ethanol) and long chain TAG, those developed by He, Singh and Thompson (2006), Cerón Sánchez (2010) and Prasertsit, Mueanmas and Tongurai (2013) can be highlighted. Among the studies only carried out by simulation, these from Mueanmas, Prasertsit and Tongurai (2010) and Xiao et al. (2014)

can be highlighted. In these works, basically three possible configurations were observed for the RDC.

One configuration adopts the RDC containing a pre-reactor, where the reaction mixture is kept in contact for a certain time before reaching equilibrium. In this case, the mixture containing vegetable oil, alcohol (fresh and recycled distillate) and alkali catalyst is fed on the top of the column, above the reactive zone, with reflux and top product containing almost pure alcohol and bottom product containing biodiesel and glycerol (HE, SINGH, THOMPSON, 2006; PRASERTSIT; MUEANMAS; TONGURAI, 2013). The second configuration also adopts the vegetable oil stream fed in the top, however, without including both pre-reactor and methanol recycles (SIMASATITKUL et al., 2011). The last configuration considers the alcohol fed in some plate below the reactive zone, not necessarily above the reboiler. In this case, oil is fed above the reactive zone together with the alkali homogeneous catalyst or without the catalyst in the case of a heterogeneous catalysis (packing) (BOON-ANUWAT et al., 2015; PÉREZ-CISNEROS et al., 2016; SILVA, 2013; SOUZA et al., 2014; XIAO et al., 2014).

Regarding to esterification reaction, experimental studies from RDC were reported by Steinigeweg and Gmehling (2003). Among the studies only carried out by simulation, the works of Omota, Dimian and Bliek (2003a; b), Dimian et al. (2009), Gómez-Castro (2010; 2011), Cossio-Vargas et al. (2011), Machado et al. (2011) and Banchero, Kusumaningtyas and Gozzelino (2014) are highlighted. In the older works, more complex configurations were observed including other unit operations in the purification step after reactive distillation.

Steinigeweg and Gmehling (2003) studied RDC in the esterification of decanoic acid with methanol in the presence of catalyst (ion exchange resin). The mixture was initially fed to a pre-reactor as for the transesterification process. Water was distilled and withdrawn as a top product making it easy to obtain the products in the bottom. The authors concluded that an excellent countercurrent flow of the reactants in the reaction zone is more important than the presence of a pre-reactor, so that there were not great advantages in using it. Omota, Dimian and Bliek (2003a,b) proposed another configuration, where alcohol was fed on the bottom with the heterogeneous catalyst distributed as a packing inside a CDC.

Noshadi, Amin and Parnas (2012) carried out an innovative experimental study applied to a RDC using a heterogeneous solid acid catalyst (HSAC), the heteropolyacid $H_3PW_{12}O_{40}.6H2O$ (12-tungstophosphoric acid), to carry out esterification and transesterification reactions simultaneously. A mixer/preheater/prereactor was initially used to

convert the mixture prior to be fed on top of nine-stage column. The researchers used WCO (3.725% FFA and 1% water) and methanol in the experiments. In addition, they employed the RSM based on a CCD. The parameters studied were total feed flow, feed temperature, reboiler duty and MR of methanol to oil. Optimum column operational conditions were found obtaining maximum conversion of 94%. Each experiment was carried out at 12 h to ensure equilibrium, although experiment 1 required only 4 h.

2.7 DESIGN AND FEASIBILITY OF BIODIESEL PRODUCTION PROCESSES

Among the studies of design and feasibility of biodiesel production processes from raw materials with high FFA content, the works of Zhang et al. (2003a; b), West, Posarac and Ellis (2008), Lee, Posarac and Ellis (2011), Albuquerque, Danielski and Stragevitch (2016) and Gaurav, Ng and Rempel (2016) are highlighted.

Zhang et al. (2003a, b) used Aspen Hysys software to design and study the technical and economic feasibility of four biodiesel production processes, in which three involved WCO. All the processes proved to be technically feasible for production of high quality biodiesel (99.65 wt%) and glycerin (85 wt%). On the other hand, the processes were not economically feasible based on the economic indicators studied, mainly due to the negative value of the return of investment (ROI) obtained. The homogeneous acid-catalyzed processes using H_2SO_4 that carried out the simultaneous transesterification and esterification reactions with (ROI = –21.5%) and without (ROI = –15.6%) hexane obtained a better economic performance compared to conventional process (ROI = –51.2%). However, the kinetic of acid-catalyzed transesterification reaction is slow and all reactions were simulated in stoichiometric reactors based on specified conversion (RSTOIC from Aspen Plus).

In order to investigate more economical feasible biodiesel production processes, West, Posarac and Ellis (2008) designed and studied the techno-economic feasibility of two processes in relation to conventional and acid-catalyzed processes proposed by Zhang et al. (2003a). All four processes were technically feasible for the production of high quality biodiesel (99.65 wt%) and glycerol (98 wt%). However, the process based on solid acid-catalyzed (SAC) transesterification using SnO as catalyst showed much higher economic feasibility (ROI = 58.8%). This process required less piece of equipment and lower operation costs, since the

catalyst carried out the simultaneous reactions (no pretreatment step) and required a smaller amount of methanol in the reactor (MR of methanol to oil of 4.5). In addition, SAC process did not need water washing after transesterification and produced a purer glycerol using less energy.

Lee, Posarac and Ellis (2011) designed and studied the simulation and economic feasibility of biodiesel production process under supercritical conditions relative to conventional process applied to FFA and edible oils. All of these processes have already been demonstrated to be technically feasible by Zhang et al. (2003a, b) and West, Posarac and Ellis (2008). However, Lee, Posarac and Ellis (2011) considered a plant capacity five times higher than those studied by the aforementioned authors and conducted the economic feasibility study using the Aspen In-Plant Cost Estimator module of Aspen® software. In addition, in order to improve the reliability of the results, they inserted the boiling temperature of triolein obtained experimentally by thermogravimetric analysis. The supercritical process required a plug-flow reactor (PFR) and obtained better economic results in comparison to the other two processes due to its lower operating cost offsets its high investment cost.

Albuquerque, Danielski and Stragevitch (2016) designed and studied the techno-economic feasibility of an alternative process of biodiesel production from ROF. Liquid-liquid extraction (LLEx) was used to separate FFA from TAG with methanol as solvent. More reliable thermophysical properties of fatty compounds, kinetic data and a rigorous thermodynamic modeling were used in the simulations. Both processes proved to be technically feasible based on a 99.65 wt% of ester as product specification. The alternative process proved to be slightly more economically feasible than the conventional one based on the selected economic indicators and therefore a promising alternative for biodiesel production from ROF.

Gaurav, Ng and Rempel (2016) investigated the SAC process from yellow grease by Aspen Plus simulations with $HWSi/Al_2O_3$ as catalyst. They compared a base case with a set of plug-flow reactor (PFR)/distillation column to an alternative process with a CDC. Greenhouse gas emissions, investment and energy costs decreased using a CDC, so that the alternative process showed to be more economical and environmental feasible than the base case. However, CDC process was not optimized and the same MR was adopted for both processes.

Some studies on the design and feasibility of biodiesel production processes using low levels of FFA in oils (below 0.5%), which does not require pretreatment, can be found in the literature. Among these, studies employing RDC that reduces investment and operation costs (lower cost with alcohol and energy to carry out the reaction) can be highlighted. Souza et al.

(2014) simulated and evaluated the economic performance of a batch biodiesel production plant located in Caetés, Pernambuco. The results obtained in the simulation agreed with the obtained ones from a real plant using cotton oil, methanol and NaOH catalyst. In this case, the authors proposed a continuous process using a RDC and proved to be more economic feasible than the conventional process.

Boon-anuwat et al. (2015) designed two biodiesel production processes from edible oils by homogeneous (NaOH) and heterogeneous (MgO) catalysis. Each process was designed for the case of a set of reactor/distillation column and a RDC (or CDC) totalizing four processes. The process by CDC with heterogeneous catalysts showed advantages over processes with homogeneous catalysis, since there was no need for water washing and biodiesel purification.

As a consequence, a combination of SAC process with a RDC as a CDC with catalyst inside packing has shown to be promising, since can improve economic and environment indicators as well as biodiesel yield and quality (GAURAV; NG; REMPEL, 2016). For these reasons, additional investigations from SAC process using CDC and/or other RSP deserve attention, in order to obtain more technical, economical and eco-friendly processes of biodiesel production from raw materials with high FFA content.

3 OPTIMIZATION OF THE EXTRACTION OF FREE FATTY ACIDS AND TECHNO-ECONOMIC ASSESSMENT OF BIODIESEL PRODUCTION BY REACTIVE DISTILLATION[1]

Allan A. Albuquerque, Cláudia J. S. Cavalcanti, Cícero H. M. Soares, Maria Fernanda Pimentel, Luiz Stragevitch[2]
Fuel Laboratory, Chemical Engineering Department, Federal University of Pernambuco
Av. Prof. Artur de Sá S/N, CEP 50740-521, Recife, PE, Brazil
Phone/fax: +55 81 21267235; E-mail: luiz@ufpe.br

Published in Brazilian Journal of Chemical Engineering: October 02, 2018.

Topic: CBTermo 2015

ABSTRACT

The liquid-liquid extraction of free fatty acids (FFA) from residual oils and fats for biodiesel production, employing methanol as the solvent, has been optimized using process simulation and response surface methodology. The parameters investigated were temperature, number of stages and solvent-to-feed ratio (S/F). Responses evaluated were FFA mass fraction in the oil-rich phase ($w_{\mathrm{FFA}}^{\mathrm{B}}$) and total cost, using yellow and brown greases as the raw materials. Quadratic and linear models were fitted for $w_{\mathrm{FFA}}^{\mathrm{B}}$ and cost responses, respectively. The optimal conditions satisfying technical ($w_{\mathrm{FFA}}^{\mathrm{B}} \leq 0.5\%$) and economic (minimum cost, including capital and operation costs, except for raw material cost) criteria were 321 K, 6 stages, $S/F = 1.27$, $w_{\mathrm{FFA}}^{\mathrm{B}} = 0.41\%$, cost = \$84.93/ton (yellow grease), and 318 K, 6 stages, $S/F = 1.32$, $w_{\mathrm{FFA}}^{\mathrm{B}} = 0.49\%$, cost = \$102.89/ton (brown grease). Furthermore, an alternative process (process B) for biodiesel production from ROF based on reactive distillation column (RDC) was investigated and compared to a base case (process A) using a set of reactor/distillation column at transesterification unit. These processes were designed, sized and evaluated related to techno-economic feasibility. Both processes showed to be technical feasible; however, each one presented advantages and disadvantages for some economic indicators as total capital cost, total operation, total annualized cost, income, net annual profit after taxes, break-even price, payback period and return of investment. As a result, both processes demonstrated to be comparable economically. Related to environment impacts, process A presented lower net Carbon fee/tax, while process B showed lower waste treatment costs. Therefore, optimal process can be chosen based on the more onerous environment indicator expected for the future.

Keywords: Biodiesel. Free fatty acids (FFA). Liquid-liquid extraction (LLEx). Reactive distillation column (RDC). Residual oils and fats (ROF). Response surface methodology.

[1] This is an extended version of the manuscript "Optimization of the extraction of free fatty acids applied to biodiesel production" published at *Brazilian Journal of Chemical Engineering* (*BJCE*) and presented at the *VIII Brazilian Congress of Applied Thermodynamics – CBTermo 2015*, Aracaju, Brazil.

[2] Corresponding author.

3.1 INTRODUCTION

Biodiesel production is usually carried out through a transesterification reaction, which consists of a chemical reaction of a vegetable oil, animal fat or residual oil and fat (ROF) with a short chain alcohol (methanol or ethanol) in the presence of a catalyst (Van Gerpen, 2005; Gnanaprakasam et al., 2013). Refined vegetable oils are largely employed as raw materials in the biodiesel industry; they can represent up to 85% of biodiesel costs. Thus, less costly raw materials, such as ROF, have been gaining more attention (AVHAD; MARCHETTI, 2015; CANAKCI; SANLI, 2008).

ROF can be 40% to 70% cheaper than refined vegetable oils (CAI et al., 2015; REFAAT, 2010). In addition, environmental and economic issues related to the improper disposal of ROF are a concern. Further, sewage treatment plants are subjected to increasing costs to treat ROF (IASMIN et al., 2014; ORTNER et al., 2016). Among ROFs, waste frying oils are derived from various vegetable oils, such as sunflower, corn, and especially soybean oil (JORGE et al., 2005; TSOUTSOS et al., 2016). ROFs such as from waste frying oils and animal fat wastes have high levels of free fatty acids (FFA) (GNANAPRAKASAM et al., 2013). ROFs can be generally found as yellow or brown greases depending on whether the FFA content is between 5% and 15% (yellow) or above 15% (brown) (ADEWALE; DUMONT; NGADI, 2015; AVHAD; MARCHETTI, 2015; CANAKCI; SANLI, 2008).

High FFA levels in the raw material cause operational drawbacks in the achievement of high biodiesel yields, mainly due to the occurrence of competitive reactions of FFA saponification and triacylglycerol (TAG) hydrolysis (GNANAPRAKASAM et al., 2013). To increase the production yield, ROF is usually subjected to an initial pretreatment step with an acid-catalyzed esterification reaction; then, the resulting stream undergoes an alkali-catalyzed transesterification step, which is known as the conventional process (CANAKCI; VAN GERPEN, 2001). The acid-catalyzed pretreatment step increases capital and operation costs since it requires additional equipment and a glycerol washing stage (ZHANG et al., 2003).

On the other hand, alternative processes employing the FFA separation from the oil have proven to be economically more attractive (ALBUQUERQUE; DANIELSKI; STRAGEVITCH, 2016). FFA separation is widely used in the food industry to produce edible oils. FFA separation can be carried out by liquid-liquid extraction (LLEx) using a short-chain alcohol as the solvent, making it a potentially interesting process for the biodiesel industry

(BHOSLE; SUBRAMANIAN, 2005; RODRIGUES et al., 2007; VAISALI et al., 2015). Despite this, studies using LLEx to separate FFA, including cost estimates, have not been found in the literature, except in the refining of edible oils with ethanol and ethanol/water mixtures as solvents (BATISTA; ANTONIASSI; WOLF MACIEL, 2002; BATISTA; WOLF MACIEL; MEIRELLES, 1999; PINA; MEIRELLES, 2000). Because the biodiesel industry predominantly uses methanol as the reaction agent, development of a LLEx process to separate FFA with methanol as the solvent may be of interest to the industry.

Among other processes, reactive distillation column (RDC) has been shown to be one of the most economic feasible operation for biodiesel production since just one equipment is used instead of a set of reactor/distillation column. For that reason, capital cost is decreased (SUNDMACHER; KIENLE, 2003). Furthermore, less alcohol is fed in the RDC because of the higher molar ratio (MR) of alcohol to ROF (or TAG or FFA) inside the stages generated from the reflux rate (HE; SINGH; THOMPSON, 2005; 2006). Consequently, lower operation cost is also obtained (SOUZA et al., 2014). However, not always a process using RDC can be more economical than a conventional process, mainly if there is a temperature mismatch between reaction and separation. Other reasons can be unfavorable volatilities, slow reaction rates, limitation to liquid-phase reactions inside stages of RDC and other restrictions (LUYBEN; YU, 2008). Therefore, both conventional and alternative processes need to be designed and compared to have certainty what it is more economical.

In this work, the LLEx of FFA from ROF employing methanol as the solvent was optimized using response surface methodology (RSM) and Aspen Plus for process simulation. The parameters investigated were temperature (T), number of stages (N) and solvent to feed ratio (S/F). The FFA mass fraction (solvent free basis) in the oil-rich phase ($w_{\mathrm{FFA}}^{\mathrm{B}}$) and the total cost were the responses evaluated. The study goals were: to attain $w_{\mathrm{FFA}}^{\mathrm{B}}$ values below the recommended FFA concentration in TAG (a mass fraction of 0.5%) for the alkali-catalyzed transesterification step; and to attain technical and economic feasibility of the process with a minimum total cost (MA; HANNA, 1999). Moreover, an alternative process based on RDC applied to transesterification reaction was compared to a base case using a set of reactor/distillation column and a LLEx column for FFA separation from ROF.

3.2 METHODOLOGY

3.2.1 Thermophysical properties prediction and thermodynamic modeling

Thermophysical properties for ROF were predicted by Constituent Fragments (CF) and Extended Constituent Fragments (ECF) approaches from Section 2.2 (CRUZ-FORERO; GONZÁLEZ-RUIZ; LÓPEZ-GIRALDO, 2012; ZONG; RAMANATHAN; CHEN, 2009). Subsequently, a rigorous thermodynamic modeling applied to vegetable oil/FFA/methanol systems was carried out to represent the liquid-liquid equilibrium (LLE) in the LLEx column. The Non-Random Two-Liquid (NRTL) model was used (RENON; PRAUSNITZ, 1968).

Experimental LLE data from Batista et al. (1999a), Mohsen-Nia and Dargahi (2007), Liu et al. (2008) and Mohsen-Nia and Khodayari (2008) were used to estimate the NRTL binary interaction parameters to be used in the process simulation. The NRTL parameters were estimated by minimization of the objective function given by Equation 3.1,

$$F = \sum_{i=1}^{N_{c,k}} \sum_{j=1}^{N_{t,k}} \sum_{k=1}^{N_D} \sum_{l=1}^{2} \left(w_{ijk}^{(l),\mathrm{exp}} - w_{ijk}^{(l),\mathrm{cal}} \right)^2 \tag{3.1}$$

where w is the phase composition (mass fraction); exp and cal denote experimental and calculated compositions; $N_{c,k}$ and $N_{t,k}$ are the number of components and tie lines in the k-th data set; N_D is the number of data sets simultaneously correlated; subscripts i, j and k denote components, tie lines and data sets; and superscript l denotes phases in equilibrium (STRAGEVITCH; D'AVILA, 1997). Experimental and calculated compositions involved in LLE systems were compared using the root mean square deviation (RMSD), according to

$$\Delta w = 100 \times \sqrt{\frac{1}{2N_t N_c} \sum_{i=1}^{N_c} \sum_{j=1}^{N_t} \sum_{l=1}^{2} \left(w_{ij}^{(l),\mathrm{exp}} - w_{ij}^{(l),\mathrm{cal}} \right)^2} \tag{3.2}$$

for each data set as well as a global deviation involving all correlated data sets.

3.2.2 Optimization of LLEx column

Aspen Plus was used in the process simulation. The ROF composition used in the simulations was defined based on a mixture of the vegetable oils found in the vegetable oil/FFA/methanol LLE systems available (BATISTA et al., 1999; LIU et al., 2008; MOHSEN-NIA; DARGAHI, 2007; MOHSEN-NIA; KHODAYARI, 2008).

Figure 3.1 illustrates the LLEx column, which was operated at constant pressure (101.3 kPa) and was fed at the top stage with 1050 kg/h of ROF, while the methanol (M) (solvent) was fed at the bottom stage. Two cases were studied to evaluate the FFA/ROF separation from a wide range of FFA content. For case 1, a ROF composed of 10% FFA was adopted; while for case 2, a ROF with 20% of FFA was used. In both cases the remaining content was the TAG. Cases 1 and 2 are representative of common ROFs found, known as yellow and brown greases, respectively (CANAKCI; SANLI, 2008; MOHITE et al., 2015).

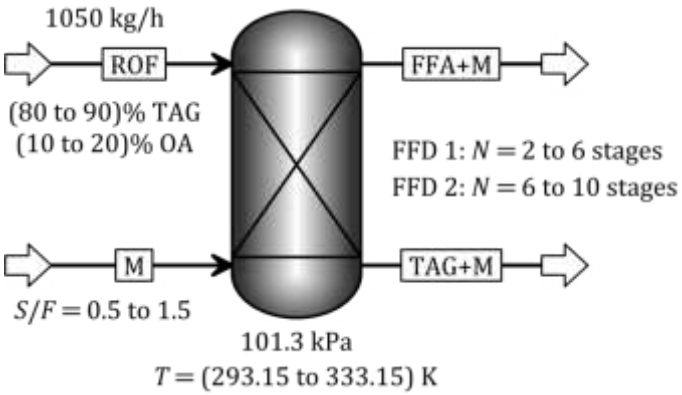

Figure 3.1 – Flowsheet of FFA separation from ROF using a LLEx column

3.2.3 Full Factorial Design and Response Surface Methodology

In order to optimize the FFA separation from ROF using a LLEx process, initially a 2^3 full factorial design (FFD) including a central point was carried out. The parameters investigated were T, N and S/F as presented in Table 3.1 and in Figure 3.1, where FFD 1 (design 1) and FFD 2 (design 2) differ only in the levels used for N. The levels for N and S/F were chosen based on the process simulation of an alternative process to produce biodiesel applying FFA separation from ROF by LLEx, while temperature levels were defined by the

temperature range from the available LLE data (ALBUQUERQUE; DANIELSKI; STRAGEVITCH, 2016).

The FFA mass fraction (solvent free basis) in the oil-rich phase ($w_{\mathrm{FFA}}^{\mathrm{B}}$), found at the bottom output stream of the extraction column, and the total cost involved in the first year of the LLEx column operation, were the responses evaluated. The goal was to achieve the design and operational conditions that simultaneously satisfied the recommended specification of $w_{\mathrm{FFA}}^{\mathrm{B}} \leq 0.5\%$ and minimum total cost in the first year of operation. The latter took into account capital and operation costs.

Capital costs included the LLEx column and heaters or coolers (purchase cost) adopting the preliminary Chemical Engineering's Plant Cost Index (CEPCI) of 537.7 (December, 2015). In this study, the LLEx column was designed as a rotating disk contactor. This type was chosen following selection schemes for extractors based on heuristics from commercial extractors (SEADER; HENLEY; ROPER, 2011). The extractor diameter and height were calculated based on Seider, Seader and Lewin (2009) and Seader, Henley and Roper (2011). Following the former authors, the heat exchangers were designed as a double-tube type (area less than 150 ft^2) or shell and tube type (area greater than 150 ft^2) (SEIDER; SEADER; LEWIN, 2009). A detailed description of the design procedure can be found in Albuquerque, Danielski and Stragevitch (2016).

Operation costs included utility costs (vapor or water in heat exchangers) and solvent (methanol) cost and were calculated as presented by Albuquerque, Danielski and Stragevitch (2016). The methanol cost was calculated multiplying the price of methanol ($0.85/kg) by the methanol mass flow rate fed plus a factor to account for the solvent make-up, 7.4% and 8.5% for cases 1 and 2, respectively (ALBUQUERQUE; DANIELSKI; STRAGEVITCH, 2016). The raw material (ROF) cost was not included in the operation costs to avoid masking since it is significantly higher than the capital and other operation costs. Nonetheless, it is constant for a constant flow rate of ROF, as used in this work, thus, not affecting the conclusions obtained.

After the results of the 2^3 design were evaluated, new computational experiments, using a central composite design (CCD), were carried out to estimate the coefficients of a quadratic model. Statistica Ultimate Academic software was employed in all calculations.

Table 3.1 – Factors and levels of factorial design

	FFD 1 (design 1)			FFD 2 (design 2)		
	Level			Level		
Factor	–	0	+	–	0	+
Temperature, T/K	293.15	313.15	333.15	293.15	313.15	333.15
Number of stages, N	2	4	6	6	8	10
Methanol to oil mass ratio, S/F	0.5	1	1.5	0.5	1	1.5

3.2.4 Design and techno-economic assessment

After optimization of LLEx column, an alternative process based on RDC for transesterification reaction was designed and compared to base case process using a set of reactor/distillation column. In this comparison, the optimal design for LLEx from case 2 was considered since 20% of FFA was adopted. Both processes were designed to achieve standard from National Agency of Petroleum, Natural Gas and Biofuels (ANP) for biodiesel as shown in Table 3.2 as well as pharmaceutical glycerol purity (99.5%) (ANP, 2014).

Table 3.2 – Biodiesel specifications from ANP standard

Minimum ester (% mass)	Maximum ($mg \cdot kg^{-1}$)	Maximum (% mass)		
	Water	Total/free Glycerol	Methanol	FFA/TAG/DAG/MAG
96.5	200	0.25/0.02	0.20	0.25/0.20/0.20/0.70

Source: Adapted from ANP (2014).

For the base case, denominated process A, the same kinetic models from our previous work were adopted as shown in Sections 2.1.4.2 and 2.1.5.2 (UNNITHAN; TIWARI, 1987; VICENTE et al., 2005). Furthermore, the kinetic model for esterification was also used to reactor from alternative process, denominated process B, based on RDC at transesterification unit. However, the kinetic model proposed by Mueanmas, Prasertsit and Tongurai (2010) from Section 2.1.4.2 was used in order to take in account the continuous separation of products and the high liquid hold up inside the stages of RDC caused by the high reflux ratio (RR).

Related to economic feasibility both processes were compared using the Economic Evaluation tool from Aspen Plus. As a result some economic indicators were adopted such as: total capital cost (C_{TC}), operation cost (C_{oper}), total annualized cost (TAC), income, net annual

profit after taxes (A_{NNP}), break-even price (BEP), payback period (PBP) and return of investment (ROI) (ALBUQUERQUE; DANIELSKI; STRAGEVITCH, 2016; SEIDER; SEADER; LEWIN, 2009). For all calculations, some values of parameters were kept constants, such as: an operation year of 8,766 h, an operating life of plant of 30 years, a length of plant start-up of 4 months and starting the basic engineering in March 12th, 2018. Furthermore, some environment indicators were compared as waste stream cost (C_{waste}) and carbon emission fees (C_{CO_2}). C_{CO_2} were calculated based on method proposed by United States Environment Protection Agency (EPA), in order to evaluate more environment friendly conditions (EPA, 2009).

3.3 RESULTS AND DISCUSSION

3.3.1Thermophysical properties prediction and thermodynamic modeling

Trilinolein (LLL) was adopted as the representative TAG of ROF in the process simulations. LLL was chosen based on the FFA compositions of the vegetable oils found in the oil/FFA/methanol LLE systems used, which indicated linoleic acid as the most abundant fragment (BATISTA et al., 1999; LIU et al., 2008; MOHSEN-NIA; DARGAHI, 2007; MOHSEN-NIA; KHODAYARI, 2008). Furthermore, LLL was also the most important TAG composed of homogeneous fragments. Use of a TAG composed of only one carbon chain simplifies the transesterification reaction modeling since only one diacylglycerol and one monoacylglycerol need to be used. The TAG composition of the ROF used is shown in Table 3.3, and was calculated from the FFA composition of a mixture of canola, corn, sunflower and jatropha curcas oils present in the LLE data available. The methodology proposed by Antoniosi Filho, Mendes and Lanças (1995) was used. Only the main FFAs (palmitic 11.7%, stearic 3.2%, oleic 33.3%, linoleic 48.3% and linolenic 3.5% wt) were used to calculate the TAG composition, since they represented 98.7% of the FFA composition of canola oil, 98.2% of corn oil, 99.7% sunflower oil and 99.4% of jatropha curcas oil (ANTONIOSI FILHO; MENDES; LANÇAS, 1995).

Table 3.3 – TAG composition of the ROF used

TAG name			
Shorthand [a]	Abbreviation [b]	M/(g/mol) [c]	w/% [d]
48:0	PPP	807.339	0.1
50:0	SPP	835.393	0.1
50:1	POP	833.377	1.3
50:2	PLP	831.361	1.9
50:3	PLnP	829.345	0.1
52:1	SOP	861.431	0.7
52:2	POO	859.415	4.9
52:3	PLO	857.399	11.2
52:4	PLL	855.383	8.8
52:5	PLnL	853.367	1.2
54:1	SOS	889.485	0.1
54:2	SOO	887.469	1.2
54:3	OOO	885.453	6.9
54:4	OLO	883.437	18.8
54:5	OLL	881.421	25.1
54:6	LLL	879.405	14.8
54:7	LLnL	877.389	2.6
54:8	LLnLn	875.373	0.2
		Overall:	100.0

[a] The two numbers separated by a colon stand for the chain length and number of double bonds;
[b] Abbreviation for trivial names of TAG chains: P = palmitic, S = stearic, O = oleic, L = linoleic, Ln = linolenic;
[c] Molar mass;
[d] Mass fraction.

A number of thermophysical properties were predicted for the ROF, for example: enthalpy of vaporization at 298.15 K (166 kJ/mol), vapor pressure, liquid heat capacity, density and viscosity. Density and viscosity were estimated by the CF method, while the others were estimated by the ECF method. The results were compared to several vegetable oils for which the properties measured are reported in the literature, as shown in Figure 3.2 (CERIANI et al., 2008; MORAD et al., 2000; NOUREDDINI; TEOH; CLEMENTS, 1992; PERRY; WEBER; DAUBERT, 1949). Differences were encountered since the oils are different; Figure 3.2 shows that the predicted values for the ROF used, however, were consistent with common oils.

LLE data reported in the literature were employed to carry out the thermodynamic modeling. The systems used were: canola oil (CnO)/oleic acid (OA)/methanol (M) at 293.15 K and 303.15 K; jatropha curcas oil (JO)/OA/M at 303.1, 313.1, 323.1 and 333.1 K; corn oil (CO)/OA/M at 303.15 K and 313.15 K and sunflower oil (SuO)/OA/M at 303.15 K and 313.15 K (BATISTA et al., 1999; LIU et al., 2008; MOHSEN-NIA; DARGAHI, 2007; MOHSEN-

NIA; KHODAYARI, 2008). The NRTL interaction parameters obtained are shown in Table 3.4. Table 3.5 shows the RMSD obtained using the NRTL model. Agreement between experimental and calculated LLE was satisfactory to develop a reliable simulation of the extraction process. A comparison of experimental and calculated LLE data using the NRTL model is shown in Figure 3.3 for some selected systems for each oil at different temperatures.

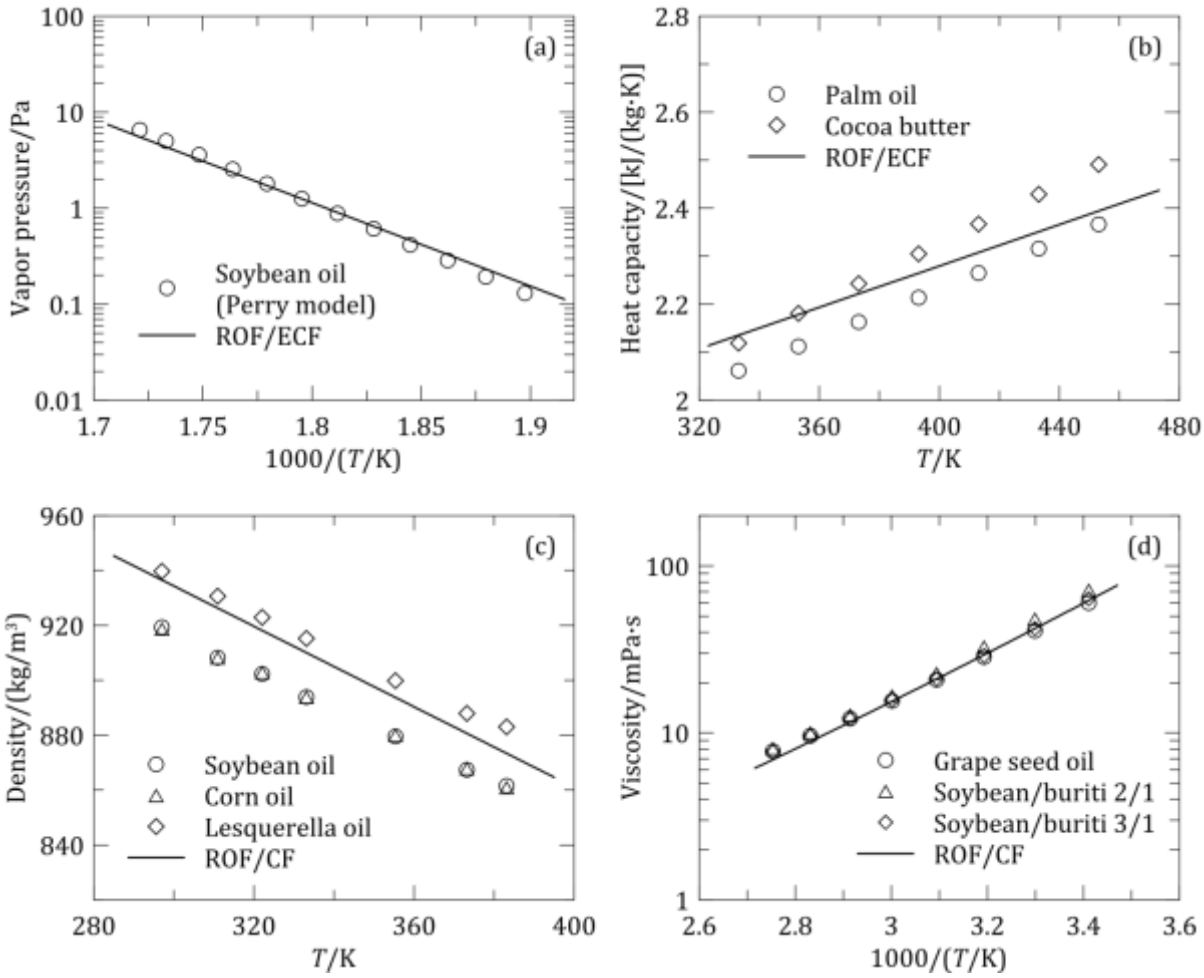

Figure 3.2 – Thermophysical properties for some vegetable oils (experimental) and estimated for ROF
Source: Ceriani et al. (2008), Morad et al. (2000), Noureddini, Teoh and Clements (1992) and Perry, Weber and Daubert (1949).

Table 3.4 – NRTL binary interaction parameters for ROF (1)/OA (2)/M (3) system [a,b]

Pair	$A_{ij}^{(0)}$/K	$A_{ji}^{(0)}$/K	$A_{ij}^{(1)}$	$A_{ji}^{(1)}$	$\alpha_{ij} = \alpha_{ji}$
12	438.71	–4592.83	–1.2224	14.495	0.47
13	2619.72	931.84	–9.3260	5.0573	0.2764
23	1478.22	–6632.54	–6.2877	25.036	0.4408

[a] ROF was represented by trilinolein (LLL) in LLE regression and in the simulation.
[b] NRTL model with temperature dependent parameters as $A_{ij} = A_{ij}^{(0)} + A_{ij}^{(1)}T$

Table 3.5 – RMSD obtained in the LLE correlation with NRTL

System	T/K	Δw/%
Canola oil (CnO)/oleic acid (OA)/methanol (M)	293.15	0.81
Canola oil (CnO)/oleic acid (OA)/methanol (M)	303.15	0.73
Corn oil (CO)/oleic acid (OA)/methanol (M)	303.15	0.98
Corn oil (CO)/oleic acid (OA)/methanol (M)	313.15	0.77
Sunflower oil (SuO)/oleic acid (OA)/methanol (M)	303.15	1.49
Sunflower oil (SuO)/oleic acid (OA)/methanol (M)	313.15	0.90
Jatropha curcas oil (JO)/oleic acid (OA)/methanol (M)	303.10	0.42
Jatropha curcas oil (JO)/oleic acid (OA)/methanol (M)	313.10	0.67
Jatropha curcas oil (JO)/oleic acid (OA)/methanol (M)	323.10	1.03
Jatropha curcas oil (JO)/oleic acid (OA)/methanol (M)	333.10	0.40
Overall		0.90

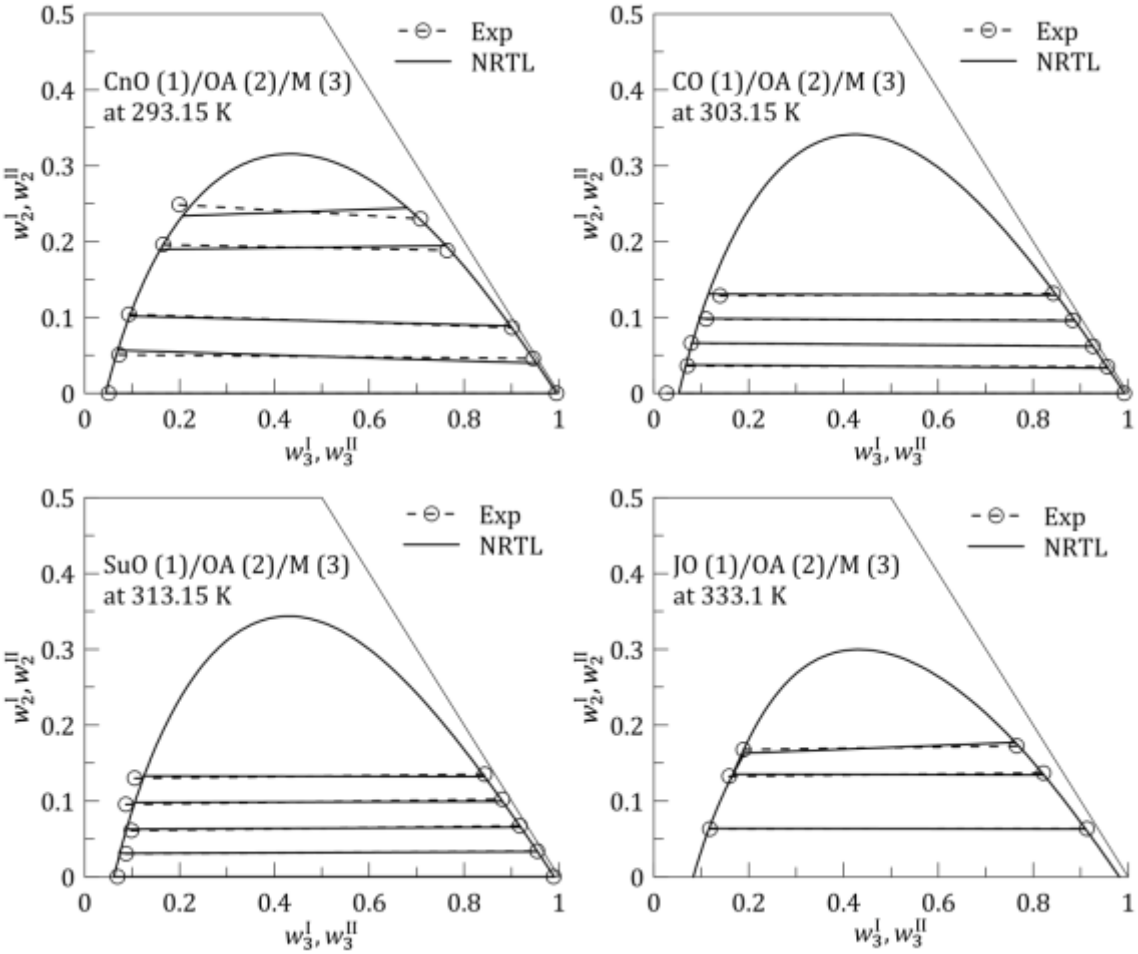

Figure 3.3 – Experimental and calculated LLE data
Source: Batista et al. (1999), Liu et al. (2008), Mohsen-Nia and Dargahi (2007) and Mohsen-Nia and Khodayari (2008).

3.3.2 Optimization of the liquid-liquid extraction process

Table 3.6 shows the values of the two responses evaluated for the 2^3 factorial designs, including a central point (lines 1-9 in Table 3.6). A test on the $w_{\mathrm{FFA}}^{\mathrm{B}}$ response showed a significant curvature, suggesting that a quadratic model may be more appropriate, for both cases 1 and 2. Therefore, extra computational experiments were carried out to complete a central composite design (CCD) (lines 10-15 in Table 3.6). A CCD with $\beta = 1$ was used due to the impossibility of using larger β values since N is an integer variable.

The coefficients of a quadratic model were then estimated. The significance of the coefficients was evaluated using normal probability plots (Figure 3.4) (BRUNS; SCARMINIO; BARROS NETO, 2006). Based on these results, the quadratic coefficient of N and all the interaction coefficients did not significantly affect the $w_{\mathrm{FFA}}^{\mathrm{B}}$ response for case 1 (Figure 3.4a). For case 2, Figure 3.4b shows that the interaction T by N (1L by 2L) and the linear coefficient of T [T(L)] were not significant in the range studied. For the total cost response, Figure 3.4c and 3.4d clearly show that only the linear coefficient of S/F [S/F(L)] was significant.

Table 3.6 – Values of $w_{\mathrm{FFA}}^{\mathrm{B}}$ and total cost responses obtained for FFD 1 and CCD 1

				Case 1		Case 2	
Run	T	N[a]	S/F	$w_{\mathrm{FFA}}^{\mathrm{B}}$/%	Cost/($/yr)	$w_{\mathrm{FFA}}^{\mathrm{B}}$/%	Cost/($/yr)
1	–	–	–	7.26	294,743	13.35	335,828
2	+	–	–	6.45	296,133	14.03	337,212
3	–	+	–	6.73	299,077	10.72	340,197
4	+	+	–	5.76	300,580	12.77	341,685
5	–	–	+	3.86	866,390	5.92	989,597
6	+	–	+	2.25	870,427	4.48	993,630
7	–	+	+	1.85	872,569	1.84	995,808
8	+	+	+	0.29	876,823	0.39	1,000,052
9	0	0	0	2.10	585,372	3.63	667,544
10	–	0	0	4.02	583,343	5.22	665,507
11	0	–	0	3.63	585,373	7.21	667,544
12	0	0	–	5.87	298,222	11.57	339,332
13	+	0	0	2.09	586,166	4.15	668,320
14	0	+	0	1.41	585,372	2.03	667,544
15	0	0	+	0.69	872,359	1.10	995,592

[a] N is relative to FFD 1: levels (–), (0) and (+) correspond to 2, 4 and 6 stages, respectively.

A quadratic model for $w_{\mathrm{FFA}}^{\mathrm{B}}$ and a linear model for total cost responses were appropriately fitted. Table 3.7 shows the models obtained for FFD 1, the coefficient of determination (R^2) and the residual mean square (MS_r) values. The predicted results were also compared to the observed ones, as shown in Figure 3.5 for $w_{\mathrm{FFA}}^{\mathrm{B}}$ and total cost responses for each case. Satisfactory agreement between predicted and observed results was obtained.

Equation 3.3 gives a linear relationship of the response $w_{\mathrm{FFA}}^{\mathrm{B}}$ with N for case 1. Since the slope is less than zero, the maximum value for the N level ($N = 6$ stages) can be adopted. For case 2, although there are additional effects of N according to Equation 3.5, minimum $w_{\mathrm{FFA}}^{\mathrm{B}}$ is also found for $N = 6$. The contour plots for $w_{\mathrm{FFA}}^{\mathrm{B}}$, using $N = 6$, are shown in Figure 3.6. Optimum temperature agreed to avoid too high or low value since can decrease solubility curve or increase mixture viscosity, respectively.

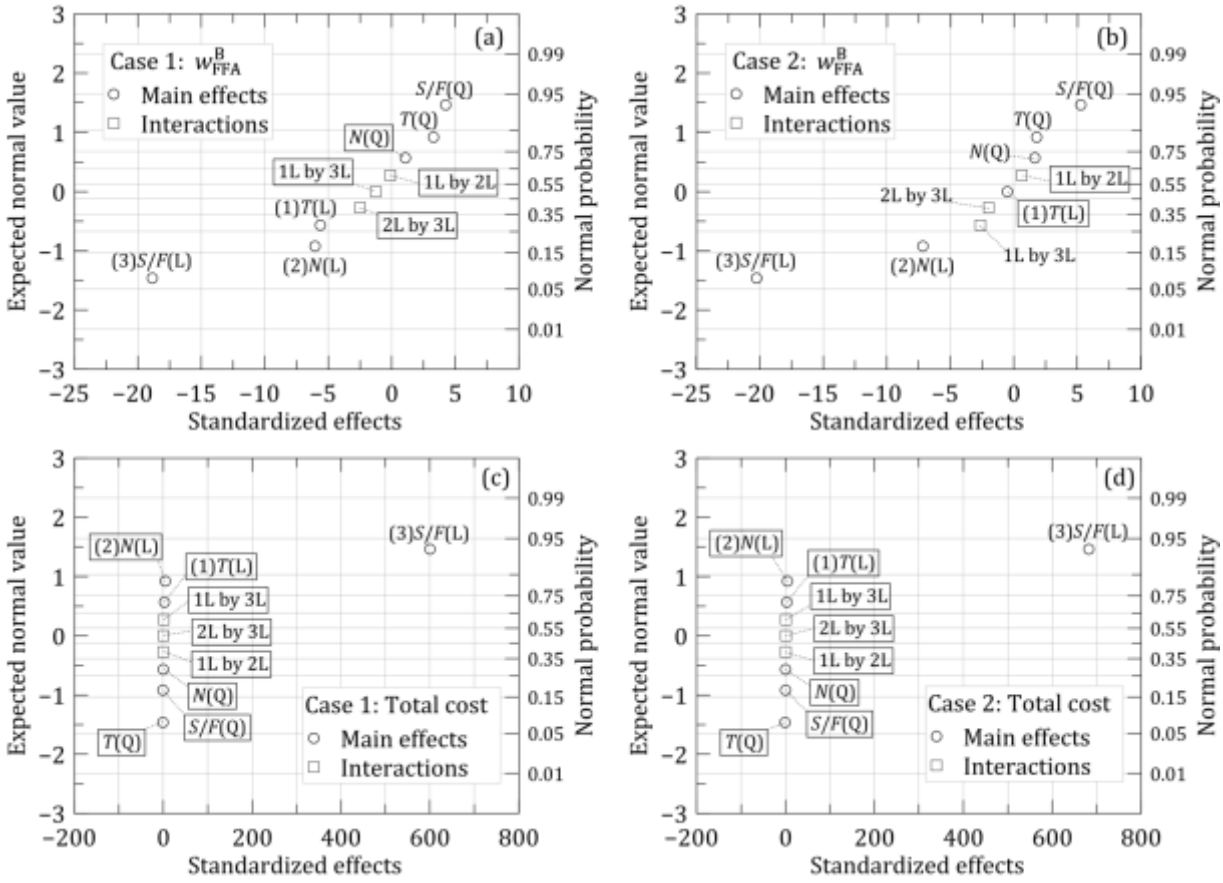

Figure 3.4 – Normal probability plots for FFD 1 (negligible effects are enclosed in borders)

Table 3.7 – Fitted models for FFD 1[a]

Case	Model		R^2	MS_r
1	$\widehat{w}_{\mathrm{FFA}}^{\mathrm{B}} = 2.301 - 0.6878x_T + 0.8739x_T^2 - 0.7403x_N - 2.312x_{S/F} + 1.099x_{S/F}^2$	(3.3)	0.9718	0.24
	$\hat{C} = 0.5849 + 0.2870x_{S/F}$	(3.4)	0.9999	6.45×10^{-6}
2	$\widehat{w}_{\mathrm{FFA}}^{\mathrm{B}} = 3.788 + 0.8565x_T^2 - 1.724x_N + 0.7941x_N^2 - 4.871x_{S/F} + 2.509x_{S/F}^2 - 0.7061x_T x_{S/F} - 0.5356x_N x_{S/F}$	(3.5)	0.9896	0.47
	$\hat{C} = 0.6670 + 0.3280x_{S/F}$	(3.6)	0.9999	6.50×10^{-6}

[a] The total cost in the first year of operation ($\hat{C}$) is given as 10^6 \$/yr.

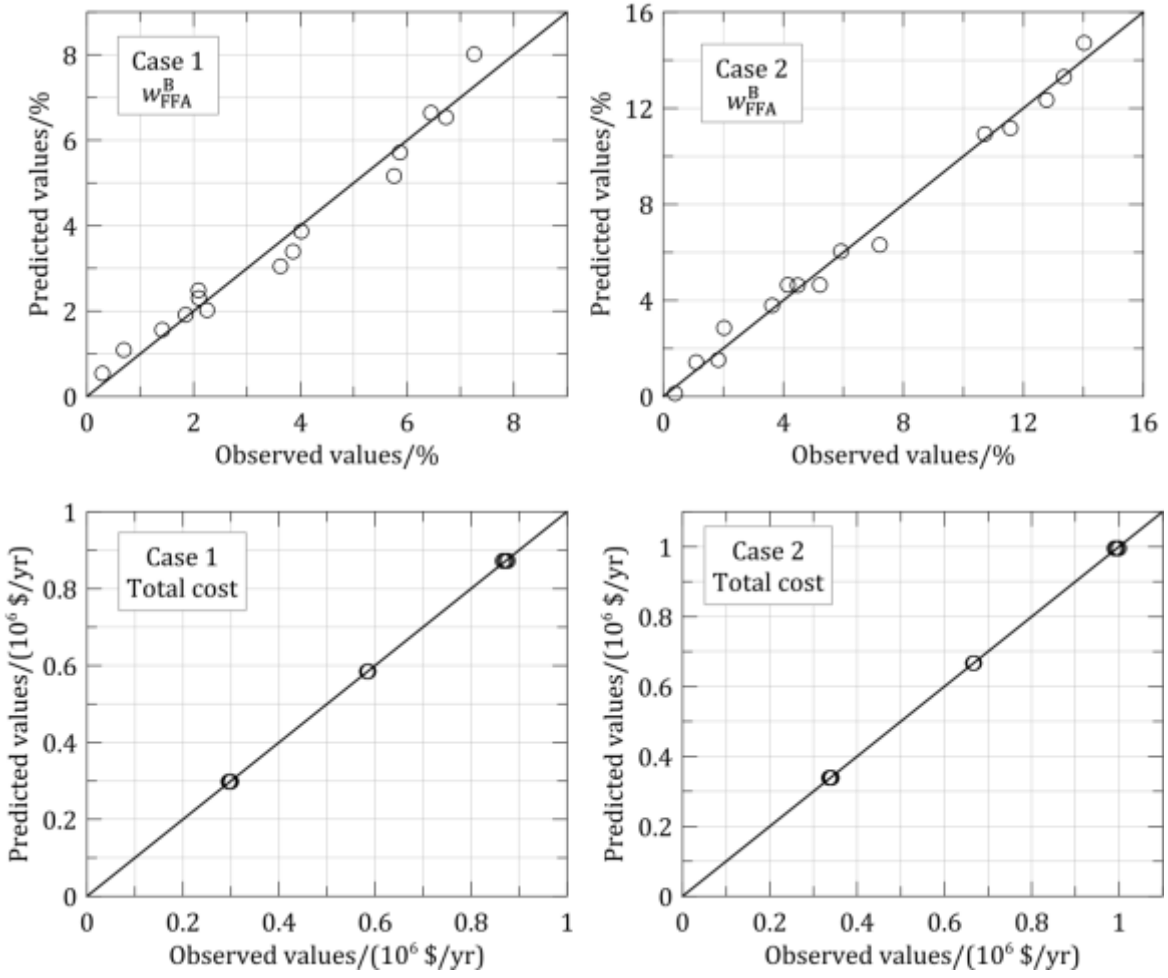

Figure 3.5 – Observed and predicted values

To assess if the technical benchmark ($w_{\mathrm{FFA}}^{\mathrm{B}} \leq 0.5\%$) could be satisfied by the rigorously modeled process, new simulations were run in Aspen under the optimal conditions predicted by the models in Table 3.7. For case 1, a mass fraction of 0.41% was obtained for $w_{\mathrm{FFA}}^{\mathrm{B}}$, thus satisfying the required specification. For case 2, however, it was necessary to increase slightly

the S/F ratio to 1.32 to meet the specification, resulting in $w_{FFA}^{B} = 0.49\%$. The corresponding costs were then calculated as \$742,143/yr for case 1 and \$899,049/yr for case 2. On the basis of a ROF feed flow rate of 1050 kg/h and a plant operation factor of 95% (8322 h per year) (Albuquerque et al., 2016), specific costs (raw material cost not included) can be expressed as \$84.93/ton and \$102.89/ton for cases 1 and 2, respectively.

The optimal design and operation conditions determined above both satisfy technical ($w_{FFA}^{B} \leq 0.5\%$) and economic (minimum cost) criteria for the separation of FFA from ROF. However, for both cases 1 and 2, the optimal condition was located at $N = 6$ stages. In order to investigate further if a number of stages greater than 6 could significantly shift the optimal point, a new factorial design was carried out over an extended range of N while preserving the previous levels for T and S/F, according to Table 3.1.

Results for the new 2^3 FFD (FFD 2) are presented in Table 3.8 (lines 1-9, including a central point) and extra computational experiments to complete a CCD (CCD 2, lines 10-15 in Table 3.8). For both cases 1 and 2, the same trend obtained in the FFD 1 was observed again: only the linear effect of S/F was significant for the total cost responses; and, a test on the w_{FFA}^{B} responses showed significant curvatures, suggesting again quadratic models. However, contrary to FFD 1, the number of stages did not affect the w_{FFA}^{B} response significantly, for both cases 1 and 2, as shown in Figure 3.7 and in Table 3.9, thus, indicating that $N = 6$ stages, as discussed above, is acceptable as the optimal condition. This conclusion is in agreement with Albuquerque, Danielski and Stragevitch (2016) who observed that w_{FFA}^{B} is not considerably affected by increasing the number of stages above five.

As mentioned before, similar studies using methanol as the solvent were not found in the literature. There are, however, extraction studies using ethanol and ethanol/water mixtures as solvents for the refining of edible oils with considerably lower FFA concentrations (BATISTA; ANTONIASSI; WOLF MACIEL, 2002; PINA; MEIRELLES, 2000). Although these authors demonstrated that it was possible to attain $w_{FFA}^{B} \leq 0.5\%$, in general, this required a higher number of stages with S/F ratios varying from 1.27 to 2. According to Mohsen-Nia and Khodayari (2008), methanol presents selectivities from 2.5 to 4 times higher than ethanol for oleic acid extraction from sunflower oil. In addition, the higher the water concentration, the more difficult the FFA separation becomes (BATISTA; ANTONIASSI; WOLF MACIEL, 2002; RODRIGUES et al., 2007). As a result, methanol presented better extraction properties than ethanol and ethanol/water mixtures requiring fewer stages and lower S/F ratios.

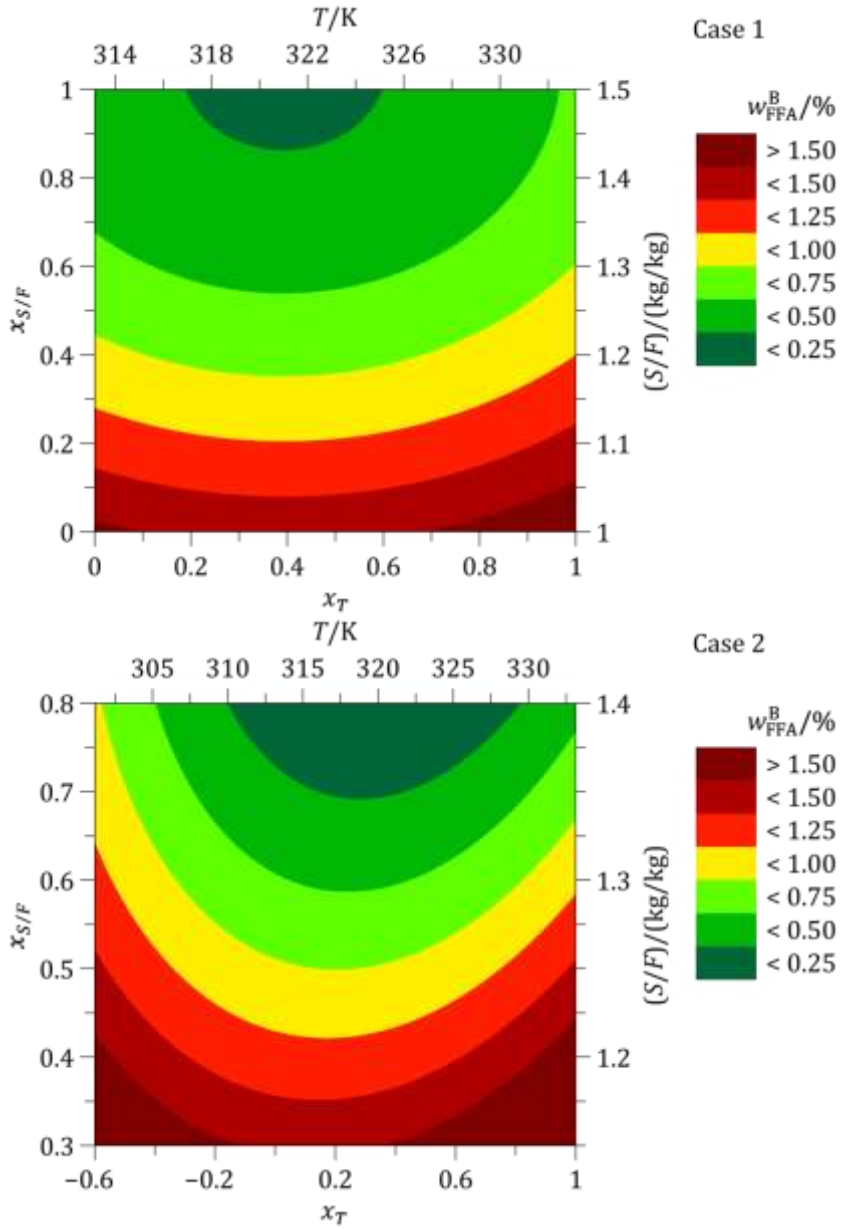

Figure 3.6 – Contour plots for $w_{\mathrm{FFA}}^{\mathrm{B}}$ at $N = 6$ stages ($x_N = 1$)

Table 3.8 – Values of $w_{\mathrm{FFA}}^{\mathrm{B}}$ and total cost responses obtained from FFD 2 and CCD 2

				Case 1		Case 2	
Run	T	N[a]	S/F	$w_{\mathrm{FFA}}^{\mathrm{B}}$/%	Cost/(\$/yr)	$w_{\mathrm{FFA}}^{\mathrm{B}}$/%	Cost/(\$/yr)
1	–	–	–	6.73	299,077	10.72	340,197
2	+	–	–	5.76	300,580	12.77	341,685
3	–	+	–	6.68	302,930	10.05	344,083
4	+	+	–	5.74	304,536	12.56	345,662
5	–	–	+	1.85	872,569	1.84	995,808
6	+	–	+	0.29	876,823	0.39	1,000,052
7	–	+	+	1.33	878,063	1.05	1,001,331
8	+	+	+	0.05	882,511	0.04	1,005,763
9	0	0	0	1.01	587,815	1.20	669,999
10	–	0	0	3.32	588,289	3.28	670,486
11	0	–	0	1.41	585,372	2.03	667,544
12	0	0	–	5.72	300,213	10.80	341,336
13	+	0	0	1.06	591,270	1.68	673,448
14	0	+	0	0.75	590,160	0.71	672,357
15	0	0	+	0.08	875,209	0.07	998,454

[a] N is relative to FFD 2: levels (–), (0) and (+) correspond to 6, 8 and 10 stages, respectively.

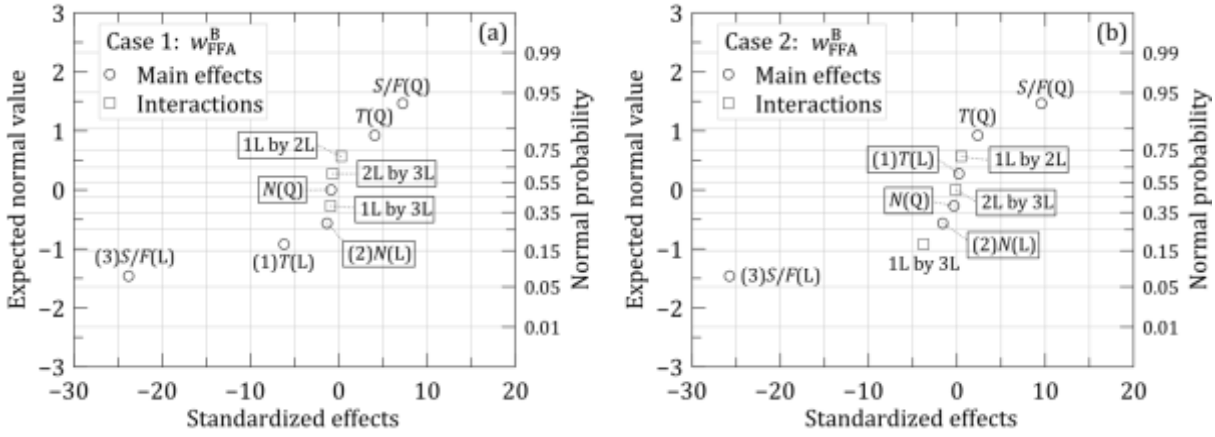

Figure 3.7 – Normal probability plots for FFD 2 (negligible effects are enclosed in borders).

Table 3.9 – Fitted models for FFD 2[a]

Case	Model		R^2	$\mathrm{MS_r}$
1	$\widehat{w}_{\mathrm{FFA}}^{\mathrm{B}} = 1.167 - 0.7032x_T + 0.8602x_T^2 - 2.702x_{S/F} + 1.567x_{S/F}^2$	(3.7)	0.9878	0.11
	$\hat{C} = 0.5890 + 0.2878x_{S/F}$	(3.8)	0.9999	7.40×10^{-6}
2	$\widehat{w}_{\mathrm{FFA}}^{\mathrm{B}} = 1.410 + 0.9235x_T^2 - 5.352x_{S/F} + 3.881x_{S/F}^2 - 0.8803x_T x_{S/F}$	(3.9)	0.9903	0.35
	$\hat{C} = 0.6712 + 0.3288x_{S/F}$	(3.10)	0.9999	7.43×10^{-6}

[a] The total cost in the first year of operation ($\hat{C}$) is given as 10^6 \$/yr.

3.3.3 Design and techno-economic assessment

In this section, some flowsheets were designed and in order to keep standardized block and stream names, a convention was adopted. For instance, flowsheet block names are represented by Y-1ZZ or Y-2ZZ, wherein numbers 1 and 2 were related to processes A and B, respectively. Y denotes E, P, R, T, M or X representing the heat exchanger (heater or cooler), pump, reactor, tower (distillation or extraction column), mixer or separator (separator or hydrocyclone), respectively. ZZ denotes an integer counter related to the amount of specific equipment. For instance, Y-1ZZ = R-103 and T-202 means a reactor and a distillation column present in processes A and B, respectively (ALBUQUERQUE; DANIELSKI; STRAGEVITCH, 2016).

Analogously, the stream names are represented by 1ZZ or 2ZZ. For example, stream 101 represents ROF feed stream to process A as shown in Figure 3.8. In addition, some streams can be accompanied by a letter (A, B or C); that was used when the stream pressure (e.g., 102A) or temperature (e.g., 103A) changed while almost keeping constant the composition, or, before or after a mixer (e.g., 122A and 122B in flowsheet from process A) (ALBUQUERQUE; DANIELSKI; STRAGEVITCH, 2016).

The base case and alternative processes were designed following the flowsheet from our previous work as shown in Figure 3.8, Figure 3.9 and Figure 3.10, where esterification unit from Figure 3.8 was equally defined for both processes. In this pretreatment unit, ROF, fresh and recycled methanol are fed to LLEx column T-101 for FFA separation from TAG. After FFA-rich stream 104 is fed in an esterification reactor to produce fatty acid methyl ester (FAME) and water using H_2SO_4 as catalyst and methanol present in the stream as reagent. Posteriorly, methanol purification T-102, neutralization of acid catalyst in a reactor R-102 using $Ca(OH)_2$ and $CaSO_4$ separation from FAME in a hydrocyclone X-101 are carried out.

On the other hand, transesterification units were similarly defined including just one difference: a set of a reactor (R-103) and a distillation column (T-103) for the base case and a RDC (T-203) for the alternative process (ALBUQUERQUE; DANIELSKI; STRAGEVITCH, 2016). As a result, the TAG-rich stream 105 is fed with methanol and NaOH as catalyst to a reactor R-103 for transesterification reaction followed by a column of methanol purification T-103 in process A, while these reactants are fed to RDC T-203 in process B. Biodiesel and glycerol are produced in 118 or 218 streams. After, FAME-rich stream 111 or 211 is mixed

with stream 118 or 218 for water washing in LLEx column T-104 or T-204 and biodiesel purification is carried out at T-105 or T-205 to produce biodiesel achieving ANP standard from Table 3.2. Posteriorly, neutralization of the alkali catalyst in a reactor R-104 or R-203 using H_3PO_4 and Na_3PO_4 separation from glycerol-rich stream 127 or 227 in a hydrocyclone X-103 or X-203 are carried out. Finally, glycerol purification using a vacuum distillation column T-106 or T-206 is performed to obtain pharmaceutical glycerol (99.5 wt%).

Other changes were adopted in separation equipment from transesterification units compared to previous process proposed by Albuquerque, Danielski and Stragevitch (2016), such as: use of distillation columns (RADFRAC) instead of flash vessels in the methanol recovery (T-103) and in the glycerol purification (T-106 or T-206). Furthermore, a distillation column (T-105 or T-205) was added to purify the biodiesel in order to attain the ANP standard related to water impurity. The same design specifications from our previous work were defined from the other equipment. Furthermore, optimal conditions obtained for case 2 from RSM study were employed for LLEx column from esterification unit. However, when the complete flowsheet was designed a lower S/F = 1.16 was required using N = 6 and T = 318.15 K. As an explanation, the small amount of water ($w_{water} \leq 6$ %) in 108 stream contributed for the FFA separation from TAG, since increased the partition coefficient (ALBUQUERQUE; DANIELSKI; STRAGEVITCH, 2016; GONÇALVES; BATISTA; MEIRELLES, 2002).

Results streams from processes A and B are showed in Table 3.10 to Table 3.12, where Table 3.10 is related to pre-treatment unit of process A. Same results were obtained for process B and for that reason were omitted, while results from transesterification units differed between processes A and B and are showed in Table 3.11 and Table 3.12. As a result, biodiesel and glycerol achieved specifications from both processes, so that processes A and B are both technical feasible. Furthermore, both presented two purges that composed the waste streams.

As a consequence, both processes were sized and compared related to economic assessment, so that design specifications, equipment sizes and capital costs for esterification and transesterification units are shown in Table 3.13. From these results process B confirmed to have a lower total capital cost than process A, since just one RDC is adopted instead a set of reactor/distillation column. This was also observed by Souza et al. (2014) and Gaurav, Ng and Rempel (2016). Among the reasons that contributes for it, low reaction time in transesterification reaction; temperature match between separation and reaction; and favorable volatilities.

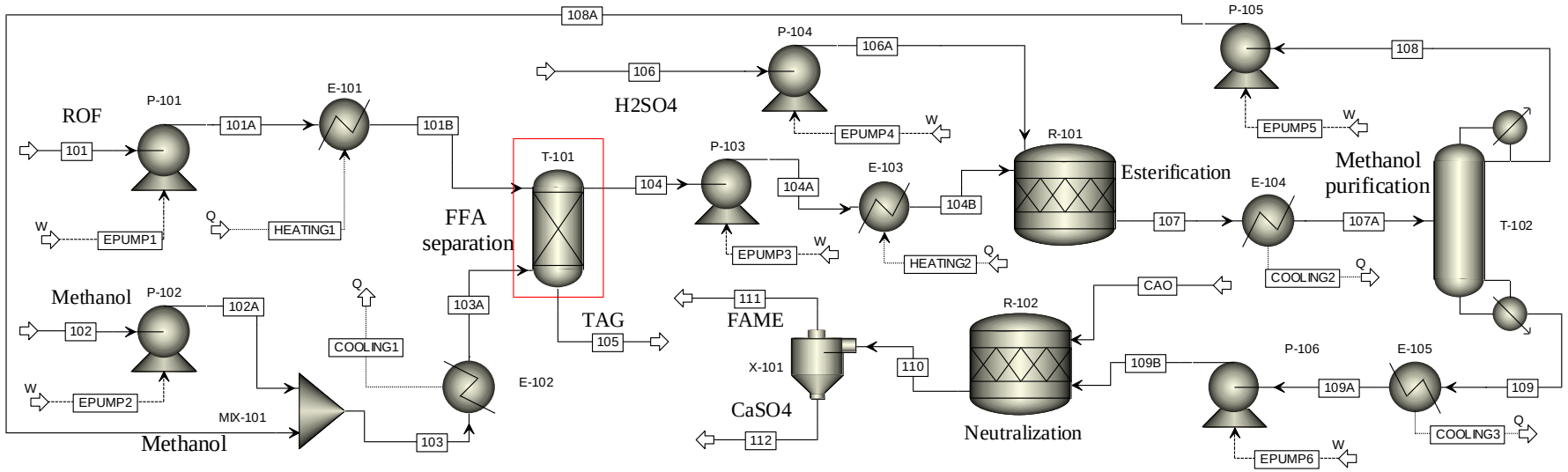

Figure 3.8 – ROF pretreatment unit for biodiesel production by acid-catalyzed esterification reaction for processes A and B using a LLEx column
Source: Adapted from Albuquerque, Danielski and Stragevitch (2016)

Table 3.10 – Main stream results of ROF pretreatment unit (FFA separation) to produce biodiesel in process A

Variables\Streams	101	102	103	104	105	106	107	108	109	111	112
Mole flow (kmol/hr)	1.70	2.03	42.29	41.73	2.25	0.02	41.75	40.26	1.49	1.49	0.02
Mass flow (kg/h)	1050.0	65.0	1295	1462.4	882.6	2.1	1464.5	1230	234.5	232.8	2.9
Pressure (kPa)	100.0	100.0	200.0	100.0	100.0	100.0	480.0	100.0	104.0	100.0	100.0
Temperature (K)	298.2	298.2	352.9	302.6	318.4	298.2	383.0	339.0	380.5	318.2	318.2
Oleic acid (wt)	0.2000	0.0000	0.0000	0.1424	0.0020	0.0000	0.0000	0.0000	0.0000	0.0000	0.0000
Methanol (wt)	0.0000	1.0000	0.9405	0.8050	0.0462	0.0000	0.7877	0.9374	0.0027	0.0028	0.0000
Water (wt)	0.0000	0.0000	0.0595	0.0524	0.0004	0.0000	0.0614	0.0626	0.0550	0.0570	0.0000
Methyl oleate (wt)	0.0000	0.0000	0.0000	0.0000	0.0000	0.0000	0.1492	0.0000	0.9320	0.9387	0.0000
Trilinolein (wt)	0.8000	0.0000	0.0000	0.0002	0.9513	0.0000	0.0002	0.0000	0.0015	0.0015	0.0000
Glycerol (wt)	0.0000	0.0000	0.0000	0.0000	0.0000	0.0000	0.0000	0.0000	0.0000	0.0000	0.0000
H2SO4 (wt)	0.0000	0.0000	0.0000	0.0000	0.0000	1.0000	0.0014	0.0000	0.0088	0.0000	0.0000
CaSO4 (wt)	0.0000	0.0000	0.0000	0.0000	0.0000	0.0000	0.0000	0.0000	0.0000	0.0000	1.0000

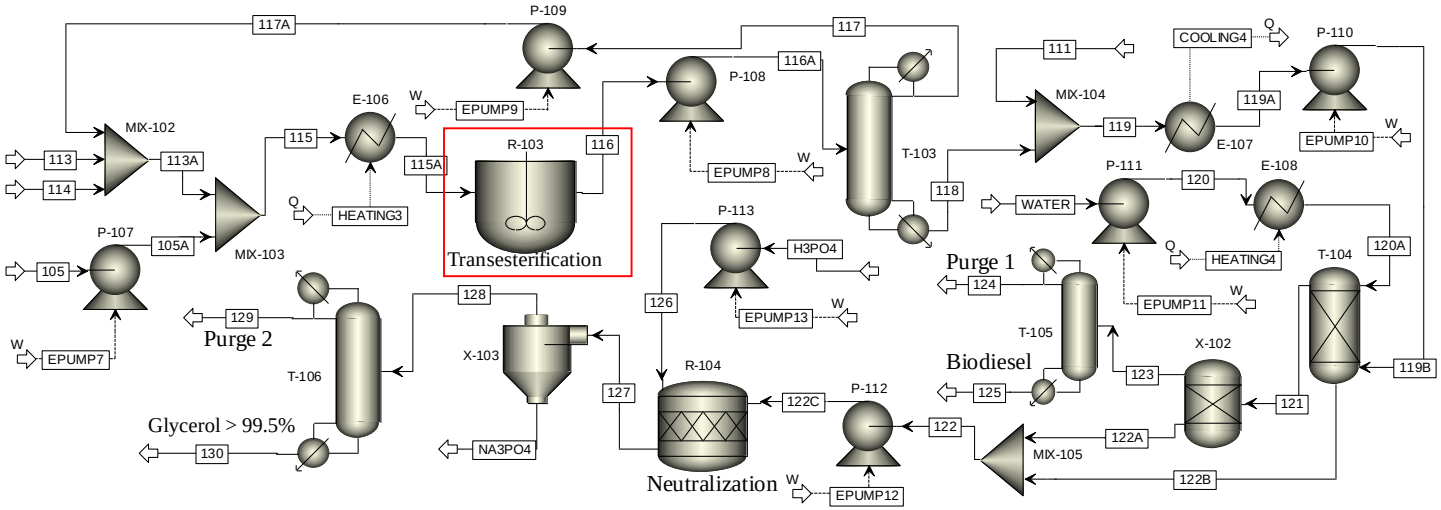

Figure 3.9 – Alkali-catalyzed transesterification unit for biodiesel production by process A (base case) using a set of reactor/distillation column
Source: Adapted from Albuquerque, Danielski and Stragevitch (2016)

Table 3.11 – Main stream results of transesterification unit to produce biodiesel in process A using a set of reactor/distillation column

Variables\Streams	105	113	114	116	117A	118	124	125	128	129	130
Mole flow (kmol/hr)	2.25	1.76	0.21	6.92	2.7	4.2	0.15	3.62	3.13	2.17	0.96
Mass flow (kg/h)	882.6	56.4	8.3	1033.8	86.4	947.4	3.4	1064	129.3	41	88.4
Pressure (kPa)	100.0	100.0	100.0	105.0	200.0	100.1	30.0	30.0	100.0	0.4	0.7
Temperature (K)	318.4	298.2	298.2	338.2	338.4	439.5	321.2	506.7	318.2	262.0	414.7
Oleic acid (wt)	0.0020	0.0000	0.0000	0.0017	0.0000	0.0019	0.0000	0.0015	0.0011	0.0000	0.0017
Methanol (wt)	0.0462	1.0000	0.0000	0.0887	0.9986	0.0057	0.4833	0.0001	0.0333	0.1051	0.0000
Water (wt)	0.0004	0.0000	0.0000	0.0005	0.0013	0.0004	0.5165	0.0001	0.2837	0.8946	0.0003
Methyl oleate (wt)	0.0000	0.0000	0.0000	0.0000	0.0000	0.0000	0.0000	0.2054	0.0000	0.0000	0.0000
Trilinolein (wt)	0.9513	0.0000	0.0000	0.0000	0.0000	0.0000	0.0000	0.0003	0.0000	0.0000	0.0000
Glycerol (wt)	0.0000	0.0000	0.0000	0.0851	0.0000	0.0928	0.0000	0.0000	0.6799	0.0002	0.9951
Methyl linoleate (wt)	0.0000	0.0000	0.0000	0.8159	0.0000	0.8904	0.0002	0.7925	0.0020	0.0000	0.0028
NaOH(wt)	0.0000	0.0000	1.0000	0.0081	0.0000	0.0088	0.0000	0.0000	0.0000	0.0000	0.0000

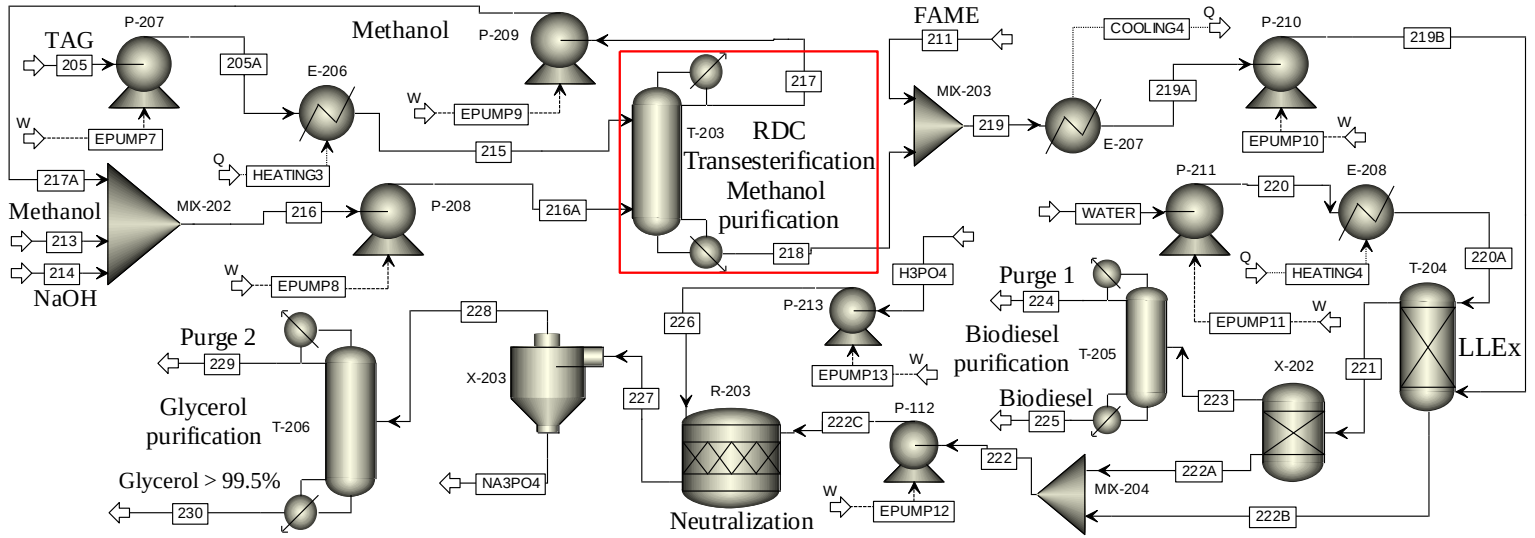

Figure 3.10 – Alkali-catalyzed transesterification unit for biodiesel production by process B (base case) using a reactive distillation column (RDC)

Table 3.12 – Main stream results of transesterification unit to produce biodiesel in process B using a RDC

Variables\Streams	205	213	214	216	217A	218	224	225	228	229	230
Mole flow (kmol/hr)	2.25	1.61	0.21	2.76	0.94	4.07	0.11	3.62	3.02	2.08	0.94
Mass flow (kg/h)	882.6	51.5	8.3	90	30.1	942.4	2.1	1064.2	125.4	38.8	86.7
Pressure (kPa)	100.0	100.0	100.0	100.0	100.0	100.6	30.0	30.1	100.0	0.1	0.6
Temperature (K)	318.4	298.2	298.2	312.4	337.4	517.0	330.3	510.9	318.2	252.4	423.1
Oleic acid (wt)	0.0020	0.0000	0.0000	0.0000	0.0000	0.0019	0.0000	0.0016	0.0005	0.0006	0.0004
Methanol (wt)	0.0462	1.0000	0.0000	0.9072	0.9997	0.0008	0.1909	0.0000	0.0081	0.0261	0.0000
Water (wt)	0.0004	0.0000	0.0000	0.0001	0.0003	0.0004	0.8087	0.0002	0.2929	0.9472	0.0000
Methyl oleate (wt)	0.0000	0.0000	0.0000	0.0000	0.0000	0.0000	0.0000	0.2054	0.0000	0.0000	0.0000
Trilinolein (wt)	0.9514	0.0000	0.0000	0.0000	0.0000	0.0001	0.0000	0.0004	0.0000	0.0000	0.0000
Glycerol (wt)	0.0000	0.0000	0.0000	0.0000	0.0000	0.0923	0.0000	0.0000	0.6933	0.0194	0.9950
Methyl linoleate (wt)	0.0000	0.0000	0.0000	0.0000	0.0000	0.8917	0.0003	0.7894	0.0021	0.0066	0.0000
NaOH(wt)	0.0000	0.0000	1.0000	0.0927	0.0000	0.0089	0.0000	0.0000	0.0000	0.0000	0.0000

Table 3.13 – Main Operating Conditions, Equipment Sizes, and Capital Costs for processes A and B

block	description	process A/B	block	description	process A	process B	block	description	process A	process B
T-101	S/F[a]	1.23	R-103	P (kPa)[b]	105		T-105	RR[g]	0.5	0.5
T-201	P (kPa)[b]	100		T (K)[c]	338.2		T-205	D/F[h]	0.040	0.029
	T (K)[c]	302.6/318.4		$D \times L$ (m)[e]	0.91 × 3.66			P (kPa)[b]	30/30.05	30/30.05
	N/FS[d]	6/1,6		cost ($k)[f]	226.1			T (K)[c]	321.2/506.7	330.3/510.9
	$D \times L$ (m)[e]	0.91 × 3.66	T-103	RR[g]	0.5	25		Q (kW)[i]	-2.6/128.2	-1.9/131.2
	cost ($k)[f]	97.0	T-203	D/F[h]	0.39	0.188		N/FS[d]	3/2	3/2
R-101	P (kPa)[b]	480		P (kPa)[b]	100/100.11	100/100.63		$D \times L$ (m)[e]	0.3 × 4.88	0.3 × 4.88
R-201	T (K)[c]	383		T (K)[c]	337.4/439.5	337.4/517		cost ($k)[f]	366.7	366.7
	$D \times L$ (m)[e]	0.46 × 2.59		Q (kW)[i]	-39.8/99.9	-238.6/400.1	T-106	RR[g]	0.5	0.5
	cost ($k)[f]	183.9		$N/FS/N_{RX}$[d]	4/2	12/2,11/2-11	T-206	D/F[h]	0.694	0.689
T-102	RR[g]	2		$D \times L$ (m)[e]	0.3 × 5.33	0.61 × 9.3		P (kPa)[b]	0.40/0.73	0.13/0.60
T-202	D/F[h]	0.964		cost ($k)[f]	379.4	439.6		T (K)[c]	262/414.7	252.4/423.1
	P (kPa)[b]	100/104	T-104	S/F[a]	0.017	1		Q (kW)[i]	-41.8/45.2	-41.9/45.5
	T (K)[c]	273.2/273.2	T-204	P (kPa)[b]	100	100		N/FS[d]	3/2	3/2
	Q (MW)[i]	-1.21/1.24		T (K)[c]	319.3/319.2	319.1/319.1		$D \times L$ (m)[e]	0.46 × 4.88	0.46 × 4.88
	N/FS[d]	5/2		N/FS[d]	3/1 and 3	3/1 and 3		cost ($k)[f]	413.7	437.5
	$D \times L$ (m)[e]	0.76 × 6.71		$D \times L$ (m)[e]	0.91 × 3.66	0.91 × 3.66	Heat exchangers cost ($k)[f]		427.1	428.9
	cost ($k)[f]	498.0		cost ($k)[f]	97.0	97.0	Pumps cost ($k)[f]		384.5	357.8
R-102	P (kPa)[b]	100	R-104	P (kPa)[b]	100	100	Others cost ($k)[f]		221.0	225.4
R-202	T (K)[c]	318.2	R-203	T (K)[c]	318.2	318.2	Total installed cost ($MM)[f]		3.61	3.47
	$D \times L$ (m)[e]	0.3 × 1.98		$D \times$ L (m)[e]	0.3 × 1.83	0.46 × 2.44	Lang factor, f_L		4.66	4.67
	cost ($k)[f]	161.8		cost ($k)[f]	157.6	179.3	Total capital cost ($MM)[f]		16.83	16.21

[a]S/F is solvent (methanol) to feed ratio in mass basis; [b]P is pressure; [c]T is temperature; [d]$N/FS/N_{RX}$ means number of stages, feed stage and reactive stages; [e]$D \times L$ are diameter and length; [f]$k and $MM mean thousand and million dollars; [g]RR is reflux mole ratio; [h]D/F is distillate to feed mole ratio; [i]Q means condenser or reboiler duty.

Other economic results were also obtained including other indicators previously defined as shown in Table 3.14. From these results, Process A showed some advantages compared to process B as lower C_{OP} and BEP; and higher income and A_{NNP}. Furthermore, biodiesel productivity from process A was slightly higher than process B. On the other hand, process B showed lower TAC, ROI and PBP.

Table 3.14 – Main costs and economic and environment indicators

Cost and Environment indicators	Process A	Process B
Raw material cost ($MM/year)	3.451	3.415
Brown grease cost ($MM/year)	2.451	2.451
Methanol cost ($MM/year)	0.900	0.863
Catalyst cost ($MM/year)	0.041	0.041
Utilities cost ($MM/year)	0.588	0.686
Electricity cost ($MM/year)	0.110	0.097
Cooling cost ($MM/year)	0.061	0.074
LP steam cost ($MM/year)	0.351	0.35
MP steam cost ($MM/year)	0.026	0
HP steam cost ($MM/year)	0.040	0.165
Total steam cost ($MM/year)	0.417	0.515
Waste treatment cost ($MM/year)	0.128	0.118
Total operation cost, C_{oper} ($MM/year)	6.460	6.510
Total annualized cost, TAC ($MM/year)	12.070	11.910
Income ($MM/year)	9.470	9.460
Net annual profit, A_{NP} ($MM/year)	3.010	2.960
Net annual profit after taxes, A_{NNP} ($MM/year)	1.510	1.480
Return of investment, ROI (%)	23.260	22.740
Break-even price, BEP ($/kg)	1.250	1.260
Payback period, PBP (year)	4.930	4.880
Biodiesel Productivity ($k/ton)	0.927	0.926
Wastewater flowrate (kton/year)	0.389	0.359
Waste treatment cost ($MM/year)	0.128	0.118
Total CO_2 emission (kton/year)	3.716	4.249
Net Carbon fee/tax ($MM/year)	0.056	0.064

Related to environment indicators, process B showed lower wastewater flowrate and treatment cost; however, it presented higher total CO_2 emission and net carbon fee/tax as result of higher demand of HP steam in RDC T-203. From all results can be stated that both processes have comparable economic feasibility, since economic results are very close. As a consequence, the process can be chosen based on environment aspects depending from which indicator is less onerous in the future.

3.4 CONCLUSIONS

The technical and economic feasibility of the separation of FFA from a ROF using LLEx with methanol as solvent was investigated using RSM for two cases of typical FFA contents found in yellow and brown greases. All variables studied (T, N and S/F) showed significant effects on the $w_{\mathrm{FFA}}^{\mathrm{B}}$ response. On the other hand, for both cases, the total cost response was only significantly affected by the linear effect of the S/F ratio. As a result, a trade-off between $w_{\mathrm{FFA}}^{\mathrm{B}} \leq 0.5\%$ and minimum total cost in the first year of operation was adopted to obtain the optimal condition, since an increase in the S/F ratio entails a decrease in the $w_{\mathrm{FFA}}^{\mathrm{B}}$ value while increasing the total cost. Therefore, optimal design and operation conditions were $T = 321$ K, $N = 6$ stages and $S/F = 1.27$ for case 1; and $T = 318$ K, $N = 6$ stages and $S/F = 1.32$ for case 2. Under these conditions, process simulation indicated that the technical specification can be satisfied, resulting in a $w_{\mathrm{FFA}}^{\mathrm{B}}$ value of 0.41% for case 1 and 0.49% for case 2. The associated costs were \$742,143/yr for case 1 and \$899,049/yr for case 2. The corresponding specific costs for a ROF feed flow rate of 1050 kg/h were \$84.93/ton and \$102.89/ton for cases 1 and 2. The above minimum costs do not include raw material (ROF) costs as already pointed out.

An alternative process for biodiesel production from ROF based on a RDC (process B) at transesterification unit was also investigated comparing to the base case using a set of reactor/distillation column (process A). These processes were designed, sized and evaluated related to techno-economic feasibility. Design specifications and results were very similar for the processes in pre-treatment unit, since there is no change in equipment and operational conditions. Both processes showed to be technical feasible; however, each one presented advantages and disadvantages for some economic indicators. For instance, process A showed lower C_{OP} and BEP; and higher income, A_{NNP}, ROI and slightly higher biodiesel productivity. On the other hand, process B showed lower TAC and PBP. As a result, both processes demonstrated to be economically comparable. Related to environment impacts, process A presented lower net Carbon fee/tax, while process B showed lower waste treatment costs. As a consequence, optimal process can be chosen based on the more onerous environment indicator expected for the future. Therefore, not always a process based on RDC is more economic feasible than a conventional process based on a set of reactor/distillation column. For this reason, it is worth to study the techno-economic assessment of RDC processes compared to base case processes.

ACKNOWLEDGMENTS

The authors acknowledge FACEPE/NUQAAPE, INCTAA, CNPq and FINEP for financial support. A. A. A. is also grateful to Capes for a Ph.D. scholarship.

NOMENCLATURE

A_{ij}	NRTL binary interaction parameter (K)
$A_{ij}^{(0)}$	Coefficient in the NRTL binary interaction parameter equation (K)
$A_{ij}^{(1)}$	Coefficient in the NRTL binary interaction parameter equation
A_{NP}	Net annual profit ($MM/year)
A_{NNP}	Net annual profit after taxes ($MM/year)
BEP	Break-even price ($/kg or $/ton)
C	Total cost in the first year of operation ($MM/year)
C_{CO_2}	Carbon emission fees
C_{oper}	Total operation cost ($MM/year)
C_{TC}	Total capital cost ($MM)
C_{waste}	Waste stream cost
F	Objective function (see Equation 3.1)
FAME	Fatty acid methyl ester
M	Molar mass (g/mol)
MS_r	Residual mean square
N	Number of stages
N_c	Number of components
N_D	Number of data sets
N_t	Number of tie lines
PBP	Payback period (year)
R^2	Coefficient of determination
ROI	Return of Investment (%)
S/F	Solvent to feed mass ratio
T	Temperature (K)
TAC	Total annualized cost ($MM/year)

w	Mass fraction (%)
$w_{\mathrm{FFA}}^{\mathrm{B}}$	FFA mass fraction (solvent free) in the oil-rich output bottom stream of the extraction column (%)
x_N	Coded number of stages
$x_{S/F}$	Coded solvent to feed mass ratio
x_T	Coded temperature

Greek Symbols

α_{ij}	NRTL non-randomness parameter
β	Distance of each axial point (also called star point) from the center

Subscripts

FFA	Free fatty acid
i	i-th component
j	j-th experimental LLE tie line
k	k-th data set
N	Number of stages
S/F	Solvent to feed mass ratio
T	Temperature

Superscripts

B	Bottom output stream of the extraction column
cal	Calculated
exp	Experimental
I, II	Liquid phases in equilibrium
l	l-th phase

Abbreviations

ANP	National Agency of Petroleum, Natural Gas and Biofuels
CCD	central composite design
CEPCI	Chemical Engineering's Plant Cost Index
CF	Constituent Fragments
CnO	canola oil
CO	corn oil

ECF	Extended Constituent Fragments
EPA	United States Environment Protection Agency
FFA	free fatty acid
FFD	full factorial design
JO	jatropha curcas oil
L	linoleic
Ln	linolenic
LLE	liquid-liquid equilibrium
LLEx	liquid-liquid extraction
LLL	trilinolein
M	methanol
NRTL	Non-Random Two-Liquid
O	oleic
OA	oleic acid
P	palmitic
Process A	base case process for biodiesel production by FFA separation from ROF using a set of reactor/distillation column in the transesterification unit
Process B	alternative process for biodiesel production by FFA separation from ROF using a reactive distillation column (RDC) in the transesterification unit
RDC	reactive distillation column
RMSD	root mean square deviation
ROF	residual oil and fat
RSM	response surface methodology
S	stearic
SuO	sunflower oil
TAG	triacylglycerol

REFERENCES

ADEWALE, P.; DUMONT, M.-J.; NGADI, M. Recent trends of biodiesel production from animal fat wastes and associated production techniques. **Renewable and Sustainable Energy Reviews,** v. 45, p. 574−588, 2015.

ALBUQUERQUE, A. A.; DANIELSKI, L.; STRAGEVITCH, L. Techno-Economic Assessment of an Alternative Process for Biodiesel Production from Feedstock Containing High Levels of Free Fatty Acids. **Energy & Fuels**, v. 30, n. 11, p. 9409−9418, 2016.

ANTONIOSI FILHO, N.; MENDES, O. L.; LANÇAS, F. **Computer predition of triacylglycerol composition of vegetable oils by HRGC**, v. 40, n. 9−10, p. 557−562, 1995.

AVHAD, M. R.; MARCHETTI, J. M. A review on recent advancement in catalytic materials for biodiesel production. **Renewable and Sustainable Energy Reviews,** v. 50, p. 696−718, 2015.

BATISTA, E.; ANTONIASSI, R.; WOLF MACIEL, M. R. Liquid-liquid extraction for deacidification of vegetable oils. In: International Solvent Extraction Conference, 16, 2002, Cape Town, South Africa. **Proceedings...** Cape Town, South Africa: ISEC, 2002. p.638−643.

BATISTA, E.; MONNERAT, S.; KATO, K.; STRAGEVITCH, L.; MEIRELLES, A. J. A. Liquid−Liquid Equilibrium for Systems of Canola Oil, Oleic Acid, and Short-Chain Alcohols. **Journal of Chemical & Engineering Data,** v. 44, n. 6, p. 1360−1364, 1999.

BATISTA, E.; WOLF MACIEL, M. R.; MEIRELLES, A. J. A. Simulation of the Deacidification of Vegetable Oil by Liquid-Liquid Extraction. In: Conference on Process Integration, Modelling and Optimisation for Energy Saving and Pollution Reduction, 2, 1999, Budapest, Hungary. **Proceedings...** Budapest, Hungary: PRES, 1999.

BHOSLE, B.; SUBRAMANIAN, R. New approaches in deacidification of edible oils—a review. **Journal of Food Engineering,** v. 69, n. 4, p. 481−494, 2005.

BRUNS, R. E.; SCARMINIO, I. S.; BARROS NETO, B. **Statistical Design - Chemometrics**. 1. ed. Campinas: Elsevier, 2006. 422p.

CAI, Z.-Z.; WANG, Y.; TENG, Y.-L.; CHONG, K.-M.; WANG, J.-W.; ZHANG, J.-W.; YANG, D.-P. A two-step biodiesel production process from waste cooking oil via recycling

crude glycerol esterification catalyzed by alkali catalyst. **Fuel Processing Technology,** v. 137, p. 186−193, 2015.

CANAKCI, M.; SANLI, H. Biodiesel production from various feedstocks and their effects on the fuel properties. **Journal of industrial microbiology & biotechnology,** v. 35, n. 5, p. 431−441, 2008.

CANAKCI, M.; VAN GERPEN, J. Biodiesel production from oils and fats with high free fatty acids. **Transactions of the ASAE,** v. 44, n. 6, p. 1429, 2001.

CERIANI, R.; PAIVA, F. R.; GONÇALVES, C. B.; BATISTA, E. A. C.; MEIRELLES, A. J. A. Densities and Viscosities of Vegetable Oils of Nutritional Value. **Journal of Chemical & Engineering Data,** v. 53, n. 8, p. 1846−1853, 2008.

CRUZ-FORERO, D.-C.; GONZÁLEZ-RUIZ, O.-A.; LÓPEZ-GIRALDO, L.-J. Calculation of thermophysical properties of oils and triacylglycerols using an extended constituent fragments approach. **CT&F-Ciencia, Tecnología y Futuro,** v. 5, n. 1, p. 67−82, 2012.

GNANAPRAKASAM, A.; SIVAKUMAR, V. M.; SURENDHAR, A.; THIRUMARIMURUGAN, M.; KANNADASAN, T. Recent strategy of biodiesel production from waste cooking oil and process influencing parameters: a review. **Journal of Energy,** v. 2013, 2013.

GONÇALVES, C. B.; BATISTA, E.; MEIRELLES, A. J. A. Liquid−Liquid Equilibrium Data for the System Corn Oil + Oleic Acid + Ethanol + Water at 298.15 K. **Journal of Chemical & Engineering Data,** v. 47, n. 3, p. 416−420, 2002.

HE, B. B.; SINGH, A. P.; THOMPSON, J. C. Experimental optimization of a continuous-flow reactive distillation reactor for biodiesel production. **American Society of Agricultural and Biological Engineers (ASABE),** v. 48, n. 6, p. 2237−2243, 2005.

_____. A novel continuous-flow reactor using reactive distillation for biodiesel production. **American Society of Agricultural and Biological Engineers (ASABE),** v. 49, n. 1, p. 107−112, 2006.

IASMIN, M.; DEAN, L. O.; LAPPI, S. E.; DUCOSTE, J. J. Factors that influence properties of FOG deposits and their formation in sewer collection systems. **Water Res,** v. 49, p. 92−102, 2014.

JORGE, N.; SOARES, B. B. P.; LUNARDI, V. M.; MALACRIDA, C. R. Physico-chemical alterations of sunflower, corn and soybean oils in deep fat frying. **Química Nova,** v. 28, n. 6, p. 947, 2005.

LIU, Y.; LU, H.; LIU, C.; LIANG, B. Solubility Measurement for the Reaction Systems in Pre-Esterification of High Acid Value Jatropha curcas L. Oil†. **Journal of Chemical & Engineering Data,** v. 54, n. 5, p. 1421−1425, 2008.

LUYBEN, W. L.; YU, C. **Reactive Distillation Design and Control**. 1. ed. New Jersey: John Wiley & Sons, Inc., 2008. 577p.

MA, F.; HANNA, M. A. Biodiesel production: a review. **Bioresource technology,** v. 70, n. 1, p. 1−15, 1999.

MOHITE, S.; KUMAR, S.; PAL, A.; MAJI, S. Biodiesel Production from High Free Fatty Acid Feed Stocks through Transesterification. In: International Conference of Advance Research and Innovation, 2015, New Delhi, India. **Proceedings...** New Delhi, India: ICARI, 2015. p. 113-115.

MOHSEN-NIA, M.; DARGAHI, M. Liquid-liquid equilibrium for systems of (corn oil+ oleic acid+ methanol or ethanol) at (303.15 and 313.15) K. **Journal of Chemical & Engineering Data,** v. 52, n. 3, p. 910−914, 2007.

MOHSEN-NIA, M.; KHODAYARI, A. De-acidification of sunflower oil by solvent extraction:(Liquid+ liquid) equilibrium data at T=(303.15 and 313.15) K. **The Journal of Chemical Thermodynamics,** v. 40, n. 8, p. 1325−1329, 2008.

MORAD, N. A.; KAMAL, A. A. M.; PANAU, F.; YEW, T. W. Liquid specific heat capacity estimation for fatty acids, triacylglycerols, and vegetable oils based on their fatty acid composition. **Journal of the American Oil Chemists' Society,** v. 77, n. 9, p. 1001−1006, 2000.

MUEANMAS, C.; PRASERTSIT, K.; TONGURAI, C. Transesterification of triolein with methanol in reactive distillation column: simulation studies. **International Journal of Chemical Reactor Engineering,** v. 8, n. 1, 2010.

NATIONAL AGENCY OF PETROLEUM, NATURAL GAS AND BIOFUELS (ANP). **ANP Resolution nº 45, of Aug. 25, 2014 - DOU Aug. 26, 2014**. ANP, Brasília, Brazil, 2014.

NOUREDDINI, H.; TEOH, B. C.; CLEMENTS, L. D. Densities of vegetable oils and fatty acids. **Journal of the American Oil Chemists Society,** v. 69, n. 12, p. 1184−1188, 1992.

ORTNER, M. E.; MÜLLER, W.; SCHNEIDER, I.; BOCKREIS, A. Environmental assessment of three different utilization paths of waste cooking oil from households. **Resources, Conservation and Recycling,** v. 106, p. 59−67, 2016.

PERRY, E. S.; WEBER, W. H.; DAUBERT, B. F. Vapor pressures of phlegmatic liquids. I. Simple and mixed triglycerides. **Journal of the American Chemical Society,** v. 71, n. 11, p. 3720−3726, 1949.

PINA, C. G.; MEIRELLES, A. J. A. Deacidification of corn oil by solvent extraction in a perforated rotating disc column. **Journal of the American Oil Chemists' Society,** v. 77, n. 5, p. 553−559, 2000.

REFAAT, A. Different techniques for the production of biodiesel from waste vegetable oil. **International Journal of Environmental Science & Technology,** v. 7, n. 1, p. 183−213, 2010.

RENON, H.; PRAUSNITZ, J. M. Local compositions in thermodynamic excess functions for liquid mixtures. **AIChE journal,** v. 14, n. 1, p. 135−144, 1968.

RODRIGUES, C. E.; GONÇALVES, C. B.; BATISTA, E.; MEIRELLES, A. J. Deacidification of vegetable oils by solvent extraction. **Recent Patents on Engineering,** v. 1, n. 1, p. 95−102, 2007.

SEADER, J. D.; HENLEY, E. J.; ROPER, D. K. **Separation process principles: chemical and biochemical operations**. 3. ed. USA: John Wiley & Sons, 2011. 849p.

SEIDER, W. D.; SEADER, J. D.; LEWIN, D. R. **Product & Process Design Principles: Synthesis, Analysis and Evaluation**. 3. ed. USA: John Wiley & Sons, 2009. 736p.

SOUZA, T. P. C.; STRAGEVITCH, L.; KNOECHELMANN, A.; PACHECO, J. G. A.; SILVA, J. M. F. Simulation and preliminary economic assessment of a biodiesel plant and comparison with reactive distillation. **Fuel Processing Technology,** v. 123, p. 75−81, 2014.

STRAGEVITCH, L.; D'AVILA, S. Application of a generalized maximum likelihood method in the reduction of multicomponent liquid-liquid equilibrium data. **Brazilian Journal of Chemical Engineering,** v. 14, 1997.

SUNDMACHER, K.; KIENLE, A. **Reactive Distillation: Status and Future Directions**. 1. ed. Magdeburg, Germany: Wiley-VCH, 2003. 308p.

TSOUTSOS, T. D.; TOURNAKI, S.; PARAÍBA, O.; KAMINARIS, S. D. The Used Cooking Oil-to-biodiesel chain in Europe assessment of best practices and environmental performance. **Renewable and Sustainable Energy Reviews,** v. 54, p. 74−83, 2016.

UNITED STATES ENVIRONMENTAL PROTECTION AGENCY (EPA). **Mandatory Reporting of Greenhouse Gases; Final Rule**. Environmental Protection Agency, Washington, 2009. Available at: <https://www.epa.gov/regulations-emissions-vehicles-and-engines/final-rule-mandatory-reporting-greenhouse-gases>. Accessed on: 2018/07/21.

UNNITHAN, U.; TIWARI, K. Kinetics of esterification of oleic-acid and mixtures of fatty-acids with methanol using sulfuric-acid and paratoluenesulphonic acid as catalysts. **Indian J. Technol.,** v. 25, p. 477−479, 1987.

VAISALI, C.; CHARANYAA, S.; BELUR, P. D.; REGUPATHI, I. Refining of edible oils: a critical appraisal of current and potential technologies. **International Journal of Food Science & Technology,** v. 50, n. 1, p. 13−23, 2015.

VICENTE, G.; MARTÍNEZ, M.; ARACIL, J.; ESTEBAN, A. Kinetics of Sunflower Oil Methanolysis. **Industrial & Engineering Chemistry Research,** v. 44, n. 15, p. 5447−5454, 2005.

ZHANG, Y.; DUBE, M.; MCLEAN, D.; KATES, M. Biodiesel production from waste cooking oil: 1. Process design and technological assessment. **Bioresource technology,** v. 89, n. 1, p. 1−16, 2003.

ZONG, L.; RAMANATHAN, S.; CHEN, C.-C. Fragment-based approach for estimating thermophysical properties of fats and vegetable oils for modeling biodiesel production processes. **Industrial & engineering chemistry research,** v. 49, n. 2, p. 876−886, 2009.

4 PHASE EQUILIBRIUM MODELING FOR BIODIESEL REACTION SYSTEMS

Allan Almeida Albuquerque[a,b], Flora T. T. Ng[b], Leandro Danielski[a], Luiz Stragevitch[a,*]
[a]LAC/DEQ/UFPE - Fuel Laboratory, Department of Chemical Engineering, Federal University of Pernambuco. Av. Prof. Artur de Sá s/n - CEP 50740-521, Recife, PE, Brazil.
[b]Department of Chemical Engineering, University of Waterloo, Waterloo, N2L 3G1, Canada
*Phone/fax: +55 81 21267235. *E-mail: luiz@ufpe.br*

Extended paper to be submitted to Fluid Phase Equilibria, Qualis A1 IF 2.197

ABSTRACT

Biodiesel production from residual oil and fats by a solid acid-catalyzed (SAC) route using catalytic distillation column (CDC) has shown to be more economically attractive than conventional processes. As a result, accurate representation of phase equilibrium (PE) including vapor-liquid-liquid equilibrium (VLLE), vapor-liquid equilibrium (VLE) and liquid-liquid equilibrium (LLE) are required in process simulators, since high cost are involved with catalysts, solvents and to design the CDC. Despite these, many authors have not given much attention to PE, so that generally a limited number of existing binary interaction parameters are considered in commercial simulators and cannot represent simultaneously the tri-phase equilibrium. As a consequence, in order to obtain more reliable and robust simulations of biodiesel production processes, a PE modeling is required. This work aims to develop a PE modeling for biodiesel reaction systems including components from esterification and transesterification reactions. Firstly, components were defined and thermophysical properties for acylglycerols were estimated and compared to experimental data. VLE, LLE and VLLE databanks of experimental data for biodiesel reaction systems were developed and a thermodynamic modeling using NRTL model was proposed. The experimental data sets were selected based on the range of pressure and temperature of interest, thermodynamic consistency and type of raw materials. A suitable description of PE data was obtained for most systems up to 750 kPa. Moreover, experimental results reported to SAC and homogeneous alkali-catalyzed (HAC) processes using CDC and reactive distillation column (RDC) were used to validate simulations accomplished in Aspen Plus. Finally, three sets of binary interaction parameters for NRTL model were obtained which can be used for more reliable design and simulation of SAC and HAC biodiesel processes based on CDC and RDC.

Keywords: Biodiesel, Esterification, *NRTL*, Phase equilibrium (PE), Transesterification, Vapor-liquid-liquid equilibrium (VLLE).

4.1 INTRODUCTION

Biodiesel is a renewable biofuel employed more commonly as a blend with diesel fuel (VAN GERPEN, 2007). Biodiesel has been added mainly to improve engine performance, reduce negative environment impacts, reduce dependence from fossil fuels and aims to improve the economic development of countryside (ARANSIOLA et al., 2014; CALISKAN, 2017; CARNEIRO et al., 2017; ŽIVKOVIĆ et al., 2017). Improvement on engine performance are observed because biodiesel has high cetane number, more suitable combustion point, flash point and lubricity (ABBASZAADEH et al., 2012; KNOTHE; KRAHL; VAN GERPEN, 2010; ŽIVKOVIĆ et al., 2017).

Biodiesel is also sulfur-free, aromatic-free, non-toxic, biodegradable and reduces global warming since the CO_2 emission into the atmosphere could be absorbed in the process of oilseeds growth (ARANSIOLA et al., 2014; ŽIVKOVIĆ et al., 2017). The possible depletion of oil reserves in future years has also encouraged the biodiesel production (HÖÖK; TANG, 2013). For these reasons, in recent years, some countries such as Brazil have given more attention to increase the volume of biodiesel added to petrodiesel (RATHMANN; SZKLO; SCHAEFFER, 2012). Since 2008 Brazil started to add 2% of biodiesel to diesel (B2) and has changed to 10% (B10) in March 2018 (BRAZIL, 2016). Moreover, a B15 mixture is expected for 2023 in Brazil (BRAZIL, 2018).

Biodiesel is commonly produced by a homogeneous alkali-catalyzed (HAC) process using edible oils, also known as first generation biodiesel process (VAN GERPEN, 2005; ZHANG et al., 2003). However, competition with food industry and high raw material costs has encouraged the production of second and third generation biodiesel using non-edible oils, and residual oil and fats (ROF) (FADHIL; AL-TIKRITY; ALBADREE, 2017; HAJJARI et al., 2017; RIAYATSYAH et al., 2017). Furthermore, production of non-edible oils is a problem for small countries since large areas of land are required (HAJJARI et al., 2017). For these reasons, biodiesel production using ROF has potential economic benefit, since waste cooking oil (WCO) and animal fats and wastes (AFW) are cheaper raw materials and their use can solve the waste disposal problem (HAJJARI et al., 2017; RUIZ et al., 2017).

On the other hand, ROF contains high free fatty acid (FFA) level which is a challenge to convert to biodiesel using the HAC process involving only the use of alkaline to facilitate the transesterification reaction step (CANAKCI, M; SANLI, 2008). For that reason, a prior

acid-catalyzed pretreatment via esterification reaction is used to process ROF in order to reduce the FFA content to lower levels (CANAKCI, MUSTUFA; VAN GERPEN, 2001; ZHANG et al., 2003).

Despite this conventional process has been applied in the last years, suggestions of changes and improvements have been proposed by many authors, in order to reduce capital and operation costs, such as: use of solid-catalysts, supercritical conditions, FFA separation from ROF, reactive distillation column (RDC) and catalytic distillation column (CDC) (ALBUQUERQUE et al., 2018; ALBUQUERQUE; DANIELSKI; STRAGEVITCH, 2016; BOON-ANUWAT et al., 2015; GAURAV et al., 2013; GAURAV; NG; REMPEL, 2016; LEE; POSARAC; ELLIS, 2011; PETCHSOONGSAKUL et al., 2017; WEST; POSARAC; ELLIS, 2008).

Recently the solid acid-catalyzed (SAC) process using a CDC to convert oils with high FFA content has been reported to reduce investment and operation costs (GAURAV; NG; REMPEL, 2016). As a result, many efforts have been made to improve this technology as well as to develop lower costs heterogeneous acid-catalysts more actives and easier to be reused (CAO et al., 2008; FERNANDES; CARDOSO; SILVA, 2012; KAUR; ALI, 2015; KONWAR et al., 2016; QING et al., 2011; TALEBIAN-KIAKALAIEH et al., 2013). In addition, since new improvements in SAC process using CDC are anticipated, thus accurate representation of phase equilibrium (PE) including vapor-liquid-liquid equilibrium (VLLE) and vapor-liquid equilibrium (VLE) must be found in process simulators, since high cost are involved with catalysts, solvents and to design the column.

On the other hand, regardless of the kind of process chosen, vapor-liquid and liquid-liquid separations are almost always required in pre-treatment and purification steps of biodiesel production processes, so that VLE and liquid-liquid equilibrium (LLE) behavior must be accurately represented in commercial simulators (ALBUQUERQUE et al., 2018; ALBUQUERQUE; DANIELSKI; STRAGEVITCH, 2016; KALVELAGE et al., 2017; LEE; POSARAC; ELLIS, 2011; WEST; POSARAC; ELLIS, 2008; ZHANG et al., 2003).

Unfortunately, many authors have not given much attention to PE, mainly because it requires a wide range of PE data and is a very complex problem. Instead they use the limited number of binary interaction parameters existent in commercial simulators and they include a safety margin in equipment design in order to compensate for this drawback (GAURAV et al., 2013; GAURAV; NG; REMPEL, 2016; LEE; POSARAC; ELLIS, 2011; WEST; POSARAC;

ELLIS, 2008; ZHANG et al., 2003). However, in order to obtain more reliable and robust simulations of biodiesel production processes compared to real plants, a PE modeling simultaneously valid for VLLE, VLE and LLE region is required (LUYBEN, 2013; LUYBEN; YU, 2008; SANDLER, 2015; SEADER; HENLEY; ROPER, 2011).

For all those above reasons and the lack of a realistic thermodynamic modeling in commercial simulators that can represent simultaneously the tri-phasic equilibrium (VLE, LLE and VLLE) involved in biodiesel systems, this work has been proposed (ANDRADE, 1991; 1997). Therefore, it aims to develop a PE modeling for biodiesel reaction systems including components from esterification and transesterification reactions.

Firstly, an evaluation and an estimation of the thermophysical properties for acylglycerols (ACG) was carried out in order to solve problems for the representation of pure component properties in process simulators, as found in Aspen Plus V8.8 (CERIANI; GANI; LIU, 2013; SU et al., 2011; ZONG; RAMANATHAN; CHEN, 2009; 2010). Then, VLE, LLE and VLLE databanks for biodiesel reaction systems were developed and a thermodynamic modeling using the Non-Random two-liquid (NRTL) model was proposed. Finally, experimental results reported for SAC and HAC processes using CDC and RDC were validated through Aspen simulations based on the PE modeling developed and kinetic data reported (HE; SINGH; THOMPSON, 2006; NOSHADI; AMIN; PARNAS, 2012). Two and one set of interaction parameters for NRTL model were obtained for SAC and HAC processes, respectively.

4.2 MATERIALS AND METHODS

4.2.1 Definition of the components

Triolein (OOO), oleic acid (OA), methanol (M), methyl oleate (MO), water (W) and glycerol (G) were chosen as representative components based on esterification and transesterification reactions. Only one TAG, FFA and FAME derived from the oleic fragment were adopted in order to simplify the simulation and the thermodynamic modeling. Moreover, WCO derived from frying oils are composed mainly by TAG containing oleic fragments after frying due to the double-bond oxidation in linoleic fragments (ALCANTARA et al., 2000;

NASERI et al., 2013). Methanol was chosen as the alcohol due to the higher conversion obtained by methanolysis and its cheaper price, besides of there is no azeotrope formation with water (MA; HANNA, 1999). In accordance with the triolein choice, diolein and monoolein were the diacylglycerols (DAG) and monoacylglycerols (MAG) chosen for this study.

4.2.2 Evaluation and estimation of thermophysical properties

In this step, the pure components properties were evaluated. For triolein the estimation of some properties by group contribution (GC) and constituent fragments (CF) methods were necessary, such as: vapor pressure, liquid heat capacity, liquid density (liquid molar volume), heat of vaporization and liquid viscosity (CERIANI; GANI; LIU, 2013; SU et al., 2011; ZONG; RAMANATHAN; CHEN, 2009). The other acylglycerols (DAG and MAG) properties were estimated using the same methods, except vapor pressure that was also calculated by a CF approach (ZONG; RAMANATHAN; CHEN, 2010). Furthermore, other acylglycerols pure properties were estimated using methods found in the Estimation mode of Aspen Plus V8.8 software, such as: ideal gas heat capacity (C_P^{ig}) by Benson's method, critical pressure (P_c) by Gani's method, critical temperature (T_c) and critical volume (V_c) by Fedors' method (COHEN; BENSON, 1993; CONSTANTINOU; GANI, 1994; FEDORS, 1982; POLING; PRAUSNITZ; O'CONNELL, 2001).

4.2.3 Phase equilibrium databank

In order to build a VLE, LLE and VLLE databank for multicomponent mixtures involved in biodiesel production, our research group carried out an extensive survey on Web of Science website from January 2nd, 2017 to December 30th, 2017 as proposed by Corrêa et al. (2015).

4.2.3.1 Vapor-liquid equilibrium (VLE) databank

For the VLE data, 19,300 results from vapor liquid equilibr* keyword were obtained, where * is a truncation symbol meaning any number of characters including none. Subsequent refinements were carried out using other keywords such as: biodiesel, edible oil, fat*, methyl ester, methyl oleate, ethyl ester, ethyl oleate, vegetable oil, acylglycerol, non-edible oil, soybean, palm and glycerol (CORRÊA; RIBEIRO; CERIANI, 2015; PONTES; ALBUQUERQUE; STRAGEVITCH, 2017). Some binary VLE data were also retrieved from Aspen Plus V8.8 through TDE NIST tool, mainly for well-known binary mixtures as methanol-water, methanol-glycerol and water-glycerol.

Other features were also analyzed as the most frequently used thermodynamic models, pressure and temperature ranges, the amount of experimental data, and whether thermodynamic consistency tests were used to evaluate the data obtained. Experimental data that had not been submitted to the consistency test were analyzed by the Redlich-Kister area test (RKAT) through Aspen Plus V8.8 software (HERINGTON, 1947; PONTES; ALBUQUERQUE; STRAGEVITCH, 2017; REDLICH; KISTER, 1948).

4.2.3.2 Liquid-liquid equilibrium (LLE) databank

From LLE data survey on Web of Science website, 67,013 results were obtained from liquid liquid equilibr* keyword. As for VLE data, the same keywords were used to refine the survey for the same period of time. In addition, some features were added to LLE databank based on reported papers such as: thermodynamic models, number of tie lines, mixtures separated by temperature, use of Hand (H) or Othmer Tobias (OT) correlation, mole or mass fraction and the type of mixture (CARNITI; CORI; RAGAINI, 1978; CORRÊA; RIBEIRO; CERIANI, 2015; OTHMER; TOBIAS, 1942; PONTES; ALBUQUERQUE; STRAGEVITCH, 2017). It is worth to mention that H and/or OT correlations are commonly used in the literature as a quality test of LLE data. However, Carniti, Cori and Ragaini (1978) proved that even when LLE data agree to these correlations, they are unsuitable as a check of LLE data. As a result, H and/or OT correlations were not applied in this work, since few data were found for some systems of interest.

4.2.3.3 Vapor liquid-liquid equilibrium (VLLE) databank

From VLLE data survey on Web of Science website, 412 results were obtained from vapor-liquid-liquid equilibr* keyword. As for VLE and LLE data, the same keywords were used to refine the survey and the same features were considered to classify the VLLE data. However, thermodynamic consistency was not tested since VLLE data are scarce in the literature.

4.2.4 Thermodynamic modeling

In order to obtain more safety on the design and simulation steps of separation and coupled reactive separation processes, a thermodynamic modeling including the main components involved in biodiesel production processes was developed. The NRTL model was chosen since it takes in account the presence of strong polar compounds and deals easier with pseudo-components (RENON; PRAUSNITZ, 1968). Ideal behavior was considered for vapor phase because low to moderate pressures are usually adopted in biodiesel production processes (30–750 kPa). In addition, when phase equilibrium data involving two components were not found, NRTL binary interaction pairs were estimated by Universal Functional-group Activity Coefficients (UNIFAC) model using the Estimation tool from Aspen Plus V8.8 (FREDENSLUND; GMEHLING; RASMUSSEN, 1977).

The data were chosen based on some criteria, such as: PE data including methanol instead of ethanol; VLE data approved on thermodynamic consistent test consisting of PTxy data, besides of some PTx, Px and Tx data; data from low to moderate pressures and some VLE data for well-known systems retrieved from TDE NIST tool on Aspen Plus V8.8 including data published from 1970 onwards; LLE data including the interactions between the pure components chosen, LLE data for vegetable oils and FAME with major 18 carbons in FFA composition as derived from soybean, sunflower, canola and jatropha curcas oils; and all ternary VLLE data were included

The regression of VLE data was carried out through Barker's modified method based on minimization of objective function F_{BM} given by Equation 4.1 from tml-vle code,

$$F_{BM} = \sum_{n=1}^{N_{exp}} \left[\left(\frac{P_n^{exp} - P_n^{cal}}{\sigma_P} \right)^2 + \sum_{i=1}^{N_c} \left(\frac{y_{i,n}^{exp} - y_{i,n}^{cal}}{\sigma_y} \right)^2 \right] \quad (4.1)$$

where σ_P and σ_y are uncertainties observed in P and y_i; N_c are the total number of components i (BARKER, 1953). The experimental (exp) and calculated (cal) results involved in VLE systems were compared using the average absolute deviation (AAD) according to Equation 4.2.

$$AAD(V) = \frac{1}{N_{exp}} \sum_{n=1}^{N_{exp}} \left| V_n^{exp} - V_n^{cal} \right| \quad (4.2)$$

In Equation 4.2, V represents the variable temperature (T), pressure (P) or vapor phase composition (y) in mole fraction; N_{exp} are the total number of experimental points n.

The LLE data were correlated through simplex method based on minimization of objective function (F_S) proposed by Stragevitch and d'Ávila (1997) through tml-lle code,

$$F_S = \sum_{i=1}^{N_{c,k}} \sum_{j=1}^{N_{t,k}} \sum_{k=1}^{N_D} \sum_{l=1}^{2} \left(w_{ijk}^{(l),\mathrm{exp}} - w_{ijk}^{(l),\mathrm{cal}} \right)^2 \quad (4.3)$$

where w is the phase composition (mass fraction); $N_{c,k}$ and $N_{t,k}$ are, respectively, the number of components and tie lines in the k-th data set; N_D is the number of data sets simultaneously correlated; subscripts i, j and k denote components, tie lines and data sets, respectively; and superscript l denotes liquid phases in equilibrium (STRAGEVITCH; D'AVILA, 1997). Experimental and calculated compositions involved in LLE systems were compared using the root mean square deviation at mass fraction units ($RMSD_w$), according to

$$RMSD_w = 100\sqrt{\frac{1}{2N_t N_c}\sum_{i=1}^{N_c-1}\sum_{j=1}^{N_t}\sum_{l=1}^{2}\left(w_{ij}^{(l),\exp} - w_{ij}^{(l),\mathrm{cal}}\right)^2} \tag{4.4}$$

for each data set as well as a global deviation involving all correlated LLE data sets.

These both procedures were developed and implemented by Stragevitch and d'Ávila (1997) in tml-vle and tml-lle codes in Fortran language (ANDRADE, 1991; 1997; STRAGEVITCH; D'AVILA, 1997). The VLLE data regression was initially carried out through the minimization of Maximum Likelihood objective function (F_{ML}) given by Equation 4.5 in Aspen Plus V8.8.

$$F_{ML} = \sum_{k=1}^{N_D}\omega_k \sum_{n=1}^{N_{exp}}\left\{\left(\frac{P_n^{exp} - P_n^{cal}}{\sigma_{P_n}}\right)^2 + \left(\frac{T_n^{exp} - T_n^{cal}}{\sigma_{T_n}}\right)^2 + \sum_{i=1}^{N_c}\left[\sum_{l=1}^{2}\left(\frac{x_{in}^{(l),\exp} - x_{in}^{(l),\mathrm{cal}}}{\sigma_{x_{i,n}}}\right)^2\right] + \left(\frac{y_{i,n}^{exp} - y_{i,n}^{cal}}{\sigma_{y_{i,n}}}\right)^2\right\} \tag{4.5}$$

In Equation 4.5 σ_T and σ_x are uncertainties observed in T and x_i, ω_k is a weight of data group n, while all other variables were defined in the same way as for Equations 4.1 and 4.3. However, Barker's modified method given by Equation 4.1 was left as a contingent plan just in case unsuccessful results was obtained from simultaneously correlation of VLLE, LLE and VLE data using the ML method. Experimental and calculated compositions involved in VLLE systems were compared using the root mean square deviation with mole fraction units ($RMSD_x$) instead of mass fractions in Equation 4.4. As stated by Andrade (1997), there is not available a procedure to carry out simultaneous VLE, LLE and VLLE correlation in order to obtain a unique set of binary interaction parameters. Furthermore, the procedure proposed by Andrade (1997) to correlate the phase equilibrium data was not successful, so that the following steps were adopted to obtain more suitable binary interaction parameters (ANDRADE, 1991):

1. VLE data for well-known binary mixtures (methanol-water, methanol-glycerol and water-glycerol) were evaluated using tml-vle code based on binary interaction parameters found in Aspen Plus V8.8 software;
2. The binary interaction parameter between methanol and methyl oleate found in Aspen Plus V8.8 software was evaluated using tml-vle code;
3. Binary and ternary VLE data involving FAME/methanol/glycerol were correlated by regression of methyl oleate-glycerol interaction.
4. The binary parameters obtained on step 3 was used to evaluate ternary LLE data for the same mixture although unsuccessful results suggested to correlate methyl oleate-glycerol interaction to obtain new parameters;
5. The parameters obtained from LLE data regression were used to evaluate the VLE data from step 3; however, unsuccessful results were also obtained. Therefore, steps 3 to 5 were repeated until to realize that no evidence of changes was found.
6. After many unsuccessful results, step 4 was repeated including an initial estimation for a temperature-dependent parameter for methanol-glycerol interaction. Suitable agreement to LLE data was obtained suggesting to return to steps 3 to 5.
7. After some successful correlations of VLE and LLE data for mixture FAME/methanol/glycerol, VLLE data was evaluated using Aspen Plus V8.8 software obtaining properly results, although VLE binary mixtures methanol-glycerol had some deviations mainly for conditions close to pure glycerol;
8. VLE, LLE and VLLE data were correlated simultaneously using Aspen Plus V8.8 based on F_{ML} from Equation 4.5; however, unsuccessful results were obtained mainly because large temperature variations were detected;
9. After unsuccessful correlation of the PE data, temperature-dependent (a_{ij} and a_{ji}) interactions for methanol-glycerol mixture were correlated based on Barker's modified method from Equation 4.1. More suitable results for VLE for this mixture were found and comparable deviations relative to other VLE, LLE and VLLE data based on previously parameters from step 6 were obtained.
10. Similar procedure was carried out to correlate VLE and LLE data for other mixtures following steps 1 to 6.

4.2.5 Kinetic models

Unlike the conventional HAC transesterification reaction, where most researchers consider three equilibrium reaction steps, for SAC route the reaction kinetic has only been considered from the global reaction. The reason is that higher molar ratio (MR) of methanol to oil (10 to 70) is commonly adopted for SAC processes compared to conventional HAC process, so that the kinetic constants from forward reactions are favored. As for transesterification case, esterification has been also considered by many authors as one-step reaction (FERNANDES; CARDOSO; SILVA, 2012; GAURAV; NG; REMPEL, 2016; TALEBIAN-KIAKALAIEH et al., 2013).

In order to validate the SAC process using a CDC, the kinetic models developed by Fernandes, Cardoso and Silva (2012) and Talebian-Kiakalaieh et al. (2013) were adopted for each reaction. Both transesterification and esterification kinetics were defined as pseudo-first-order rate law given by Equations 4.6 to 4.7,

$$\frac{dC_{TAG}}{dt} = -k'_{trans} \cdot C_{TAG} \tag{4.6}$$

$$\frac{dC_{FFA}}{dt} = -k'_{ester} \cdot C_{FFA} \tag{4.7}$$

where C_{TAG} and C_{FFA} are molarity of TAG (OOO) and FFA (OA) components at mol·L^{-1}; k'_{trans} and k'_{ester} are pseudo-kinetic constants (high MR of methanol to oil) for the transesterification and esterification reactions at sec^{-1}; and t is the reaction time. In addition, the kinetic constants for both reactions can be obtained from Arrhenius equation given by Equation 4.8,

$$k'_r = k_0 \cdot exp\left(\frac{-E_a}{RT}\right) \tag{4.8}$$

where k_0 is the pre-exponential factor at sec^{-1}, E_a is the activation energy at $kJ \cdot (mol \cdot K)^{-1}$, T is temperature at K and k'_r is a pseudo-kinetic constant for reaction r (FERNANDES; CARDOSO; SILVA, 2012; GAURAV; NG; REMPEL, 2016; TALEBIAN-KIAKALAIEH et al., 2013).

In order to also validate the NRTL parameters for the HAC process using RDC, the kinetic model proposed by Mueanmas, Prasertsit and Tongurai (2010) was adopted, so that DAG and MAG were also considered.

4.2.6 Kinetic and phase equilibrium model validation

From the kinetic models, thermophysical properties of ACG and PE modeling, a kinetic and PE validation was carried out based on reported experiments. The CDC and RDC simulation results were compared to experimental ones from SAC process studied by Noshadi, Amin and Parnas (2012) and HAC process studied by He, Singh and Thompson (2006), respectively. The SAC process also included a preheater/mixer/reactor, in order to obtain higher reaction conversions at lower time as shown in Figure 4.1. FAME yield (%) was the response evaluated based on response surface methodology (RSM) and central composite design (CCD) methodology by varying the following variables: total feed flow rate F (mol/h), reboiler duty Q_{reb} (kW), inlet temperature T (°C) and MR of methanol to oil. In addition, some temperature profiles were also measured. On the other hand, results from He, Singh and Thompson (2006) without prereactor were also compared to simulated ones based on component mass fractions (w_i), conversion (X_A), yield and reboiler temperature (T_{reb}).

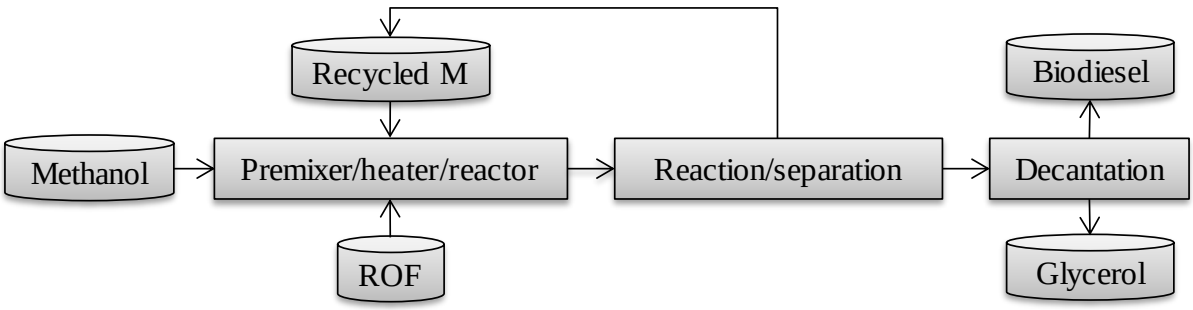

Figure 4.1 – SAC biodiesel production by reaction/separation including a preheater/mixer/reactor
Source: Adapted from Noshadi, Amin and Parnas et al. (2012).

4.3 RESULTS AND DISCUSSION

4.3.1 Evaluation and estimation of thermophysical properties

The pure properties from all components were compared with those from literature through the more recognized online databanks as NIST and REAXYS from Elsevier. Most part of temperature-dependent pure properties for triolein were estimated based on GC and CF methods. Vapor pressure of triolein (P_{OOO}^{vap}) was calculated based on methods proposed by Ceriani, Gani and Liu (2013) and Ceriani and Meirelles (2004). Figure 4.2a shows the comparison between calculated P_{OOO}^{vap} and experimental data available for soybean oil, tristearin (SSS) and for triolein (GOODRUM; GELLER, 2002; LEE; POSARAC; ELLIS, 2011; PERRY; WEBER; DAUBERT, 1949; SANTANDER et al., 2012). From these results, the method proposed by Ceriani and Meirelles (2004) method could be judged as the most suitable since agree to data on higher temperatures. However, the approach proposed by Ceriani, Gani and Liu (2013) was also shown to be an excellent choice. This could also be concluded by comparing the estimated boiling point to experimental data as shown in Table 4.1.

On the other hand, when enthalpy of vaporization of triolein (ΔH_{OOO}^{vap}) was calculated from those methods an unexpected behavior was estimated from Ceriani and Meirelles' model as shown in Figure 4.2b (CERIANI; MEIRELLES, 2004). For this reason, Ceriani, Gani and Liu (2013) proposed an update, including a correction factor for higher temperatures, so that the expected behavior of decreasing ΔH_{OOO}^{vap} when temperature increases was observed. In addition, from this method a ΔH_{OOO}^{vap} = 172 kJ/mol was estimated, which is very close to experimental one for soybean oil 185 kJ/mol between 527 and 581 K (PERRY; WEBER; DAUBERT, 1949). Therefore, this model was adopted to estimate the P_{OOO}^{vap}. The definition method from Aspen Plus V8.8 based on Clausius-Clayperon equation was used to calculate ΔH_{OOO}^{vap} as shown in Figure 4.2b (CERIANI; GANI; LIU, 2013).

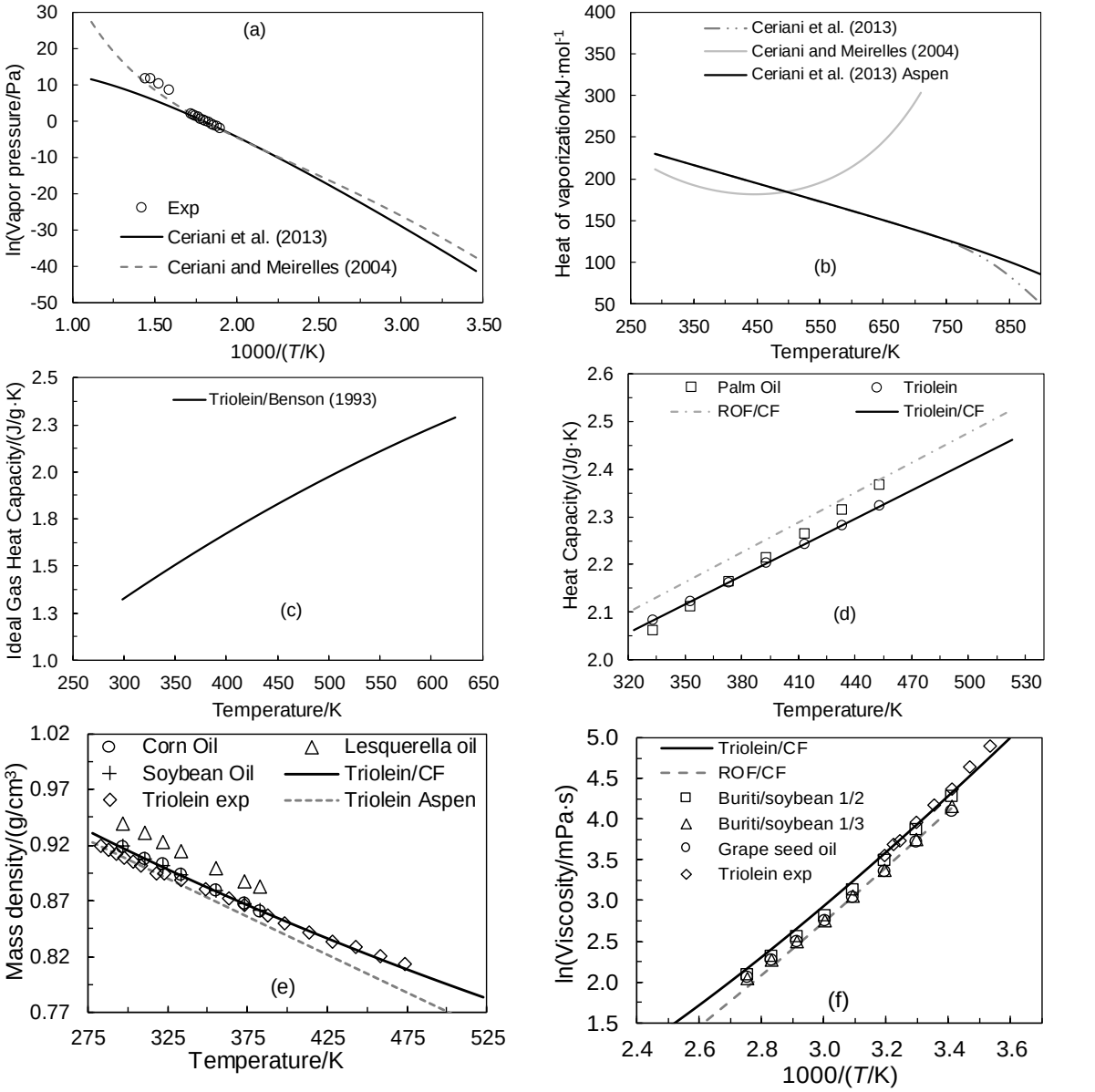

Figure 4.2 – Thermophysical properties for some vegetable oils and triolein (experimental) and for ROF and triolein (predicted)

Source: Adapted from Albuquerque et al. (2018), Benson (1976), Ceriani, Gani and Liu (2013), Ceriani and Meirelles (2004), Ceriani et al. (2008), Dickinson, McLure and Al-Nakash (1980), Exarchos, Tasioula-Margari and Demetropoulos (1995), Goodrum and Geller (2002), Jaeger (1917), Knothe and Steidley (2007), Lee, Posarac and Ellis (2011), Morad et al. (2000), Noureddini, Teoh and Clements (1992), Perry, Weber and Daubert (1949), Santander et al. (2012) and Zong, Ramanathan and Chen (2009).

Table 4.1 – Comparison between experimental and calculated boiling points for triolein

Experimental (K)	GC1[c] (K)	ARD (%)[d]	GC2 (K)[e]	ARD (%)[d]	Aspen (K)	ARD (%)[d]
685.95[a] (692.25)[b]	709.15	3.4 (2.4)	899.15	31.1 (29.9)	1120	63.3 (61.8)

[a] Lee, Posarac and Ellis (2011); [b] Santander et al. (2012); [c] GC1 refers to group contribution approach proposed by Ceriani and Meirelles (2004); [d] ARD means average relative deviation calculated by $ARD(\%) = 100 \cdot \left|\frac{exp-cal}{exp}\right|$; [e] GC2 refers to group contribution approach proposed Ceriani, Gani and Liu (2013).

It is worth to mention that critical properties were required and estimated using the Estimation mode of Aspen Plus V8.8, since no experimental data of critical properties is currently available for long chain TAG compounds. From the experimental boiling point (T_B) of triolein, values of T_c = 1043.29 K, P_c = 3.22 bar and V_c = 3.1 cm^3/kmol were estimated. These values were very close to T_c = 977.88 K and P_c = 3.34 bar presented by Glišić et al. (2007), while the V_c value was the same found in Aspen Plus V8.8. Furthermore, C_P^{ig} of triolein was estimated from Benson's method on Estimation mode of Aspen Plus V8.8 as shown in Figure 4.2c (BENSON, 1976).

Liquid heat capacity (C_p^l), mass density (ρ^l) and viscosity (η) of triolein were estimated by the CF approach and compared to experimental data from vegetable oils and triolein as shown in Figure 4.2d-f. From these results, estimated C_p^l, ρ^l and η of triolein agreed with experimental data and ROF calculated by the same method (ALBUQUERQUE et al., 2018; CERIANI et al., 2008; DICKINSON; MCLURE; AL-NAKASH, 1980; EXARCHOS; TASIOULA-MARGARI; DEMETROPOULOS, 1995; JAEGER, 1917; KNOTHE; STEIDLEY, 2007; NOUREDDINI; TEOH; CLEMENTS, 1992; ZONG; RAMANATHAN; CHEN, 2009).

4.3.2 Phase equilibrium databank

4.3.2.1 Vapor-liquid equilibrium (VLE) databank

The VLE databank was composed of 181 mixtures and 5,961 data obtained from 100 papers as shown on Table 4.2. As expected this new databank has more mixtures and VLE data than that developed by Corrêa, Ribeiro and Ceriani (2015). However, mixtures containing more than three compounds were not found as shown on Table 4.2 and an update needs to be carried out in the future. It is worth to note that a distinction between mixture and system was adopted in this work. For instance, Table 4.2 shows the number of systems from different authors. Moreover, alcohol/water refers mostly to methanol/water systems and less to ethanol/water systems. In this case, only two mixtures have been included.

Table 4.2 – Classification of VLE data for mixtures involved in the biodiesel production

Class of compounds	Type of systems	Number of systems	Number of experimental data
Alcohol/Water	Binary (Bin)	80	1,235
Alcohol/Glycerol		61	609
Water/Glycerol		49	575
Fatty Acid/Fatty Acid		17	167
Fatty Acid/Fatty Ester		1	9
Alcohol/Fatty Ester		89	1,093
Water/Fatty Ester		1	8
Fatty ester/Fatty ester		44	399
Alcohol/Triglyceride		8	46
Fatty Acid/Monoglyceride		2	24
Fatty acid/Monoglyceride		2	22
Alcohol/Fatty Acid		2	25
Alcohol/Vegetable oil	Pseudobinary (Pbin)	12	387
Alcohol/Biodiesel		70	930
Alcohol/Glycerol/Water	Ternary (Tern)	18	84
Alcohol/Fatty Ester/Fatty Ester		1	34
Alcohol/Glycerol/Fatty ester		18	51
Alcohol/Biodiesel/Water	Pseudoternary (Ptern)	40	100
Alcohol/Biodiesel/Glycerol		43	134
Alcohol/Biodiesel/Vegetable oil		7	48
Total		**565**	**5,980**

Source: Adapted from Pontes, Albuquerque and Stragevitch (2017).

During the construction of VLE databank, we also analyzed the most used thermodynamic models, pressure and temperature ranges and the amount of experimental data as shown in Table 4.3. In addition, we evaluated if tests of thermodynamic consistency were reported to evaluate the data. Therefore, experimental data for low to moderate pressures (until 10 bar) that had not been subjected to these tests were analyzed through the Redlich-Kister area test (RKAT) using Aspen Plus V8.8 software (HERINGTON, 1947; PONTES; ALBUQUERQUE; STRAGEVITCH, 2017; REDLICH; KISTER, 1948). However, only VLE data including vapor molar fraction (y) could be tested by RKAT, since the root mean-square (RMS) error in y is commonly within experimental error of y (PRAUSNITZ; LICHTENTHALER; AZEVEDO, 1999). For that reason, only some Px, Tx and PTx data were considered in the thermodynamic modeling.

Among the 181 mixtures, 33 were reported as thermodynamically consistent, while for the other systems only 61 mixtures presented PTxy data, applicable to the RKAT. These were subjected to consistency test adopting a tolerance of 10%, a standard criterion from Aspen Plus

V8.8. From these PTxy data, 28 mixtures (46%) were accepted and 17 mixtures (28%) were rejected by the test indicating thermodynamic inconsistencies; while 16 mixtures (26%) could not be tested due to the lack of enough experimental points. Furthermore, 16 mixtures were not tested because 5 and 8 were ternary and high-pressure systems, respectively, while 3 systems were both ternary with high pressures. In this work, high pressures systems (greater than 10 bar) were not considered since high temperatures can cause decomposition reactions of fatty compounds.

Table 4.3 – Classification of mixtures based on type of data, correlation and GC models used

Type	Type of data				Correlation model			GC model	
	PTx	PTxy	Isobaric P (kPa)	Isothermic T (K)	UNIQ[a]	NRTL	Other	UNIF[b]	ASOG[c]
Bin	192	164	172 (0.1-1x10^4)	98 (244-573)	123	137	239	110	24
Pbin	79	3	42 (6.7-101.3)	17 (348-573)	52	2	20	14	
Tern	12	25	19 (6.7-100.4)	18 (493-523)	13	2	19		
Ptern	90		80 (6.7-66.7)		80				

[a] UNIQ means Universal QuasiChemical (UNIQUAC) model;
[b] UNIF means UNIFAC model;
[c] ASOG means Analytical Solutions of Groups model.

4.3.2.2 Liquid-liquid equilibrium (LLE) databank

The LLE databank was composed of 185 systems and 2,411 data obtained from 74 papers as shown on Table 4.4. As expected this new databank has more systems and LLE data than that developed by Corrêa, Ribeiro and Ceriani (2015). It should be noted that there can be less than 185 mixtures since some mixtures were reported in more than one paper. However, these systems were considered separately because the components can present difference in purities.

During the elaboration of LLE databank, we also analyzed the most used thermodynamic models, temperature ranges, number of tie line data and number of systems that reported use of H and/or OT correlation as shown in Table 4.5 (CARNITI; CORI; RAGAINI, 1978; OTHMER; TOBIAS, 1942).

Table 4.4 – Classification of LLE data for mixtures involved in the biodiesel production

Class of compounds	Type of mixtures	Number of systems	Number of tie lines
TAG/Glycerol	Binary (Bin)	1	9
Fatty acid alkyl ester (FAAE)/Glycerol		1	14
Alcohol/Vegetable oil (VO)	Pseudobinary (Pbin)	11	79
VO/Glycerol		1	3
Biodiesel/Glycerol		1	3
Alcohol/FAAE/Glycerol	Ternary (Tern)	13	238
Alcohol/FAAE/Water		8	121
Alcohol/TAG/FFA		2	22
Alcohol/FFA/Water		2	10
MAG/FAAE/Glycerol		1	4
FAAE/Glycerol/Water[a,b]		4	31
Alcohol/VO/FFA	Pseudoternary (Ptern)	15	122
Alcohol/VO/Biodiesel		6	73
Alcohol/VO/Glycerol		1	9
Alcohol/Biodiesel/Glycerol		33	418
Alcohol/Biodiesel/Water		20	222
Alcohol/VO/Water		4	32
Alcohol/FFA/Water		1	8
VO/Biodiesel/Glycerol		1	9
Biodiesel/Glycerol/Water		9	108
Alcohol/FAAE/Glycerol/NaCl	Quaternary (Quat)	1	9
Alcohol/FFA/FAAE/Water		1	10
Alcohol/VO/Biodiesel/Glycerol	Pseudo quaternary (Pquat)	1	3
Alcohol/Biodiesel/Glycerol/Water		8	76
Alcohol/VO/FFA/Water		21	481
Alcohol/Biodiesel/Glycerol/NaOH		2	22
Alcohol/VO/DAG/MAG/FFA	Pseudoquinary (Pquin)	3	34
Alcohol/VO/FFA/FFA/Water		2	55
Alcohol/VO/DAG/MAG/FAAE[b]		7	107
Alcohol/VO/DAG/MAG/Biodiesel/Glycerol	Pseudosixnary (Psix)	2	34
Alcohol/VO/FFA/DAG/MAG/FAAE[b]		2	45
Total		185	2411

[a] Four systems have glycerin instead glycerol
[b] Four, two and two systems with pressure below atmospheric pressure for Tern, Pquin and Psix mixtures.

Table 4.5 – Classification of systems, range of T, data quality, correlation and GC models

Type	Number of systems	Range of T (K)	NRTL	UNIQ[a]	Other	UNIF[b]	ASOG	H/OT
Bin	2	323-383			2			
Pbin	13	298-341	13	3				5
Tern	30	293-408	17	9	5	15	2	19
Ptern	90	293-343	41	53	2	10	2	33
Quat	2	323-346	1	2		1		1
Pquat	32	283-338	23	22				6
Pquin	12	298-318	12	2		7		
Psix	4	298-333	3	1		2		
Total	185	283-408	110	92	9	35	4	64

[a] UNIQ means UNIQUAC model
[b] UNIF means UNIFAC model

4.3.2.3 Vapor-liquid-liquid equilibrium (VLLE) databank

VLLE data for systems involved in biodiesel production are scarce, so that VLLE databank was only composed from two systems relative to one ternary mixture as shown in Table 4.6. These systems were reported by Andreatta et al. (2008) and Barreau et al. (2010) as isothermic PTxx data. Andreatta et al. (2008) modelled the systems using GC with association equation of state (GCA-EOS) and UNIFAC with association (UNIFAC-A), while Barreau et al. (2010) employed a GC method with a statistical associated fluid theory equation of state (GC-PPC-SAFT).

Table 4.6 – Classification of VLLE data for systems involved in the biodiesel production

Class of compound	Type of		Number of		Isothermic	Range of
	mixture	data	systems	data	T (K)	P (kPa)
Alcohol/FAAE/Glycerol	Ternary	PTxx	2	46[a]	2 (333-473)	60-2660

[a] Five data from Barreau et al. (2010) were reported in VLE region, in this case number of data could be 41.

4.3.3 Thermodynamic modeling

The results obtained from the thermodynamic modeling of phase equilibrium for VLE, LLE and VLLE systems were compared to experimental ones as shown in Table 4.7 and Table 4.8 according to NRTL1. According to these results, values of AAD for pressure (AAD_P), temperature (AAD_x) and vapor mole fraction (AAD_y) and $RMSD$ for mass ($RMSD_w$) and mole ($RMSD_x$) fractions for NRTL1 can be considered to be low since difficulties were found to correlate simultaneously VLE, LLE and VLLE data. Furthermore, the binary parameters available on Aspen Plus databank for methanol-water, water-glycerol and methanol-methyl oleate (M-MO) interactions were kept constant. The unique exception was the methanol-glycerol (M-G) interaction parameter, where a temperature-dependent parameter (a_{ij} and a_{ji}) was regressed in order to agree simultaneously with VLE, LLE and VLLE data from binary and ternary mixtures of methyl oleate/methanol/glycerol. Related to the interaction parameters for the other components, they were obtained through VLE and LLE data as described by steps 1 to 6 presented in methodology section 4.2.4. All these binary interaction parameters for NRTL1 are showed in Table 4.9.

Some binary experimental data for VLE data were compared to NRTL calculated ones as shown in Figure 4.3 for isobaric systems methanol (M)/glycerol (G) at 66.7 kPa, methanol/soybean FAME (MO) at 66.7 kPa, methanol/methyl oleate (MO) at 101.325 kPa and methanol/water (W) at 101.325 kPa (FU; WANG; HU, 1989; GAO et al., 2006; OCHI; KOJIMA, 1987; OLIVEIRA et al., 2010; SILVA, et al., 2016; VENERAL et al., 2013; VERHOEYE; DE SCHEPPER, 1973). From these results, it can be concluded that the diagrams calculated by NRTL1 model agreed with the binary VLE data. However, some deviations were found in the systems M/G between 66.7 kPa (Figure 4.3a) to 101.325 kPa due to regression of a temperature-dependent parameter for M-G interaction in order to fit VLE, LLE and VLLE data simultaneously. The M-MO system at 101.325 kPa was also found to have some deviation close to pure MO compositions. Parameters retrieved from Aspen Plus V8.8 can be the reason since was obtained from VLE data with methanol mole fraction between 0.36 and 0.90 besides of pressure range from 6.7 to 66.7 kPa. On the other hand, higher values of uncertainties are expected to obtain pure biodiesel at temperatures above 548.15 K (decomposition temperature). For example, according to NIST TDE tool from Aspen Plus V8.8, vapor pressure data of MO at 101.325 kPa has nearly ±50% uncertainty related to pressure.

Table 4.7 – Average absolute deviations for VLE systems correlated by NRTL model

Class of compounds	NRTL	Number of systems	Number of exp data	AAD_P /kPa	AAD_T /K	AAD_y
Methanol/Water	1	73	1136	1.52	0.48	0.0092
	2					
	3			1.52	0.50	0.0091
Methanol/Glycerol	1	16	190	10.46	4.07	
	2			9.77	3.54	
	3			9.87	1.83	
Water/Glycerol	1	54	563	8.17	5.7	0.0521
	2					
	3			7.05	6.95	0.0628
Methanol/FAME[b]	1	18	187	6.39	2.75	0.0011
	2			3.77	1.35	0.0012
	3			7.73	2.40	0.0012
Methanol/Edible oil[a]	1	2	60	5.24		
	2			3.08		
	3			4.33		
Methanol/oleic acid	1	1	13	0.61		
	2					
	3			0.61		
Methanol/Glycerol/FAME[b]	1	10	30	0.41	0.30	
	2			0.24	0.19	
	3			0.34	0.25	
Methanol/FAME/Water[b]	1	10	20	0.55	0.38	
	2					
	3			0.68	0.46	
Methanol/FAME/Edible oil[a]	1	3	16	3.77		
	2			6.23		
	3			4.03		
Total	1	187	2215	6.29-4.49[c]	2.52-2.36[c]	0.0011-0.0197[c]
	2	49	483	5.13	1.74	0.0012
	3	187	2215	6.55-4.32[c]	1.65-2.22[c]	0.0012-0.0223[c]

[a] Fatty acid methyl esters (FAME) was represented by methyl oleate as a pseudocomponent;
[b] Edible oil was represented by triolein as a pseudocomponent and all data were correlated from soybean oil;
[c] Values before and after hyphen are relative to transesterification and transesterification-esterification systems.

Table 4.8 – Root mean square deviations ($RMSD$) for LLE and VLLE systems correlated by three set of binary interaction parameters for NRTL model

Class of compounds	NRTL	Number of systems	Number of tie lines	$RMSD_w$/ % LLE	$RMSD_x$/ % VLLE
Vegetable oil (VO)/Glycerol[a]	1	3	3	1.05	
	2			0.23	
	3			0.21	
Methanol/FAME/Glycerol[b]	1	5 (5)[c]	31 (38)[c]	1.44	1.69
	2			1.93	3.48
	3			1.25	2.82
Methanol/FAME/Water (W)[b]	1	6	30	1.52	
	2				
	3			1.67	
Methanol/VO/oleic acid[a]	1	10	43	1.97	
	2				
	3			1.99	
Methanol/VO/Glycerol (G)[a]	1	3	9	1.55	
	2			1.22	
	3			0.74	
VO/FAME/Glycerol[b]	1	3	9	0.67	
	2			0.98	
	3			0.88	
FAME/Glycerol/Water[b]	1	3	18	1.32	
	2				
	3			1.32	
Methanol/VO/FAME/G[a,b]	1	3	3	2.32	
	2			0.78	
	3			0.94	
Methanol/FAME/Glycerol/W[b]	1	3	8	1.23	
	2				
	3			1.07	
Total	1	39 (5)[c]	154 (38)[c]	1.41-1.55[d]	1.69
	2	17 (5)[c]	55 (38)[c]	1.13	3.48
	3	39 (5)[c]	154 (38)[c]	0.86-1.32[d]	2.82

[a] Vegetable oil (VO) was represented by triolein as a pseudocomponent and all data correlated were from soybean, *jatropha curcas*, corn, sunflower and canola oils;
[b] Fatty acid methyl esters (FAME) was represented by methyl oleate as a pseudocomponent;
[c] Number inside brackets is relative to VLLE and outside one to LLE;
[d] Values before and after hyphen are relative to transesterification and transesterification-esterification systems.

Table 4.9 – NRTL1 and NRTL3 binary interactions parameters for methanol (1)/triolein (2)/ oleic acid (3)/methyl oleate (4)/glycerol (5)/water (6) systems

i	j	NRTL	a_{ij} [a]	a_{ji} [a]	b_{ij}/K [a]	b_{ji}/K [a]	α_{ij}	Source
1	2	1	14.52	-4.60	-2,621.50	1,784.00	0.47	Regressed[b]
		3	14.62	-4.69				
1	3	1	0	0	459.09	-80.76	0.30	Regressed[b]
		3						
1	4	1	*Aspentech copyright*					NISTV88 NIST-IG[c]
		3	9.84	-3.37	-1,548.00	1,351.00	0.47	Regressed[b]
1	5	1	2.75	-1.22	*Aspentech copyright*			Regressed[b]
		3	2.79	-0.97	-774.97	165.55	0.47	Regressed
1	6	1	*Aspentech copyright*					APV88 VLE-IG[c]
		3	-1.39	2.39	358.23	-423.33	0.20	Regressed
2	3	1	-0.26	3.25	-604.23	-988.85	0.30	Regressed[b]
		3	-0.84	3.50	-433.32	-1,031.40		Regressed
2	4	1	10.80	9.28	701.51	-3,000.00	0.30	Regressed[b]
		3	-5.88	2.78	552.24	-672.19	0.30	Regressed[b]
2	5	1	-0.11	14.84	4,672.20	-2,713.60	0.30	Regressed[b]
		3	-1.45	5.96	2,133.30	140.66	0.20	Regressed
2	6	1	-0.49	21.22	780.49	1,0054.78	0.30	UNIFAC[d]
		3	-1.18	15.92	1,196.67	13,239.88	0.30	
3	4	1	0.15	-0.29	-177.92	343.97	0.30	UNIFAC[d]
		3	-0.04	0.02	-6.46	91.87	0.30	
3	5	1	0.76	2.92	863.90	927.08	0.30	UNIFAC[d]
		3	-0.65	1.99	1,723.76	1,499.41	0.30	
3	6	1	0.43	7.72	402.86	2,673.78	0.30	UNIFAC[d]
		3	-0.71	6.74	1,095.37	3,261.17	0.30	
4	5	1	5.33	-5.83	-506.85	3,501.40	0.27	Regressed[b]
		3	-1.17	0.01	1,871.10	1,209.50	0.20	Regressed
4	6	1	0	0	1,565.60	2,709.20	0.20	Regressed[b]
		3	0	0	1,536.10	3,000.00	0.20	Regressed[b]
5	6	1	*Aspentech copyright*					APV88 VLE-IG[c]
		3	-0.7	-1.18	324.23	179.16	0.20	Regressed[b]

[a] Binary interaction parameters were organized according to Aspen Plus: $\tau_{ij} = exp\left(a_{ij} + {}^{b_{ij}}/_{T}\right)$;

[b] Regressed means that binary interaction parameters were obtained by regression;
[c] NISTV88 NIST-IG and APV88 VLE-IG are databanks from Aspen Plus V8.8;
[d] UNIFAC means that NRTL parameters were obtained from original UNIFAC.

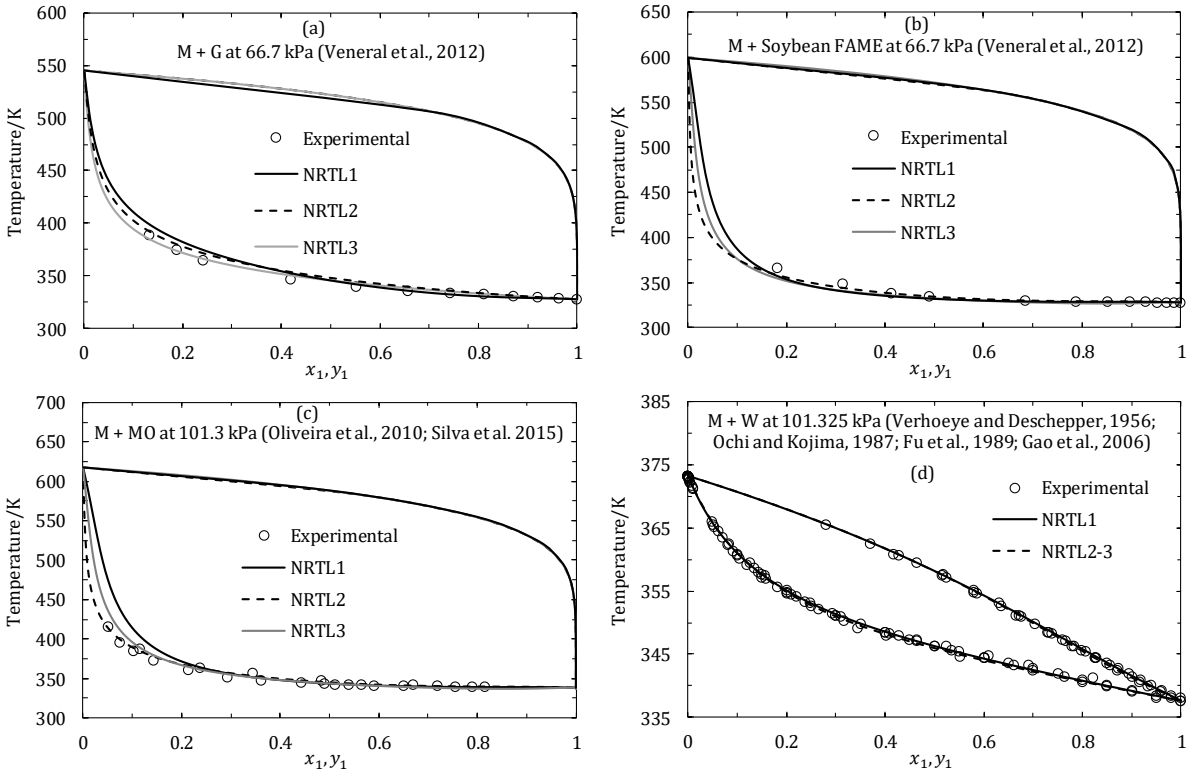

Figure 4.3 – Txy diagrams comparing VLE experimental data to calculated ones by NRTL model for systems: (a) methanol (M)/glycerol (G) at 66 kPa, (b) methanol/soybean FAME (MO) at 66.7 kPa, (c) methanol/methyl oleate (MO) at 101.325 kPa and (d) methanol/water (W) at 101.325 kPa
Source: Adapted from Fu, Wang and Hu (1989), Gao et al. (2006), Ochi and Kojima (1987), Oliveira et al. (2010), Silva et al. (2016), Veneral et al. (2013) and Verhoeye and de Schepper (1973).

Some isothermal VLE systems were also compared as shown in Figure 4.4 for the following systems: methanol (M)/methyl oleate (MO) at 373.15 K, methanol/soybean oil (OOO) at 373.15 K, water/glycerol (G) at 363.15 K and methanol/oleic acid (OA) at 318.15 K (BELTING et al., 2015; CHIU; GOFF; SUPPES, 2005; EDULJEE; BOYES, 1981; ZAOUI-DJELLOUL-DAOUADJI et al., 2014). These results confirmed the reliability of the NRTL1 binary interaction parameters obtained to represent these isothermal VLE systems involved in the biodiesel production processes. In addition, according to Figure 4.4a–b the VLE for systems M/MO and M/soybean oil are in agreement until pressures closer to 350 kPa, so that SAC biodiesel production processes can be favored since these processes are commonly carried out in a pressure range of 101.3 to 750 kPa.

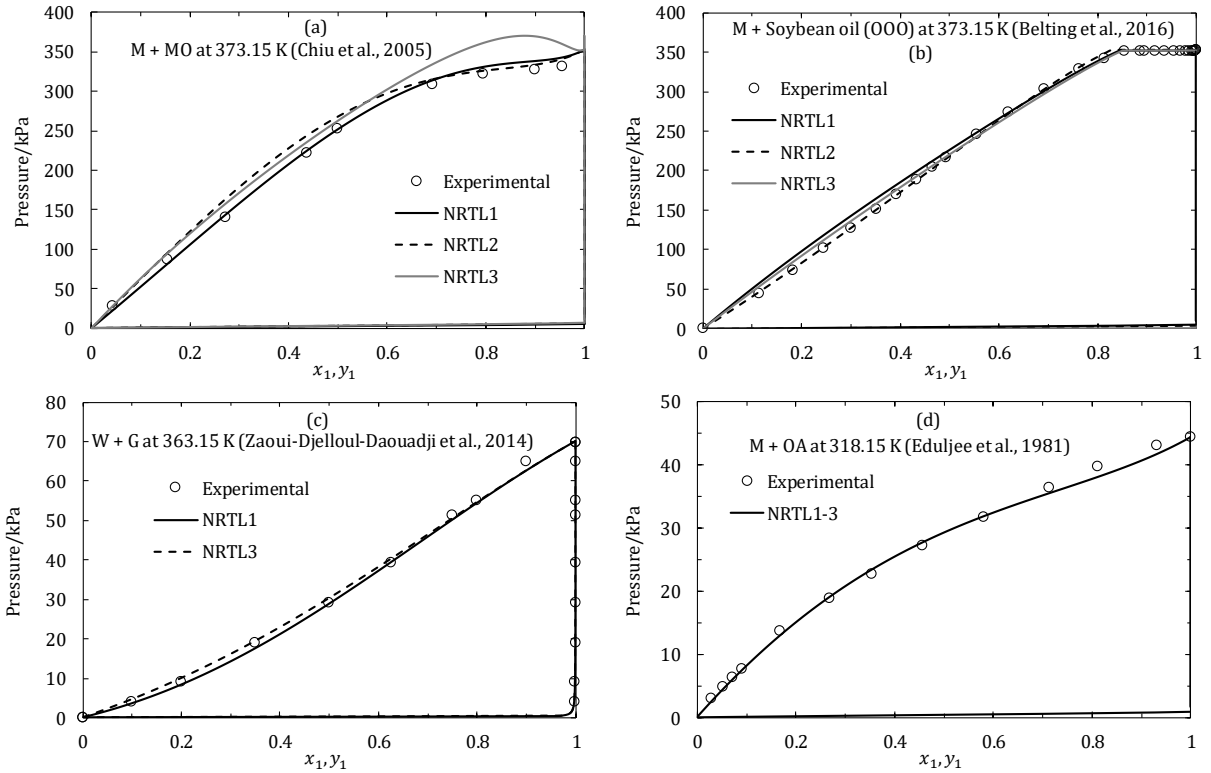

Figure 4.4 – Pxy diagrams comparing experimental VLE data to calculated ones by NRTL model for systems: (a) methanol (M)/methyl oleate (MO) at 373.15 K, (b) methanol/soybean oil (OOO) at 373.15 K, (c) water/glycerol (G) at 363.15 K and (d) methanol/oleic acid (OA) at 318.15 K
Source: Adapted from Belting et al. (2015), Chiu, Goff and Suppes (2005), Eduljee and Boyes (1981) and Zaoui-Djelloul-Daouadji et al. (2014).

Some ternary VLE data were also correlated and results are showed in Figure 4.5 to NRTL1 for the following systems: methanol (M)/soybean FAME (MO)/glycerol (G), methanol/water (W)/soybean FAME and methanol/soybean oil (OOO)/soybean FAME for two different set of mass fractions (w_M, w_{OOO}, w_{MO}) = (16.6, 41.6, 41.8)% and (w_M, w_{OOO}, w_{MO}) = (20.0, 16.6, 63.4)%. A mixture of methanol (M)/soybean oil (OOO)/soybean FAME (MO) was found to have reasonable deviations at higher MO concentration as shown in Figure 4.5d (SILVA, et al., 2013; VENERAL et al., 2013). This could be related to the binary interaction parameter M-MO that was found in Aspen Plus databank and obtained through binary VLE data with maximum MO mole fraction of 0.64. Despite some deviations, the VLE data agreed with the most part of ternary VLE data correlated.

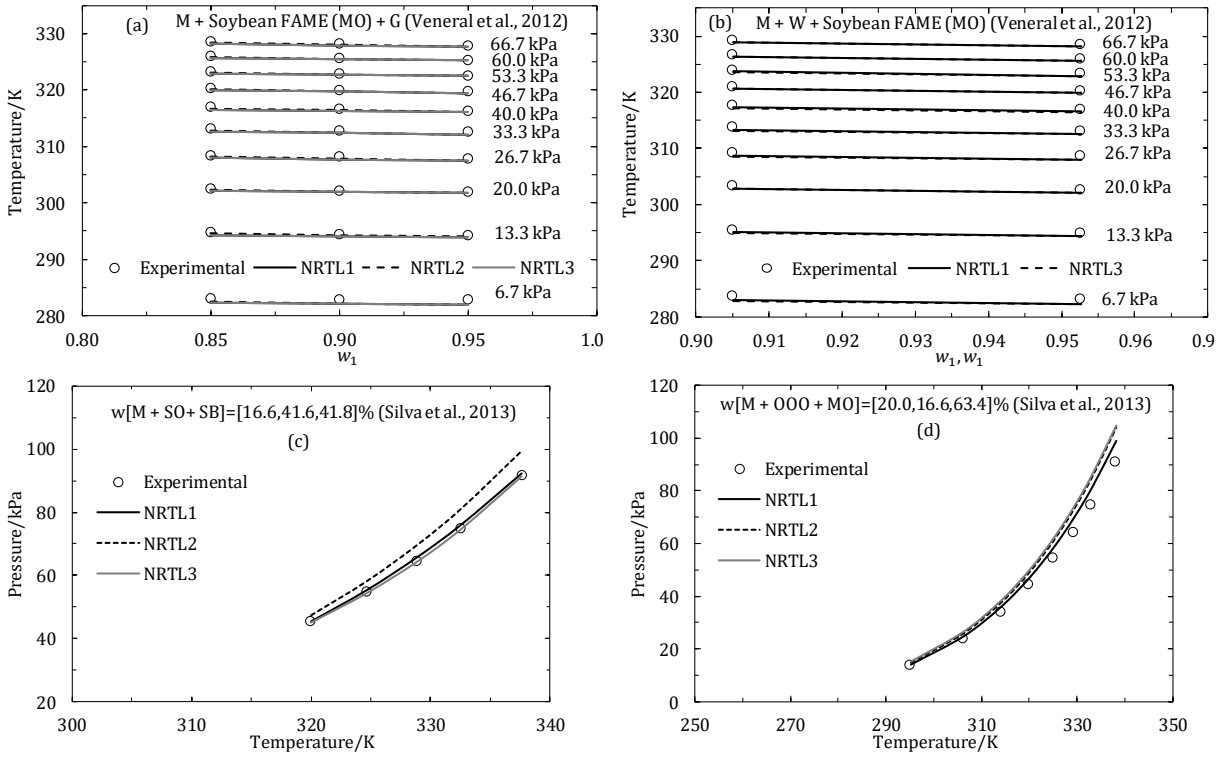

Figure 4.5 – (a,b) Tx and (c,d) PT diagrams at mass fractions (w_i) comparing experimental ternary VLE data to calculated ones by NRTL model for systems: (a) methanol (M)/soybean FAME (MO)/glycerol (G), (b) methanol/water (W)/soybean FAME and (c,d) methanol/soybean oil (OOO)/soybean FAME
Source: Adapted from Silva et al. (2013) and Veneral et al. (2013).

LLE data was also compared to NRTL1 calculated values at mass fractions using ternary diagrams as shown in Figure 4.6 for the following systems: jatropha curcas oil (OOO)/oleic acid (OA)/methanol (M) at 333 K, glycerol (G)/soybean oil (OOO)/soybean FAME (MO) at 341.85 K, soybean oil/glycerol/methanol at 341.85 K and soybean oil/soybean FAME/glycerol/water (W) at 318.85 K (CASAS et al., 2014; LIU et al., 2008). According to Figure 4.6, LLE data agreed with calculated ones and a slight difference in tie line slope was found for quaternary system from Figure 4.6d that can be related to conversion of these LLE data from mole fraction (x_i) to mass fraction (w_i) since pseudocomponents MO and OOO was used to represent soybean FAME and soybean oil.

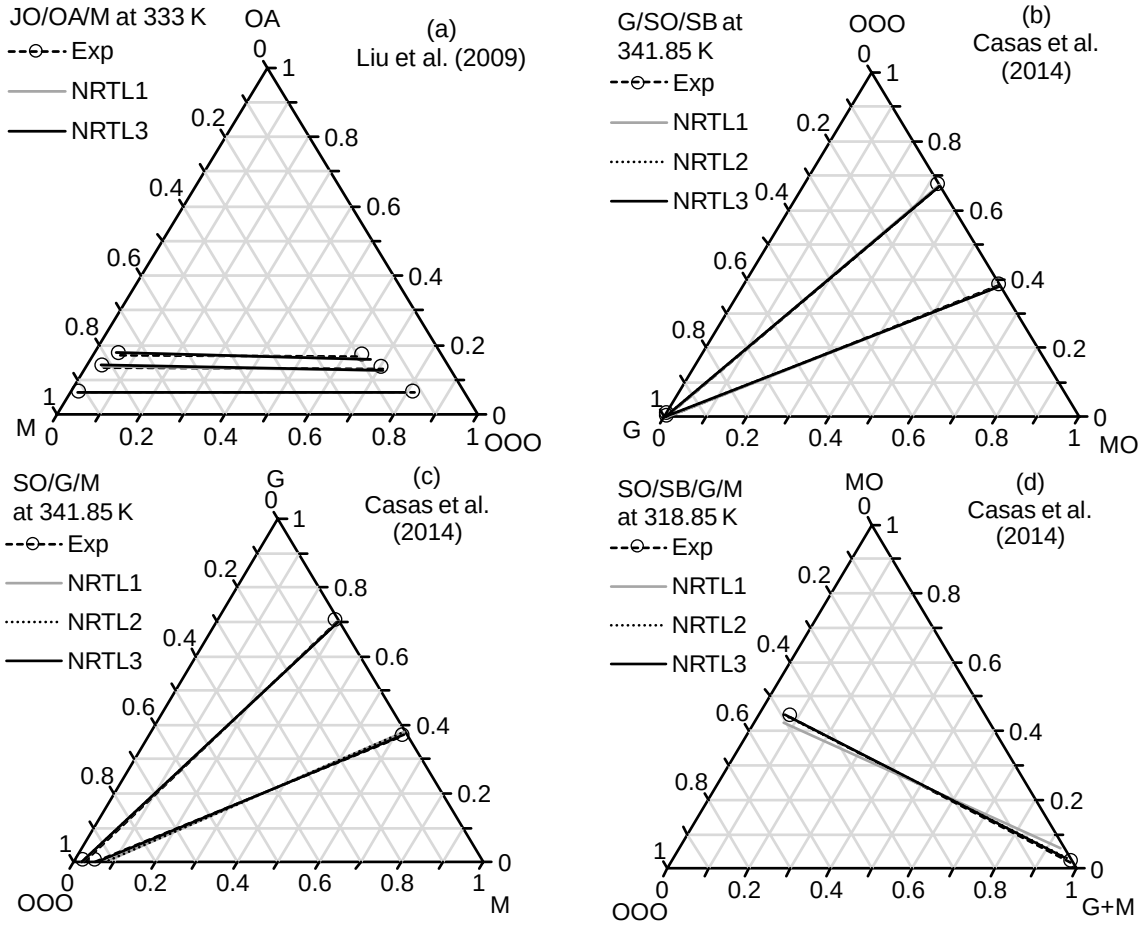

Figure 4.6 – Ternary diagrams comparing LLE data to NRTL calculated ones at mass fractions for systems: (a) jatropha curcas oil (OOO)/oleic acid (OA)/methanol (M) at 333 K, (b) glycerol (G)/soybean oil (OOO)/soybean FAME (MO) at 341.85 K, (c) soybean oil/glycerol/methanol at 341.85 K and (d) soybean oil/soybean FAME/glycerol/water (W) at 318.85 K
Source: Adapted from Casas et al. (2014) and Liu et al. (2008).

Other LLE data were also compared to NRTL1 results at mass fractions as shown in Figure 4.7 for the following systems: methyl oleate (MO)/methanol (M)/ glycerol (G) at 353 K, water (W)/methanol/ methyl oleate at 318.2 K, soybean FAME (MO)/glycerol/water at 333.15 K and soybean FAME/methanol/water/glycerol at 318.15 K (ANDREATTA et al., 2008; ARO; FATEHI, 2017; MAZUTTI et al., 2013). According to Figure 4.7, the LLE data agreed with NRTL1 calculated values including those systems containing water.

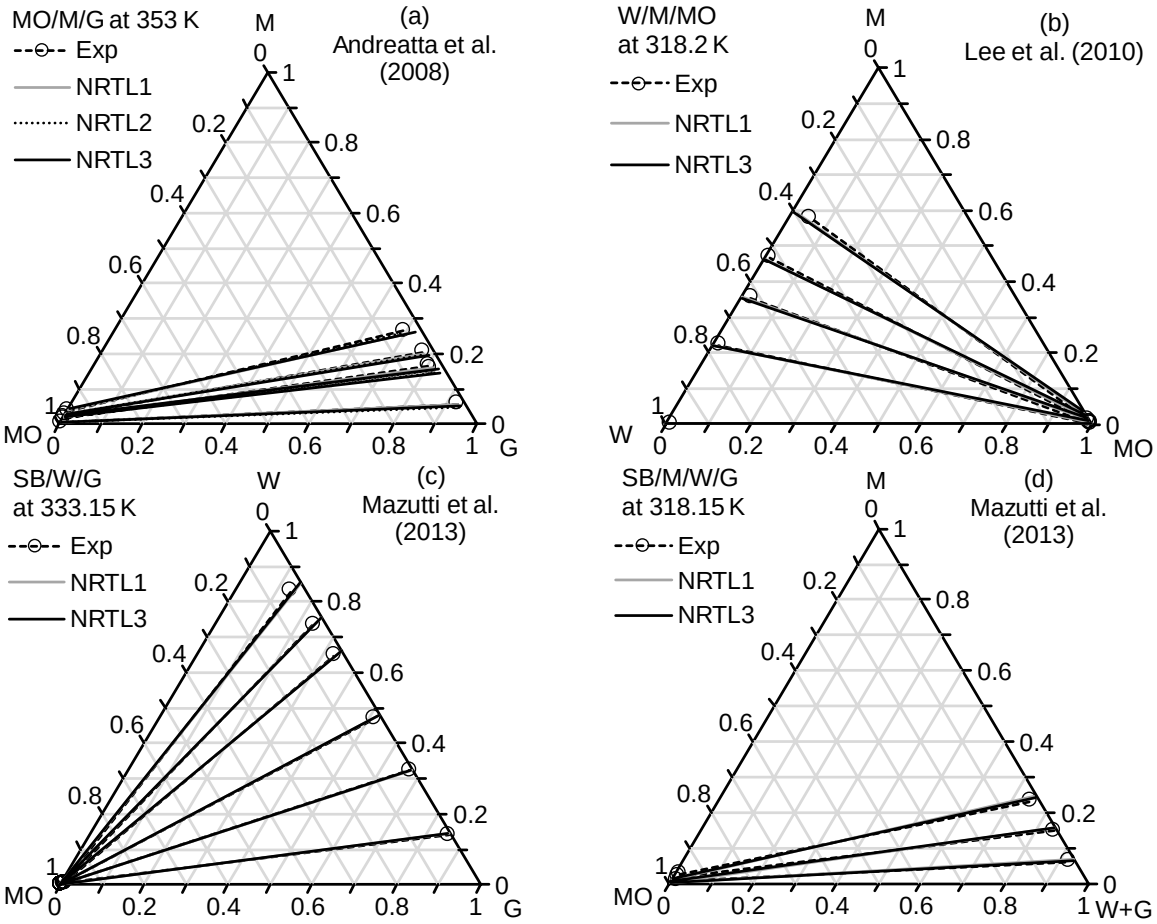

Figure 4.7 – Ternary diagrams comparing LLE data to NRTL calculated ones at mass fractions for systems: (a) methyl oleate (MO)/methanol (M)/ glycerol (G) at 353 K, (b) water (W)/methanol/ methyl oleate at 318.2 K, (c) soybean FAME (MO)/glycerol/water at 333.15 K and (d) soybean FAME/methanol/water/glycerol at 318.15 K
Source: Adapted from Andreatta et al. (2008), Aro and Fatehi (2017) and Mazutti et al. (2013).

VLLE data were also compared to NRTL1 calculated values at mole fractions using ternary diagrams as shown in Figure 4.8 for isothermal systems methyl oleate (MO)/methanol (M)/glycerol (G) at (a) 333.15 K from 60 to 80 kPa, (b) 353 K from 131 to 150 kPa, (c) 373 K from 157 to 259 kPa, (d) 393 K from 177 to 512 kPa, (e) 403 K from 280 to 750 kPa and (f) 473 K from 870 to 2200 kPa (ANDREATTA et al., 2008; BARREAU et al., 2010). According to Figure 4.8, VLLE data reasonably agreed with calculated ones and slight differences in tie line slopes were found mainly for higher temperatures systems (403 K and 473 K) since higher pressures are found. However, it is worth to mention that the ternary system MO/M/G at 473 K was not correlated because the pressures for this system was too high to represent the vapor phase as ideal. As a result, this system was only evaluated with parameters obtained from the thermodynamic modeling.

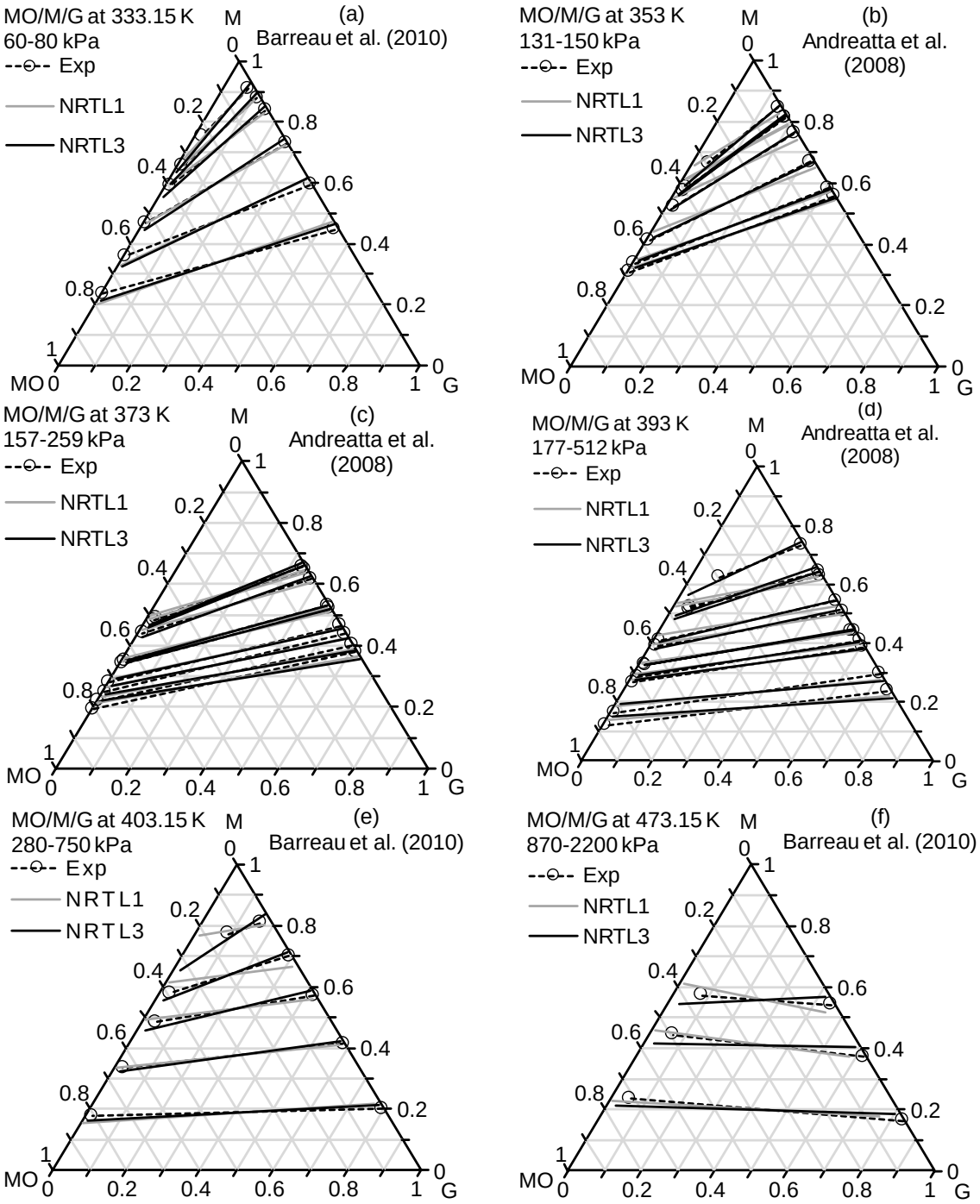

Figure 4.8 – VLLE ternary diagrams for systems methyl oleate (MO)/methanol (M)/glycerol (G) comparing experimental data to NRTL calculated ones (mole fraction) at (a) 333.15 K from 60 to 80 kPa, (b) 353 K from 131 to 150 kPa, (c) 373 K from 157 to 259 kPa, (d) 393 K from 177 to 512 kPa, (e) 403 K from 280 to 750 kPa and (f) 473 K from 870 to 2200 kPa
Source: Adapted from Andreatta et al. (2008) and Barreau et al. (2010).

Despite of some deviations found to represent VLE, LLE and VLLE data involved in biodiesel production processes, the thermodynamic modeling using NRTL1 was considered acceptable because to model the three-phase equilibrium data with the same set of interaction

parameters is very challenge. Furthermore, the modeling was carried out adopting MO and OOO as pseudocomponents to FAME biodiesel and vegetable oil in some mixtures, respectively. Other reasons for these deviations can be related to the large range of pressure and temperature adopted, difficulty to correlate all data simultaneously, data obtained for a wide variety number of references and systems.

4.3.4 Kinetic and phase equilibrium validation

The SAC biodiesel production process using CDC was simulated and validated as shown in Figure 4.9 based on experimental results obtained by Noshadi, Amin and Parnas (2012). WCO was composed in mass percentage of 95.275% of TAG (triolein), 3.725% of FFA (oleic acid) and 1% of water. Esterification and transesterification reactions on pre-reactor were simulated using kinetic models proposed by Fernandes, Cardoso and Silva (2012) and Talebian-Kiakalaieh et al. (2013). This last model was also used on CDC, while an FFA conversion (X_{OA}) of 95.44% was adopted on the 2nd stage of the CDC, since only small amounts of FFA were detected in pre-reactor product stream (CAO et al., 2008). According to Table 4.10 and Figure 4.10, simulation results using NRTL1 agreed with experimental values for yield and temperature profiles obtained from the CDC.

The homogeneous alkali-catalized process (HAC) was also simulated and compared to experimental results obtained by He, Singh and Thompson (2006) and simulated results from Mueanmas, Prasertsit and Tongurai (2010) as shown in Figure 4.11 and Table 4.11. Canola oil was represented by pure triolein and the kinetic model proposed by Mueanmas, Prasertsit and Tongurai (2010) for HAC in RDC was used. However, reasonable deviations were found related to mass fraction (w_i), yield, conversion (X_A) and reboiler temperature (T_{reb}) according to Table 4.11. The reason for these deviations could be related to the difficulty of M-MO interaction parameter to represent VLE of this binary mixture close to ambient pressure. In order to overcome this drawback, an alternative thermodynamic modeling including only transesterification systems, denoted by NRTL2, was developed. In this model, contrary to NRTL1, all binary interactions parameters were regressed.

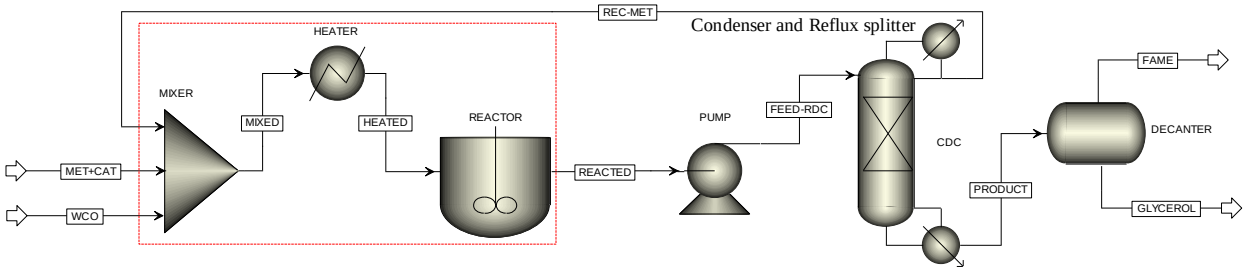

Figure 4.9 – Flowsheet for SAC ($H_3PW_{12}O_{40}{\cdot}6H_2O$) biodiesel production from CDC including a preheater/mixer/reactor
Source: Adapted from Noshadi, Amin and Parnas (2012).

Table 4.10 – Experimental design inputs and results for transesterification and esterification of WCO

Run	Type	F/mol·h^{-1}	Q_{reb}/kW	T_{in}/°C[a]	MR	$Yield$/%[b]	ARD/%[c]	T_{reb}/°C[b]	ARD/%[d]
3	Exp	150.0	1.50	30	70	88.70		139.30	
	NRTL1					88.60	0.12	140.44	0.82
	NRTL3					87.89	0.91	141.00	1.22
8	Exp	132.5	1.25	25	50	89.90		131.89	
	NRTL1					89.92	0.02	131.36	0.40
	NRTL3					88.88	1.13	131.92	0.02

[a] T_{in} means inlet temperature; [b] $Yield$ is related to yield in biodiesel after decanter; [c] Absolute relative deviation (ARD/%) for $Yield$; [d] ARD/% for T_{reb}
Source: Adapted from Noshadi, Amin and Parnas (2012).

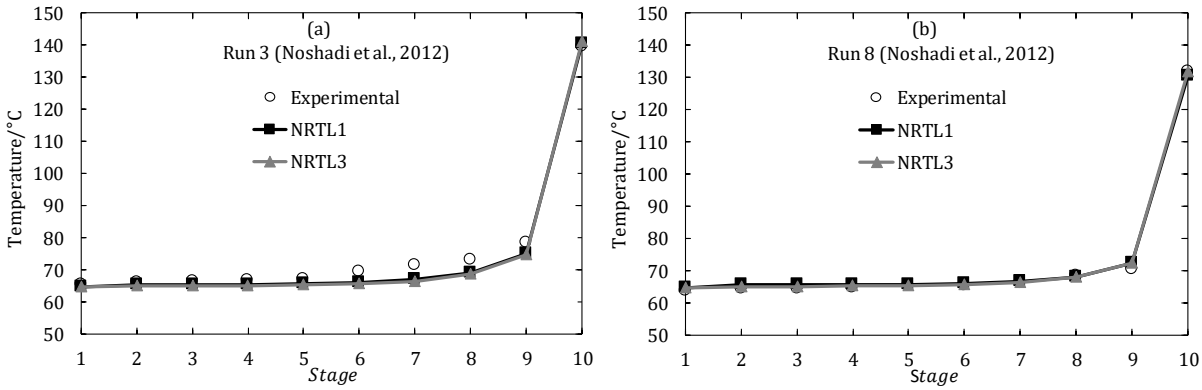

Figure 4.10 – Experimental and simulated temperatures profiles in the CDC from the SAC process
Source: Adapted from Noshadi, Amin and Parnas (2012).

According to Figure 4.4 to Figure 4.7, NRTL2 results showed better agreement with the VLE binary M-MO mixture and LLE pseudo-quaternary soybean oil/soybean FAME/M/G mixture. On the other hand, NRTL2 results only agreed with VLLE ternary mixtures for pressures close to ambient. Table 4.7 and Table 4.8 showed that the global AAD values for VLE mixtures and the global $RSMD_w$ value for LLE mixtures are lower than obtained by NRTL1 for transesterification systems. Although, a higher deviation based on $RSMD_x$ was obtained for VLLE systems mainly for higher pressures (P > 150 kPa). Therefore, NRTL2 could be used to

simulate HAC biodiesel production processes, since HAC is commonly carried out close to ambient pressure. As a result, simulation results from HAC process using NRTL2 parameters were closer to experimental ones as shown in Table 4.11. Therefore, parameters from NRTL1 and NRTL2 showed in Table 4.9 and Table 4.12 should be applied to SAC and HAC using CDC and RDC, respectively.

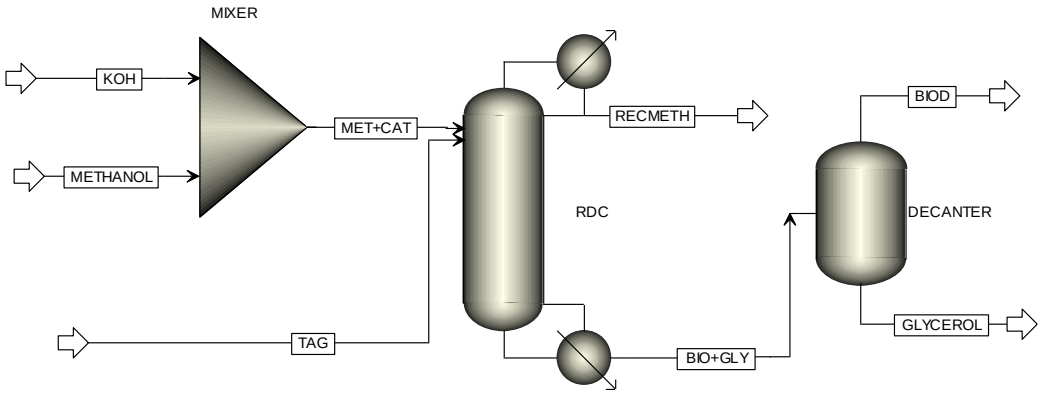

Figure 4.11 – Flowsheet for HAC process using KOH as catalyst for biodiesel production from RDC
Source: Adapted from He, Singh and Thompson (2006).

Table 4.11 – Some experimental design inputs and results for transesterification of canola oil

MR[a]	Type	ME[b]	MG[b]	DG[b]	TG[b]	MeOH[b]	$Yield$/%	X_{TG}/%-X_{AG}/%[c]	T_{reb}/K
3.0:1	Exp[d]	79.90	2.30	3.00	12.70	2.10	61.9	64.5	408.15
	Muenmas[e]	74.28	2.35	3.31	19.21	0.85			
	NRTL1	74.27	0.50	3.40	20.85	0.83	74.7	78.9-72.8	413.57
	NRTL2	77.42	0.37	3.03	18.58	0.60	77.6	81.3-76	404.87
3.5:1	Exp[d]	79.00	1.40	3.60	14.60	1.40	77.2	78.4	399.15
	Muenmas[e]	84.60	1.30	1.91	11.26	0.93			
	NRTL1	78.03	0.41	2.87	17.59	0.94	78.6	82.2-77.0	408.56
	NRTL2	79.98	0.33	2.68	16.37	0.64	80.2	83.5-78.8	403.14
4.0:1	Exp[d]	92.00	0.40	0.90	5.80	0.90	93.0	93.8	396.15
	Muenmas[e]	91.84	0.59	0.93	5.66	0.98			
	NRTL1	90.69	0.18	1.16	7.08	0.71	91.2	92.8-90.7	428.64
	NRTL2	91.94	0.16	1.04	6.23	0.64	92.3	93.7-91.8	406.91
4.5:1	Exp[d]	93.80	0.60	0.70	3.40	1.50	94.3	95.1	368.15
	Muenmas[e]	95.51	0.26	0.45	2.76	1.01			
	NRTL1	92.88	0.10	0.73	4.54	1.57	94.2	95.4-94.1	389.78
	NRTL2	93.86	0.08	0.64	3.98	1.42	94.8	96.0-94.8	382.05

[a] MR means molar ratio; [b] ME, MG, DG, TG and MeOH mean methyl ester, monoacylglycerol, diacylglycerol, triacylglycerol and methanol; [c] X_{TG} and X_{AG} mean TG and acylglycerols (TG, DG and MG) conversion; [d] Exp means experimental results from He, Singh and Thompson (2006) adapted and normalized by Muenmas, Prasertsit and Tongurai (2010); [e] Simulation results obtained by Muenmas, Prasertsit and Tongurai (2010).

Table 4.12 – NRTL2 binary interactions parameters for methanol (1)/triolein (2)/ diolein (3)/monolein (4)/methyl oleate (5)/glycerol (6) systems

i	j	a_{ij} [a]	a_{ji} [a]	b_{ij}/K [a]	b_{ji}/K [a]	α_{ij}	Source
1	2	13.81	-4.94	-2,621.50	1,784.00	0.47	Regressed[b]
1	3	-8.21	12.18	3,364.24	-4,000.54	0.30	UNIFAC[c]
1	4	-3.77	9.81	369.60	-1,451.04	0.30	UNIFAC[c]
1	5	0.00	0.00	1,061.30	-184.51	0.35	Regressed[b]
1	6	0.00	0.00	201.63	-255.76	0.47	Regressed[b]
2	3	-0.61	0.51	179.83	-2.36	0.30	UNIFAC[c]
2	4	-1.55	1.24	730.00	380.55	0.30	UNIFAC[c]
2	5	-5.88	2.78	552.24	-672.19	0.30	Regressed[b]
2	6	3.68	-3.01	141.24	2,944.90	0.30	Regressed[b]
3	4	-0.75	0.85	230.10	30.82	0.30	UNIFAC[c]
3	5	3.47	-3.33	-1,308.95	1,397.38	0.30	UNIFAC[c]
3	6	-0.04	5.40	1,461.45	2,600.53	0.30	UNIFAC[c]
4	5	-0.39	0.03	149.94	666.10	0.30	UNIFAC[c]
4	6	-0.34	2.81	538.51	621.58	0.30	UNIFAC[c]
5	6	28.31	0.15	-6,626.70	1,462.00	0.20	Regressed[b]

[a] Binary interaction parameters were organized according to Aspen Plus: $\tau_{ij} = exp\left(a_{ij} + {}^{b_{ij}}/_{T}\right)$;

[b] Regressed means that binary interaction parameters were obtained by regression;
[c] UNIFAC means that NRTL parameters were obtained from original UNIFAC.

On the other hand, the set of parameters from NRTL1 must be used inside Aspen software, since some interactions from Aspen Plus V8.8 were kept constants. Therefore, in order to overcome this drawback a new set of binary interaction parameters, denoted NRTL3, was obtained by data regression for simultaneous esterification and transesterification reactions. Related to VLE systems, NRTL3 showed the highest and lowest values of AAD_P for transesterification and transesterification-esterification systems as shown in Table 4.7. Furthermore, NRTL3 presented the lowest value of AAD_T. Despite these results, the system M/MO was difficult to correlate for pressures close to 300 kPa as shown in Figure 4.4a.

For LLE systems and VLLE, NRTL3 results also agreed to experimental results according to Figure 4.6 to Figure 4.8. However, NRTL3 presented the lowest values of $RMSD_w$ for LLE systems and a value of $RMSD_x$ higher than NRTL1 for VLLE systems. Despite these results, NRTL3 was considered suitable to correlate VLE, LLE and VLLE systems for biodiesel production since low deviations and properly representation of phase equilibrium data were obtained. As a consequence, SAC process was simulated using these parameters and close results were found for temperature profile and yield as shown in Figure 4.10 and Table 4.10.

Comparing NRTL1 to NRTL3, both agreed to temperature profile presented by Noshadi, Amin and Parnas (2012); however, NRTL1 obtained closer yield results.

4.4 CONCLUSIONS

Pure properties of acylglycerols involved in biodiesel production were evaluated and estimated using group contribution and constituent fragments approaches. Large VLE, LLE and VLLE databanks were also developed in order to accurately represent phase equilibrium in reactive separation processes found in biodiesel production. VLE and LLE data were chosen based on thermodynamic consistency, simplicity, type of vegetable oils and range of pressure and temperature. Some VLE, LLE and VLLE data were successfully correlated by NRTL model based on comparison to experimental results as shown by phase diagrams and low deviation values. The phase equilibrium modeling assured more safety to design and simulate a SAC biodiesel production process using CDC from ROF. As a result, two set of binary interaction parameters were obtained for this process from NRTL model. The first set, denoted NRTL1, is recommended when Aspen Plus is used, since some well-known interaction parameters were kept fixed and VLLE data was successfully correlated obtaining the lowest value of $RMSD_x$. On the other hand, the another set, denoted NRTL3, was obtained regressing all parameters including experimental data and also agreed to VLE, LLE and VLLE data. Moreover, NRTL3 presented the lowest values of AAD_P and AAD_T for VLE systems and $RMSD_w$ for LLE systems involved in simultaneous transesterification and esterification reactions. However, a higher value of $RMSD_x$ for VLLE systems and a higher value of ARD for yield from SAC process demonstrated that this set of parameters should be used when other commercial simulators are adopted. Despite this, interaction parameters from NRTL3 can be used in any software, since was also able to properly model biodiesel reaction systems. Finally, parameters from NRTL2 also agreed to phase equilibrium data from transesterification systems, despite of the highest value of $RMSD_x$ for VLLE systems caused by deviation for higher pressures. In addition, HAC process on RDC was also simulated and closer results were obtained using NRTL2 parameters, since VLE data were better correlated close to ambient pressure. Therefore, NRTL2 is recommended for HAC process operated until pressures of 150 kPa.

ACKNOWLEDGMENTS

The authors would like to acknowledge CNPQ, FINEP and NSERC for financial support. A. A. A. is also grateful to CAPES for the PhD scholarship.

NOMENCLATURE

a_{ij}	coefficient in the NRTL binary interaction parameter equation (K)
AAD	average absolute deviation
ARD	average relative deviation
b_{ij}	coefficient in the NRTL binary interaction parameter equation
C	concentration (molarity) ($mol \cdot L^{-1}$)
C_p	mass heat capacity ($J \cdot g^{-1} \cdot K^{-1}$)
E_a	activation energy at $kJ \cdot mol^{-1} \cdot K^{-1}$
F_{BM}	Barker's modified objective function
F_{ML}	maximum likelihood objective function
F_S	simplex objective function
k'	pseudo-kinetic constant (sec^{-1})
k_0	pre-exponential factor (sec^{-1})
N_C	total number of experimental points
N_D	number of data sets
N_{exp}	number of experimental data
N_t	number of tie lines data
P	pressure (kPa)
R	universal gas constant (8.314 $J \cdot mol^{-1} \cdot K^{-1}$)
$RMSD$	root mean square deviation
t	time
T	temperature (K)
V	variable (temperature, pressure or vapor mole fraction)
w	mass fraction
x	liquid mole fraction
y	vapor mole fraction

Greek Symbols

ΔH	enthalpy of vaporization (kJ·mol^{-1})
α_{ij}	NRTL non-randomness parameter
η	viscosity (mPa·s^{-1})
ρ	mass density (g·cm^{-3})
σ	Uncertainty
ω	weight (see Equation 4.5)

Subscripts

c	critical
i	component
j	tie line
k	data set
n	experimental point
OOO	triolein
P	pressure
r	reaction
T	temperature
w	liquid mass fraction
x	liquid mole fraction
y	vapor mole fraction

Superscripts

cal	calculated
exp	experimental
ig	ideal gas
l	liquid phase in equilibrium
vap	vapor

Abbreviations

ACG	acylglycerols
ARD	average relative deviation
ASOG	Analytical Solutions of Groups

Bin	binary
CCD	central composite design
CDC	catalytic distillation column
CF	constituent fragments
DAG or DG	diacylglycerols
Exp	experimental results
FAAE	fatty acid alkyl ester
FAME	fatty acid methyl ester
FFA	free fatty acids
G	glycerol
GC	group contribution
GCA-EOS	group contribution with association equation of state
GC-PPC-SAFT	GC method with a statistical associated fluid theory equation of state
HAC	homogeneous alkali-catalyzed
LLE	liquid-liquid equilibrium
M	methanol
MAG or MG	monoacylglycerols
ME	methyl ester
ML	maximum Likelihood
MO	methyl oleate
MR	molar ratio of methanol to FFA or TAG
NRTL	Non-Random two-liquid
NRTL1	binary interaction parameters for both reactions using some Aspen parameters
NRTL2	binary interaction parameters for transesterification reaction with all parameters regressed
NRTL3	binary interaction parameters for both reactions with all parameters regressed
OA	oleic acid
OOO	triolein
Pbin	pseudobinary
PE	phase equilibrium
Pquat	pseudoquaternary
Pquin	pseudoquinary
Psix	pseudosixnary

Ptern	pseudoternary
Quat	quaternary
RDC	reactive distillation column
RKAT	Redlich-Kister area test
RMSD	root mean square deviation
ROF	residual oil and fats
RSM	response surface methodology
SAC	solid acid-catalyzed
SSS	tristearin
TAG or TG	triacylglycerols
Tern	ternary
UNIFAC	Universal Functional-group Activity Coefficients
UNIFAC-A	UNIFAC with association
UNIQUAC	Universal QuasiChemical
VLE	vapor-liquid equilibrium
VLLE	vapor-liquid-liquid equilibrium
VO	vegetable oil
W	water
WCO	waste cooking oil

REFERENCES

ABBASZAADEH, A.; GHOBADIAN, B.; OMIDKHAH, M. R.; NAJAFI, G. Current biodiesel production technologies: a comparative review. **Energy Conversion and Management**, v. 63, p. 138−148, 2012.

ALBUQUERQUE, A. A.; CAVALCANTI, C. J. S.; SOARES, C. H. M.; PIMENTEL, M. F.; STRAGEVITCH, L. Optimization of the extraction of free fatty acids applied to biodiesel production. **Brazilian Journal of Chemical Engineering**, v. 35, n. 2, p. 327−340, 2018.

ALBUQUERQUE, A. A.; DANIELSKI, L.; STRAGEVITCH, L. Techno-economic assessment of an alternative process for biodiesel production from feedstock containing high levels of free fatty acids. **Energy & Fuels**, v. 30, n. 11, p. 9409−9418, 2016.

ALCANTARA, R.; AMORES, J.; CANOIRA, L. T.; FIDALGO, E.; FRANCO, M.; NAVARRO, A. Catalytic production of biodiesel from soy-bean oil, used frying oil and tallow. **Biomass and bioenergy**, v. 18, n. 6, p. 515−527, 2000.

ANDRADE, M. H. C. **Vapor-liquid-liquid equilibrium of ternary mixtures: algorithm of calculation and thermodynamic terms (in portuguese)**. MSc Dissertation. Campinas: University of Campinas, 1991. 173p.

_____. **Thermodynamic modeling of vapor-liquid-liquid equilibrium and simulation of three-phase distillation columns**. PhD Thesis. Campinas: University of Campinas, 1997. 184p.

ANDREATTA, A. E.; CASÁS, L. M.; HEGEL, P.; BOTTINI, S. B.; BRIGNOLE, E. A. Phase equilibria in ternary mixtures of methyl oleate, glycerol, and methanol. **Industrial & Engineering Chemistry Research**, v. 47, n. 15, p. 5157−5164, 2008.

ARANSIOLA, E.; OJUMU, T.; OYEKOLA, O.; MADZIMBAMUTO, T.; IKHU-OMOREGBE, D. A review of current technology for biodiesel production: State of the art. **Biomass and bioenergy**, v. 61, p. 276−297, 2014.

ARO, T.; FATEHI, P. Tall oil production from black liquor: Challenges and opportunities. **Separation and Purification Technology**, v. 175, p. 469−480, 2017.

BARKER, J. Determination of activity coefficients from total pressure measurements. **Australian Journal of Chemistry**, v. 6, n. 3, p. 207−210, 1953.

BARREAU, A.; BRUNELLA, I.; DE HEMPTINNE, J.-C.; COUPARD, V.; CANET, X.; RIVOLLET, F. Measurements of liquid− liquid equilibria for a methanol+ glycerol+ methyl oleate system and prediction using group contribution statistical associating fluid theory. **Industrial & Engineering Chemistry Research**, v. 49, n. 12, p. 5800−5807, 2010.

BELTING, P. C.; GMEHLING, J.; BÖLTS, R.; RAREY, J.; CERIANI, R.; CHIAVONE-FILHO, O.; MEIRELLES, A. J. Measurement, correlation and prediction of isothermal vapor–liquid equilibria of different systems containing vegetable oils. **Fluid Phase Equilibria**, v. 395, p. 15−25, 2015.

BENSON, S. Methods for the estimation of thermochemical data and rate parameters. **Thermochemical Kinetics**, p. 217, 1976.

BOON-ANUWAT, N.-N.; KIATKITTIPONG, W.; AIOUACHE, F.; ASSABUMRUNGRAT, S. Process design of continuous biodiesel production by reactive distillation: Comparison

between homogeneous and heterogeneous catalysts. **Chemical Engineering and Processing: Process Intensification**, v. 92, p. 33−44, 2015.

BRAZIL. **LEI Nº 13.263, DE 23 DE MARÇO DE 2016**. Republic President, 2016.

_____. **Resolution N° 16 from October 29, 2018**. Presidency of the republic, Brasília, Brazil, 2018.

CALISKAN, H. Environmental and enviroeconomic researches on diesel engines with diesel and biodiesel fuels. **Journal of Cleaner Production**, v. 154, p. 125−129, 2017.

CANAKCI, M.; SANLI, H. Biodiesel production from various feedstocks and their effects on the fuel properties. **Journal of industrial microbiology & biotechnology**, v. 35, n. 5, p. 431−441, 2008.

CANAKCI, M.; VAN GERPEN, J. Biodiesel production from oils and fats with high free fatty acids. **Transactions of the ASAE**, v. 44, n. 6, p. 1429, 2001.

CAO, F.; CHEN, Y.; ZHAI, F.; LI, J.; WANG, J.; WANG, X.; WANG, S.; ZHU, W. Biodiesel production from high acid value waste frying oil catalyzed by superacid heteropolyacid. **Biotechnology and bioengineering**, v. 101, n. 1, p. 93−100, 2008.

CARNEIRO, M. L. N.; PRADELLE, F.; BRAGA, S. L.; GOMES, M. S. P.; MARTINS, A. R. F.; TURKOVICS, F.; PRADELLE, R. N. Potential of biofuels from algae: Comparison with fossil fuels, ethanol and biodiesel in Europe and Brazil through life cycle assessment (LCA). **Renewable and Sustainable Energy Reviews**, v. 73, p. 632−653, 2017.

CARNITI, P.; CORI, L.; RAGAINI, V. A critical analysis of the hand and Othmer-Tobias correlations. **Fluid Phase Equilibria**, v. 2, n. 1, p. 39−47, 1978.

CASAS, A.; RODRÍGUEZ, J. F.; DEL PESO, G. L.; RODRÍGUEZ, R.; VICENTE, G.; CARRERO, A. Liquid–Liquid Phase Equilibria for Soybean Oil Methanolysis: Experimental, Modeling, and Data Prediction. **Industrial & Engineering Chemistry Research**, v. 53, n. 9, p. 3731−3736, 2014.

CERIANI, R.; GANI, R.; LIU, Y. Prediction of vapor pressure and heats of vaporization of edible oil/fat compounds by group contribution. **Fluid Phase Equilibria**, v. 337, p. 53−59, 2013.

CERIANI, R.; MEIRELLES, A. J. Predicting vapor–liquid equilibria of fatty systems. **Fluid Phase Equilibria**, v. 215, n. 2, p. 227−236, 2004.

CERIANI, R.; PAIVA, F. R.; GONCALVES, C. B.; BATISTA, E. A.; MEIRELLES, A. J. Densities and viscosities of vegetable oils of nutritional value. **Journal of Chemical & Engineering Data**, v. 53, n. 8, p. 1846−1853, 2008.

CHIU, C. W.; GOFF, M. J.; SUPPES, G. J. Distribution of methanol and catalysts between biodiesel and glycerin phases. **AIChE Journal**, v. 51, n. 4, p. 1274−1278, 2005.

COHEN, N.; BENSON, S. Estimation of heats of formation of organic compounds by additivity methods. **Chemical Reviews**, v. 93, n. 7, p. 2419−2438, 1993.

CONSTANTINOU, L.; GANI, R. New group contribution method for estimating properties of pure compounds. **AIChE Journal**, v. 40, n. 10, p. 1697−1710, 1994.

CORRÊA, L.; RIBEIRO, L.; CERIANI, R. Survey of vapor-liquid and liquid-liquid equilibrium experimental data of grease and biodiesel systems. **Blucher Chemical Engineering Proceedings**, v. 1, n. 2, p. 16304−16311, 2015.

DICKINSON, E.; MCLURE, I. A.; AL-NAKASH, A. Equation of state of glycerol trioleate. **The Journal of Chemical Thermodynamics**, v. 12, n. 4, p. 349−354, 1980.

EDULJEE, G. H.; BOYES, A. P. Excess Gibbs energy for eight oleic acid-solvent and triolein-solvent mixtures at 318.15 K. **Journal of Chemical and Engineering Data**, v. 26, n. 1, p. 55−57, 1981.

EXARCHOS, N. C.; TASIOULA-MARGARI, M.; DEMETROPOULOS, I. N. Viscosities and densities of dilute solutions of glycerol trioleate+ octane,+ p-xylene,+ toluene, and+ chloroform. **Journal of Chemical and Engineering Data**, v. 40, n. 3, p. 567−571, 1995.

FADHIL, A. B.; AL-TIKRITY, E. T.; ALBADREE, M. A. Biodiesel production from mixed non-edible oils, castor seed oil and waste fish oil. **Fuel**, v. 210, p. 721−728, 2017.

FEDORS, R. A relationship between chemical structure and the critical temperature. **Chemical Engineering Communications**, v. 16, n. 1−6, p. 149−151, 1982.

FERNANDES, S. A.; CARDOSO, A. L.; SILVA, M. J. A novel kinetic study of H 3 PW 12 O 40-catalyzed oleic acid esterification with methanol via 1 H NMR spectroscopy. **Fuel processing technology**, v. 96, p. 98−103, 2012.

FREDENSLUND, A.; GMEHLING, J.; RASMUSSEN, P. **Vapor-liquid equilibria using UNIFAC : a group contribution**. 1. ed. Amsterdam: Elsevier Scientific Publishers B.V., 1977. 380p.

FU, J.; WANG, K.; HU, Y. H. X. Studies on vapor-liquid and liquid-liquid vapor equilibria for the ternary system methanol-methyl methacrylate-water (I) three binary systems. **Journal of Chemical Industry and Engineering**, n. 1, p. 1−13, 1989.

GAO, D.; CHENG, H.; DING, M.; ZHU, D. Study on Isobaric Vapor-liquid Equilibrium of Methanol-Propionic Acid-H2O Multisystems. **Journal of Nanchang University**, v. 28, n. 4, p. 319−325, 2006.

GAURAV, A.; LEITE, M. L.; NG, F. T.; REMPEL, G. L. Transesterification of triglyceride to fatty acid alkyl esters (biodiesel): comparison of utility requirements and capital costs between reaction separation and catalytic distillation configurations. **Energy & Fuels**, v. 27, n. 11, p. 6847−6857, 2013.

GAURAV, A.; NG, F. T.; REMPEL, G. L. A new green process for biodiesel production from waste oils via catalytic distillation using a solid acid catalyst–Modeling, economic and environmental analysis. **Green Energy & Environment**, v. 1, n. 1, p. 62−74, 2016.

GLIŠIĆ, S.; MONTOYA, O.; ORLOVIĆ, A.; SKALA, D. Vapor-liquid equilibria of triglycerides-methanol mixtures and their influence on the biodiesel synthesis under supercritical conditions of methanol. **Journal of the Serbian Chemical Society**, v. 72, n. 1, p. 13−27, 2007.

GOODRUM, J. W.; GELLER, D. P. Rapid thermogravimetric measurements of boiling points and vapor pressure of saturated medium-and long-chain triglycerides. **Bioresource Technology**, v. 84, n. 1, p. 75−80, 2002.

HAJJARI, M.; TABATABAEI, M.; AGHBASHLO, M.; GHANAVATI, H. A review on the prospects of sustainable biodiesel production: A global scenario with an emphasis on waste-oil biodiesel utilization. **Renewable and Sustainable Energy Reviews**, v. 72, p. 445−464, 2017.

HE, B.; SINGH, A.; THOMPSON, J. A novel continuous-flow reactor using reactive distillation for biodiesel production. **Transactions of the ASABE**, v. 49, n. 1, p. 107−112, 2006.

HERINGTON, E. A thermodynamic test for the internal consistency of experimental data on volatility ratios. **Nature**, v. 160, n. 4070, p. 610−611, 1947.

HÖÖK, M.; TANG, X. Depletion of fossil fuels and anthropogenic climate change—A review. **Energy Policy**, v. 52, p. 797−809, 2013.

JAEGER, F. M. On the temperature dependence of the molecular free surface energy of liquids in the temperature range of -80 to 1650°C. **Journal of Inorganic and General Chemistry**, v. 101, n. 1, p. 1−214, 1917.

KALVELAGE, P. M.; ALBUQUERQUE, A. A.; BARROS, A. A.; BERTOLI, S. L. (Vapor+ Liquid) Equilibrium for Mixtures Ethanol+ Biodiesel from Soybean Oil and Frying Oil. **International Journal of Thermodynamics**, v. 20, n. 3, p. 159−164, 2017.

KAUR, N.; ALI, A. Lithium zirconate as solid catalyst for simultaneous esterification and transesterification of low quality triglycerides. **Applied Catalysis A: General**, v. 489, p. 193−202, 2015.

KNOTHE, G.; KRAHL, J.; VAN GERPEN, J. **The biodiesel handbook**. 2. ed. Elsevier, 2010. 494p.

KNOTHE, G.; STEIDLEY, K. R. Kinematic viscosity of biodiesel components (fatty acid alkyl esters) and related compounds at low temperatures. **Fuel**, v. 86, n. 16, p. 2560−2567, 2007.

KONWAR, L. J.; WÄRNÅ, J.; MÄKI-ARVELA, P.; KUMAR, N.; MIKKOLA, J.-P. Reaction kinetics with catalyst deactivation in simultaneous esterification and transesterification of acid oils to biodiesel (FAME) over a mesoporous sulphonated carbon catalyst. **Fuel**, v. 166, p. 1−11, 2016.

LEE, S.; POSARAC, D.; ELLIS, N. Process simulation and economic analysis of biodiesel production processes using fresh and waste vegetable oil and supercritical methanol. **Chemical Engineering Research and Design**, v. 89, n. 12, p. 2626−2642, 2011.

LIU, Y.; LU, H.; LIU, C.; LIANG, B. Solubility measurement for the reaction systems in pre-esterification of high acid value Jatropha curcas L. oil. **Journal of Chemical & Engineering Data**, v. 54, n. 5, p. 1421−1425, 2008.

LUYBEN, W. L. **Distillation design and control using Aspen simulation**. 2. ed. Hoboken, New Jersey: John Wiley & Sons, 2013. 512p.

LUYBEN, W. L.; YU, C.-C. **Reactive distillation design and control**. 1. ed. Hoboken, New Jersey: John Wiley & Sons, 2008. 580p.

MA, F.; HANNA, M. A. Biodiesel production: a review. **Bioresource technology**, v. 70, n. 1, p. 1−15, 1999.

MAZUTTI, M. A.; VOLL, F. A.; CARDOZO-FILHO, L.; CORAZZA, M. L.; LANZA, M.; PRIAMO, W. L.; OLIVEIRA, J. V. Thermophysical properties of biodiesel and related systems:(liquid+ liquid) equilibrium data for soybean biodiesel. **The Journal of Chemical Thermodynamics**, v. 58, p. 83−94, 2013.

MORAD, N. A.; KAMAL, A. M.; PANAU, F.; YEW, T. Liquid specific heat capacity estimation for fatty acids, triacylglycerols, and vegetable oils based on their fatty acid composition. **Journal of the American Oil Chemists' Society**, v. 77, n. 9, p. 1001−1006, 2000.

MUEANMAS, C.; PRASERTSIT, K.; TONGURAI, C. Transesterification of triolein with methanol in reactive distillation column: simulation studies. **International Journal of Chemical Reactor Engineering**, v. 8, n. 1, p., 2010.

NASERI, M.; ABEDI, E.; MOHAMMADZADEH, B.; AFSHARNADERI, A. Effect of frying in different culinary fats on the fatty acid composition of silver carp. **Food science & nutrition**, v. 1, n. 4, p. 292−297, 2013.

NOSHADI, I.; AMIN, N.; PARNAS, R. S. Continuous production of biodiesel from waste cooking oil in a reactive distillation column catalyzed by solid heteropolyacid: optimization using response surface methodology (RSM). **Fuel**, v. 94, p. 156−164, 2012.

NOUREDDINI, H.; TEOH, B.; CLEMENTS, L. D. Densities of vegetable oils and fatty acids. **Journal of the American Oil Chemists Society**, v. 69, n. 12, p. 1184−1188, 1992.

OCHI, K.; KOJIMA, K. A measurement of vapor-liquid equilibria at extreme dilution. **Journal of chemical engineering of Japan**, v. 20, n. 1, p. 6−10, 1987.

OLIVEIRA, M. B.; MIGUEL, S. I.; QUEIMADA, A. J.; COUTINHO, J. A. Phase equilibria of ester+ alcohol systems and their description with the cubic-plus-association equation of state. **Industrial & Engineering Chemistry Research**, v. 49, n. 7, p. 3452−3458, 2010.

OTHMER, D.; TOBIAS, P. Liquid-liquid extraction data-the line correlation. **Industrial & Engineering Chemistry**, v. 34, n. 6, p. 693−696, 1942.

PERRY, E.; WEBER, W.; DAUBERT, B. Vapor pressures of phlegmatic liquids. I. Simple and mixed triglycerides. **Journal of the American Chemical Society**, v. 71, n. 11, p. 3720−3726, 1949.

PETCHSOONGSAKUL, N.; NGAOSUWAN, K.; KIATKITTIPONG, W.; AIOUACHE, F.; ASSABUMRUNGRAT, S. Process design of biodiesel production: Hybridization of ester-and transesterification in a single reactive distillation. **Energy Conversion and Management**, v. 153, p. 493−503, 2017.

POLING, B. E.; PRAUSNITZ, J. M.; O'CONNELL, J. P. **The Properties of Gases and Liquids**. 5. ed. New York: McGraw-Hill, 2001. 803p.

PONTES, F. C.; ALBUQUERQUE, A. A.; STRAGEVITCH, L. **Vapor-liquid equilibrium of systems involved in biodiesel production**. Brazilian Congress of Research and Development in Oil and Gas. Macéio/AL: Brazilian Association of R&D in Oil and Gas: 6 p. 2017.

PRAUSNITZ, J.; LICHTENTHALER, R. N.; AZEVEDO, E. G. D. **Molecular thermodynamics of fluid-phase equilibria**. 3. ed. New York: Prentice Hall, 1999. 896p.

QING, S.; JIXIAN, G.; YUHUI, L.; JINFU, W. Reaction kinetics of biodiesel synthesis from waste oil using a carbon-based solid acid catalyst. **Chinese Journal of Chemical Engineering**, v. 19, n. 1, p. 163−168, 2011.

RATHMANN, R.; SZKLO, A.; SCHAEFFER, R. Targets and results of the Brazilian biodiesel incentive program–has it reached the promised land? **Applied Energy**, v. 97, p. 91−100, 2012.

REDLICH, O.; KISTER, A. Algebraic representation of thermodynamic properties and the classification of solutions. **Industrial & Engineering Chemistry**, v. 40, n. 2, p. 345−348, 1948.

RENON, H.; PRAUSNITZ, J. M. Local compositions in thermodynamic excess functions for liquid mixtures. **AIChE journal**, v. 14, n. 1, p. 135−144, 1968.

RIAYATSYAH, T. M. I.; ONG, H. C.; CHONG, W. T.; ADITYA, L.; HERMANSYAH, H.; MAHLIA, T. M. I. Life Cycle Cost and Sensitivity Analysis of Reutealis trisperma as Non-Edible Feedstock for Future Biodiesel Production. **Energies**, v. 10, n. 7, p. 877, 2017.

RUIZ, M. S.; OLIVEIRA, R. B. D.; STRUFFALDI, A.; GABRIEL, M. L. D. D. S.; BOCATTO, E. Cooking oil waste recycling experiences worldwide: a preliminary analysis of the emerging networks in the São Paulo Metropolitan Region, Brazil. **International Journal of Energy Technology and Policy**, v. 13, n. 3, p. 189−206, 2017.

SANDLER, S. I. **Using Aspen Plus in thermodynamics instruction: a step-by-step guide**. 1. ed. Hoboken, New Jersey: John Wiley & Sons, 2015. 368p.

SANTANDER, C. M. G.; RUEDA, S. M. G.; DA SILVA, N. D. L.; DE CAMARGO, C. L.; KIECKBUSCH, T. G.; MACIEL, M. R. W. Measurements of normal boiling points of fatty acid ethyl esters and triacylglycerols by thermogravimetric analysis. **Fuel**, v. 92, n. 1, p. 158−161, 2012.

SEADER, J.; HENLEY, E. J.; ROPER, D. K. **Separation Process Principles: Chemical and Biochemical Operations**. 3. ed. Hoboken, New Jersey: Wiley, 2011, 821p.

SILVA, C.; SOH, L.; BARBERIO, A.; ZIMMERMAN, J.; SEIDER, W. D. Phase equilibria of triolein to biodiesel reactor systems. **Fluid Phase Equilibria**, v. 409, p. 171−192, 2016.

SILVA, D. I. S.; MAFRA, M. R.; SILVA, F. R.; NDIAYE, P. M.; RAMOS, L. P.; CARDOZO FILHO, L.; CORAZZA, M. L. Liquid–liquid and vapor–liquid equilibrium data for biodiesel reaction–separation systems. **Fuel**, v. 108, p. 269−276, 2013.

STRAGEVITCH, L.; D'AVILA, S. Application of a generalized maximum likelihood method in the reduction of multicomponent liquid-liquid equilibrium data. **Brazilian Journal of Chemical Engineering**, v. 14, p., 1997.

SU, Y.-C.; LIU, Y.; DIAZ TOVAR, C. A.; GANI, R. Selection of prediction methods for thermophysical properties for process modeling and product design of biodiesel manufacturing. **Industrial & Engineering Chemistry Research**, v. 50, n. 11, p. 6809−6836, 2011.

TALEBIAN-KIAKALAIEH, A.; AMIN, N. A. S.; ZAREI, A.; NOSHADI, I. Transesterification of waste cooking oil by heteropoly acid (HPA) catalyst: optimization and kinetic model. **Applied energy**, v. 102, p. 283−292, 2013.

VAN GERPEN, J. Biodiesel processing and production. **Fuel processing technology**, v. 86, n. 10, p. 1097−1107, 2005.

_____. **Biodiesel production**. In RANALLI, P. (Ed.). *Improvement of crop plants for industrial end uses*. Dordrecht: Springer, 2007. p. 281−289.

VENERAL, J. G.; JUNIOR, D. L.; MAZUTTI, M. A.; VOLL, F. A.; CARDOZO-FILHO, L.; CORAZZA, M. L.; OLIVEIRA, J. V. Thermophysical properties of biodiesel and related

systems: Low-pressure vapour–liquid equilibrium of methyl/ethyl Jatropha curcas biodiesel. **The Journal of Chemical Thermodynamics**, v. 60, p. 46−51, 2013.

VERHOEYE, L.; DE SCHEPPER, H. The vapour—liquid equilibria of the binary, ternary and quaternary systems formed by acetone, methanol, propan-2-ol, and water. **Journal of Chemical Technology and Biotechnology**, v. 23, n. 8, p. 607−619, 1973.

WEST, A. H.; POSARAC, D.; ELLIS, N. Assessment of four biodiesel production processes using HYSYS. Plant. **Bioresource Technology**, v. 99, n. 14, p. 6587−6601, 2008.

ZAOUI-DJELLOUL-DAOUADJI, M.; NEGADI, A.; MOKBEL, I.; NEGADI, L. (Vapor-liquid) equilibria and excess Gibbs free energy functions of (ethanol+ glycerol), or (water+ glycerol) binary mixtures at several temperatures. **The Journal of Chemical Thermodynamics**, v. 69, p. 165−171, 2014.

ZHANG, Y.; DUBE, M.; MCLEAN, D.; KATES, M. Biodiesel production from waste cooking oil: 1. Process design and technological assessment. **Bioresource technology**, v. 89, n. 1, p. 1−16, 2003.

ŽIVKOVIĆ, S. B.; VELJKOVIĆ, M. V.; BANKOVIĆ-ILIĆ, I. B.; KRSTIĆ, I. M.; KONSTANTINOVIĆ, S. S.; ILIĆ, S. B.; AVRAMOVIĆ, J. M.; STAMENKOVIĆ, O. S.; VELJKOVIĆ, V. B. Technological, technical, economic, environmental, social, human health risk, toxicological and policy considerations of biodiesel production and use. **Renewable and Sustainable Energy Reviews**, v. 79, p. 222−247, 2017.

ZONG, L.; RAMANATHAN, S.; CHEN, C.-C. Fragment-based approach for estimating thermophysical properties of fats and vegetable oils for modeling biodiesel production processes. **Industrial & engineering chemistry research**, v. 49, n. 2, p. 876−886, 2009.

_____. Predicting thermophysical properties of mono-and diglycerides with the chemical constituent fragment approach. **Industrial & Engineering Chemistry Research**, v. 49, n. 11, p. 5479−5484, 2010.

5 REACTIVE SEPARATION PROCESSES APPLIED TO BIODIESEL PRODUCTION: design, optimization and techno-economic assessment of solid acid-catalyzed route from residual oil and fats

Allan Almeida Albuquerque[a,b], Flora T. T. Ng[b], Leandro Danielski[a], Luiz Stragevitch[a,*]

[a]LAC/DEQ/UFPE - Fuel Laboratory, Department of Chemical Engineering, Federal University of Pernambuco. Av. Prof. Artur de Sá s/n - CEP 50740-521, Recife, PE, Brazil.
[b]Department of Chemical Engineering, University of Waterloo, Waterloo, N2L 3G1, Canada
*Phone/fax: +55 81 21267235. *E-mail: luiz@ufpe.br*

Extended version from paper to be submitted to Applied Energy, Qualis A1 IF 7.900

ABSTRACT

Reactive distillation column (RDC) has attracted attention in the development of more techno-economic feasible processes and to increase performance of equilibrium-limited reactions as found in biodiesel production. Despite this, few studies evaluated the possibility to produce biodiesel by esterification and transesterification reactions simultaneously. This route can result in lower biodiesel prices since cheaper residual oil and fats (ROF) can be used with less equipment and use of methanol. On the other hand, given that the use of homogeneous catalysts by RDC is a disadvantage, catalytic distillation column (CDC) is gaining attention for biodiesel production, since advantages from solid catalysts and the RDC concept are combined. For this reason, improvements in this technology have been encouraged as the development of cheaper solid acid catalysts with higher activity and reusability. Recently, a solid acid-catalyzed (SAC) process using $HWSi/Al_2O_3$ as catalyst was designed in Aspen Plus based on CDC and showed to be more economic feasible than using a plug-flow reactor. However, optimization was not carried out for CDC as well as other reactive separation processes (RSP) were not investigated and/or compared to industrial processes achieving requirements from biodiesel standard. In this work, two processes based on catalytic absorption column (CAC) and hydro-esterification using CDC were designed and compared to CDC process. The three processes were optimized by decision maker. Heat integration and a flexibility study from a wide range of free fatty acids (FFA) composition were also developed, so that a final design was obtained for raw materials with FFA content between 5 to 25 wt%. The CDC process was chosen as the best process since it was the most economical, environmental friendly and the simplest before the heat integration. A global optimization for this process through connection between Matlab, Visual Basic for Applications (VBA) from Microsoft Excel and Aspen Plus was also developed obtaining the optimal design specifications.

Keywords: Biodiesel. Catalytic distillation column (CDC). Esterification. Free fatty acids (FFA). Solid acid-catalyzed (SAC).

5.1 INTRODUCTION

Reactive separation processes (RSP) have been widely studied in recent years since companies have looked for ways to reduce environmental impact and investment, operation and energy costs (KISS; BILDEA, 2012; MAZUBERT; POUX; AUBIN, 2013). As a result, the keyphrase has been “doing more with less, but being sustainable”. For this reason, process intensification has gained more attention: it facilitates achieving the objectives of generating higher profits, lower costs and lower penalties relative to environment issues (KISS, 2014; MAZUBERT; POUX; AUBIN, 2013; QIU; ZHAO; WEATHERLEY, 2010). Among these processes, reactive distillation column (RDC) has shown some advantages relative to reactor/separator set. For instance, simultaneous vapor-liquid separation and reaction in the same equipment, lower capital costs, lower horizontal space required, higher production rate and product selectivity (LUYBEN; YU, 2008; SUNDMACHER; KIENLE, 2002). For all these features, RDC has attracted attention in the development of more techno-economic feasible processes to increase the performance of equilibrium-limited reactions such as those found in biodiesel production (LUYBEN; YU, 2008; SUNDMACHER; KIENLE, 2002).

Biodiesel is a renewable fuel composed of fatty acid alkyl esters (FAAE) and has been applied in some countries as a blend with diesel (HASAN; RAHMAN, 2017; MAHMUDUL et al., 2017; POUSA; SANTOS; SUAREZ, 2007; SORDA; BANSE; KEMFERT, 2010). Biodiesel is still being produced in many industries by transesterification reaction using edible oils since design and operation conditions from the reaction are well-known and less complicated (MEHER; VIDYA SAGAR; NAIK, 2006; ZHANG et al., 2003a). However, high prices of edible oils and competition with food industry have encouraged producers to use cheaper raw materials such as residual oil and fats (ROF). On the other hand, ROF requires a pretreatment step before the transesterification step. ROF commonly contain high free fatty acids (FFA) content, which requires that a homogeneous acid-catalyzed process by esterification reaction be carried out to decrease FFA levels. That resulting pretreatment step increases capital and operation costs for biodiesel production reflecting on biodiesel price (ALBUQUERQUE; DANIELSKI; STRAGEVITCH, 2016; ZHANG et al., 2003a; b). In addition, homogeneous catalysts used in these processes increase the separation and waste

treatment costs making environmental impact another problem (GAURAV; NG; REMPEL, 2016; WEST; POSARAC; ELLIS, 2008).

For those reasons, many authors have suggested alternative processes to reduce costs, such as the use of solid catalyst and RDC (HE; SINGH; THOMPSON, 2006; SIMASATITKUL et al., 2011; SOUZA et al., 2014; STEINIGEWEG; GMEHLING, 2003; WEST; POSARAC; ELLIS, 2008). For instance, West, Posarac and Ellis (2008) studied a design of a solid acid-catalyzed (SAC) process based on simultaneous transesterification and esterification reactions of waste cooking oil (WCO) using SnO catalyst in a reactor. The researchers showed that SAC process is more economically feasible than the conventional process and presented higher value of return of investment, since the pretreatment step was eliminated. Furthermore, they showed that more highly-purified biodiesel and glycerol can be obtained when solid catalyst is employed making easier purification steps and decreasing waste treatment generation. Given that RDC's use of homogeneous catalysts is a disadvantage, catalytic distillation (CDC) is gaining attention for biodiesel production (BOON-ANUWAT et al., 2015; GAURAV; NG; REMPEL, 2016).

CDC is a green reactor technology, which combines a heterogeneous catalytic reaction and distillation in the same column. CDC has the same advantages of RDC; however, a solid catalyst usually inserted as a packing is used instead a homogeneous catalyst (NG; REMPEL, 2002). Therefore, when CDC is applied to biodiesel production from ROF, advantages from solid catalysts and RDC concept are combined. As a result, Noshadi, Amin and Parnas (2012) investigated a set of preheater/mixer/reactor followed by a CDC applied to biodiesel production using $H_3PW_{12}O_{40}\cdot 6H_2O$ as solid catalyst. They obtained conversions of WCO close to 89% for optimum conditions. However, higher conversion is required to achieve biodiesel standards, since separation costs are high.

For this reason, Gaurav, Ng and Rempel (2016) measured kinetic data and developed a kinetic model for simultaneous esterification and transesterification of yellow grease in presence of $HWSi/Al_2O_3$ obtaining maximum conversion in optimal conditions. Furthermore, they investigated two flowsheet designed in Aspen Plus, where a process containing a set of plug-flow reactor (PFR) and distillation column was adopted as the base case. The alternative process based on CDC concept showed to be more economic feasible and environmental friendly based on lower costs, waste streams and CO_2 emissions (GAURAV; NG; REMPEL,

2016). On the other hand, Gaurav, Ng and Rempel (2016) employed the same molar ratio (MR) of methanol to ROF for both processes in order to keep the MR higher than 21.3. However, many authors have shown that when RDC or CDC is used, a lower amount of alcohol can be fed in the column, because reflux ratio (RR) supplies higher liquid holdup (HE; SINGH; THOMPSON, 2005; 2006; MUEANMAS; PRASERTSIT; TONGURAI, 2010; SOUZA et al., 2014). Moreover, CDC process designed by Gaurav, Ng and Rempel (2016) did not achieve all requirements from biodiesel standards, such as free and glycerol total minimum purity. Furthermore, this process was not compared to other RSP and/or industrial processes including CDC.

Consequently, in order to investigate innovative RSP from SAC route, achieving all requirements from biodiesel standards, and to obtain optimized conditions for CDC process, this work was suggested. As a result, an alternative process based on a catalytic absorption column (CAC) was proposed since CDC designed by Gaurav, Ng and Rempel (2016) presented a very low RR. In addition, a SAC process based on industrial hydro-esterification was investigated using niobium oxide (Nb_2O_5) as catalyst from hydrolysis reaction in a PFR reactor and $HWSi/Al_2O_3$ as catalyst from esterification reaction in a CDC column (ARANDA; SILVA; DETONI, 2009; MACHADO et al., 2016). The three processes were optimized by decision maker (DM) based on two approaches applied to costliest equipment: direct simulation and cost calculation in Aspen Plus V8.8; and sensitivity analysis and use of an external cost calculation procedure in spreadsheets (LUYBEN; YU, 2008; SEGOVIA-HERNÁNDEZ; GÓMEZ-CASTRO, 2017).

Subsequently, all processes were compared relative to techno-economic feasibility and a heat integration (HI) was proposed for the most economic feasible processes (SEIDER; SEADER; LEWIN, 2009). Moreover, a stochastic optimization based on simulated annealing (SA) method was carried out to compare with optimal conditions from the most economic process found by DM (LUYBEN; YU, 2008; SEGOVIA-HERNÁNDEZ; GÓMEZ-CASTRO, 2017). Finally, flexibility from the most economical process was investigated based on raw materials with FFA content varying between 5 to 25 wt% as commonly faced by industry.

5.2 MATERIALS AND METHODS

5.2.1 Definition of the components

Components were defined based on the same assumptions from our previous work (ALBUQUERQUE et al., 2019). As a result, triolein (OOO), oleic acid (OA), methanol (M), methyl oleate (MO), water (W) and glycerol (G) were chosen as representative components for hydrolysis, esterification and transesterification reactions (ALBUQUERQUE et al., 2019).

5.2.2 Thermophysical properties, phase equilibrium and kinetic model

Thermophysical properties models and a phase equilibrium modeling previously validated were used in simulations. The pure properties of triolein were obtained mainly by constituent fragments approach and group contribution method, while vapor-liquid-liquid equilibrium (VLLE) was modeled using Non-Random two liquid (NRTL) model with binary parameters from NRTL1 previously obtained and validated by our research group (ALBUQUERQUE et al., 2019; CERIANI; MEIRELLES, 2004; ZONG; RAMANATHAN; CHEN, 2010). On the other hand, for higher-pressure conditions as for hydro-esterification process, the NRTL-Redlich Kwong (RK) model was adopted (GÓMEZ-CASTRO et al., 2011; GOMEZ-CASTRO et al., 2010).

In relation to reaction modeling, pseudo-first order kinetic models for esterification and transesterification reactions through HWSi/Al_2O_3 obtained by Gaurav, Ng and Rempel (2016) were adopted, as shown in Appendix A, to represent reactions in processes using CDC and CAC. In addition, a reversible second order model developed by Machado et al. (2016) from experimental results of Layla et al. (2010) using Nb_2O_5 was considered for the hydrolysis reaction modeling in a plug flow reactor (PFR) reactor.

5.2.3 Design, optimization and techno-economic feasibility of the processes

Three different processes of biodiesel production based on RSP were studied using Aspen Plus V8.8. First, process A proposed by Gaurav, Ng and Rempel (2016) based on catalytic distillation column (CDC) applied to simultaneous esterification and transesterification reactions was designed and optimized. Second, process B based on catalytic absorption column (CAC) using the same reactions and kinetic models from process A was proposed, designed and optimized (KISS, 2009). Finally, the well-known industrial process C based on hydro-esterification was designed and optimized including a PFR for hydrolysis reaction using Nb_2O_5 as catalyst and a CDC for esterification reaction through $HWSi/Al_2O_3$ (GAURAV; NG; REMPEL, 2016; GÓMEZ-CASTRO et al., 2011; GOMEZ-CASTRO et al., 2010; MACHADO et al., 2016). A mass flow rate close to 34,875 ton/year of ROF with 85 wt% of TAG and 15 wt% FFA was adopted for all processes as used by Gaurav, Ng and Rempel (2016).

A scheme for the SAC process based on simultaneous esterification, transesterification and separation using CDC or CAC is shown in Figure 5.1. Furthermore, a scheme for the SAC process based on hydrolysis reaction and esterification reaction is shown in Figure 5.2. For both schemes are observed reaction steps and separation (SEP) steps, such as: liquid-liquid equilibrium (LLE) SEP, vapor-liquid equilibrium (VLE) SEP and VLLE SEP. Figure 5.1 and 5.2 also show majority components in the streams as capital letter, while minority components as lower case.

For all processes, specifications from National Agency of Petroleum, Natural Gas and Biofuels (ANP) standard were taken in account to produce biodiesel as shown in Table 5.1 (ANP, 2014). On the other hand, pharmaceutical glycerol 99.5 wt% was preferred as a by-product than glycerin since is more valuable (LDC, 2017; ROSARIA et al., 2014). As a result, processes achieving these specifications for biodiesel and glycerol were judged as technical feasible. Moreover, designed flowsheets were optimized to reduce costs using a decision maker (DM) approach (LUYBEN; YU, 2008; SEGOVIA-HERNÁNDEZ; GÓMEZ-CASTRO, 2017). Two approaches were adopted for costliest equipment indicated by Aspen Economic Analyzer tool from Aspen Plus V8.8: design and economic evaluation directly from Aspen Plus; and sensitivity analysis, design and economic evaluation using an external spreadsheet based on installed (C_{inst}), utility (C_{util}), waste stream (C_{waste}) and total annualized (TAC) costs.

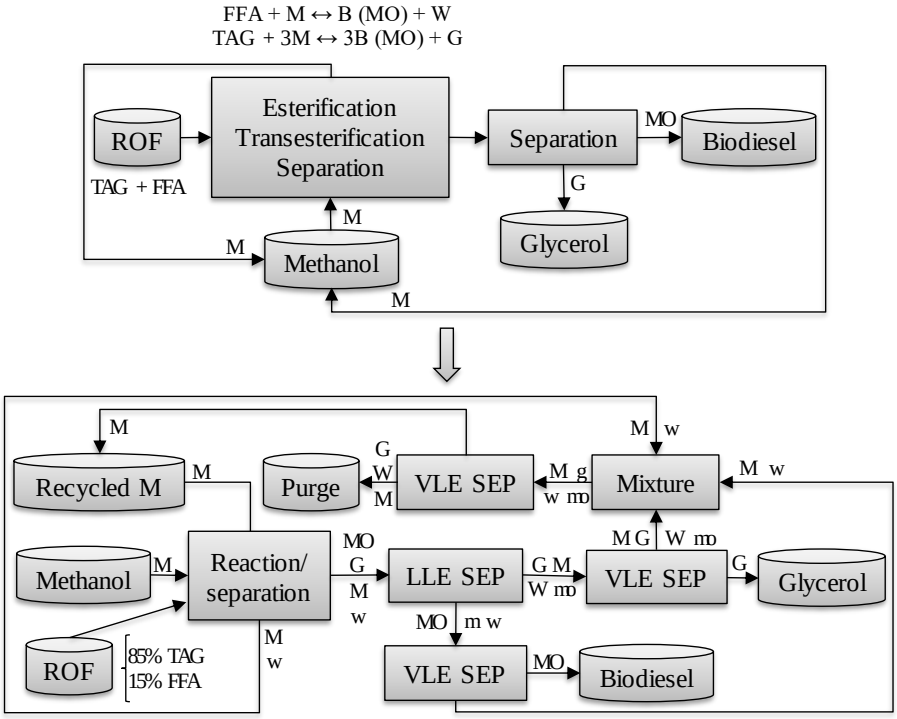

Figure 5.1 – Scheme of SAC process for biodiesel production from ROF using CDC or CAC concept in simultaneous esterification and transesterification reactions
Source: Adapted from Gaurav, Ng and Rempel (2016).

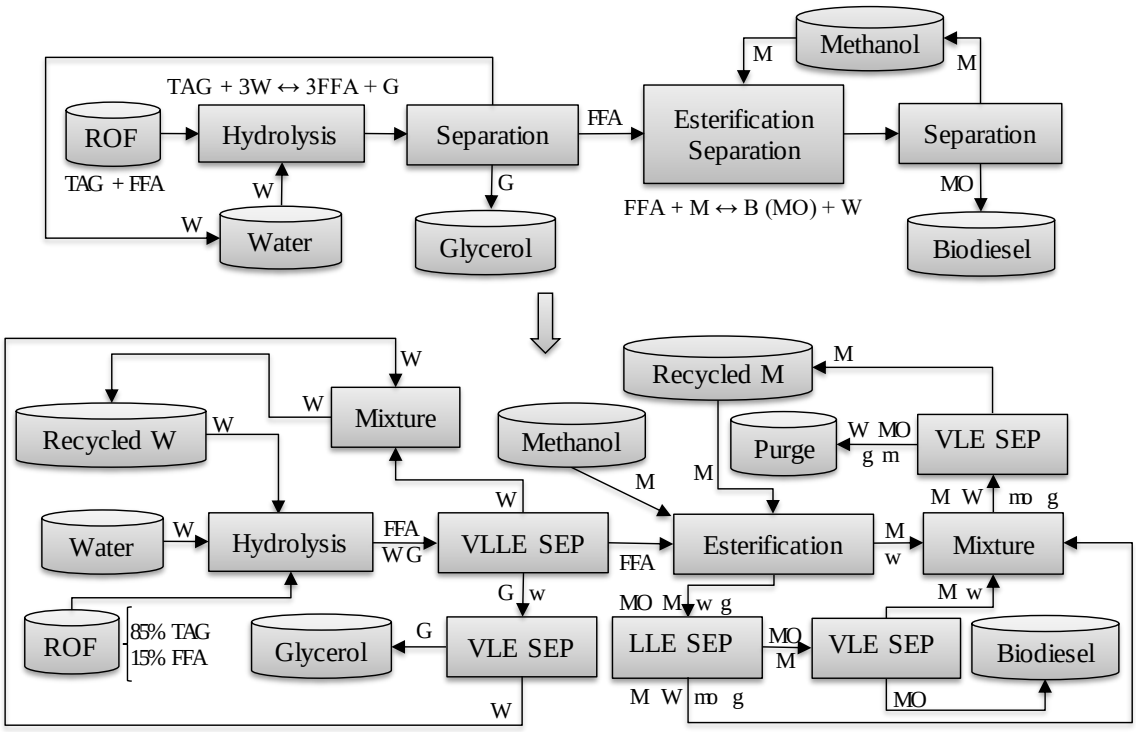

Figure 5.2 – Scheme of SAC hydro-esterification process for biodiesel production from ROF using CDC
Source: Adapted from Machado et al. (2016).

Table 5.1 – Biodiesel specifications from ANP standard

Minimum ester (% mass)	Maximum ($mg \cdot kg^{-1}$)	Maximum (% mass)		
	Water	Total/free Glycerol	Methanol	FFA/TAG/DAG/MAG
96.5	200	0.25/0.02	0.20	0.25/0.20/0.20/0.70

Source: Adapted from ANP (2014).

After the optimization step by DM, each process was compared in terms of economic feasibility based on some economic indicators, such as: TAC, total production cost (C_{TP}), income, annual net profit (A_{NNP}), return on investment (ROI), break-even price (BEP) and payback period (PBP) (ALBUQUERQUE; DANIELSKI; STRAGEVITCH, 2016; SEIDER; SEADER; LEWIN, 2009). For all calculations, some values of parameters were kept constants, such as: an operation year of 8,766 h, an operating life of plant of 30 years, a length of plant start-up of 4 months and starting the basic engineering in March 12th, 2018. Carbon dioxide (CO_2) emissions were also calculated based on method proposed by United States Environment Protection Agency (EPA), in order to evaluate more environment friendly conditions (EPA, 2009).

For the more techno-economical feasible processes was also investigated the possibility of heat integration (HI) in order to reduce utility cost and TAC. For this reason, heuristics rules were adopted. However, HI between streams located closer to each other were prioritized, since the convergence became easier. Finally, the heat integrated processes were also compared to each other and to other processes not including HI related to techno-economic feasibility and eco-friendly aspects (PERLINGEIRO, 2005; SEIDER; SEADER; LEWIN, 2009).

5.2.4 Stochastic Optimization

In order to find an optimal global solution or at least a solution close enough to it, a stochastic optimization approach was adoped based on simulated annealing (SA) method found in Optimization Toolbox of Matlab 2017a. This method simulates the annealling process in solids, where a hypothetical temperature (T) is firstly increased causing random behavior and slowly decreased to achieve a new equilibrium. During this process a solution x_0 is chosen based on initial T. Then, an objetive function $f(x_0)$ is obtained and another solution x is

proposed to compare $f(x)$ to $f(x_0)$, where x is accepted as solution if $f(x) \geq f(x_0)$, otherwise a probability of acceptance $\Psi(x, x_0)$ for x is calculated based on Equation 5.1. Thereafter, just in case x is not accepted, if $\Psi(x, x_0) \geq r$ for a given random number r, then x can be still chosen as new solution. Finally, the procedure is repeated until T decreases to a stable freezing temperature (T_{frez}), where a optimal solution x is found or at least close enough to it (KISS et al., 2012; SEGOVIA-HERNÁNDEZ; GÓMEZ-CASTRO, 2017).

$$\Psi(x, x_0) = \exp\left(\frac{f(x_0) - f(x)}{T}\right) \tag{5.1}$$

As Aspen Plus V8.8 software does not include an internal stochastic optimization method, a similar procedure based on SA, as proposed by Segovia-Hernández and Gómez-Castro (2017), was implemented connecting Matlab 2017a, Microsoft Excel 2016 through Visual Basic for Applications (VBA) and Aspen Plus V8.8 (KISS et al., 2012; SEGOVIA-HERNÁNDEZ; GÓMEZ-CASTRO, 2017). In this procedure, Matlab 2017a works as the "brain" from the optimization sending values of vector of input variables $[I]$ to Microsoft Excel 2016. After Excel via VBA sends input variables to Aspen Plus V8.8 that returns simulation results as a vector of output variables $[O]$ to calculate an objetive function $F = TAC$ in Excel. Finally, value of TAC is returned to Matlab to evaluate by SA if $[I]$ leads F for an optimum value (KISS et al., 2012; SEGOVIA-HERNÁNDEZ; GÓMEZ-CASTRO, 2017). A simplified block diagram for this approach is shown in Figure 5.3, while Equations 5.2 and 5.3 show how the minimum value of the objective function $Min(F)$ was calculated in Microsoft Excel 2016. It is worth to mention that a stochastic optimization method needs long number of iterations (i) to achieve the optimal solution since has less dependence from initial condition

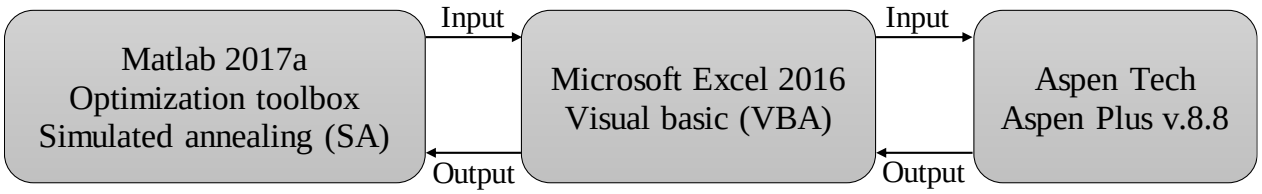

Figure 5.3 – Block diagram from the procedure of stochastic optimization by SA method
Source: Adapted from Kiss et al. (2012) and Segovia-Hernández and Gómez-Castro (2017)

$$Min\ (F) = f\left[n_{feed}^{M}, \left(N, RR, \frac{D}{F}\right)_{c}\right]\ for\ c = 1, 2, 3, \dots, n_c \tag{5.2}$$

$$F = TAC = C_{util} + \left(\frac{C_{inst}}{3}\right) + C_{waste} \tag{5.3}$$

From Equation 5.2, the input variables (I) from Matlab 2017a are n_{feed}^{M} that corresponds to feed mole flow of methanol, N that means number of stages, RR that means reflux ratio and D/F that means distillate to feed ratio (mol/mol). In addition, subscript n_c represents number of c distillation columns. On the other hand, Equation 5.3 shows how F is calculated based on output variables (O) from Aspen Plus V8.8 to Microsoft Excel 2016, where C_{util} means utility cost, C_{inst} means installed cost for the distillation columns considered and C_{waste} means waste stream cost. Finally, in the end of the procedure, I values obtained in $Min(F)$ was used to calculate costs directly from Aspen Plus V8.8 in order to compare the economic indicators from DM approach and SA method.

5.2.5 Flexibility

As a final step, plant flexibility of the most techno-economical feasible process was investigated based on range of FFA content in ROF between 5 to 25 wt%. In this case, a process design was proposed in order to attend this common range of FFA composition found in industries. In addition, economic indicators were calculated in order to compare different scenarios including yellow grease and brown grease.

5.3 DESIGN AND OPTIMIZATION

In this section, some flowsheets were designed and in order to keep standardized block and stream names, a convention was adopted. For instance, flowsheet block names are represented by Y-1ZZ, Y-2ZZ or Y-3ZZ, wherein numbers 1, 2 and 3 were related to processes A, B and C, respectively. Y denotes E, P, R, T, V, M or S representing the heat exchanger (heater or cooler), pump, reactor, tower (distillation or absorption column), vessel (flash drum, decanter or extraction column), mixer or splitter. ZZ denotes an integer counter related to the amount of specific equipment. For instance, Y-1ZZ = T-101 means distillation column 1 present in process A (ALBUQUERQUE; DANIELSKI; STRAGEVITCH, 2016).

Analogously, the stream names are represented by 1ZZ, 2ZZ or 3ZZ. For example, stream 103 represents ROF feed stream to process A as shown in Figure 5.4. In addition, some streams can be accompanied by a letter (A, B, C, D, E or F); that was used when the stream pressure (e.g., 102A) or temperature (e.g., 103B) changed while almost keeping constant the composition, or, after a splitter (e.g., 215B and 215C in flowsheet from process B1) (ALBUQUERQUE; DANIELSKI; STRAGEVITCH, 2016).

5.3.1 Solid-acid catalyzed process from catalytic distillation

The SAC process based on simultaneous esterification and transesterification reactions using catalytic distillation (CDC), denominated Process A1, was designed as shown in Figure 5.4, where only few changes from the flowsheet proposed by Gaurav, Ng and Rempel (2016) were adopted, such as: presence of more pumps, heat exchangers and a flash tank (V-102) instead of a distillation column in the glycerol purification step. This last change was applied because low pressure is a more important issue than number of stages (N) for a distillation column to avoid higher temperatures since degradation of glycerol could occur after 423.15 K (ALMAZROUEI; SAMAD; JANAJREH, 2017; CRNKOVIC et al., 2012; DOU et al., 2009).

Stream results for the same feed conditions adopted by Gaurav, Ng and Rempel (2016) can be found in Table 5.2. From these results, it can be observed that almost all specifications from biodiesel standard from Table 5.1 were achieved. Exceptions were found to achieve

minimum free glycerol content in biodiesel and maximum purity of glycerol of 99.5 wt% for pharmaceutical glycerol (ANP, 2014).

As mentioned before, RDC and CDC can supply higher molar ratio (MR) of methanol to ROF due to alcohol reflux, so that lower amount of alcohol can be fed into the column (HE; SINGH; THOMPSON, 2005; 2006). For that reason optimization was carried out to reduce the MR of methanol to ROF, since the kinetic model proposed by Gaurav, Ng and Rempel (2016) is valid for MR higher than 21.27. As a first approach, an optimization by decision maker was adopted using the sensitivity analysis tool from Aspen Plus V8.8. However, presence of recycle stream dumped simulation convergence during sensitivity analysis, so that separated simulations were considered (LUYBEN; YU, 2008; SEGOVIA-HERNÁNDEZ; GÓMEZ-CASTRO, 2017). For this optimization, a strategy was adopted keeping almost all design conditions from Table 5.3 constants. One exception was MR of methanol to ROF before CDC column (T-101) that was reduced, so that MR in all stages could still be above 21.27 (GAURAV; NG; REMPEL, 2016). From these changes, the number of stages (N) from T-101 and distillate to feed ratio (D/F) from columns T-101, T-102 and T-103 needed to be changed to achieve results close to SAC process based on 126.15 kmol·h^{-1} (base case) of alcohol designed in Table 5.3.

For the base case, the minimum MR was 106.2 for stage 2 that was adopted as feed stage (FS) from both input streams, since lower RR can be used feeding in that stage. Capital and operation costs were higher than obtained by Gaurav, Ng and Rempel (2016) since was adopted an operating life of plant of 30 years, a length of plant start-up of 4 months and starting the basic engineering in March 12th, 2018. Results from the optimization are shown in Figure 5.5, where bottom abscissa is a continuous axis for MR, while top abscissa is a discrete axis for each values of minimum MR inside stage 2 ($MR_{min}^{N=2}$) considered. From results from Figure 5.5e-f, cost (capital, utility and total annualized costs) and emission indicators decrease as expected when MR is reduced, since lower values of diameter and reboiler duties were obtained. For design parameters this is also true with exception to packing height (L_p), since N of T-101 increased when MR of methanol to ROF decreased as shown in input values from the sensitivity analysis in Table 5.3.

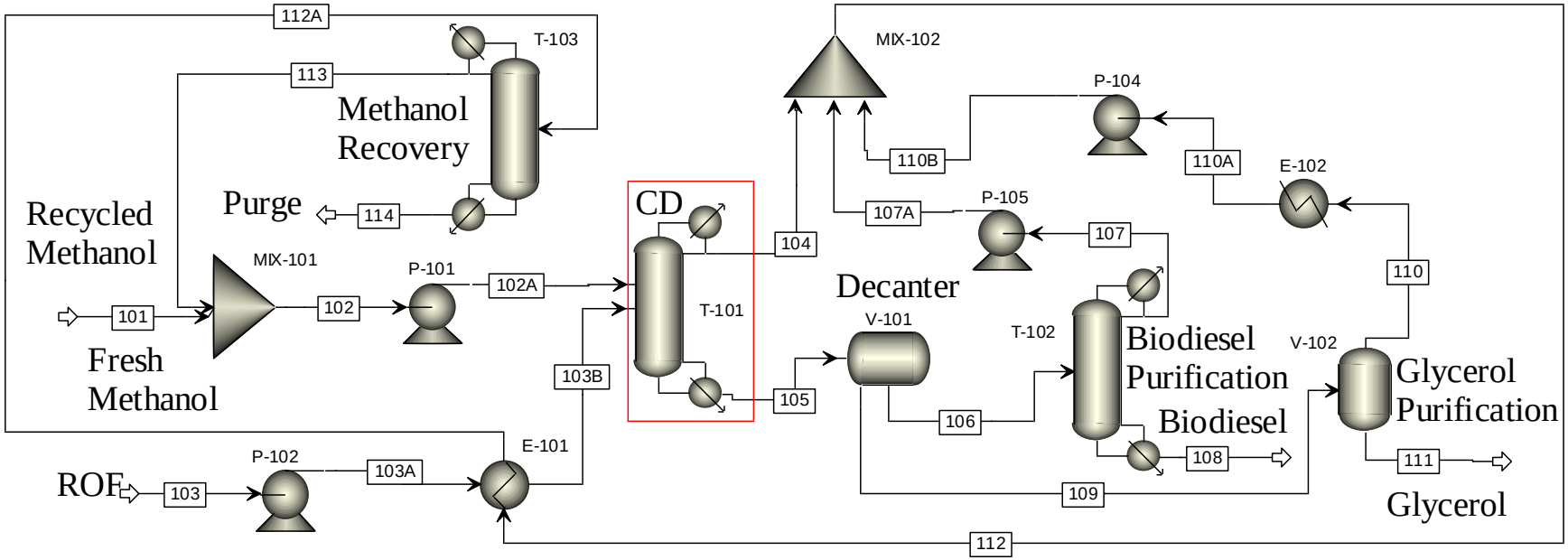

Figure 5.4 – Flowsheet for the solid acid-catalyzed (SAC) biodiesel production process from catalytic distillation (CDC) column
Source: Adapted from Gaurav, Ng and Rempel (2016).

Table 5.2 – Stream results for the base case of Process A1 based on SAC biodiesel production process from CD column

Stream number	101	102A	103B	104	105	106	107A	108	109	110B	111	113
Temperature (°C)	25.0	60.8	96.6	112.1	162.1	110.0	54.8	238.4	110.0	10.6	149.0	64.6
Pressure (kPa)	101.3	506.6	511.3	506.6	506.6	101.3	506.6	65.9	101.3	506.6	4.7	101.3
Mole flow (kmol/hr)	14.8	126.7	5.9	106.6	26.0	17.8	4.0	13.8	8.2	5.0	3.2	111.8
Mass flow (kg/hr)	475.0	4051.1	3978.4	3401.9	4627.6	4148.9	127.0	4021.9	478.7	183.5	295.3	3576.1
Mass fraction												
Methanol (M)	1.0000	0.9977	0.0000	0.9947	0.0483	0.0322	0.9919	0.0018	0.1885	0.4911	0.0005	0.9974
Triolein (OOO)	0.0000	0.0000	0.8502	0.0000	0.0012	0.0013	0.0000	0.0014	0.0000	0.0000	0.0000	0.0000
Oleic acid (OA)	0.0000	0.0000	0.1498	0.0000	0.0000	0.0000	0.0000	0.0000	0.0000	0.0000	0.0000	0.0000
Water (W)	0.0000	0.0023	0.0000	0.0052	0.0064	0.0002	0.0068	0.0000	0.0597	0.1529	0.0018	0.0026
Glycerol (G)	0.0000	0.0000	0.0000	0.0000	0.0759	0.0014	0.0008	0.0014	0.7213	0.2865	0.9914	0.0000
Methyl oleate (MO)	0.0000	0.0000	0.0000	0.0000	0.8682	0.9649	0.0004	0.9954	0.0305	0.0695	0.0063	0.0000

Table 5.3 – Input conditions used to obtain results from optimization by decision maker (DM) of Process A1

n_{102}^{M} [a]	MR [b]	$MR_{min}^{N=2}$ [c]	T-101					T-102					T-103					V-101		V-102	
			P[e]	N	RR	FS	D/F[f]	P[e]	N	RR	FS	D/F[f]	P[e]	N	RR	FS	D/F[f]	P[e]	T[g]	P_t [h]	T[g]
126.1	21.3	106.2[d]	5	11	0.5	2	0.804	0.65	5	0.3	2	0.224	1	10	0.3	4	0.968	1	110	35	149
110.0	18.5	88.7[d]	5	11	0.5	2	0.777	0.65	5	0.3	2	0.223	1	10	0.3	4	0.962	1	110	35	149
95.0	16.0	74.6[d]	5	12	0.5	2	0.744	0.65	5	0.3	2	0.219	1	10	0.3	4	0.956	1	110	35	149
80.0	13.5	60.9[d]	5	13	0.5	2	0.701	0.65	5	0.3	2	0.214	1	10	0.3	4	0.946	1	110	35	149
65.0	11.0	48.0[d]	5	14	0.5	2	0.638	0.65	5	0.3	2	0.212	1	10	0.3	4	0.931	1	110	35	149
50.0	8.4	35.8[d]	5	16	0.5	2	0.540	0.65	5	0.3	2	0.211	1	10	0.3	4	0.905	1	110	35	149
45.0	7.6	32.0[d]	5	18	0.5	2	0.495	0.65	5	0.3	2	0.210	1	10	0.3	4	0.891	1	110	35	149
35.0	5.9	24.7[d]	5	19	0.5	2	0.371	0.65	5	0.3	2	0.208	1	10	0.3	4	0.845	1	110	35	149
45.0[i]	**7.6**	**27.1[d]**	**5**	**19**	**0.1**	**2**	**0.495**	**0.66**	**4**	**0.1**	**3**	**0.210**	**1**	**9**	**0.3**	**4**	**0.891**	**1**	**110**	**35**	**149**
43.2[j]	**7.3**	**26.4[d]**	**5**	**20**	**0.1**	**2**	**0.496**	**0.66**	**4**	**0.2**	**3**	**0.180**	**1**	**9**	**0.3**	**4**	**0.900**	**1**	**110**	**34.6**	**149**

[a] n_{102}^{M} means mole flow of methanol on stream 102 at kmol·h^{-1}; [b] MR means molar ratio of methanol to ROF (mol/mol) before the catalytic distillation (CD) column T-101; [c] $MR_{min}^{N=2}$ means minimum molar ratio of methanol to ROF (mol/mol) inside the CD T-101 found on stage 2; [d] Hot inlet temperature (T_{in}^{H}) minus cold outlet temperature (T_{out}^{C}) equals 10°C (ΔT = 10°C) for $n_{102}^{M} \geq$ 110 kmol·h^{-1} or hot outlet temperature (T_{out}^{H}) equals 64°C for n_{102}^{M} < 110 kmol·h^{-1};[e] P means pressure at atm; [f] D/F means distillate to feed ratio in CD T-101; [g] T means temperature at °C; [h] P_t means pressure at Torr; [i] Optimization condition for column T-101 obtained by decision maker (DM) [j] Optimization condition for column T-101 obtained by stochastic optimization using Simulated Annealing (SA) method from Matlab.

Table 5.4 – Raw material, product, catalyst and utilities prices used in process simulations

Chemicals	LRP[a] ($/kg)	HRP[b] ($/kg)	Chemicals	LPP[a] ($/kg)	HPP[b] ($/kg)	Utility	Cost ($/GJ)	Utility	Cost
Yellow grease	0.35	0.60	Biodiesel	0.85	1.00	HP steam[c]	9.88	Chilled water	4.43 $/GJ
Brown grease	0.20	0.33	Glycerol	0.63	0.98	MP steam[c]	8.22	Cooling water	6 x 10^{-5} $/kg
Methanol	0.30	0.50	$HWSi/Al_2O_3$	150.00		LP steam[c]	7.78	Electricity	0.12 $/kW·h
Water	5.4 x 10^{-4}	1.2 x 10^{-3}	Nb_2O_5	44.33		Freon	7.89	Wastewater	0.33 $/kg

[a] LRP and LPP refer to the lowest raw material price and lowest product price; [b] HRP and HPP refer to the highest raw material price and highest product price; [c] LP steam refers to low-pressure steam, MP steam refers to moderate-pressure steam and HP steam refers to high-pressure steam.

Source: Adapted from HBI (2018), ICIS (2018), Intratec (2018), Jolis and Martis (2012), Kiss (2013), Luyben (2013), McGarvey and Tyner (2018), Methanex (2018), Neste (2018), Perlingeiro (2005), Segovia-Hernández and Gómez-Castro (2017), Seider, Seader and Lewin (2009) and United States Department of Agriculture (2018).

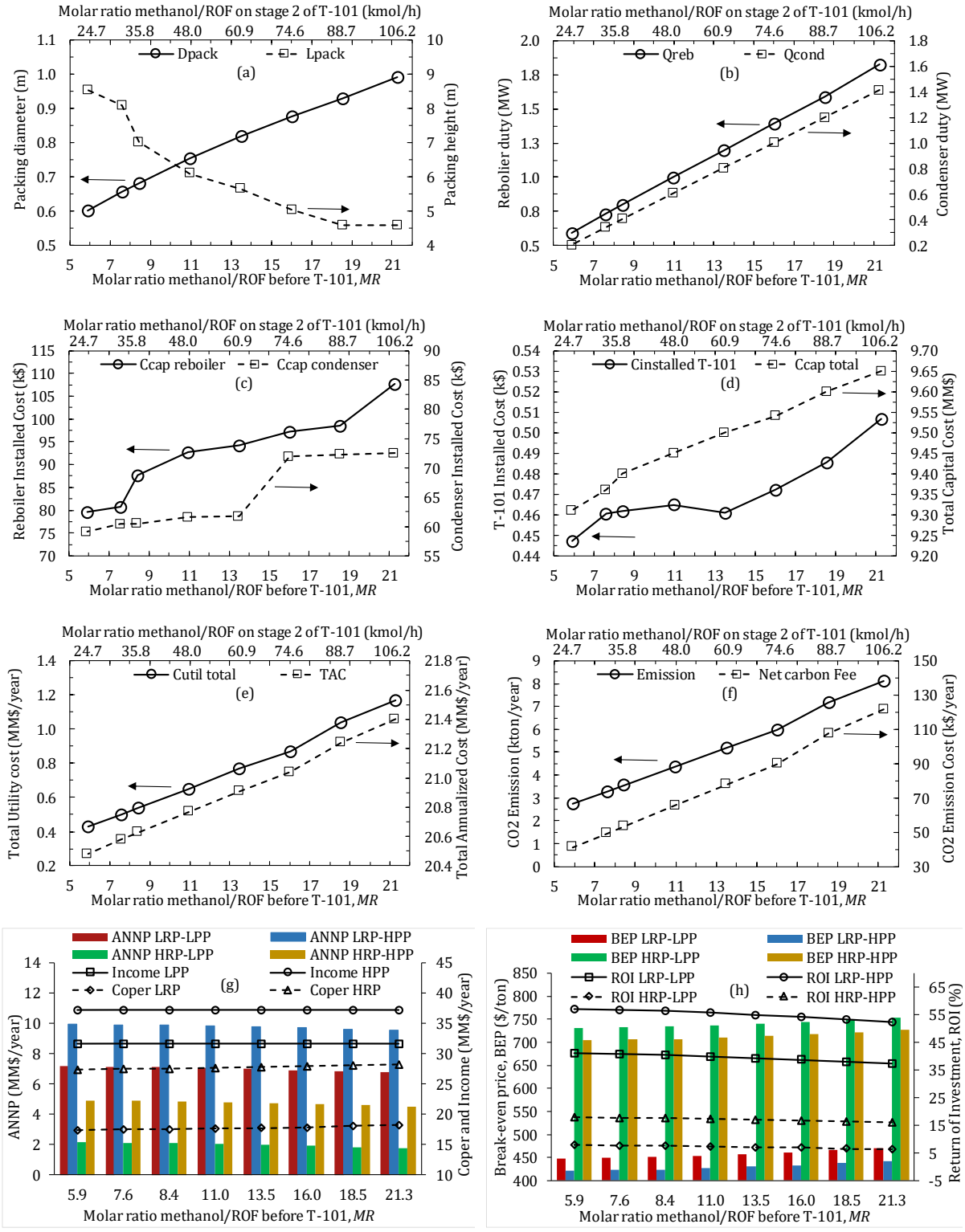

Figure 5.5 – Results for optimization of Process A1 by decision maker varying molar ratio (*MR*)

Figure 5.5g-h show more four types of economic indicators that takes account the minimum and maximum prices of raw materials and products as shown in Table 5.4. In order to make easier the differences between the four cases of prices, an abbreviation was defined containing first three letters relative to raw materials price and other three letters in the final relative to product prices. The first letter was defined as L or H referring to lowest or highest prices, while second letter was referred R to raw materials and P to product. The last letter P refers to price. Therefore, for instance LRP-HPP refers to lowest raw material price and highest product price.

Clearly, all economic results are enhanced when MR was decreased, since costs (TAC, capital, utility and operation costs) decreased and other indicators based on product sales increased, such as: income, net annual profit after taxes (A_{NNP}) and return of investment (ROI). Results from break-even price (BEP) and payback period also decreased when MR decreased as shown in Figure 5.5h and Table 5.5, respectively. Consequently, from these results the lowest MR value of 5.9 should be chosen. However, a MR of 8.4 was chosen as optimal, since other technical parameters were considered for these cases, so that they should keep close to values from the base case. For instance, besides of a MR > 21.27 on stages from T-101 column, biodiesel specifications should be satisfied as in the base case including the exceptions mentioned before. In addition, reboiler temperature (T_{reb}) of T-101 and T-102 columns should be close to 162°C and 238°C to avoid decomposition of glycerol and biodiesel, waste stream mass flow rate (m_{214}) in the range of 136 to 140 kg/h and mass fraction of methanol before T-101 (w_{202}^{M}) greater than 0.99. This latter helped the decision to choose a feed of 45 kmol/h of methanol resulting in a MR of 8.4, minimum molar ratio ($MR_{min}^{N=2}$) greater than 21.27 on stage 2 and w_{202}^{met} > 0.99.

After optimization of methanol feed rate, an evaluation was carried out based on the most expensive equipment as indicated on Aspen Plus, so that the three distillation columns T-101, T-102 and T-103 were investigated. In this case, in order to obtain minimum TAC, two main input variables were changed: number of stages (N) and reflux ratio (RR). Furthermore, two different approaches were adopted in this optimization. First, column T-101 was optimized as previously presented using Aspen Plus cost analyzer tool according to the following reasons: presence of recycle stream, highest equipment cost, highest utility costs and difficult to converge many input variables in the same time on sensitivity analysis. Second, columns T-102 and T-103 were optimized based on sensitivity analysis including an external cost calculation

procedure for TAC, since this approach is easier and faster to obtain cost results for the secondary costlier equipment (capital, utility and waste treatment costs). As this last approach is simplified some differences on sizing and costs can be evidenced related to the final optimized flowsheet to be evaluated on Aspen Plus cost analyzer tool. However, these approximate approach was applied with relative success to obtain faster optimized results for Process A1 based on SAC process with CDC.

Table 5.5 – Input conditions and PBP results from optimization by decision maker of Process A1

n_{102}^{M} [a]	MR [b]	$MR_{min}^{N=2}$ [c]	E-101	T-201					PBP[g] LRP-		PBP[g] HRP-	
			ΔT or T[d]	P[e]	N	RR	FS	D/F[f]	LPP	HPP	LPP	HPP
126.1	21.3	106.2	10	5	11	0.5	2	0.804	2.86	2.13	11.56	4.50
110.0	18.5	88.7	10	5	11	0.5	2	0.777	2.82	2.11	11.09	4.42
95.0	16.0	74.6	64	5	12	0.5	2	0.744	2.78	2.08	10.58	4.33
80.0	13.5	60.9	64	5	13	0.5	2	0.701	2.75	2.07	10.24	4.26
65.0	11.0	48.0	64	5	14	0.5	2	0.638	3.94	2.05	9.90	4.20
50.0	8.4	35.8	64	5	16	0.5	2	0.540	2.68	2.03	9.62	4.14
45.0	7.6	32.0	64	5	18	0.5	2	0.495	2.67	2.02	9.51	4.11
35.0	5.9	24.7	64	5	19	0.5	2	0.371	2.65	2.01	9.31	4.07
45.0	**7.6**	**27.1**	**64**	**5**	**19**	**0.1**	**2**	**0.495**	**2.62**	**1.98**	**9.37**	**4.04**

[a] n_{102}^{M} means mole flow of methanol on stream 102 at kmol·h^{-1}; [b] MR means molar ratio of methanol to ROF (mol/mol) before the CDC T-101; [c] $MR_{min}^{N=2}$ means minimum molar ratio of methanol to ROF (mol/mol) inside the CDC T-101 found on stage 2; [d] One of two conditions were adopted to E-101 to become easier convergence, such as: hot inlet temperature (T_{in}^{H}) minus cold outlet temperature (T_{out}^{C}) equals 10°C (ΔT = 10°C) for $n_{102}^{M} \geq$ 110 kmol·h^{-1} or hot outlet temperature (T_{out}^{H}) equals 64°C for n_{102}^{M} < 110 kmol·h^{-1}; [e] P means pressure at atm; [f] D/F means distillate to feed ratio (mol/mol) in CDC T-101; [g] PBP means payback period at year.

Similar qualitative results for optimization of column T-101 were found for design variables as well as for cost and emission indicators as shown in Figure 5.6. However, for that case N and reflux ratio (RR) were changed in T-101 column keeping n_{102}^{M} = 45 kmol·h^{-1} and FS = 2, while D/F were varied in T-102 and T-103 columns in order to achieve biodiesel specifications close to the base case. From these results N = 20 and RR = 0.001 should be chosen. However, problems to carry out sensitivity analysis close to this low value of RR suggested that is closer or below minimum reflux ratio (RR_{min}). For that reason, N = 19 and RR = 0.1 was chosen as optimal point as shown in Table 5.3, since no problems with sensitivity analysis were found with FS kept on stage 2. Furthermore, a test to obtain an estimative from RR_{min} showed that $RR_{min} \leq 0.05$ for N = 19. It is worth to mention that in Figure 5.6, bottom abscissa is a continuous axis for N, while top abscissa is a discrete axis for RR in T-101 column.

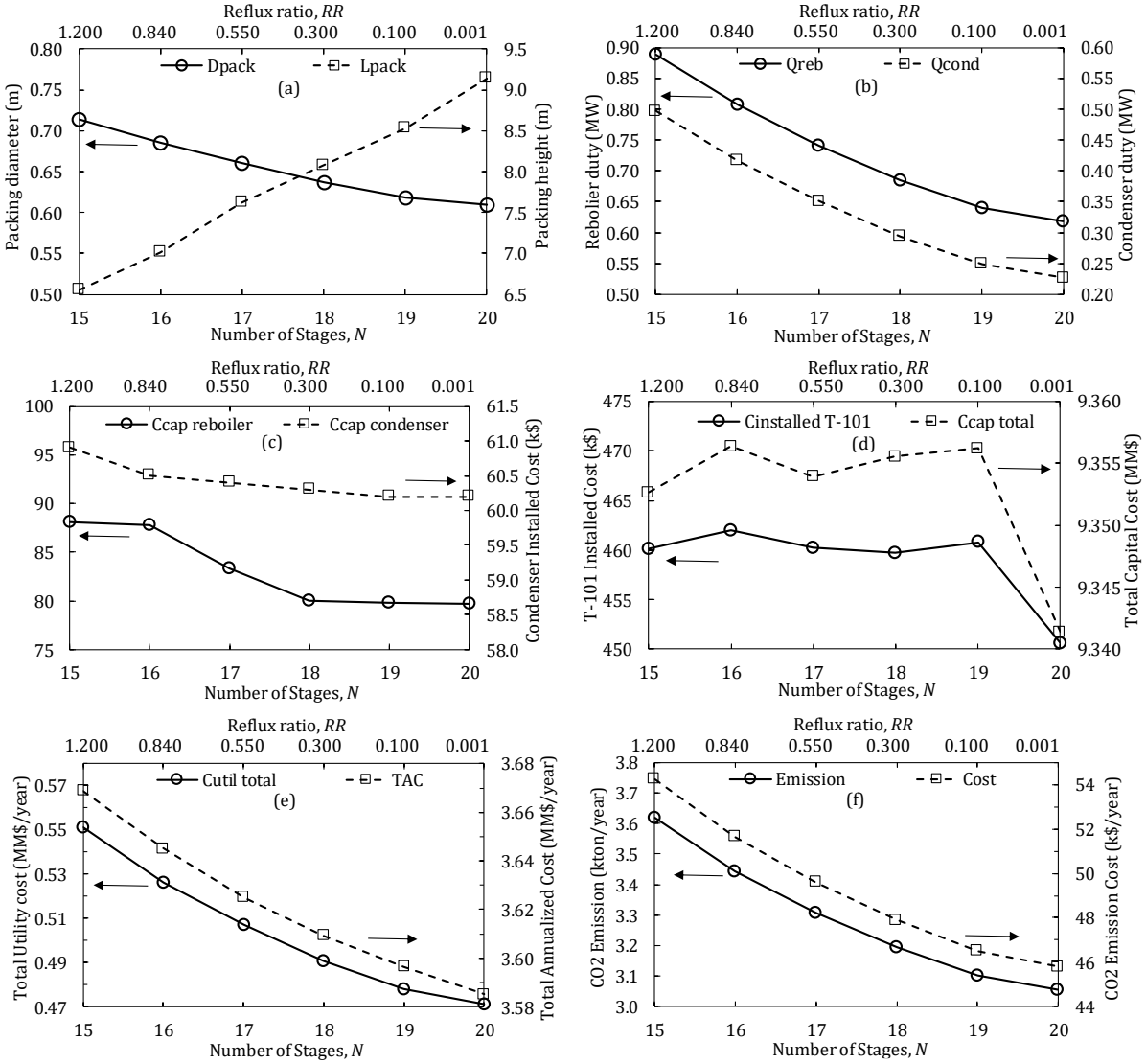

Figure 5.6 – Sensitivity analysis results for the CDC (T-101) from Process A1 obtained varying *N* and reflux ratio (*RR*)

Results of optimization design of biodiesel purification column (T-102) was obtained by sensitivity analysis including an external cost calculation as shown in Figure 5.7. Results of these designs were obtained without include stream 113, since when recycle was included a long time was required to converge and some error results were found. For all variables, the lower RR the lower dimensions, required energy and costs. Relative to N, the lower N the lower installed cost (C_{inst}). However, a minimum was found for utility cost (C_{util}) and consequently also to TAC in N = 4, despite the lower capital cost. It is worth to remind that feed stage (FS) was set as $N - 1$ on sensitivity analysis since was the best FS value for all N values. In relation to D/F, the higher D/F the higher biodiesel purity (w_{108}^{MO}), packing diameter (D_p), required energy and costs; and also the lower methanol purity (w_{108}^{M}). Therefore, based on a trade-off,

T-102 column design was set up in N = 4, FS = 3, RR = 0.1 and D/F = 0.2103 as shown in Table 5.3. Values closer to N and FS were also varied to calculate costs directly from Aspen Plus V8.8 keeping RR and D/F in the same values. This approach confirmed a minimal cost point in these conditions.

Optimization design of methanol recovery column (T-103) was carried out in the same way as applied to T-102 column as shown in Figure 5.8. For all variables, the lower RR the lower tray diameter, required energy and costs. Relative to N, the lower N the lower column height and consequently, the lower installed cost (C_{inst}). Despite to be difficult to identify a minimum TAC point in Figure 5.8h, N = 9 and RR = 0.1 showed the lowest TAC value for higher methanol purity in recycle stream 113 (w_{113}^{M}). It is worth to remind that optimum feed stage (FS) was set up as FS = 2 for $N \leq 6$, FS = 3 for 7 ≤ N ≤ 8, FS = 4 for N = 9 and FS = 5 for $10 \leq N \leq 11$. Relative to D/F, the lower D/F the higher w_{113}^{M} to be recovered; however, the lower tray diameter (D_T), required energy and costs.

Therefore, based on results from Figure 5.8, N = 9, FS = 4, RR = 0.1 and D/F = 0.887 should be chosen as optimum design conditions for T-103 column. However, when recycle stream was added, lower w_{113}^{M} values were obtained. In order to investigate this issue, an additional sensitivity analysis varying D/F and RR were carried out keeping N and FS constants. Results showed that D/F should be increased when recycle stream was included, since some small amount of water returned in stream 113. A mass fraction of methanol in the stream 102 (w_{102}^{M}) greater than 0.99 was adopted as constraint for this choice. For that reason, D/F value was increased to obtain the optimal design: N = 9, FS = 4, RR = 0.1 and D/F = 0.8905 as shown in Table 5.3. Values closer to N and FS were also varied to calculate costs directly from Aspen Plus V8.8. keeping RR and D/F in the same values. This approach confirmed a minimal cost point in these conditions.

After optimization by decision maker (DM) of the most expensive pieces of equipment, a modification in the flowsheet of Process A1 was proposed in order to completely achieve the biodiesel standard and high purity pharmaceutical glycerol (99.5 wt%). For that reason, a water washing step including an extraction column (V-101), was added as shown in Figure 5.9 (ZHANG et al., 2003a).

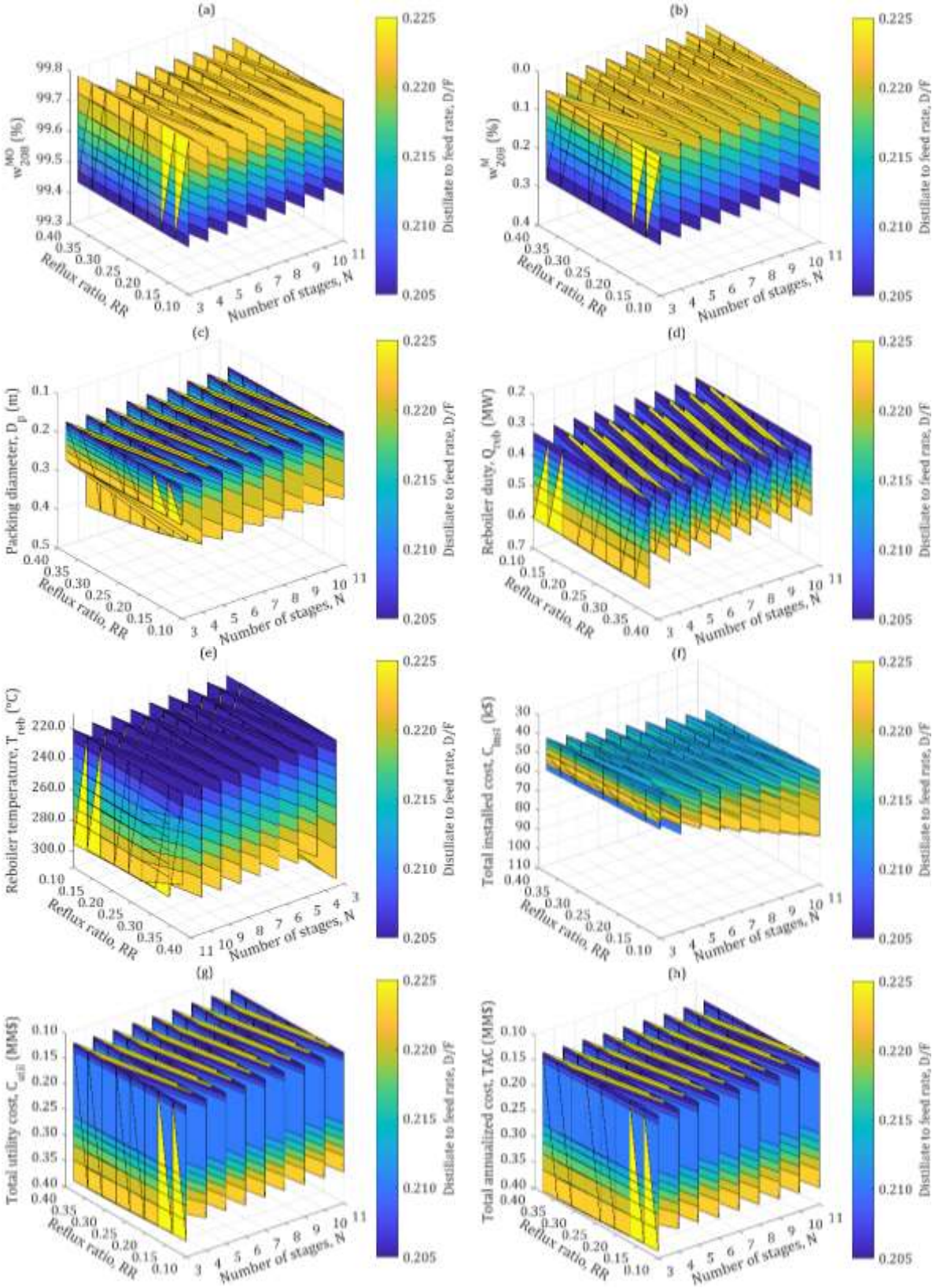

Figure 5.7 – Sensitivity analysis results for biodiesel purification (T-102 column) from Process A1

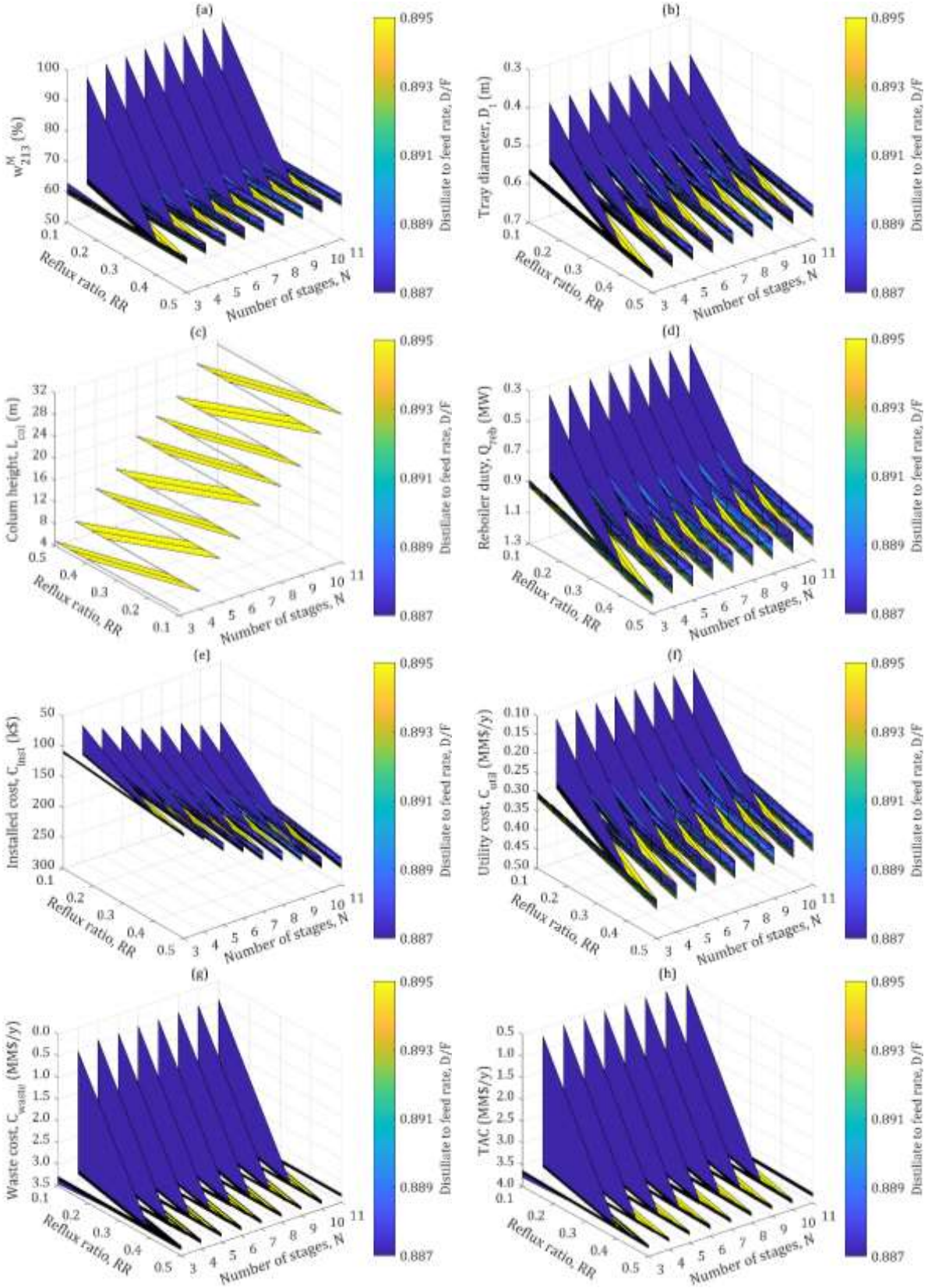

Figure 5.8 – Sensitivity analysis results for methanol recovery (T-103 column) from Process A1

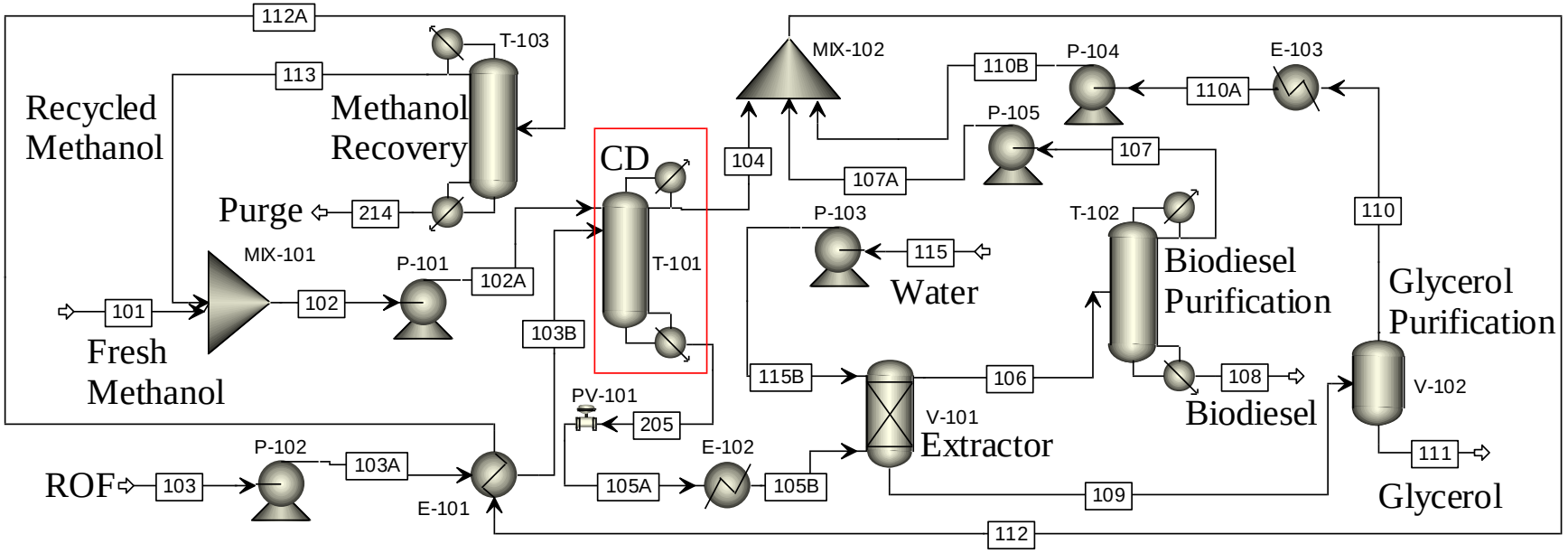

Figure 5.9 – Flowsheet for the SAC biodiesel production process from CDC column including an extractor to satisfy biodiesel specifications
Source: Adapted from Gaurav, Ng and Rempel (2016)

Table 5.6 – Stream results for optimized design of Process A2 based on SAC biodiesel production process from CD column

Stream number	101	102A	103B	104	105	106	107A	108	109	110B	111	113
Temperature (°C)	25.0	53.3	42.1	112.4	162.4	89.8	51.5	238.9	90.0	9.5	149.3	64.8
Pressure (kPa)	101.3	506.6	511.3	506.6	507.3	152.0	506.6	55.8	152.0	506.6	4.1	101.3
Mole flow (kmol/h)	14.8	45.6	5.9	25.5	26.0	17.0	3.2	13.8	9.4	6.4	3.0	30.8
Mass flow (kg/h)	474.2	1451.8	3978.4	807.3	4622.9	4122.6	100.9	4021.7	507.5	235.0	272.5	977.6
Mass fraction												
Methanol (M)	1.0000	0.9930	0.0000	0.9851	0.0459	0.0256	0.9678	0.0020	0.2102	0.4535	0.0004	0.9896
Triolein (OOO)	0.0000	0.0000	0.8502	0.0000	0.0013	0.0015	0.0000	0.0015	0.0000	0.0000	0.0000	0.0000
Oleic acid (OA)	0.0000	0.0000	0.1498	0.0000	0.0000	0.0000	0.0000	0.0000	0.0000	0.0000	0.0000	0.0000
Water (W)	0.0000	0.0070	0.0000	0.0148	0.0078	0.0008	0.0322	0.0000	0.0791	0.1688	0.0017	0.0104
Glycerol (G)	0.0000	0.0000	0.0000	0.0000	0.0760	0.0002	0.0000	0.0002	0.6907	0.3379	0.9950	0.0000
Methyl oleate (MO)	0.0000	0.0000	0.0000	0.0000	0.8690	0.9720	0.0000	0.9964	0.0200	0.0398	0.0029	0.0000

An optimization by DM was also carried out for the extraction column (V-101) in order to obtain minimum TAC and mass fraction of glycerol on biodiesel stream (w_{108}^{G}) less than or equal to 0.02 wt%, which is equivalent to mass flowrate of glycerol on stream 106 (m_{106}^{G}) less than 0.8 kg/h. From results of Figure 5.10, the lower T the lower amount of glycerol on biodiesel rich-streams (106 and 108), since partition coefficient of glycerol on glycerol rich-stream (polar phase) increases when T is decreased (ANDREATTA et al., 2008; BARREAU et al., 2010). On the other hand, the lower T the higher installed (C_{inst}) and utility (C_{util}) costs for the cooling heat exchanger, consequently the higher TAC. Therefore, higher T should be set up on V-101, because the stream 105B was fed in extractor at 90°C. For that reason, adiabatic operation was adopted keeping P = 1.5 kPa to avoid formation of a vapor phase as shown in Table 5.6. As T showed to be the most important variable affecting results, N = 2 and feed to solvent (water) mass ratio (m_{105B}/m_{115}) equals to 641.5.

After to add the extraction column, new sensitivity analysis was carried out to T-102 and T-103 column, so that only few changes were applied to achieve $w_{108}^{G} \leq 0.02$ wt% in biodiesel stream (108) and $w_{111}^{G} \geq 99.5$ wt% in glycerol stream as N = 10 and FS = 5 to column T-103. Stream results for Process A2 are showed in Table 5.6, while input conditions to obtain the results are showed in Table 5.9; and design and capital costs are showed in Table 5.7. Furthermore, some profile results from column T-101 of process A2 are plotted as shown in Figure 5.11. From these results, temperature profiles showed similar behaviour as reported by Noshadi, Amin and Parnas (2012). As an excess of methanol was added, composition profiles (mole and mass fractions) showed larger fractions of the alcohol. However, as expected methyl oleate (MO) concentration increased from top to bottom of column T-101, mainly in the 2nd liquid phase also known as MO rich-phase. The same happened to glycerol (G) in the 1st liquid phase also known as G rich-phase.

Related to MR of methanol to ROF, stage 2 showed the minimum MR (MR_{min}) greater than 21.27 and the higher reaction rate because the higher amount of ROF in this stage. Moreover, other stages showed much higher MR, so that methanol could be fed in lower stages. Actually, this was investigated; however, higher RR were required to keep MR_{min} > 21.27 and, consequently, higher reboiler duty (Q_{reb}) and higher costs were obtained. Experimental results reported by Noshadi, Amin and Parnas (2012) were also obtained feeding oil and methanol in stage 2.

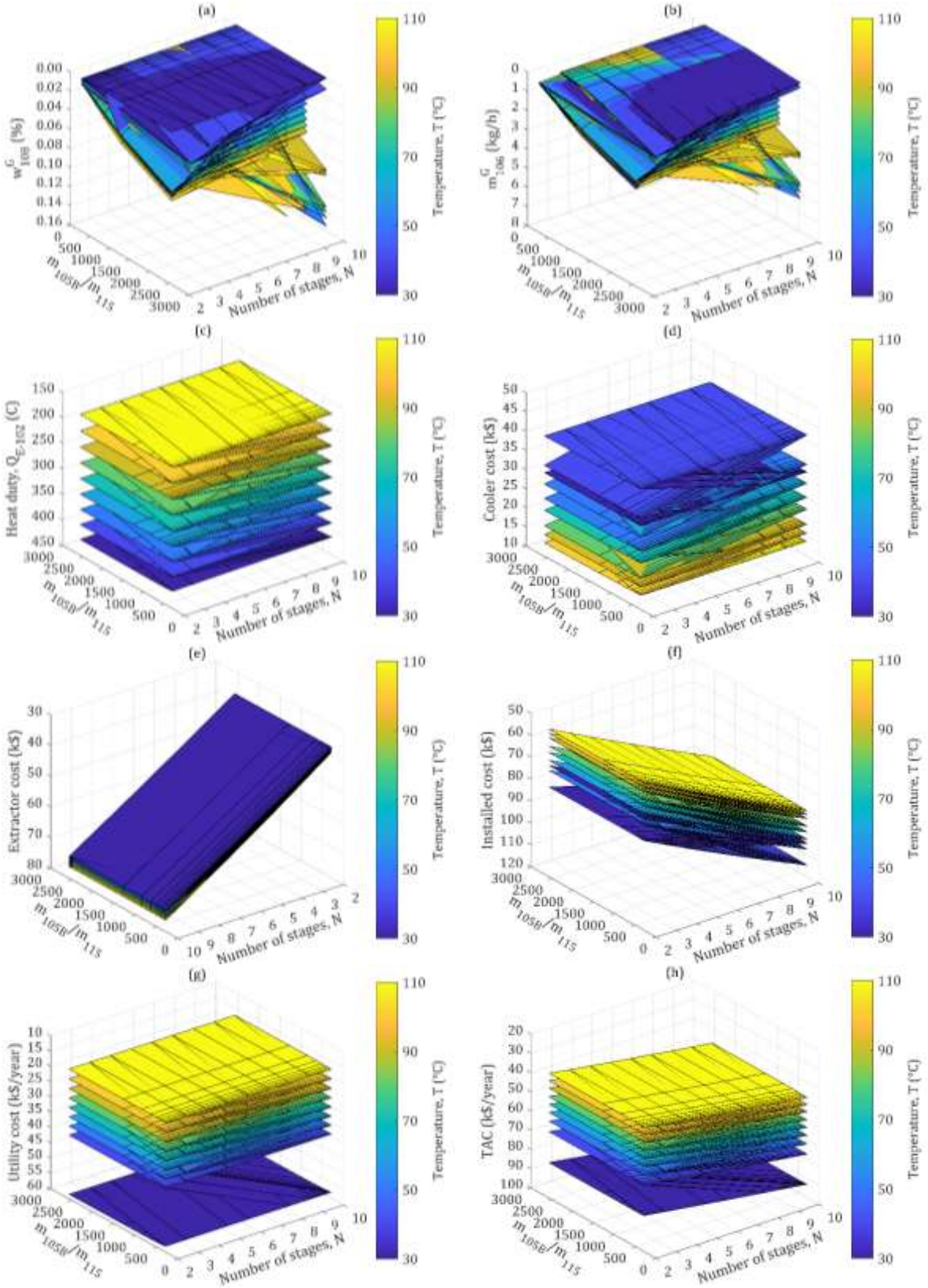

Figure 5.10 – Sensitivity analysis results for extraction column (V-101) from Process A2

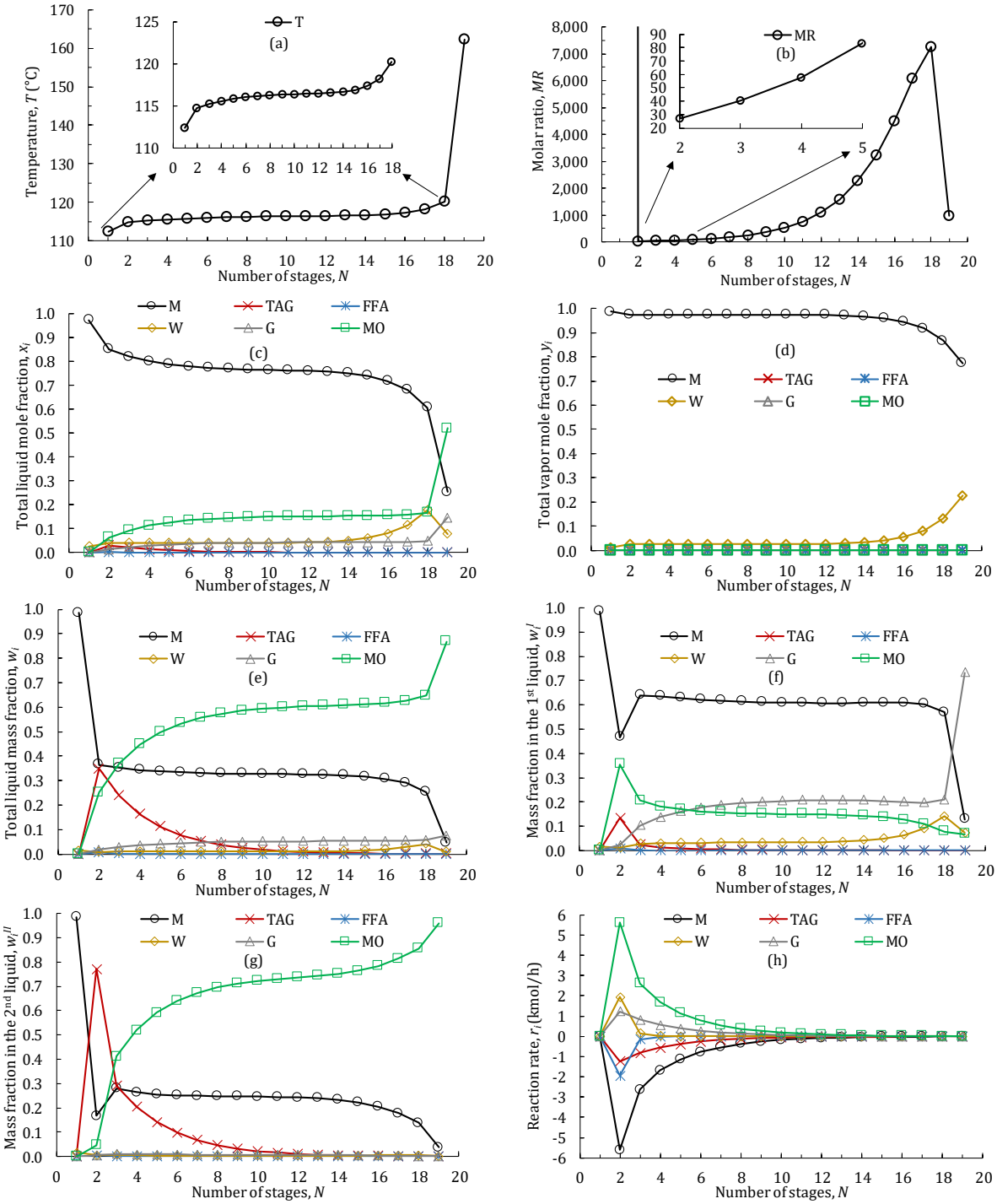

Figure 5.11 – Profiles results from column T-101 of process A2 including an extraction column

Table 5.7 – Main operating conditions, equipment sizes and capital costs

Block	Description	Process A2	Process B1	Process C1
R-301 Hydrolysis	P (kPa)/T (K)			5,600.0/540.8
	N_t/size ($D \times L$, m)			10/0.12 X 0.80
	cost (k$)			94.6
T-101/ T-201/ T-302 CDC	$RR/(D/F$ or $V/F)$	0.1/0.495	0.0/0.500	0.1/0.230
	P (kPa)	506.6/507.3	709.3/709.7	304/304.8
	T (K)	385.5/435.5	402.9/404.8	369.2/376
	heat duty, Q (kW)	-249.3/642.0	0.0/0.0	-187.6/587.0
	N (stages)/FS/NR	19/2/2-18	13/1-13/1-13	22/2/2-21
	size ($D \times L$, m)	0.76 X 12.8	0.61 X 10.82	0.76 X 14.33
	cost (k$)	460.8	179.2	474.3
V-101/ V-202/ V-302 Extractor/ Decanter	P (kPa)/T (K)	152.0/363.0	152.0/354.3	152.0/376.0
	Water mass flow, m^W(kg/h)	7.2	18.0	
	size ($D \times L$, m)	1.07 X 3.66	1.07 X 3.66	0.91 X 3.66
	cost (k$)	107.4	105.7	103.7
T-102/ T-202/ T-303 Biodiesel purification	$RR/(D/F)$	0.1/0.190	0.1/0.304	0.4/0.536
	P (kPa)	55.7/55.8	55.7/55.8	304/304.8
	T (K)	324.1/512.1	324.1/511.5	347.0/513.2
	heat duty, Q (kW)	-36.1/427.9	-69.3/472.6	-224.4/473.2
	N (stages)/FS	4/3	3/2	8/6
	size ($D \times L$, m)	0.30 X 5.33	0.30 X 4.88	0.30 X 7.32
	cost (k$)	391.3	391.0	409.7
V-102/ V-203/ T-301 Glycerol purification	$RR/(D/F)$			0.1/0.085
	P (kPa)	4.1	4.1	0.9/1.1
	T (K)	422.5	422.5	278/411.7
	heat duty, Q (kW)	93.8	180.7	-4.8/20.7
	N (stages)/FS			3/2
	size ($D \times L$, m)	0.91 X 3.66	0.91 X 3.66	0.15 X 4.88
	cost (k$)	107.4	105.1	352.2
T-103/ T-203/ T-304 Methanol purification	$RR/(D/F)$	0.3/0.880	0.3/0.865	0.9/0.777
	P (kPa)	101.3/107.5	101.3/107.5	101.3/110.3
	T (K)	338/364.7	338.1/363.4	337.9/371.0
	heat duty, Q (kW)	-393.6/399.8	-396.5/403.1	-957.7/922.6
	N (stages)/FS	10/5	10/5	14/8
	size ($D \times L$, m)	0.46 X 10.97	0.46 X 10.97	0.76 X 14.63
	cost (k$)	430.7	431.5	507.1
	heat exchangers, cost (k$)	177.6	435.8	416.3
	pumps, cost (k$)	141.0	202.9	450.3
	Total Installed cost, C_{TI} (MM$)	1.82	1.96	2.96
	Total Capital Cost, C_{TC} (MM$)	9.82	10.24	13.19

5.3.2 Solid-acid catalyzed process from Catalytic Absorption

An alternative process based on catalytic absorption column (CAC), denominated Process B1, was also designed in order to balance the distribution of methanol around the column stages as shown in flowsheet from Figure 5.12 (KISS, 2009). This process was proposed to overcome waste of alcohol in the bottom of the T-101 column, since some amount of methanol is fed as liquid on the top stage (42%) as for Process A2 and another amount is fed as vapor on the last stage. Furthermore, according to Kiss (2009) low RR values can suggest that a reactive absorption column can be more economical than a RDC. It is worth to mention that the flowsheet was designed in the same way as for Process A2 and adopting the same optimization steps by decision maker applied previously.

Stream results and design input conditions are showed in Table 5.8 and Table 5.9. From these results can be highlighted that a higher pressure (P) of 7 atm was employed. For that reason, less N were required (N = 13), since the higher P in CAC the higher T in reactive stages and consequently, the higher biodiesel conversion (GAURAV et al., 2013; PETCHSOONGSAKUL et al., 2017). Furthermore, three heat exchangers of integration were added in order to decrease utility costs. Finally, biodiesel specifications were satisfied besides of glycerol purity of pharmaceutical glycerol (99.65 wt%).

Profile results from column T-201 of process B1 were also generated as shown in Figure 5.13. From these results T profiles showed different behaviour with highest T in the middle stages, since no reboiler and condenser were presented. An excess of methanol was also detected in bottom stages, so that composition profiles showed larger fractions of the alcohol mainly in vapor phase. However, lower concentrations of methanol in liquid phases and lower MR inside stages were obtained, so that amount of methanol was balanced in column T-201. The highest reaction rate was also found in the first reactive stage as before for Process A2.

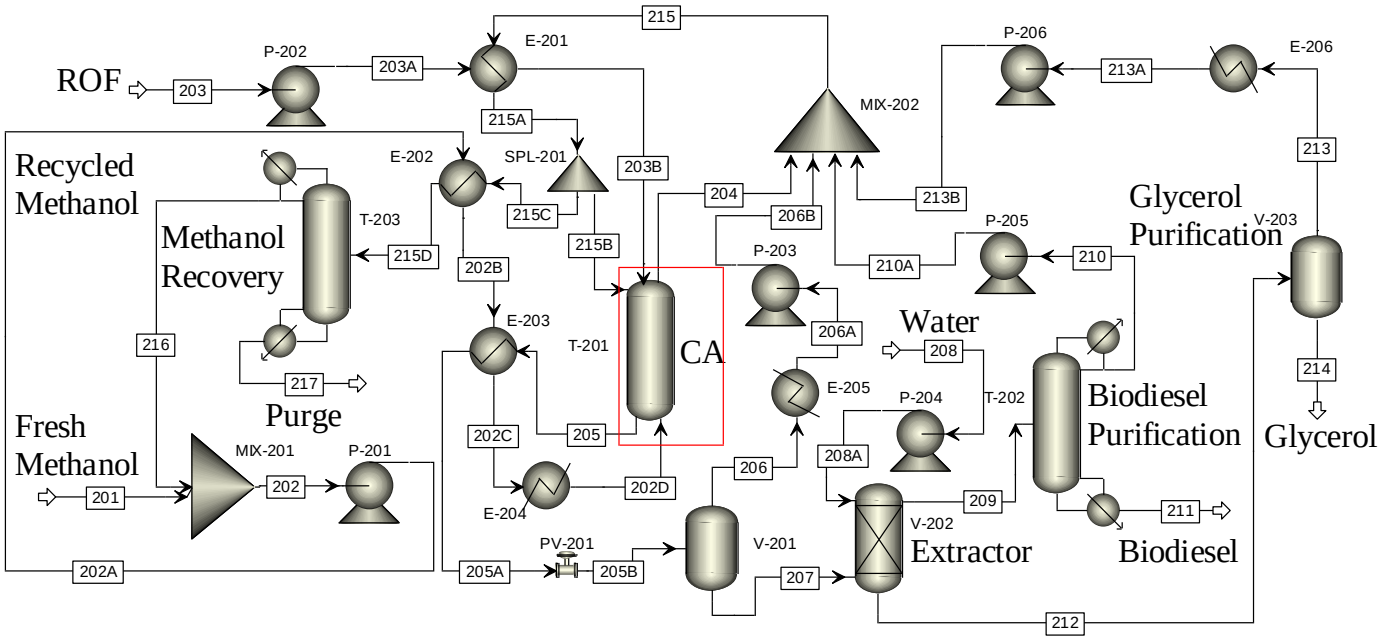

Figure 5.12 – Flowsheet for the SAC biodiesel production process from catalytic absorption (CAC) column satisfying biodiesel standard
Source: Adapted from Gaurav, Ng and Rempel (2016) and Kiss (2009).

Table 5.8 – Stream results for optimized design of Process B1 based on SAC biodiesel production process from CA column

Stream number	201	202D	203B	204	205	206	209	210A	211	213	214	216
Temperature (°C)	25.0	124.3	116.2	129.7	131.6	81.0	81.2	51.9	238.3	149.3	149.3	64.9
Pressure (kPa)	101.3	709.3	711.3	709.3	709.7	101.3	152.0	709.3	55.8	4.1	4.1	101.3
Mole flow (kmol/h)	14.8	45.7	5.9	25.8	76.7	42.0	19.8	6.0	13.8	12.8	3.1	30.9
Mass flow (kg/h)	474.5	1455.3	3978.4	796.3	6262.1	1290.2	4209.5	187.5	4022.0	493.6	286.7	980.8
Mass fraction												
Methanol (M)	1.0000	0.9907	0.0000	0.9491	0.2670	0.9446	0.0449	0.9646	0.0020	0.5356	0.0005	0.9863
Triolein (OOO)	0.0000	0.0000	0.8502	0.0000	0.0008	0.0000	0.0012	0.0000	0.0013	0.0000	0.0000	0.0000
Oleic acid (OA)	0.0000	0.0000	0.1498	0.0000	0.0000	0.0000	0.0000	0.0000	0.0000	0.0000	0.0000	0.0000
Water (W)	0.0000	0.0093	0.0000	0.0507	0.0175	0.0553	0.0016	0.0353	0.0000	0.0996	0.0011	0.0137
Glycerol (G)	0.0000	0.0000	0.0000	0.0000	0.0710	0.0001	0.0001	0.0001	0.0001	0.3209	0.9954	0.0000
Methyl oleate (MO)	0.0000	0.0000	0.0000	0.0001	0.6437	0.0000	0.9522	0.0000	0.9966	0.0439	0.0030	0.0000

Table 5.9 – Input conditions for results from optimization of Processes SA2, A2, A3, B1 and B2

Process	MR_{min}[a]	T-101/T-201					T-102/T-202					T-103/T-203					V-201		V-101/ V-202		V-102/ V-203	
		P[b]	N	RR	FS	D/F[c]	P[b]	N	RR	FS	D/F[c]	P[b]	N	RR	FS	D/F[c]	P[b]	T[d]	P[b]	T[d]	P_t[e]	T[d]
SA2	27.4	5	21	0.2	2	0.491	0.6	3	0.1	3	0.161	1	11	0.3	5	0.896			1.5	90	30.4	149.3
A2	27.2	5	19	0.1	2	0.495	0.55	4	0.1	3	0.190	1	10	0.3	5	0.875			1.5	90	30.4	149.3
B1	21.7	7	13		1/13	0.500	0.55	3	0.1	2	0.304	1	10	0.3	5	0.865	1	81	1.5	81	30.0	149.3
A3	21.4	5	21	0.6	2	0.495	0.55	4	0.1	3	0.196	1	10	0.3	5	0.876			1.5	93	15.0	136.6
B2	21.6	7	13		1/13	0.505	0.55	3	0.1	2	0.303	1	10	0.3	5	0.869	1	81	1.5	86	15.0	133.4

[a] MR_{min} means minimum molar ratio of methanol to ROF (mol/mol) inside the CDC T-101; [b] P means pressure at atm; [c] D/F means distillate to feed ratio (mol/mol) in CDC T-101; [d] T means temperature at °C; [e] P_t means pressure at Torr.

Table 5.10 – Input conditions used to obtain results from optimization by decision maker (DM) of Process C1

n_{313}^{M}[a]	MR[b]	$MR_{min}^{N=2}$[c]	T-302					T-303					T-304					V-301		V-302	
			P[d]	N	RR	FS	D/F[e]	P[d]	N	RR	FS	D/F[e]	P[d]	N	RR	FS	D/F[e]	P_t[f]	T[g]	P[d]	T[g]
112.6	8.3	13.5	3	27	0.1	2	0.470	0.6	8	0.4	6	0.575	1	14	0.9	8	0.870	7.6	60	1	101.7
100.0	7.4	12.2	3	26	0.1	2	0.400	0.6	8	0.4	6	0.579	1	14	0.9	8	0.854	7.6	60	1	101.6
85.0	6.3	10.8	3	24	0.1	2	0.300	0.6	8	0.4	6	0.581	1	14	0.9	8	0.828	7.6	60	1	101.7
77.8	5.7	9.3	3	23	0.1	2	0.275	0.6	8	0.4	6	0.567	1	14	0.9	8	0.813	7.6	60	1	101.9
70.0	5.2	9.3	3	23	0.1	2	0.250	0.6	8	0.4	6	0.548	1	14	0.9	8	0.793	7.6	60	1	102.5
65.0	**4.8**	**8.8**	**3**	**22**	**0.1**	**2**	**0.230**	**0.6**	**8**	**0.4**	**6**	**0.536**	**1**	**14**	**0.9**	**8**	**0.777**	**7.6**	**60**	**1**	**102.8**
60.0	4.4	8.3	3	21	0.1	2	0.210	0.6	8	0.4	6	0.522	1	14	0.9	8	0.760	7.6	60	1	103.2
55.0	4.1	7.8	3	21	0.1	2	0.140	0.6	8	0.4	6	0.524	1	14	0.9	8	0.738	7.6	60	1	103.1

[a] n_{102}^{M} means mole flow of methanol on stream 102 at kmol·h^{-1}; [b] MR means molar ratio of methanol to ROF (mol/mol) before the catalytic distillation column (CDC) T-302; [c] $MR_{min}^{N=2}$ means minimum molar ratio of methanol to ROF (mol/mol) inside the CDC T-302 found on stage 2; [d] P means pressure at atm; [e] D/F means distillate to feed ratio (mol/mol) in CDC T-101; [f] P_t means pressure at Torr; [g] T means temperature at °C.

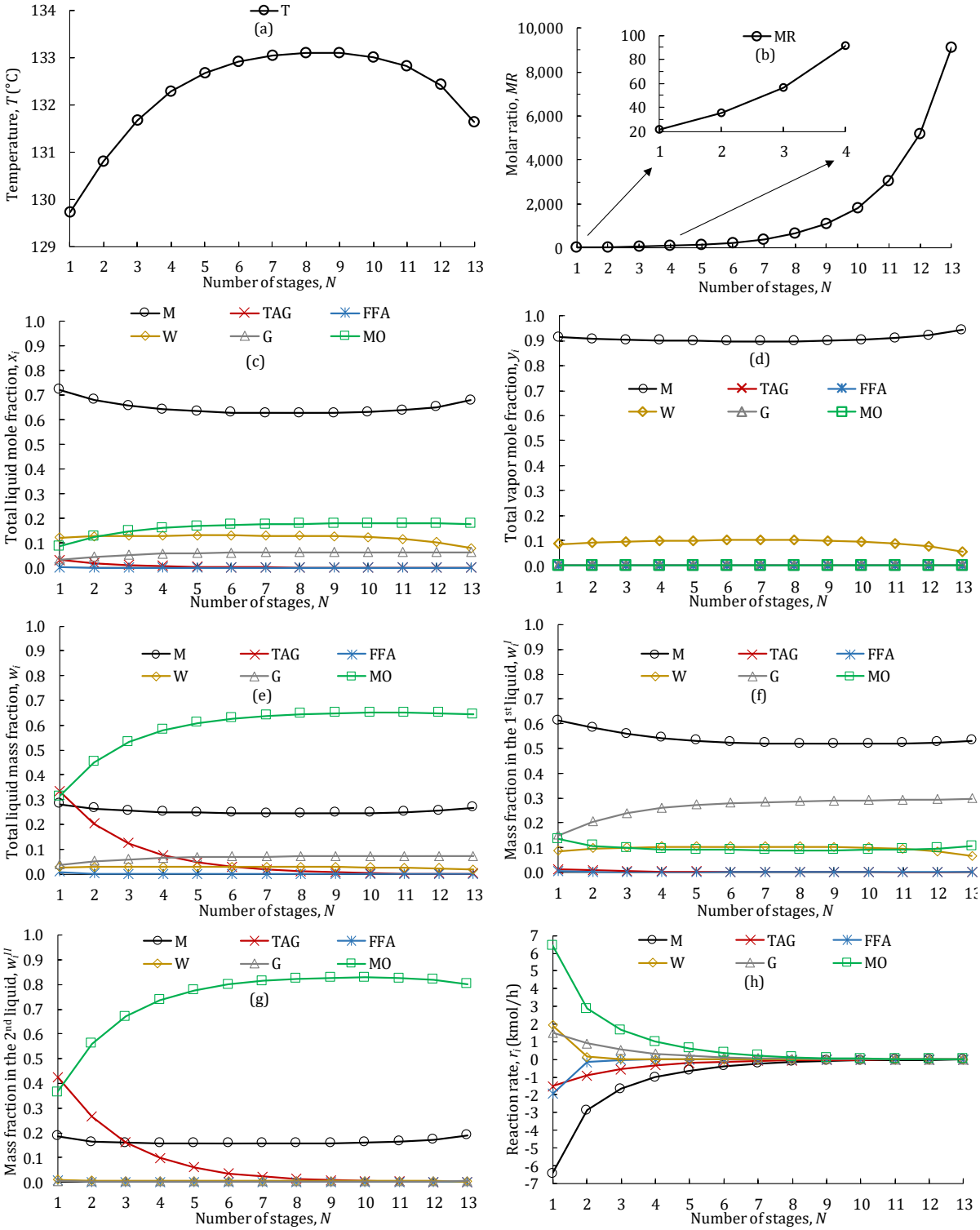

Figure 5.13 – Profiles results from column T-201 of process B1

5.3.3 Solid-acid catalyzed process from CDC based on hydro-esterification

The most well-known SAC process applied by industry for ROF was also designed in order to compare with SAC process based on simultaneous esterification and transesterification reactions (MACHADO et al., 2016). This flowsheet is based on hydro-esterification process using niobium oxide (Nb_2O_5) and $HWSi/Al_2O_3$ as solid acid catalysts for hydrolysis and esterification reactions, respectively, as shown in Figure 5.14 (GAURAV; NG; REMPEL, 2016; LAYLA et al., 2010; MACHADO et al., 2016). The flowsheet structure was also developed as other reported to supercritical conditions (GÓMEZ-CASTRO et al., 2011; GOMEZ-CASTRO et al., 2010). Furthermore, the concept of CDC was applied for the last reaction since esterification is an equilibrium-limited reaction. The same catalyst from Process A and Process B was adopted for Process C in order to keep concordance in economic analysis, since industrial tests are required to obtain the catalyst lifetime. In this work, one year of catalyst lifetime was adopted as considered in previous work from our research group (GAURAV; NG; REMPEL, 2016). This approach was judged suitable since $HWSi/Al_2O_3$ was used for all processes.

As for Process A1, an optimization by DM was carried out to reduce the MR of methanol to ROF. As the value of MR required for esterification reaction was not determined by Gaurav, Ng and Rempel (2016), a minimum MR of 8.32 was considered as a limit based on work of Tesser et al. (2005). For this optimization, a strategy was adopted keeping almost all design conditions from base case constants in Table 5.10. One exception was MR of methanol to ROF before CDC column (T-302) that was reduced, so that MR in all stages could still be above 8.32 (GAURAV; NG; REMPEL, 2016). From these changes, the number of stages (N) from T-302 and distillate to feed ratio (D/F) from columns T-302, T-303 and T-304 needed to be changed to achieve results close to base case of process C1 based on 112.63 kmol/h of alcohol designed in Table 5.10. For this base case, the minimum MR was 13.49 for stage 2. Results from that sensitivity analysis are presented in Figure 5.15, where bottom and top abscissa are continuous and discrete axis for MR and methanol mole flow, respectively. From these results, all cost and emission indicators decreased as expected when MR was reduced, since lower values of dimensions and reboiler duties were obtained. For design parameters this was also true to packing height (L_p), since N of T-302 decreased when MR of methanol to ROF decreased as shown in input values from the sensitivity analysis in Table 5.10.

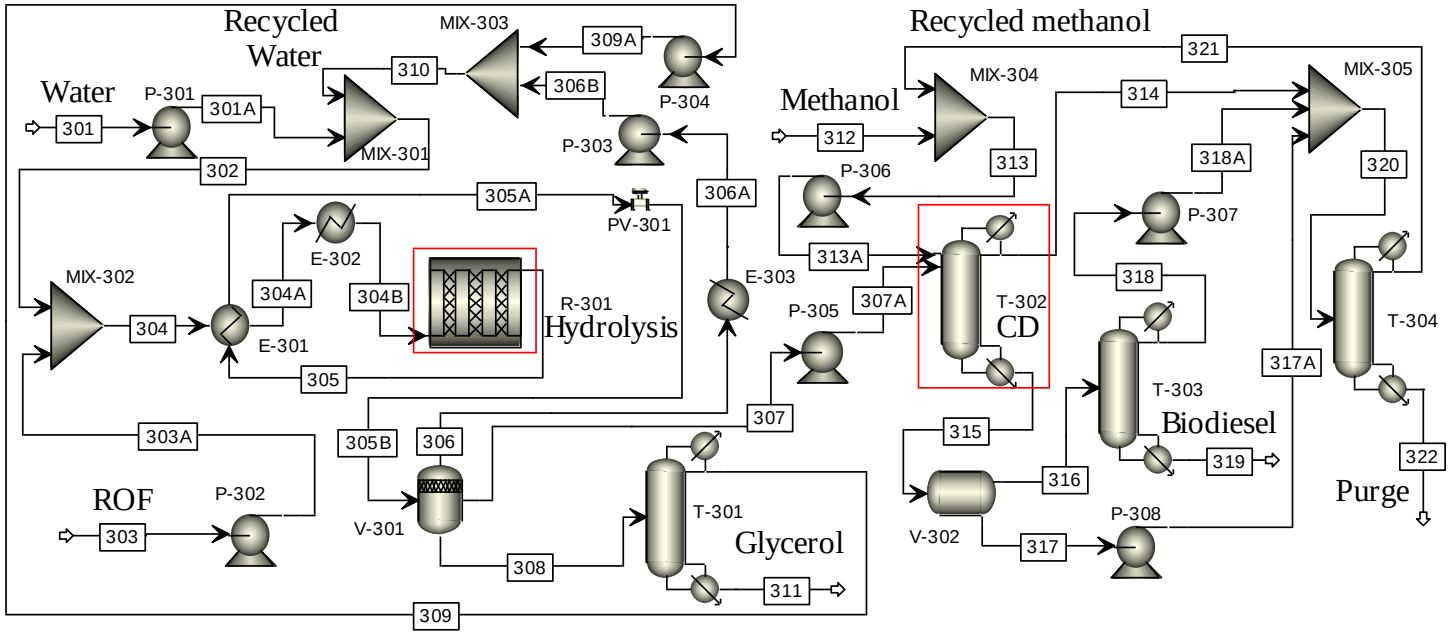

Figure 5.14 – Flowsheet for SAC hydroesterification using a PFR reactor and a CDC for hydrolysis and esterification reactions
Source: Adapted from Gómez-Castro et al. (2010, 2011) and Machado et al. (2016).

Table 5.11 – Stream results for optimized design of Process C1 including hydrolysis reaction, tri-phasic separation and glycerol purification

Stream number	301	302	303	305	306	307	308	309	310	311
Temperature (°C)	25.0	13.6	25.0	267.7	60.0	60.0	60.0	4.9	11.8	138.5
Pressure (kPa)	101.3	5600.0	101.3	5600.0	1.0	1.0	1.0	0.9	5600.0	1.1
Mole flow (kmol/h)	11.6	120.1	5.9	126.0	108.1	14.0	3.9	0.3	108.5	3.6
Mass flow (kg/h)	209.3	2170.6	3978.4	6149.0	1955.2	3858.5	335.3	6.0	1961.2	329.2
Mass fraction										
Methanol (M)	0.0000	0.0000	0.0000	0.0000	0.0000	0.0000	0.0000	0.0000	0.0000	0.0000
Triolein (OOO)	0.0000	0.0000	0.8502	0.0012	0.0000	0.0019	0.0000	0.0000	0.0000	0.0000
Oleic acid (OA)	0.0000	0.0001	0.1498	0.6223	0.0001	0.9913	0.0033	0.0005	0.0002	0.0033
Water (W)	1.0000	0.9960	0.0000	0.3181	0.9956	0.0008	0.0191	0.9913	0.9956	0.0013
Glycerol (G)	0.0000	0.0039	0.0000	0.0585	0.0043	0.0060	0.9776	0.0082	0.0043	0.9954
Methyl oleate (MO)	0.0000	0.0000	0.0000	0.0000	0.0000	0.0000	0.0000	0.0000	0.0000	0.0000

Table 5.12 – Stream results for optimized design of Process C1 including esterification reaction, biodiesel and methanol purification

Stream number	312	313	314	315	316	317	318	319	320	321	322
Temperature (°C)	25.0	56.7	96.0	102.8	102.8	102.8	53.3	219.2	87.0	64.7	97.8
Pressure (atm)	101.3	101.3	304.0	304.8	101.3	101.3	60.8	62.7	202.7	101.3	110.3
Mole flow (kmol/h)	14.3	65.6	18.3	61.3	29.3	32.0	15.7	13.6	66.0	51.3	14.7
Mass flow (kg/h)	458.5	2093.4	575.9	5376.0	4452.5	923.5	484.7	3967.8	1984.1	1634.9	349.3
Mass fraction											
Methanol (M)	1.0000	0.9948	0.9767	0.2023	0.1054	0.6694	0.9517	0.0020	0.8276	0.9933	0.0516
Triolein (OOO)	0.0000	0.0000	0.0000	0.0014	0.0017	0.0001	0.0000	0.0019	0.0000	0.0000	0.0002
Oleic acid (OA)	0.0000	0.0000	0.0000	0.0021	0.0019	0.0029	0.0000	0.0021	0.0013	0.0000	0.0076
Water (W)	0.0000	0.0052	0.0233	0.0453	0.0053	0.2385	0.0483	0.0000	0.1295	0.0067	0.7047
Glycerol (G)	0.0000	0.0000	0.0000	0.0043	0.0000	0.0250	0.0000	0.0001	0.0116	0.0000	0.0661
Methyl oleate (MO)	0.0000	0.0000	0.0000	0.7446	0.8858	0.0642	0.0000	0.9940	0.0299	0.0000	0.1697

Table 5.13 – Input conditions and PBP results from optimization by DM of Process C1

n_{313}^{M} [a]	MR [b]	$MR_{min}^{N=2}$ [c]	T-302					PBP[f] LRP-		PBP[f] HRP-	
			P[d]	N	RR	FS	D/F[e]	LPP	HPP	LPP	HPP
112.6	8.3	13.5	3	27	0.1	2	0.470	3.92	2.79	>20	6.37
100.0	7.4	12.2	3	26	0.1	2	0.400	6.27	2.78	>20	6.31
85.0	6.3	10.8	3	24	0.1	2	0.300	3.8	2.71	>20	6.15
77.7	5.7	9.3	3	23	0.1	2	0.275	3.74	2.68	>20	5.98
70.0	5.2	9.3	3	23	0.1	2	0.250	3.67	2.66	19.16	5.83
65.0	**4.8**	**8.8**	**3**	**22**	**0.1**	**2**	**0.230**	**5.69**	**2.63**	**17.94**	**5.72**
60.0	4.4	8.3	3	21	0.1	2	0.210	3.61	2.62	17.42	5.67
55.0	4.1	7.8	3	21	0.1	2	0.140	3.58	2.61	16.84	5.60

[a] n_{313}^{M} means mole flow of methanol on stream 313 at kmol·h^{-1};
[b] MR means molar ratio of methanol to ROF (mol/mol) before the catalytic distillation column (CDC) T-302;
[c] $MR_{min}^{N=2}$ means minimum molar ratio of methanol to ROF (mol/mol) inside the CDC T-302 found on stage 2;
[d] P means pressure at atm; [e] D/F means distillate to feed ratio (mol/mol) in CDC T-302;
[f] PBP means payback period at year.

Stream results from process C1 are also shown in Table 5.11 and Table 5.12, they were separated in equipment from hydrolysis unit and esterification unit.

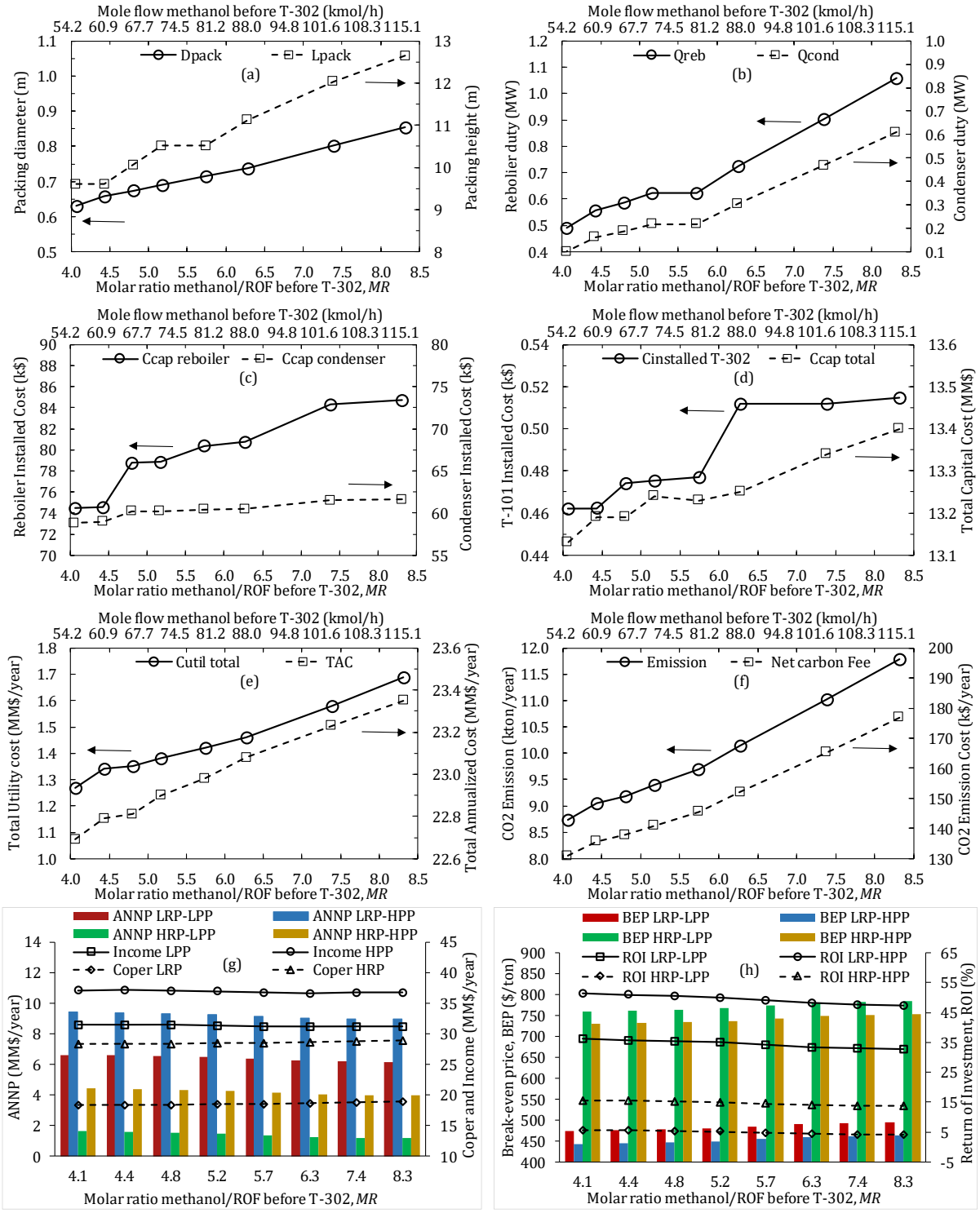

Figure 5.15 – Results for optimization of Process C1 by decision maker varying molar ratio (*MR*)

As for Process A1, all economic results were enhanced when MR decreased, because costs decreased and other indicators based on product sales increased. Results from payback period also decreased when MR decreased as shown in Table 5.13. Consequently, from these results the lowest MR = 4.1 should be chosen. However, a MR of 4.8 was chosen as optimal, since other technical parameters were take account for these cases, so that they should keep close to values from the base case. Therefore, besides of a MR > 8.32 on stages from T-302 column, biodiesel specifications should be satisfied as in the base case. In addition, reboiler temperature (T_{reb}) of column T-303 and temperature of reactive stages of T-302 column should be less than to 516.15 K and 374.15 K, waste stream mass flow rate (m_{322}) value less than 400 kg/h and mass fraction of methanol before T-302 (w_{313}^{M}) greater than 0.99. This latter helped the decision to choose a feed of 65 kmol/h of methanol resulting in a MR of 4.8, minimum molar ratio ($MR_{\min}$) greater than 8.32 on stage 2 and w_{313}^{M} > 0.99.

5.3.4 Economic comparison

Economic, energetic and environmental comparison among the optimized processes A2, B1 and C1 were also performed based on the same economic indicators showed previously as shown in Table 5.7 and Figure 5.16. According to these indicators, process A2 showed lower results of C_{TC}, C_{util}, TAC, PBP and BEP for lowest product prices (LPP). On other hand, Process B1 showed higher profit (income and A_{NNP}) and lower BEP for highest product prices (HPP), since a slightly higher biodiesel productivity was found. Despite these differences, processes A2 and B1 showed closer results, so that based on uncertainty of cost model, both processes should be considered to have equivalent economic feasibilities.

According to Figure 5.16, when comparing process C1 to processes A2 and B1 can be observed those last two are more economical feasible considering the same solid acid-catalyst. Despite this, Process C1 has been applied in industries since other commercial catalysts has been used. However, Processes A2 and B1 showed possibility to substitute this existent route and obtaining better economic results. Furthermore, these processes showed to be more environmental friendly based on CO_2 emissions and waste stream indicators. In relation to energy use, process C1 also needs more energy than processes A2 and B1, since higher T are required in hydrolysis reaction.

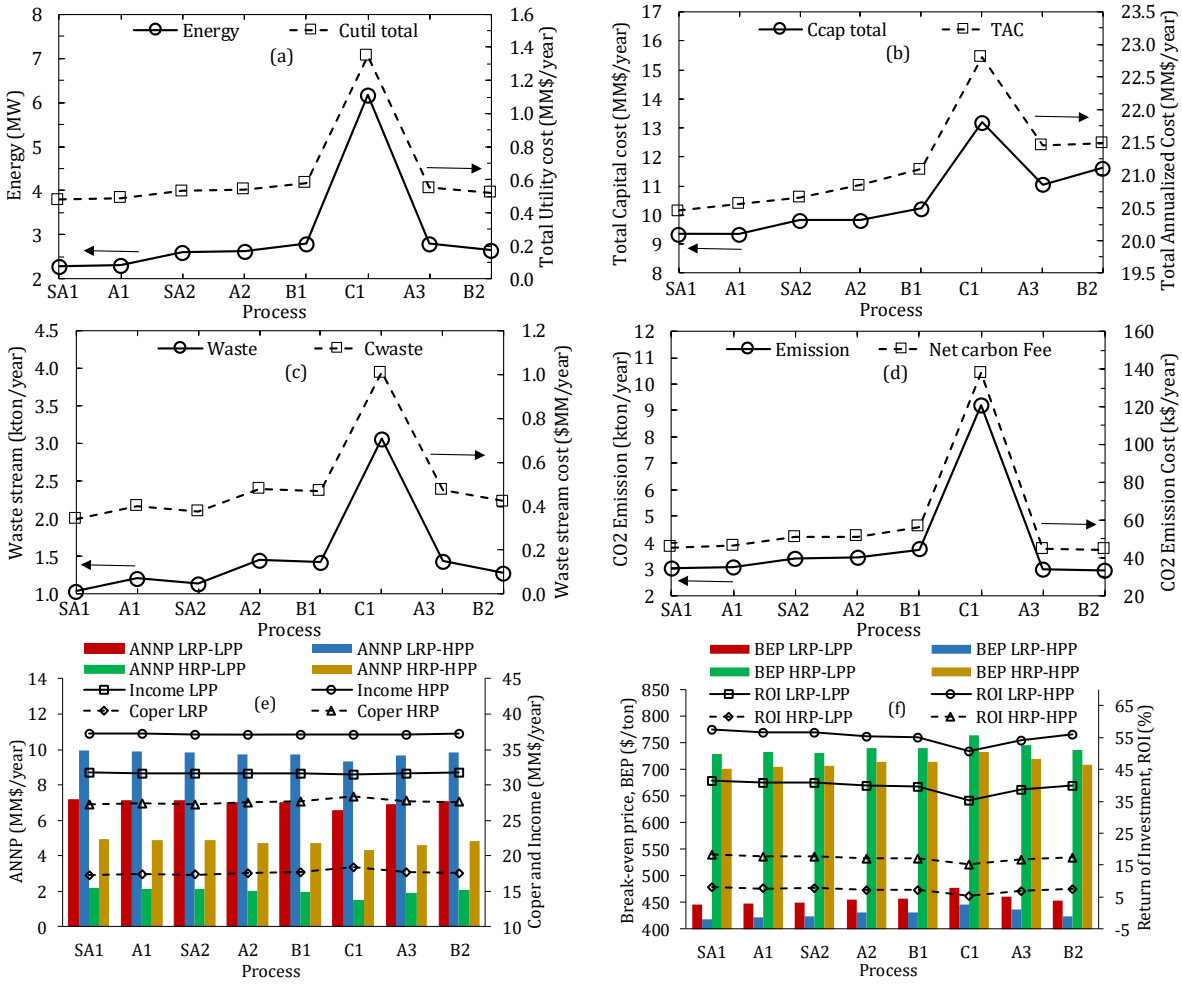

Figure 5.16 – Economic, energetic and environmental results when comparing optimized processes

Processes A2 and B1 also showed similar results of environment and energy indicators. However, process A2 showed lower CO_2 emissions and use of energy, while process B1 showed lower waste stream flow and waste stream cost. For all those reasons, the choice between process A2 and B1 can be made based on number of equipment and simplicity of flowsheet and operation conditions, so that process A2 based on CDC can be chosen instead process B1.

5.3.5 Heat integration (HI)

For processes A2 and B1, the most economical SAC processes, a HI was proposed in order to evaluate possible savings in utility costs as shown in Figure 5.17 and Figure 5.18 for Processes A3 and B2. Heuristics rules were adopted (PERLINGEIRO, 2005; SEIDER; SEADER; LEWIN, 2009). However, challenges to converge the flowsheet due to tear streams obligated to give preference to integrate nearer streams. From these HI, another economic

comparison was carried out as shown in Figure 5.16. Similar conclusions as comparing Processes A2 and B1 were observed. Nevertheless, C_{util} for Process B2 were lower than Process A3 as well as BEP for all conditions for raw materials and products prices. From these results can be concluded that Process B based on CAC can be more economical than Process A with CDC if a successful HI is applied. Stream results for Processes A3 and B2 can be found in Table 5.14 and Table 5.15.

5.3.6 Stochastic Optimization

A stochastic optimization was also carried out making a connection between Matlab, VBA from Excel and Aspen Plus V8.8. Processes A1 and A2 were chosen for this optimization since Process A based on CDC showed to be more simplified, since these included few heat exchangers integrated and tear streams. Furthermore, Process A2 showed to be more economic feasible than Processes B1 and C1. From these processes were chosen ten variables to be varied, such as: N, D/F and RR for T-101, T-102 and T-103, totalizing nine variables and mole flow rate of methanol on stream 101 (n_{101}^{M}) (KISS et al., 2012; SEGOVIA-HERNÁNDEZ; GÓMEZ-CASTRO, 2017).

For Process A1, n_{101}^{M} showed to be the most important variable to decrease TAC value, so that more than 25000 iterations were required to obtain the possible minimum global as shown in Figure 5.19. For process A2 many iterations were also required. However, close to 12500 iterations was enough to obtain the minimum TAC, probably because a narrow range for n_{101}^{M} to Process A2 (35 kmol/h to 50 kmol/h) was adopted compared to Process A1 (40 kmol/h to 116.15 kmol/h). From these results, stochastic optimization based on simulating annealing (SA) algorithmic showed to be very useful to find a point closer to the optimum for processes A1 and A2. These processes were denominated SA1 and SA2 (KISS et al., 2012).

Economic results obtained in Aspen Plus V8.8 for these cases can be found in Figure 5.16, where the design of processes SA1 and SA2 showed to have better economic, use of energy and environment indicators than processes A1 and A2. As a result, optimal input conditions obtained, as shown in Table 5.3 and Table 5.9, aided Process A to be more economically attractive.

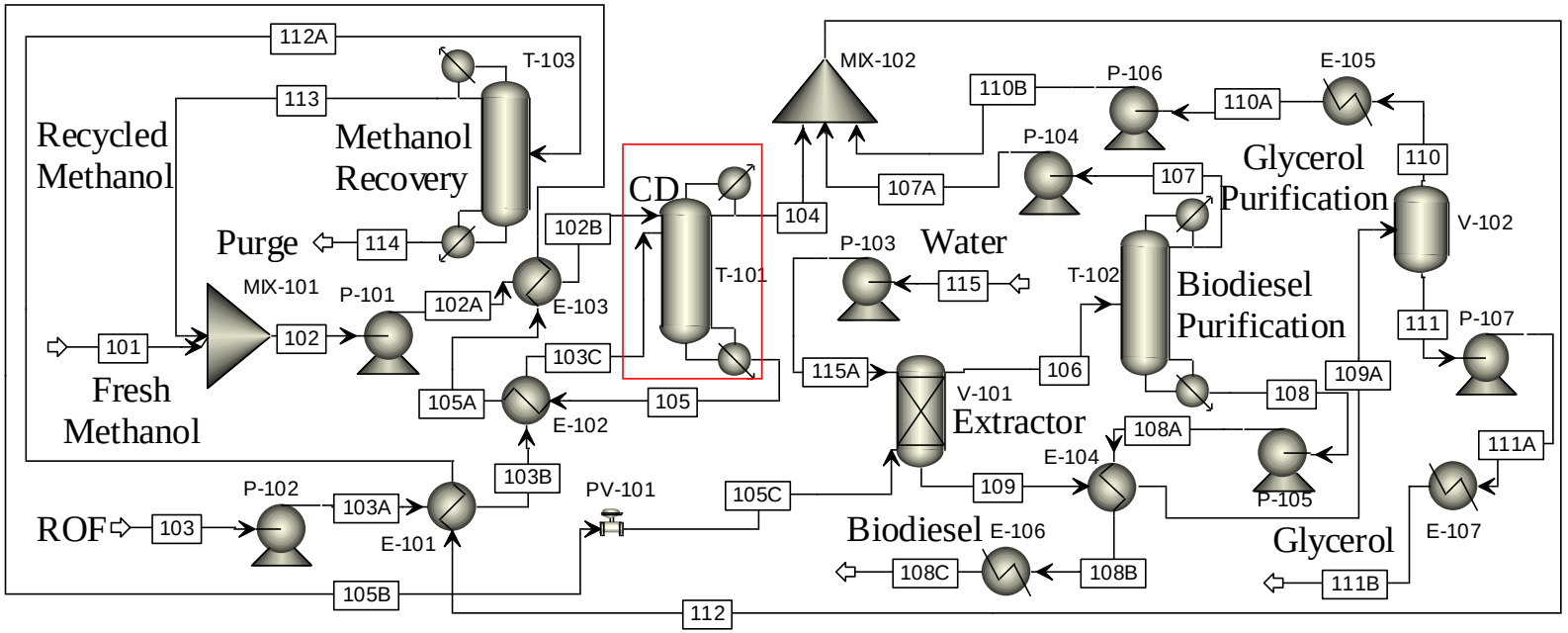

Figure 5.17 – Flowsheet for the SAC biodiesel production process from CDC column satisfying biodiesel standard and including heat integration.
Source: Adapted from Gaurav, Ng and Rempel (2016).

Table 5.14 – Stream results for optimized design of Process A3 by CD including a heat integration

Stream number	101	102B	103C	104	15B	106	107	108C	109A	110	111B	112A
Temperature (°C)	25.0	109.2	110.0	112.4	92.6	92.4	50.9	25.0	198.1	136.6	25.0	64.0
Pressure (kPa)	101.3	506.6	511.3	506.6	507.3	152.0	55.7	202.7	152.0	2.0	202.7	506.6
Mole flow (kmol/h)	14.8	45.6	5.9	25.5	26.0	17.1	3.4	13.8	9.3	6.3	3.0	35.1
Mass flow (kg/h)	474.0	1452.1	3978.4	806.5	4624.0	4126.2	104.9	4021.3	505.1	230.6	274.4	1142.1
Mass fraction												
Methanol (M)	1.0000	0.9929	0.0000	0.9835	0.0464	0.0265	0.9676	0.0020	0.2085	0.4562	0.0003	0.8756
Triolein (OOO)	0.0000	0.0000	0.8502	0.0000	0.0017	0.0019	0.0000	0.0020	0.0000	0.0000	0.0000	0.0000
Oleic acid (OA)	0.0000	0.0000	0.1498	0.0000	0.0000	0.0000	0.0000	0.0000	0.0000	0.0000	0.0000	0.0000
Water (W)	0.0000	0.0071	0.0000	0.0164	0.0076	0.0008	0.0324	0.0000	0.0769	0.1669	0.0012	0.0483
Glycerol (G)	0.0000	0.0000	0.0000	0.0000	0.0759	0.0002	0.0000	0.0002	0.6935	0.3339	0.9958	0.0674
Methyl oleate (MO)	0.0000	0.0000	0.0000	0.0000	0.8684	0.9706	0.0000	0.9959	0.0211	0.0430	0.0028	0.0087

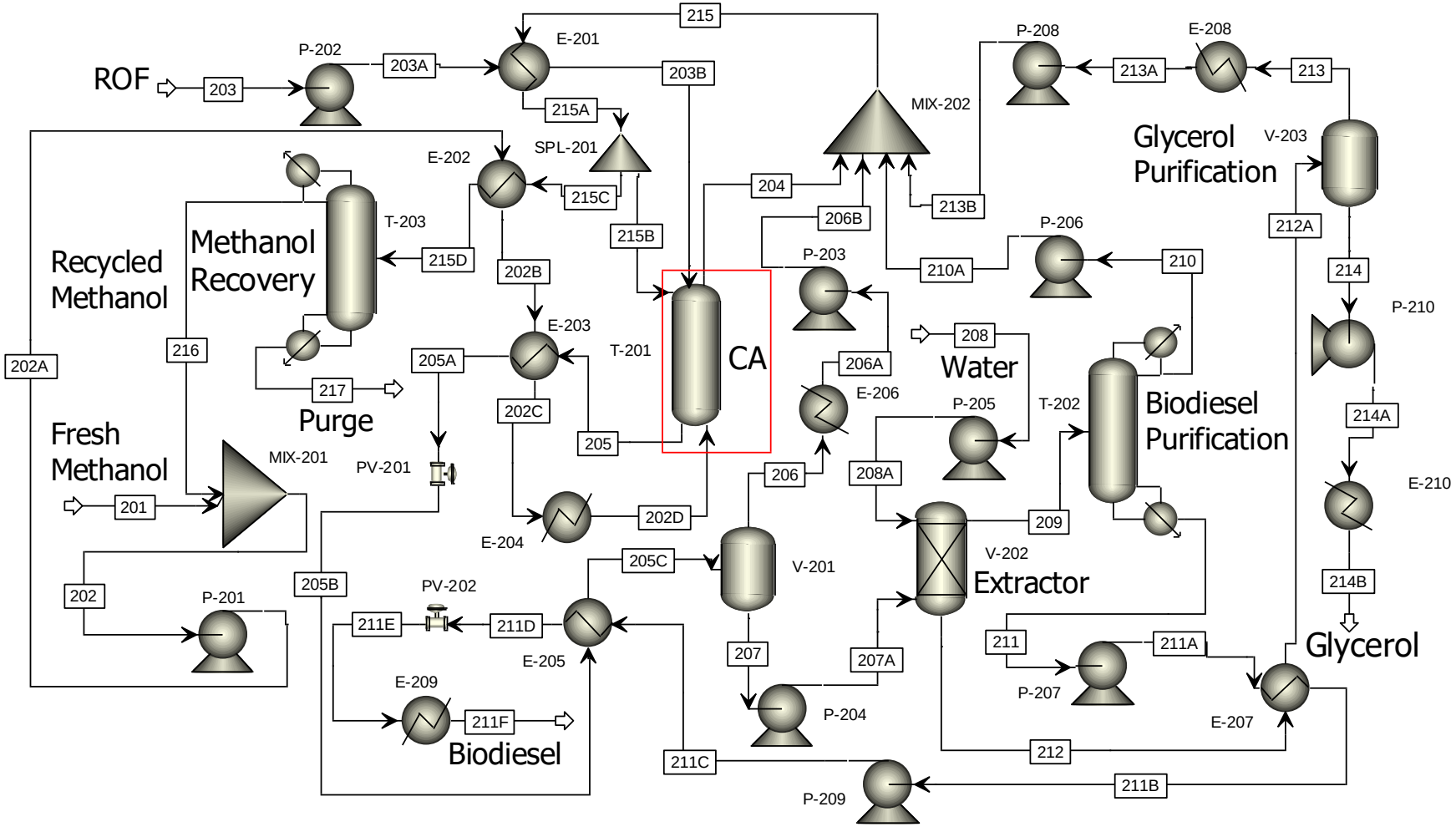

Figure 5.18 – Flowsheet for the SAC biodiesel production process from CAC column satisfying biodiesel standard and including heat integration
Source: Adapted from Gaurav, Ng and Rempel (2016) and Kiss (2009).

Table 5.15 – Stream results for optimized design of Process B2 by CA including a heat integration

Stream number	201	202D	203B	204	205C	209	211F	212A	214B
Temperature (°C)	25.0	124.3	116.1	129.7	97.3	81.1	25.0	195.6	25.0
Pressure (kPa)	101.3	709.3	711.3	709.3	202.7	152.0	202.7	152.0	202.7
Mole flow (kmol/h)	14.8	45.8	5.9	26.1	76.2	19.8	13.8	15.2	3.3
Mass flow (kg/h)	474.4	1455.8	3978.4	804.3	6232.6	4209.5	4022.4	742.7	302.3
Mass fraction									
Methanol (M)	1.0000	0.9903	0.0000	0.9471	0.2673	0.0448	0.0020	0.3394	0.0004
Triolein (OOO)	0.0000	0.0000	0.8502	0.0000	0.0008	0.0013	0.0013	0.0000	0.0000
Oleic acid (OA)	0.0000	0.0000	0.1498	0.0000	0.0000	0.0000	0.0000	0.0000	0.0000
Water (W)	0.0000	0.0097	0.0000	0.0528	0.0175	0.0016	0.0000	0.0641	0.0008
Glycerol (G)	0.0000	0.0000	0.0000	0.0000	0.0677	0.0001	0.0001	0.5677	0.9954
Methyl oleate (MO)	0.0000	0.0000	0.0000	0.0001	0.6466	0.9523	0.9966	0.0288	0.0034

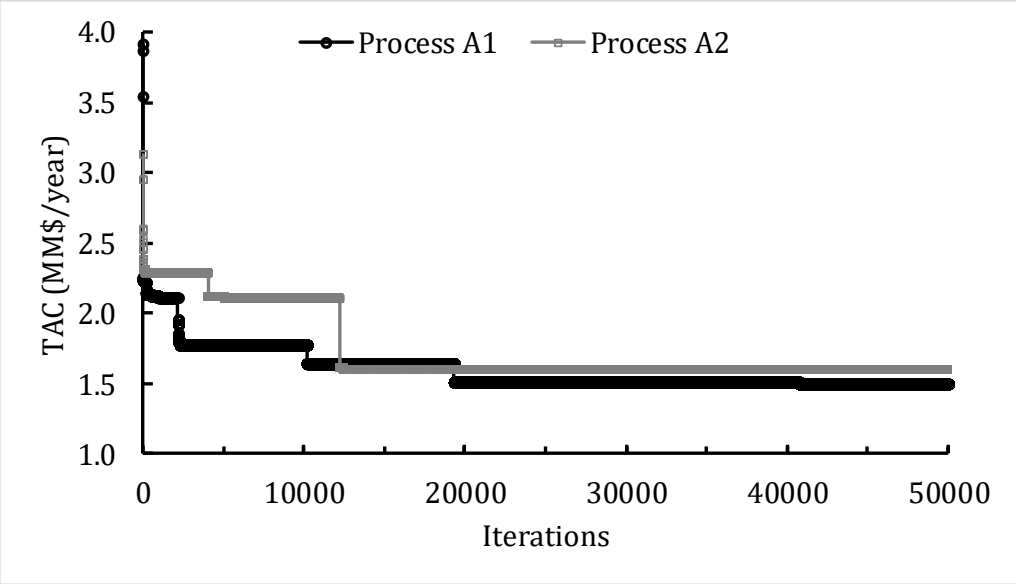

Figure 5.19 – Evolution of TAC cost during the stochastic optimization of Processes A1 and A2
Source: Adapted from Kiss et al. (2012) and Segovia-Hernández and Gómez-Castro (2017)

5.3.7 Flexibility

Flexibility was also evaluated for Process A2, since raw materials used by industries are commonly inside a range of 5 to 25 wt% of FFA in ROF. In addition, raw materials with FFA content greater than 15% as brown grease are cheaper than yellow grease. For those reasons, process A2 was designed in order to satisfy this FFA range. Optimal input conditions from process SA2 by decision maker was used as initial conditions to find the optimum design.

A process design valid for the range of 5 to 25 % of FFA in ROF was developed as shown in Table 5.16. From these results, higher N for T-101 were required to satisfy the 5% of FFA case, since more TAG needed to be converted. On the other hand, higher N for T-103 were required to satisfy the 25% of FFA case, because more water is present making more difficult the methanol recovery. A final equipment size was defined based on the wider range of conditions, larger equipment and higher C_{TC} value as shown in column 5–25% from Table 5.16 for HRP-LPP case.

Related to other economic indicators, C_{util} increased when mass fraction of FFA in ROF increased (w_{ROF}^{FFA}), while total production cost (C_{TP}), TAC and BEP increased from 5 to 15 % of FFA and decreased from 15 to 25 % of FFA. Furthermore, BEP of biodiesel from yellow grease is very close to 0.67 $/kg reported by Gaurav, Ng and Rempel (2016) and inside the BEP range of 0.48 to 1.36 $/kg for biodiesel from WCO (ARAUJO; HAMACHER; SCAVARDA, 2010; FAWAZ; SALAM, 2018; MOHAMMADSHIRAZI et al., 2014). Therefore, biodiesel price of Process A from yellow grease is competitive to diesel price, comparing to the average and range of diesel price including taxes of 1.24 $/kg and 0.08 to 3.74 $/kg in January 21st, 2019, where differences are related to different country policies, development and production capacity (PRICES, 2019).

On the other hand, PS decreased when w_{ROF}^{FFA} increased and raw materials cost (C_{RM}) kept constant until 15% when decreased for 25% of FFA, since brown grease is cheaper than yellow grease as shown in Table 5.4. Consequently, process A2 for 25% of FFA in ROF showed to be more economical feasible. Nevertheless, other pre-treatment processes applied to brown grease must be taken account as water and solids removal, since these steps can add more costs. Therefore, a future in deep investigation should be done. It is worth to mention that results of Table 5.16 were obtained for HRP-LPP case in order to evaluate the most adverse scenario.

Table 5.16 – Conditions, size and costs for HRP-LPP case of process A2 from 5 to 25 % of FFA

Block	Description\FFA (wt%)	5%	15%	25%	5-25%
T-101	RR	0.1	0.1	0.1	0.1
	D/F	0.495	0.495	0.495	0.495
	P (kPa)	506.6/507.3	506.6/507.3	506.6/507.3	506.6/507.3
	T (K)	385.3/442.2	385.5/435.7	385.8/429.3	385.3/442.2
	heat duty, Q (kW)	-241.9/628.1	-248.8/643.9	-256.1/659.7	-256.1/659.7
	N (stages)/FS/NR	20/2/2-19	20/2/2-19	20/2/2-19	20/2/2-19
	size ($D \times L$, m)	0.61 X 13.41	0.76 X 13.41	0.76 X 13.41	0.76 X 13.41
	cost (k$)	453.0	463.8	463.4	463.8
V-101	P (kPa)	152.0	152.0	152.0	152.0
	T (K)	362.9/363.1	362.9/363.1	363/363.1	362.9/363.1
	size ($D \times L$, m)	1.07 X 3.66	1.07 X 3.66	1.07 X 3.66	1.07 X 3.66
	cost (k$)	107.4	107.4	107.4	107.4
T-102	RR	0.1	0.1	0.1	0.1
	D/F	0.202	0.190	0.182	0.182-0.202
	P (kPa)	55.7/55.8	55.7/55.8	55.7/55.8	55.7/55.8
	T (K)	324.0/511.0	324.1/513.5	324.1/513.1	324.0/513.5
	heat duty, Q (kW)	-38.9/424.3	-36.1/432.6	-34.5/432.5	-38.9/432.6
	N (stages)/FS	4/3	4/3	4/3	4/3
	size ($D \times L$, m)	0.30 X 5.33	0.30 X 5.33	0.30 X 5.33	0.30 X 5.33
	cost (k$)	391.3	391.5	391.5	391.5
V-102	P (kPa)	3.0	3.0	3.0	3.0
	T (K)	422.5	422.5	422.5	422.5
	size ($D \times L$, m)	0.91 X 3.66	0.91 X 3.66	0.91 X 3.66	0.91 X 3.66
	cost (k$)	105.1	105.1	105.1	105.1
T-103	RR	0.3	0.3	0.3	0.3
	D/F	0.905	0.863	0.826	0.826-0.905
	P (kPa)	101.3/108.9	101.3/108.9	101.3/108.9	101.3/108.9
	T (K)	337.8/365.6	337.9/369.1	338.1/370.8	337.80/370.8
	heat duty, Q (kW)	-389.1/394.3	-392.3/400.2	-395.6/406.2	-395.6/406.2
	N (stages)/FS	12/6	12/6	12/6	12/6
	size ($D \times L$, m)	0.46 X 12.8	0.46 X 12.8	0.46 X 12.8	0.46 X 12.8
	cost (k$)	440.7	441.9	442.4	442.4
	C_{HE} | C_P ($k)[a]	177.8 | 141.0	189.4 | 141.0	188.1 | 141.0	189.4 | 141.0
	C_{TI} | C_{TC} ($MM)[a]	1.82 | 9.83	1.84 | 9.87	1.84 | 9.87	1.84 | 9.87
	C_{RM} | C_{util} ($MM/year)[a]	23.38 | 0.53	23.38 | 0.54	14.30 | 0.56	
	C_{TP} ($MM/year)[a]	27.54	27.70	18.04	
	PS | TAC ($MM/year)[a]	31.59 | 30.81	31.38 | 30.99	31.18 | 21.33	
	BEP ($/ton)[a]	737.33	748.46	482.01	

[a] C_{HE} means heat exchangers cost; C_P means pumps cost; C_{TI} means total installed cost; C_{TC} means total capital cost; C_{RM} means raw materials cost; C_{util} means utility cost; C_{TP} means total production or operation cost; PS means product sales or income; TAC means total annualized cost and BEP means break-even price.

5.4 CONCLUSIONS

Three SAC processes for biodiesel production from ROF based on reactive separation processes were designed, optimized and compared in relation to techno-economic feasibility. First, the SAC process for simultaneous esterification and transesterification reactions using HWSi/Al2O3 as catalyst was designed and optimized based on a DM approach. A lower MR of methanol to ROF for process A1 showed to be sufficient to keep MR > 21.27 inside stages and aided to improve economic indicators and reduce greenhouse gas emissions. Similar results were found for process C1 based on MR > 8.32 for esterification reaction. The three studied processes showed to be technical feasible; however, processes A2 and B1 showed to be more economical feasible than the industrial process C1. Processes A2 and B1 presented similar economic and environment indicators considering the uncertainties for the economic model, so that a heat integration was proposed through processes A3 and B2. Comparing these processes, process B2 showed to have lower value of utility costs and BEP, so that process B based on CAC can be more economical than process A if a successful heat integration is applied. Results from all processes were compared including two cases for SAC process from CDC (process SA1 and SA2) obtained using SA method. Search for global optimum condition (or at least close enough to it) needed high CPU capacity and number of iterations; however, stochastic optimization showed to be successful tool since economic and environment indicators were improved when comparing process SA1 to A1 and process SA2 to A2. From all processes evaluated, process A2 (or SA2 or A3) based on CDC from ROF was chosen as the most promisor since presented to be slightly more techno-economic feasible than process B1, besides of include a more simplified flowsheet and less number of equipment. Moreover, process A2 showed lowest CO_2 emissions fees and second lowest waste stream cost. Finally, an investigation of plant flexibility demonstrated that process A2 was capable to be technical feasible for raw materials with FFA levels between 5 to 25 wt% as found applying yellow grease and brown grease. A design for process A2 was proposed in these conditions and brown grease showed to be a more economical raw material reflecting a BEP price 1.5 times lower than using yellow grease.

ACKNOWLEDGMENTS

The authors would like to acknowledge CNPQ, FINEP and NSERC for financial support. A. A. A. is also grateful to CAPES for the PhD scholarship.

NOMENCLATURE

A_{NNP}	net annual profit after taxes ($MM/year)
BEP	break-even price ($/kg or $/ton)
c	refers to a distillation column
C_{HE}	heat exchangers cost ($MM)
C_{inst}	installed cost ($MM)
C_P	pumps cost ($MM)
C_{RM}	raw materials cost ($MM/year)
C_{TC}	total capital cost ($MM)
C_{TI}	total installed cost ($MM)
C_{TP}	total production or operation cost ($MM/year)
C_{util}	utility cost ($MM/year)
C_{waste}	waste stream cost
D	diameter (m)
D/F	distillate to feed ratio (mole/mole)
D_p	packing diameter (m)
F	objective function, where a minimum is desired
$f(x)$	objective function of solution x
$f(x0)$	objective function of solution x_0
FS	feed stage
I	input variables
L	length (m)
L_p	packing height (m)
MR	molar ratio of methanol to ROF (mol/mol)
N	number of stages
n	mole flow (kmol.h-1)

n_c	number of c distillation columns
n_{feed}^{M}	methanol feed mole flow rate (kmol.h-1)
O	output variables
P	pressure (atm)
PBP	payback period
P_t	pressure (Torr)
Q	heat duty (kW or MW)
r	random number
r_i	reaction rate of the ith component
ROI	return of investment (%)
RR	reflux ratio (mole/mole)
T	temperature (C or K)
TAC	total annualized cost ($MM/year)
w_i	mass fraction of ith component
x_i	liquid mole fraction of ith component
y_i	vapor mole fraction of ith component

Greek Symbols

ΔT	variation of temperature ©
$\Psi(x, x_0)$	probability of acceptance for solution x

Subscripts

106	stream 106
108	stream 108
111	stream 111
115	stream 115
201	stream 201
202	stream 202
208	Stream 208
213	stream 213
214	stream 214
313	stream 313
322	stream 322
Col	column

$frez$	freezing
in	inlet
min	minimum
out	outlet
reb	reboiler
ROF	residual oil and fats
T	tower

Superscripts

C	cold
FFA	free fatty acids
G	glycerol
H	hot
I	1st liquid phase
II	2nd liquid phase
M	methanol
MO	methyl oleate
N	stage of minimum MR of methanol to ROF

Abbreviations

$MM	million dollars
ANP	National Agency of Petroleum, Natural Gas and Biofuels
B	biodiesel
CAC	catalytic absorption column
CDC	catalytic distillation column
CF	constituent fragments
DAG	diacylglycerol
DM	decision maker
E	heat exchanger (heater or cooler)
ECF	extended constituent fragments
EPA	United States Environment Protection Agency
FAAE	fatty acid alkyl esters
FFA	free fatty acid
G	glycerol

HI	heat integration
HPP	highest product prices
HRP	highest raw material prices
LLE	liquid-liquid equilibrium
LPP	lowest product prices
LRP	lowest raw material prices
M	methanol
MAG	monoacylglycerol
MIX	mixer
MO	methyl oleate
NRTL	Non-Random Two-Liquid
OA	oleic acid
OOO	triolein
P	pump
PFR	plug-flow reactor
Process A	simultaneous esterification and transesterification by catalytic distillation
Process A1	process A using a decanter (do not achieve minimum purity of free glycerol)
Process A2	process A using a extractor (achieve minimum purity of free glycerol)
Process A2	process A1 including a heat integration
Process B	simultaneous esterification and transesterification by catalytic absorption
Process B1	process B using a extractor (achieve minimum purity of free glycerol)
Process B2	process B1 including a heat integration
Process C1	hydrolysis using a PFR reactor and esterification by catalytic distillation
Process SA1	optimized process A1 by simulated annealing method
Process SA2	optimized process A2 by simulated annealing method
R	reactor
RDC	reactive distillation column
RK	Redlich Kwong
ROF	residual oil and fats
SA	simulated annealing
SAC	solid acid-catalyzed
SEP	separation
SPL	splitter
T	tower (distillation column)

TAG	triacylglycerol
V	vessel (flash drum, decanter or extraction column with two stages)
VBA	Visual Basic for Applications
VLE	vapor-liquid equilibrium
VLLE	vapor-liquid-liquid equilibrium
W	water
WCO	waste cooking oil

REFERENCES

ALBUQUERQUE, A. D. A.; DANIELSKI, L.; STRAGEVITCH, L. Techno-Economic Assessment of an Alternative Process for Biodiesel Production from Feedstock Containing High Levels of Free Fatty Acids. **Energy & Fuels**, v. 30, n. 11, p. 9409−9418, 2016.

ALBUQUERQUE, A. D. A.; NG, F. T. T.; DANIELSKI, L.; STRAGEVITCH, L. Phase equilibrium modeling for biodiesel reaction systems (submitted). **Fluid Phase Equilibr.**, 2019.

ALMAZROUEI, M.; SAMAD, T. E.; JANAJREH, I. Thermogravimetric Kinetics and High Fidelity Analysis of Crude Glycerol. **Energy Procedia**, v. 142, p. 1699−1705, 2017.

ANDREATTA, A. E.; CASÁS, L. M.; HEGEL, P.; BOTTINI, S. B.; BRIGNOLE, E. A. Phase Equilibria in Ternary Mixtures of Methyl Oleate, Glycerol, and Methanol. **Industrial & Engineering Chemistry Research**, v. 47, n. 15, p. 5157−5164, 2008.

ARANDA, D. A. G.; SILVA, C. C. C. M.; DETONI, C. Current Processes in Brazilian Biodiesel Production. **International Rev. Chem. Eng.**, v. 1, n. 6, p. 603−608, 2009.

ARAUJO, V. K. W. S.; HAMACHER, S.; SCAVARDA, L. F. Economic assessment of biodiesel production from waste frying oils. **Bioresource Technology**, v. 101, n. 12, p. 4415−4422, 2010.

BARREAU, A.; BRUNELLA, I.; DE HEMPTINNE, J. C.; COUPARD, V.; CANET, X.; RIVOLLET, F. Measurements of Liquid−Liquid Equilibria for a Methanol + Glycerol + Methyl Oleate System and Prediction Using Group Contribution Statistical Associating Fluid Theory. **Industrial & Engineering Chemistry Research**, v. 49, n. 12, p. 5800−5807, 2010.

BOON-ANUWAT, N.-N.; KIATKITTIPONG, W.; AIOUACHE, F.; ASSABUMRUNGRAT, S. Process design of continuous biodiesel production by reactive distillation: Comparison between homogeneous and heterogeneous catalysts. **Chem. Eng. Proc.**, v. 92, p. 33−44, 2015.

CERIANI, R.; MEIRELLES, A. J. A. Predicting vapor–liquid equilibria of fatty systems. **Fluid Phase Equilibria**, v. 215, n. 2, p. 227−236, 2004.

CRNKOVIC, P. M.; KOCH, C.; ÁVILA, I.; MORTARI, D. A.; CORDOBA, A. M.; MOREIRA DOS SANTOS, A. Determination of the activation energies of beef tallow and crude glycerin combustion using thermogravimetry. **Biomass Bioenerg.**, v. 44, p. 8−16, 2012.

DOU, B.; DUPONT, V.; WILLIAMS, P. T.; CHEN, H.; DING, Y. Thermogravimetric kinetics of crude glycerol. **Bioresource Technology**, v. 100, n. 9, p. 2613−2620, 2009.

FAWAZ, E. G.; SALAM, D. A. Preliminary economic assessment of the use of waste frying oils for biodiesel production in Beirut, Lebanon. **Science of The Total Environment**, v. 637−638, p. 1230-1240, 2018.

GAURAV, A.; LEITE, M. L.; NG, F. T. T.; REMPEL, G. L. Transesterification of Triglyceride to Fatty Acid Alkyl Esters (Biodiesel): Comparison of Utility Requirements and Capital Costs between Reaction Separation and Catalytic Distillation Configurations. **Energy & Fuels**, v. 27, n. 11, p. 6847-6857, 2013.

GAURAV, A.; NG, F. T. T.; REMPEL, G. L. A new green process for biodiesel production from waste oils via catalytic distillation using a solid acid catalyst – Modeling, economic and environmental analysis. **Green Energy & Environment**, v. 1, n. 1, p. 62−74, 2016.

GÓMEZ-CASTRO, F. I.; RICO-RAMÍREZ, V.; SEGOVIA-HERNÁNDEZ, J. G.; HERNÁNDEZ-CASTRO, S. Esterification of fatty acids in a thermally coupled reactive distillation column by the two-step supercritical methanol method. **Chemical Engineering Research and Design**, v. 89, n. 4, p. 480−490, 2011.

GOMEZ-CASTRO, F. I.; RICO-RAMIREZ, V.; SEGOVIA-HERNANDEZ, J. G.; HERNANDEZ, S. Feasibility study of a thermally coupled reactive distillation process for biodiesel production. **Chem. Eng. Proc.**, v. 49, n. 3, p. 262−269, 2010.

HASAN, M. M.; RAHMAN, M. M. Performance and emission characteristics of biodiesel–diesel blend and environmental and economic impacts of biodiesel production: A review. **Renewable and Sustainable Energy Reviews**, v. 74, p. 938−948, 2017.

HBI. **Glycerine market report**. December 2017 / N°119, Hong Kong, 2018. Available at: <http://www.hbint.com/>. Accessed on: 2018/03/18.

HE, B. B.; SINGH, A. P.; THOMPSON, J. C. Experimental optimization of a continuous-flow reactive distillation reactor for biodiesel production. **Transactions of the ASAE**, v. 48, n. 6, p. 2237, 2005.

_____. A novel continuous-flow reactor using reactive distillation for biodiesel production. **Transactions of the ASABE**, v. 49, n. 1, p. 107, 2006.

ICIS. **Indicative Chemical Prices A-Z**. Chemicals, USA, 2018. Available at: <https://www.icis.com/explore/chemicals/ >. Accessed on: 2018/03/17.

INTRATEC. **Demineralized Water Price History & Forecast**. Historical Demineralized Water Price, San Antonio, TX, 2018. Available at: <https://www.intratec.us/chemical-markets/demineralized-water-price>. Accessed on: 2018/03/17.

JOLIS, D.; MARTIS, M. **Brown grease recovery and biofuel demonstration project**. Final Project Report, San Francisco, CA, 2012. Available at: <https://sfwater.org/>. Accessed on: 2018/03/17.

KISS, A. A. Novel process for biodiesel by reactive absorption. **Separation and Purification Technology**, v. 69, n. 3, p. 280−287, 2009.

KISS, A. A. **Advanced Distillation Technologies**. 1. ed. Chichester, West Sussex, United Kingdom: John Wiley & Sons, Ltd, 2013. 405p.

KISS, A. A. **Process Intensification Technologies for Biodiesel Production: Reactive Separation Processes**. 1. ed. Arnhem: Springer, 2014. 103p.

KISS, A. A.; BILDEA, C. S. A review of biodiesel production by integrated reactive separation technologies. **J. Chem. Technol. Biot.**, v. 87, n. 7, p. 861−879, 2012.

KISS, A. A.; SEGOVIA-HERNÁNDEZ, J. G.; BILDEA, C. S.; MIRANDA-GALINDO, E. Y.; HERNÁNDEZ, S. Reactive DWC leading the way to FAME and fortune. **Fuel**, v. 95, p. 352−359, 2012.

LAYLA, L. L. R.; ANDRE, L. D. R.; NELSON ROBERTO ANTONIOSI, F.; NELSON, C. F.; CARLTON, A. T.; DONATO, A. G. A. Production of Biodiesel by a Two-Step Niobium Oxide Catalyzed Hydrolysis and Esterification. **Lett. Org. Chem.**, v. 7, n. 7, p. 571−578, 2010.

LDC. **Pharmaceutical Refined Glycerin**. Louis Dreyfus Company, Wittenberg, Germany, 2017. Available at: <https://www.ldc.com.pdf>. Accessed on: 2018/06/17.

LUYBEN, W. L.; YU, C.-C. **Reactive distillation design and control**. 1. ed. Hoboken, New Jersey: John Wiley & Sons, Inc., 2008. 577p.

LUYBEN, W. L. **Distillation design and control using AspenTM simulation**. 2. ed. Hoboken, New Jersey: Wiley, 2013. 512p.

MACHADO, G. D.; DE SOUZA, T. L.; ARANDA, D. A. G.; PESSOA, F. L. P.; CASTIER, M.; CABRAL, V. F.; CARDOZO-FILHO, L. Computer simulation of biodiesel production by hydro-esterification. **Chem. Eng. Process.**, v. 103, p. 37−45, 2016.

MAHMUDUL, H. M.; HAGOS, F. Y.; MAMAT, R.; ADAM, A. A.; ISHAK, W. F. W.; ALENEZI, R. Production, characterization and performance of biodiesel as an alternative fuel in diesel engines – A review. **Renew. Sust. Energ. Rev.**, v. 72, p. 497−509, 2017.

MAZUBERT, A.; POUX, M.; AUBIN, J. Intensified processes for FAME production from waste cooking oil: A technological review. **Chem. Eng. J.**, v. 233, p. 201−223, 2013.

MCGARVEY, E.; TYNER, W. E. A stochastic techno-economic analysis of the catalytic hydrothermolysis aviation biofuel technology. **Biofuels, Bioproducts and Biorefining**, v. 12, n. 3, p. 474-484, 2018.

MEHER, L. C.; VIDYA SAGAR, D.; NAIK, S. N. Technical aspects of biodiesel production by transesterification—a review. **Renew. Sust. Energ. Rev.**, v. 10, n. 3, p. 248−268, 2006.

METHANEX. **Methanex Methanol Price Sheet**. February 28, 2018, Vancouver, Canada, 2018. Available at: <https://www.methanex.com/>. Accessed on: 2018/03/18.

MOHAMMADSHIRAZI, A.; AKRAM, A.; RAFIEE, S.; BAGHERI KALHOR, E. Energy and cost analyses of biodiesel production from waste cooking oil. **Renew. Sust. Energ. Rev.**, v. 33, p. 44−49, 2014.

MUEANMAS, C.; PRASERTSIT, K.; TONGURAI, C. Transesterification of Triolein with Methanol in Reactive Distillation Column: Simulation Studies. **International Journal of Chemical Reactor Engineering**, v. 8, n. 1, 2010.

NATIONAL AGENCY OF PETROLEUM, NATURAL GAS AND BIOFUELS (ANP). **ANP Resolution No. 45, of 25.8.2014 - DOU 26.8.2014**. 2014.

NESTE. **Biodiesel prices (SME & FAME)**. Investors, Finland, 2018. Available at: <https://www.neste.com/ >. Accessed on: 2018/03/17.

NG, F. T. T.; REMPEL, G. L. **Catalytic Distillation**. In: HORVÁTH, I. Encyclopedia of Catalysis. 1. ed. John Wiley & Sons, Inc., 2002.

NOSHADI, I.; AMIN, N. A. S.; PARNAS, R. S. Continuous production of biodiesel from waste cooking oil in a reactive distillation column catalyzed by solid heteropolyacid: Optimization using response surface methodology (RSM). **Fuel**, v. 94, p. 156−164, 2012.

PERLINGEIRO, C. A. G. **Process Engineering: Analysis, Simulation, Optimization and Synthesis of Chemical Processes (in portuguese)**. 1. ed. Rio de Janeiro: Blucher, 2005. 208p.

PETCHSOONGSAKUL, N.; NGAOSUWAN, K.; KIATKITTIPONG, W.; AIOUACHE, F.; ASSABUMRUNGRAT, S. Process design of biodiesel production: Hybridization of ester-and transesterification in a single reactive distillation. **Energy Conversion and Management**, v. 153, p. 493−503, 2017.

POUSA, G. P. A. G.; SANTOS, A. L. F.; SUAREZ, P. A. Z. History and policy of biodiesel in Brazil. **Energy Policy**, v. 35, n. 11, p. 5393−5398, 2007.

PRICES, G. P. **Diesel prices, liter**. Diesel prices, Atlanta, USA, 2019. Available at: <https://www.globalpetrolprices.com/diesel_prices/>. Accessed on: 2019.01.23.

QIU, Z.; ZHAO, L.; WEATHERLEY, L. Process intensification technologies in continuous biodiesel production. **Chem. Eng. Process.**, v. 49, n. 4, p. 323−330, 2010.

ROSARIA, C.; DELLA, P. C.; MICHELE, R.; MARIO, P. Understanding the glycerol market. **European Journal of Lipid Science and Technology**, v. 116, n. 10, p. 1432−1439, 2014.

SEGOVIA-HERNÁNDEZ, J. G.; GÓMEZ-CASTRO, F. I. **Stochastic Process Optimization using Aspen Plus®**. 1. ed. Boca Raton: CRC Press Taylor & Francis Group, 2017. 242p.

SEIDER, W. D.; SEADER, J. D.; LEWIN, D. R. **Product and process design principles: synthesis, analysis and evaluation**. 3. ed. USA: John Wiley & Sons, 2009. 766p.

SIMASATITKUL, L.; SIRICHARNSAKUNCHAI, P.; PATCHARAVORACHOT, Y.; ASSABUMRUNGRAT, S.; ARPORNWICHANOP, A. Reactive distillation for biodiesel production from soybean oil. **Korean J. Chem. Eng.**, v. 28, n. 3, p. 649−655, 2011.

SORDA, G.; BANSE, M.; KEMFERT, C. An overview of biofuel policies across the world. **Energy Policy**, v. 38, n. 11, p. 6977−6988, 2010.

SOUZA, T. P. C.; STRAGEVITCH, L.; KNOECHELMANN, A.; PACHECO, J. G. A.; SILVA, J. M. F. Simulation and preliminary economic assessment of a biodiesel plant and comparison with reactive distillation. **Fuel Processing Technology**, v. 123, p. 75−81, 2014.

STEINIGEWEG, S.; GMEHLING, J. Esterification of a Fatty Acid by Reactive Distillation. **Industrial & Engineering Chemistry Research**, v. 42, n. 15, p. 3612−3619, 2003.

SUNDMACHER, K.; KIENLE, A. **Reactive Distillation: Status and Future Directions**. 1. ed. Magdeburg, Germany: Wiley-VCH, 2002. 308p.

TESSER, R.; DI SERIO, M.; GUIDA, M.; NASTASI, M.; SANTACESARIA, E. Kinetics of Oleic Acid Esterification with Methanol in the Presence of Triglycerides. **Industrial & Engineering Chemistry Research**, v. 44, n. 21, p. 7978−7982, 2005.

UNITED STATES DEPARTMENT OF AGRICULTURE (ASDA). **National Weekly Ag Energy Round-Up**. USDA Livestock, Poultry & Grain Market News, USA, 2018. Available at: <https://www.ams.usda.gov/mnreports/lswagenergy.pdf>. Accessed on: 2018/03/17.

UNITED STATES ENVIRONMENTAL PROTECTION AGENCY (EPA). **Mandatory Reporting of Greenhouse Gases; Final Rule**. Environmental Protection Agency, Washington, 2009. Available at: <https://www.epa.gov/regulations-emissions-vehicles-and-engines/final-rule-mandatory-reporting-greenhouse-gases>. Accessed on: 2018/07/21.

WEST, A. H.; POSARAC, D.; ELLIS, N. Assessment of four biodiesel production processes using HYSYS.Plant. **Bioresource Technology**, v. 99, n. 14, p. 6587−6601, 2008.

ZHANG, Y.; DUBÉ, M. A.; MCLEAN, D. D.; KATES, M. Biodiesel production from waste cooking oil: 1. Process design and technological assessment. **Bioresource Technology**, v. 89, n. 1, p. 1−16, 2003a.

_____. Biodiesel production from waste cooking oil: 2. Economic assessment and sensitivity analysis. **Bioresource Technology**, v. 90, n. 3, p. 229−240, 2003b.

ZONG, L.; RAMANATHAN, S.; CHEN, C.-C. Fragment-Based Approach for Estimating Thermophysical Properties of Fats and Vegetable Oils for Modeling Biodiesel Production Processes. **Industrial & Engineering Chemistry Research**, v. 49, n. 2, p. 876−886, 2010.

6 BIODIESEL PRODUCTION FROM TALL OIL BY CATALYTIC DISTILLATION

Allan Almeida Albuquerque[a,b], Flora T. T. Ng[b], Leandro Danielski[a], Luiz Stragevitch[a,*]
[a]*LAC/DEQ/UFPE - Fuel Laboratory, Department of Chemical Engineering, Federal University of Pernambuco. Av. Prof. Artur de Sá s/n - CEP 50740-521, Recife, PE, Brazil.*
[b]*Department of Chemical Engineering, University of Waterloo, Waterloo, N2L 3G1, Canada*
*Phone/fax: +55 81 21267235. *E-mail: luiz@ufpe.br*

Paper to be submitted to *Energy & Fuels*, Qualis A1 IF 3.024

ABSTRACT

Pine-derived market is well-developed and expected to achieve 5.27 billion USD by 2021. As a result, by-products from Kraft pulping process as crude tall oil (CTO) has been gaining attention. For instance, CTO is commonly purified to obtain five more valuable products: heads, tall oil pitch (TOP), tall oil fatty acids (TOFA) rich in C18 free fatty acids (FFA), tall oil rosin (TOR) and distilled tall oil (DTO). This purification basically consists of five steps using vapor-liquid separation equipment: dehydration, depitching, rosin column, heads separation and FFA column. Moreover, CTO has also been reported as a potential low cost feedstock for biodiesel production by esterification reaction. However, studies of design, optimization and techno-economic assessment of biodiesel production from CTO have not been found in the literature. In this work, the techno-economic feasibility of a new process for biodiesel production from CTO was investigated. A solid acid-catalyzed (SAC) route using a catalytic distillation column (CDC) with Relite CFS as the catalyst was employed. CTO purification was needed to achieve biodiesel standard specifications. As a consequence, a base case and an alternative process for CTO purification from three and four distillation columns were designed, optimized and techno-economically assessed. The alternative process showed to be the only technically feasible for biodiesel production and also more economical and eco-friendly. Therefore, this process was investigated for biodiesel production from TOFA by SAC process using a CDC and a catalytic divided-wall column (CDWC). CDWC process was not technically feasible, so that the CDC process was globally optimized based on five inputs: feed temperature of the TOFA stream, liquid holdup, number of rectification, reactive and stripping stages. Finally, a flexibility study was also carried out, so that a final design was obtained for biodiesel production using CTO from United States of America, Canada and Scandinavia.

Keywords: Biodiesel. Catalytic distillation column (CDC). Crude tall oil (CTO). Esterification. Free fatty acids (FFA). Solid acid-catalyzed (SAC).

6.1 INTRODUCTION

Economic issues have been for years the main reason for industry to keep producing fossil fuels. However, the world has changed since global warming risk was identified, so that climate policy has been tighter creating budgets (tax) on carbon emissions (COVERT; GREENSTONE; KNITTEL, 2016). Moreover, technology improvements in renewable fuels production have enabled more competitive prices (VAN DE GRAAF, 2017; VAN DER PLOEG, 2016; ZERVOS; ADIB, 2018).

After Kyoto protocol in 1997, Paris Agreement in 2015 has guided countries to decrease greenhouse gas emissions (GHC) in order to keep global temperature increase below 2 ºC and making efforts to attain an increase less than 1.5 ºC until second half of century (UN, 2015). As a consequence, some countries have aspirated for new low carbon policies, such as Norway, Ireland, Netherlands and other countries, and plan to decrease sale of fossil fuel cars in the next years (MECKLING; NAHM, 2019). Despite this, biodiesel supply is expected to increase more than 8 billion liters from 2016 to 2025, mainly, due to United of States and developing countries as Brazil, Argentina and Indonesia (ROUHANY; MONTGOMERY, 2019).

As a result, the use of biomass and production of renewable fuels has been encouraged. As a preparation, countries and industries have invested in cheap raw materials such as waste and by-products (BABCOCK et al., 2008; DEMIRBAS, 2011). For instance, residual oil and fats (ROFs) such as waste cooking oil and animal fats and wastes have been employed for biodiesel production to decrease waste disposal and costs (CORDERO-RAVELO; SCHALLENBERG-RODRIGUEZ, 2018; SOUZA; SEABRA; NOGUEIRA, 2018). In addition, biodiesel from ROF already has been shown to be 2 to 3 times cheaper than those produced from edible oils (DEMIRBAS, 2011; ZHANG et al., 2003). However, ROF availability is still a concern to meet completely the biodiesel industry demand in some countries. Consequently, other low-cost raw materials from biomass have been studied as crude tall oil (CTO), since pine-derived market is well-developed and expected to achieve 5.27 billion USD by 2021 (ROHAN, 2016).

CTO is a viscous dark brown odorous liquid similar to wood tar and obtained as one of two by-products from Kraft pulping process for paper production using pine wood (NORLIN, 2012). Basically, CTO is separated from black liquor by settling and produced by acidification of tall oil soap using sulfuric acid (ARO; FATEHI, 2017; NORLIN, 2012; WANSBROUGH;

ROUGH; COONEY, 1987). CTO is mainly composed of free fatty acids (FFA), resin acids (RA) and neutral (unsaponifiables) compounds. Typical composition is 30–53 wt% of FFA, 30–53 wt.% of RA and 6.5–30 wt% of neutral compounds composed mainly from high molecular components such as sterols, esters, fatty alcohols and other compounds (ARO; FATEHI, 2017; BABCOCK et al., 2008; HOLMBOM; ERÄ, 1978; NOGUEIRA, 1996; NORLIN, 2012). Impurities can also be found, such as: water-oil emulsions, soap residue, sulfuric acid, lignin and salts (NORLIN, 2012).

After production, CTO is separated by fractional distillation to obtain five stream products: heads, tall oil pitch (TOP), tall oil fatty acids (TOFA) rich in C18 FFA, tall oil rosin (TOR) and distilled tall oil (DTO). The main products are TOFA and TOR (NORLIN, 2012). TOFA is commonly obtained with more than 90 wt% of FFA and has been used to obtain soaps, detergents, base for textile oils, cutting oils, lubricating greases and biodiesel (ALTIPARMAK et al., 2007; KRALOVA; SJÖBLOM, 2010; NORLIN, 2012). While TOR is composed of 85 to 96 wt% of RA and used in rubber polymerization, to produce adhesives, print inks and rosin to increase string instruments performance (NORLIN, 2012; WANSBROUGH; ROUGH; COONEY, 1987).

The other products have also become important, DTO is composed of more than 65 wt% of FFA and is used in coating, flotation, board impregnation and to produce soap, while heads and TOP are typically used as fuel (NORLIN, 2012; WANSBROUGH; ROUGH; COONEY, 1987). However, TOP can also be used as binder in cement, asphalt and rubber modifier. Sitosterol is the main neutral compound found in TOP; however, esters, FFA, RA, fatty alcohols and others compounds can also be found (HOLMBOM; ERÄ, 1978; NORLIN, 2012). Despite these characteristics, CTO composition, yield and properties can be affected by several factors, such as: type of wood species (pine, spruce or birch), type and length of wood storage, location, hardwood and others causes (ADEWALE; CHRISTOPHER, 2017; NORLIN, 2012).

CTO has been reported as a potential low cost raw material for biodiesel production by esterification reaction. However, many authors reported prior CTO purification is needed because of the presence of RA and other impurities as neutral compounds (ALTIPARMAK et al., 2007; KESKIN; GÜRÜ; ALTIPARMAK, 2007; KESKIN et al., 2010; KRALOVA; SJÖBLOM, 2010). This purification basically consists of five steps using vapor-liquid separation equipment: dehydration, depitching, rosin column, heads separation and FFA

column (NIEMELÄINEN, 2018; NORLIN, 2012; RÜTTI, 1986; WANSBROUGH; ROUGH; COONEY, 1987).

Water and short-chain molecule components are removed at the dehydration step using an evaporator, while TOP is removed at bottom stream of depitching evaporator or distillation column. The other three separation steps are carried out in distillation columns including side streams in rosin and FFA columns to obtain tall oil poor in RA and TOFA, respectively. TOR and DTO are both obtained at the bottom streams of rosin and FFA columns. Heads can be obtained from all these three last separations and is mainly composed of palmitic acid and lower boiling point compounds (NORLIN, 2012; RÜTTI, 1986; WANSBROUGH; ROUGH; COONEY, 1987).

After CTO purification, TOFA side stream, mainly composed of oleic, linoleic, linolenic and stearic acids in addition to some traces of palmitic acid, undergoes esterification reaction. In this step, homogeneous or heterogeneous catalyzed, uncatalyzed or enzymatic reactions have been reported (AVHAD; MARCHETTI, 2015). Uncatalyzed process based on supercritical conditions has advantages of low reaction time, high reaction rate, high conversion and absence of catalyst; however, this is still impracticable in large scale since high costs are involved using high pressure, temperature and molar ratio (MR) of alcohol to FFA (or oil) (VYAS; VERMA; SUBRAHMANYAM, 2010). Moreover, there is a risk for biodiesel decomposition for temperatures above 275 ºC (LIN; ZHU; TAVLARIDES, 2013).

Enzyme can completely convert FFA to fatty acid methyl esters (FAME), be regenerated and reused by immobilization besides of its by-product is easily separated. Nevertheless, high enzyme prices, high reaction time, inhibition by water and possibility of activity loss and formation of agglomerate can discourage its use (GNANAPRAKASAM et al., 2013). As a result, acid-catalyzed route has been commonly applied in industry using a homogeneous catalyst as sulfuric acid. Homogeneous acid-catalyzed reaction using H_2SO_4 has high yield and conversion besides of low price and reaction time (FARAG; EL-MAGHRABY; TAHA, 2011; JACOBSON et al., 2008). Despite these reasons, this catalyst is highly corrosive, cannot be reused, increase purification and wastewater treatment costs (ATADASHI et al., 2013; CARDOSO; NEVES; SILVA, 2008).

On the other hand, solid-acid catalysts can obtain high conversion of FFA, tolerate water, reduce waste treatment cost, produce higher purity glycerol and they are environment friendly, easily separated, reused and regenerated depending on activity and reduced leaching

of activity sites (ATADASHI et al., 2013; AVHAD; MARCHETTI, 2015; MANSIR et al., 2017). Furthermore, the solid acid-catalyzed (SAC) process for biodiesel production using catalytic distillation column (CDC) has showed advantages related to a combination of reactor/distillation column, such as: lower MR of methanol to FFA fed, less affected by water presence, higher productivity, smaller space required and lower capital and operation costs (GAURAV; NG; REMPEL, 2016; STEINIGEWEG; GMEHLING, 2003). However, the SAC process using CDC for biodiesel production from CTO was not investigated yet by process simulation as well as there are no studies of design, optimization and techno-economic assessment in this subject.

As a result, this work was proposed in order to investigate the techno-economic feasibility of a new process for biodiesel production from CTO by CDC. For this purpose, two CTO purification processes were designed and evaluated related to techno-economic and environment assessment. Furthermore, TOFA from the most technical-economic feasible process was subjected to esterification reaction inside a CDC and a catalytic distillation divided-wall column (CDWC) using Relite CFS as catalyst. Afterwards, the most technical feasible process was designed and optimized based on a stochastic optimization through connection between Matlab, Visual Basic for Applications (VBA) from Microsoft Excel and Aspen Plus simulations. Finally, a flexibility study on this process was carried out using three different common CTO composition profiles.

6.2 METHODOLOGY

6.2.1 Definition of the components

Components for CTO purification were defined based on main FFA, RA and neutral compounds from United States of America (USA) CTO showed in Table 6.1. While components for esterification unit were defined based on the same assumptions from our previous work (ALBUQUERQUE et al., 2019a) presented in Chapter 4. As a result, oleic acid (OA), methanol (M), methyl oleate (MO), water (W) and the main RA found in TOFA stream were chosen as representative components for esterification reaction.

Table 6.1 – Characteristics and composition of crude tall oil (CTO)

	Shorthand[a]	USA pine	Scandinavia	Canada
Acid number (AN)		165	145	140
Saponification number (SN)		172	160	165
Fatty acids, wt%		**45.1**	**45.0**	**41.9**
Palmitic	16:0	3.5	1.9	2.6
Stearic	18:0	1.2	0.6	1.3
Oleic	18:1	23.4	12.9	13.1
Linoleic	18:2	15.2	21.9	19.7
Linolenic	18:3	1.2	6.4	3.9
Arachidic	20:0	0.6	1.3	1.3
Resin acids, wt%		**42.0**	**30.0**	**30.0**
Pimaric	20:1:3:1:3	3.2	2.1	2.1
Palustric	20:0:3:2:3	7.5	4.1	5.4
Isopimaric	20:1:3:1:2	4.3	2.1	4.3
Abietic	20:0:3:2:2,3	16.2	12.4	10.7
Dehydroabietic	20:0:3:3:3	4.3	5.2	4.3
Neoabietic	20:1:3:1:3	6.5	4.1	3.2
Neutrals, wt%		**11.0**	**23.0**	**26.0**
Sitosterol	29:0:4:1:2	11.0	23.0	26.0
Water, wt%		**2.0**	**2.0**	**2.0**
Total		100.0	100.0	100.0

[a] The five numbers separated by a colon stand for the chain length, number of double bonds in aliphatic chain, number of rings, number of double bonds in all rings and which ring has been located the double bonds.
Source: Norlin (2012).

6.2.2 Thermophysical properties, phase equilibrium and kinetic model

For CTO purification unit, thermophysical properties of RA were reviewed and calculated based on a model proposed by Bokis, Chen and Orbey (1999) for neoabietic and dehydroabietic acids because it agreed with experimental data from DIPPR database. While phase equilibrium was modeled by UNIFAC model since no binary interaction parameters between FFA, RA and sitosterol were found in Aspen Plus from correlative models.

For the esterification unit, phase equilibrium was modeled by NRTL model previously validated for vapor-liquid-liquid equilibrium (VLLE) region (see Chapter 4), where interaction parameters involving the main RA were estimated by UNIFAC. Furthermore, a kinetic modeling based on Eley-Rideal surface reaction mechanism including the phases partition phenomenon and the ionic exchange equilibrium was validated and adopted to esterification reaction inside reactive stages of the CDC as shown in Appendix B (TESSER et al., 2010). As a result, an user kinetic model was developed in a FORTRAN code and connected to Aspen Plus simulations.

6.2.3 Design, optimization and techno-economic feasibility of the processes

6.2.3.1 Purification of crude tall oil

Two different processes for CTO purification were studied in order to produce biodiesel achieving requirements from ANP standard (ANP, 2014). In this case, process A based on conventional route with four distillation columns were designed (NORLIN, 2012; WANSBROUGH; ROUGH; COONEY, 1987). Furthermore, an alternative route, denoted as process B, adapted from steam distillation concept was studied using dry vacuum distillation (WALAS, 1990). This latter has three distillation columns including two side streams at the last one in order to obtain heads, TOFA, DTO and TOR. While for process A, all these products are also obtained in the last (fourth) column, except for TOR that is obtained in the second column. Moreover, another heads product can be obtained in other columns as a top product for both processes and TOP in the first column. Figure 6.1 shows a simplified block diagram for both

routes of CTO purification (NORLIN, 2012; RÜTTI, 1986; WALAS, 1990; WANSBROUGH; ROUGH; COONEY, 1987).

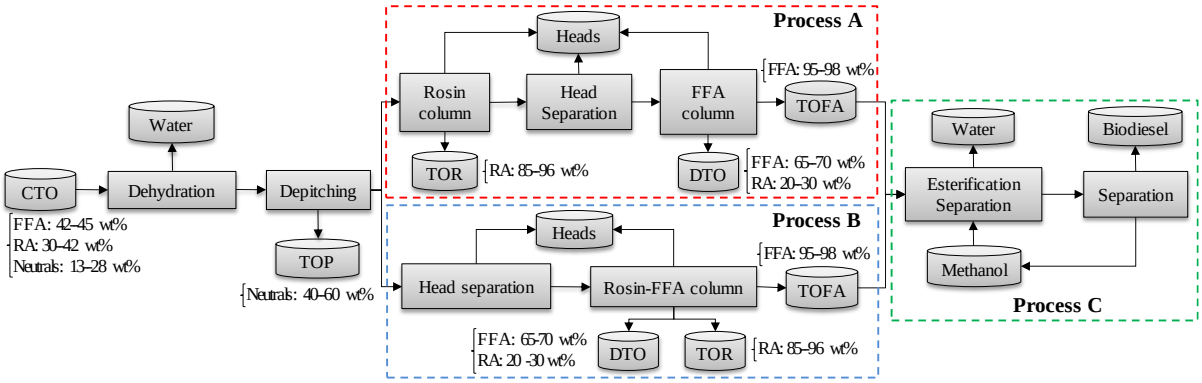

Figure 6.1 – Block diagram of processes A and B for CTO purification and process for biodiesel production from CTO using CDC
Source: Adapted from Norlin (2012), Rütti (1986), Walas (1990) and Wansbrough, Rough and Cooney (1987).

Processes A and B were designed embedding with some experimental results (RÜTTI, 1986). A CTO feed rate of 200 kton/year was adopted based on the fractionation capacity of a tall oil industry from Arizona, United States (KIRSCHNER, 2005). After both processes were evaluated related to technical feasibility and economically optimized based on sensitivity analysis tool from Aspen Plus and cost estimation using spreadsheets including installed cost (C_{inst}), utility cost (C_{util}) and total annualized cost (TAC). Subsequently, economic evaluation in Aspen Plus was carried out for base and optimized cases adopting stainless steel (SS) 316, when reasonable content of FFA or RA was found above 150 ºC, otherwise SS 304 was used. Finally, the most technical-economical process was applied for biodiesel production through process C.

6.2.2.2 Biodiesel production from esterification

In this step, TOFA stream reacted with methanol at CDC to produce biodiesel at the bottom and water at the top as shown in Figure 6.2a. Additional purification can be required, so that methanol was recycled and biodiesel was produced attaining ANP standard. The solid acid catalyst Relite CFS was considered as inside of structured packing and reaction was modeled based on Eley-Rideal kinetic model presented in Section 6.2.2 (TESSER et al., 2010).

Finally, process C based on CDC was compared to CDWC as proposed by Kiss et al. (2012) and shown in Figure 6.2b. Both configurations were investigated related to technical feasibility and the best process was also economically assessed. In addition, a global optimization was proposed since CDC or CDWC columns can involve many input variables. As a result, a procedure connecting Matlab, VBA and Aspen Plus was used to optimize esterification unit based on minimization of *TAC*. Moreover, all economic evaluated processes were compared related to energy usage and CO_2 emissions besides of other economic indicators, such as: total capital cost (C_{TC}), C_{util}, total operation cost (C_{oper}), product sales (PS), net annual profit after taxes (A_{NNP}), return of investment (ROI) and break-even price (BEP).

For all calculations using economic evaluation tool from Aspen Plus, some values of parameters were kept constants, such as: an operation year of 8,766 h, an operating life of plant of 30 years, a length of plant start-up of 4 months and starting the basic engineering in March 12th, 2018 (ALBUQUERQUE et al., 2019b). Furthermore, four cases of chemical prices were adopted to include variation effect of raw material and product prices as shown in Table 6.2 (ALBUQUERQUE et al., 2019b; DRBAL; BOSTON; WESTRA, 1996; KISS, 2013; LUYBEN, 2013; PARKASH, 2003). An abbreviation was defined containing first three letters relative to raw materials price and other three letters in the final relative to product prices. The first letter was defined as L or H referring to lowest or highest prices, while second letter R referred to raw materials and P to product. The last letter P refers to price. Therefore, for instance LRP-HPP refers to lowest raw material price and highest product price (ALBUQUERQUE et al., 2019b).

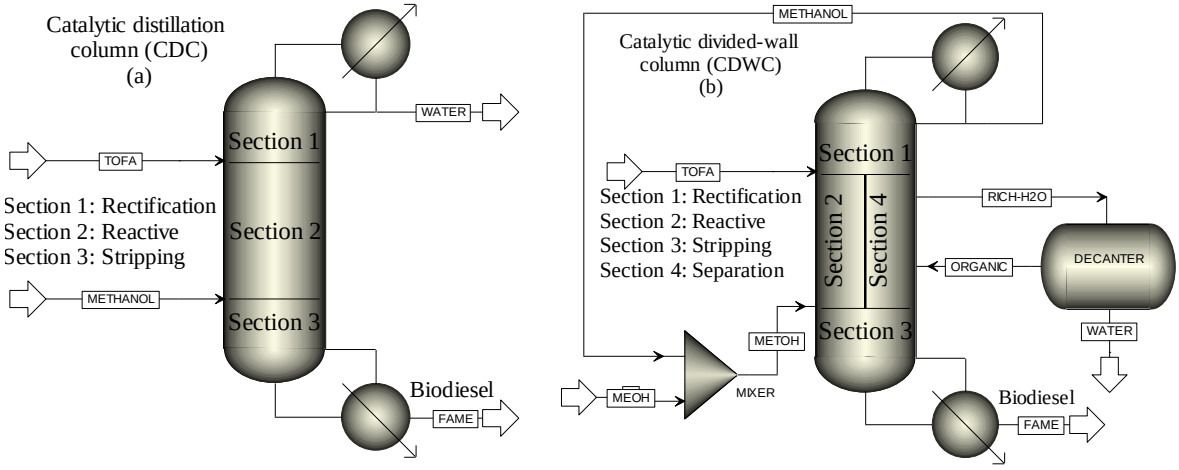

Figure 6.2 – Configuration for esterification reaction based on (a) CDC and (b) CDWC
Source: Adapted from Kiss (2012)

Carbon dioxide (CO_2) emissions were also calculated based on method proposed by United States Environment Protection Agency (EPA), in order to evaluate more environment friendly conditions (EPA, 2009).

Table 6.2 – Raw material, product, catalyst and utilities prices used in process simulations

Chemical	LRP|LPP[a] ($/kg)	HRP|HPP[b] ($/kg)	Utility	*P* (bar)| *T* (ºC)[d]	Cost	Unit
CTO	0.55	0.85	LP steam	6|160	7.78	$/GJ
Heads	0.28	0.43	MP steam	11|184	8.22	$/GJ
TOP	0.67	0.73	HP steam[c]	42|254	9.88	$/GJ
TOR	1.03	2.30	HHP steam[c]	61|273	10.44	$/GJ
DTO	1.39	2.40	HHHP steam[c]	99|308	11.27	$/GJ
Methanol	0.30	0.50	Chilled water	|5-15	4.43	$/GJ
Biodiesel	0.85	1.00	Cooling water	|30-45	0.06	$/g
Relite CFS	7.00	10.00	Electricity		0.12	$/kW·h

[a] LRP and LPP refer to the lowest raw material price and lowest product price;
[b] HRP and HPP refer to the highest raw material price and highest product price;
[c] HP steam refers to high-pressure steam, HHP steam refers to higher pressure than HP steam and HHHP steam refers to higher pressure than HHP steam;
[d] P|T refers to pressure in bar and temperature in ºC.
Source: Adapted from Albuquerque et al. (2019b), Alibaba (2018), Drbal, Boston and Westra (1996), Kiss (2013), Luyben (2013) and Parkash (2003).

6.3.2.3 Flexibility study

As a final step, plant flexibility of the more techno-economical feasible process was investigated based on three different types of CTO showed in Table 6.1, so that Scandinavian and Canadian CTO was also purified and applied for biodiesel production at the same feed rate used for USA CTO. In this case, a process design was proposed in order to attain this common composition range of FFA, RA and neutral coumpounds found in industries. In addition, economic indicators were also calculated in order to compare different scenarios including an average price for chemical compounds.

6.3 RESULTS AND DISCUSSION

6.3.1 Kinetic modeling

Kinetic model was added as user defined in order to obtain an initial FORTRAN code for CDC represented by RADFRAC block. In this case, kinetic data for esterification of oleins with Relite CFS was validated to simulated results using a batch reactor from Aspen Plus as shown in Figure 6.3. Results from Figure 6.3a–b were obtained for runs between 100 to 120ºC of the uncatalyzed and catalyzed reactions without tryacylglycerols (TAGs) (TESSER et al., 2010). On the other hand, kinetic data from Figure 6.3c–d were obtained by esterification of FFA in presence of TAGs between 50 to 85ºC for the same catalyst (TESSER et al., 2005). As a result, kinetic was considered validated between 50 to 120ºC since Pearson Correlation Coefficient (PCC) are close to one and F test ($F < F_{critical}$) is satisfied for 95% of confidence level.

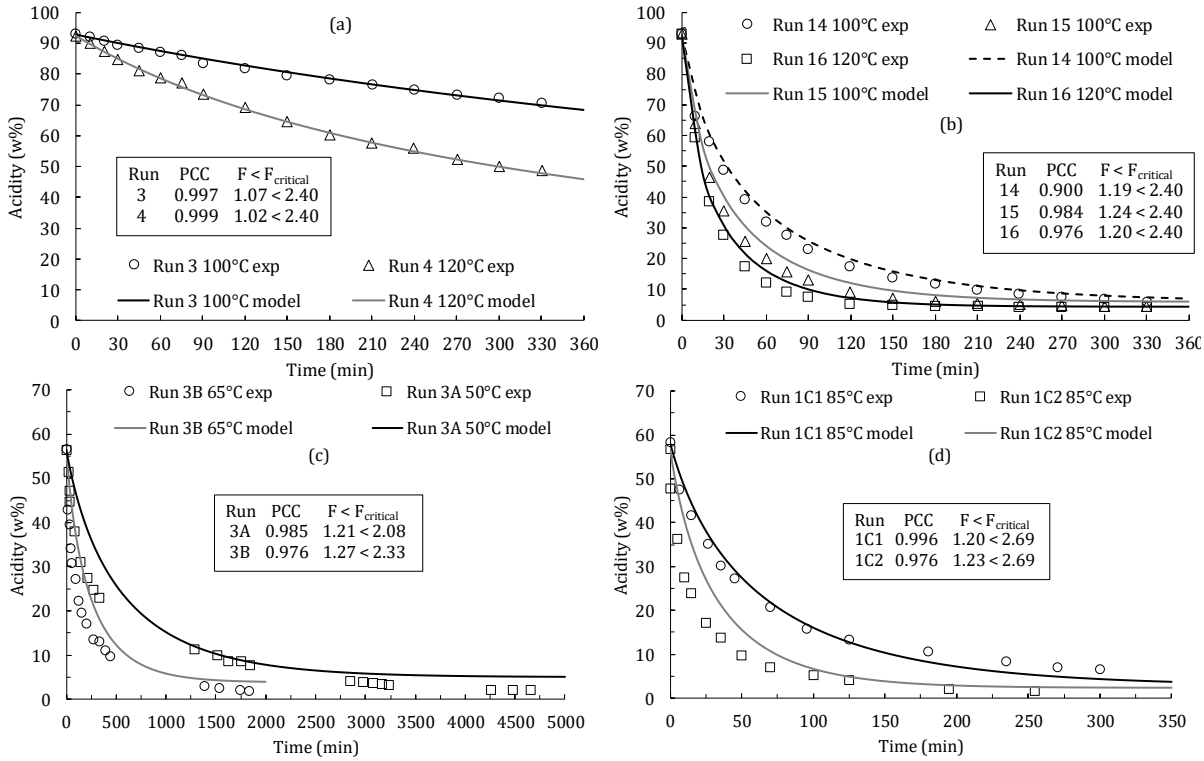

Figure 6.3 – Comparison between esterification kinetic model to experimental data using Relite CFS: (a) uncatalyzed and (b) catalyzed reaction for oleins at 100 and 120ºC without oil; catalyzed reaction for oleic acid in presence of TAGs (c) using 5 g of catalyst at 50 and 65ºC and (d) using 5 g and 10 g at 85ºC

Source: Adapted from Tesser et al. (2005, 2010).

After validation step in a batch reactor, since there is no data for kinetics inside CDC, the user kinetic model was extended to RADFRAC block. In order to validate this procedure, some results of Pérez-Cisneros (2016) were replicated for esterification reaction in CDC and obtained almost complete conversion. Furthermore, a test connecting a CDC to a continuous stirred tank reactor (CSTR) and a flash column proved that the reaction inside one stage behaves as a CSTR.

6.3.2 Design, optimization and techno-economic assessment

In this section, some flowsheets were designed and in order to keep standardized block and stream names, a convention was adopted. For instance, flowsheet block names are represented by Y-1ZZ or Y-2ZZ, wherein numbers 1 and 2 were related to processes A and B or C, respectively. Y denotes E, P, T, V, M or S representing the heat exchanger (heater or cooler), pump, tower (distillation column or CDC), vessel (flash drum), mixer or splitter. ZZ denotes an integer counter related to the amount of specific equipment. For instance, Y-1ZZ = T-101 means distillation column 1 present in process A (ALBUQUERQUE; DANIELSKI; STRAGEVITCH, 2016; ALBUQUERQUE et al., 2019b).

Analogously, the stream names are represented by 1ZZ or 2ZZ. For example, stream 101 represents CTO feed stream to process A as shown in Figure 6.4. In addition, some streams can be accompanied by a letter (A, B or C); that was used when the stream pressure (e.g., 101A) or temperature (e.g., 101B) changed while almost keeping constant the composition (ALBUQUERQUE; DANIELSKI; STRAGEVITCH, 2016; ALBUQUERQUE et al., 2019b).

6.3.2.1 Purification of crude tall oil

Purification of CTO was required to remove undesired resin acids and neutral compounds. Information about this separation it is almost always kept in secret by industry. For this reason, two flowsheets were proposed, where Processes A and B were based on four and three distillation columns as shown in Figure 6.4 and Figure 6.5 (NORLIN, 2012; RÜTTI, 1986; WALAS, 1990; WANSBROUGH; ROUGH; COONEY, 1987). Old industrial plants have still

been operated as steam distillation in order to avoid lower pressures; however, waste stream costs and environment impacts increase. As a result, until at lower pressures dry vacuum distillation has been encouraged in order to be more environment friendly and improve separation (NORLIN, 2012; RÜTTI, 1986).

For both purification processes, water impurity (2 wt%) was firstly separated from CTO in a flash vessel (V-101 and V-201) followed by TOP separation in a distillation column (T-101 and T-201) with 9 stages and feed stage (FS) at stage 4. Number of stages (N) and FS closer to recommended by Walas (1990) was adopted, since very close pressure drop (8 mbar) was obtained inside RADFRAC block compared to experimental results from Rütti (1986) in a pilot plant using Mellapak® 250Y from Sulzer Chemtech. Low drop pressure was required in order to improve separation and avoid degradation of tall oil components at reboiler temperature (T_{reb}) above 270ºC (RÜTTI, 1986). As a result, TOP was obtained composing mainly of 77 wt% of neutral (unsaponifiables) compounds and 23 wt% of resin acids.

After TOP separation, FFA/RA-rich stream (107A or 207A) was fed to a second distillation column T-102 or T-202 composed of 9 or 18 stages with FS at stage 4 or 9. In this step, heads were separated in both processes; however, heads fraction removed in stream 208 at base case of Process B, denoted as Process BB, was more than five times higher than that obtained in stream 108 from base case of Process A, denoted as Process AB. Furthermore, TOR stream (110) was obtained in this column for Process A composing of more than 95 wt% of RA, while TOFA-rich stream (109) was removed as a side-stream to feed the third column T-103 composed of 10 stages with FS at stage 5. As for first distillation column, a pressure drop close to 8 mbar was kept in tower T-102 in order to agree with experimental results obtained by Rütti (1986).

Subsequently at Process AB, more heads were removed in distillate stream 111 of T-103 in order to separate higher boiling components as RA and FFA with less than 18 carbons (palmitic acid) in the chain. After bottom stream 112 was pumped to feed at stage 26 a tower T-104 composed of 31 stages, where another distillate stream 113 composed of heads, a side stream 114 with TOFA at 95 wt% and a bottom stream 115 with DTO were obtained. For all products, AN, yield and component mass purity were compared to Norlin's results as shown in Table 6.3.

Table 6.3 – Comparison between reported and simulated yield, AN and composition for tall oil fractions

Fraction	Process	Yield/%	*AN*	RA/wt%	FFA/wt%	Neutrals/wt%
Head	Norlin (2012)	5–12	70–120	<0.5	30–50	40–60
	AB*	16.3	164.2	78.4	21.5	0.1
	AO*	14.9	171.9	60.9	39.0	0.1
	BB*	29.0	171.9	60.8	39.1	0.1
	BO*	25.7	169.8	65.7	34.2	0.1
	B8 or (C8 or CU) *	25.7	169.8	65.7	34.3	0.1
	CS*	28.2	177.2	48.6	51.3	0.1
	CC*	28.6	174.6	54.7	45.2	0.1
TOFA	Norlin (2012)	35–45	192–197	<2	95–98	1–2
	AB*	73.1	196.4	5.0	95.0	0.0
	AO*	67.7	198.2	0.8	99.2	0.0
	BB*	49.9	198.6	0.1	99.9	0.0
	BO*	51.5	198.6	0.1	99.9	0.0
	B8 or (C8 or CU) *	51.5	198.6	0.1	99.9	0.0
	CS*	49	198.6	0.0	100.0	0.0
	CC*	48.4	198.6	0.0	100.0	0.0
DTO	Norlin (2012)	5–15	180–190	20–30	65–70	4–7
	AB*	5.2	179.7	43.3	56.7	0.0
	AO*	14.9	184.3	32.7	67.3	0.0
	BB*	8.3	184.8	31.5	68.5	0.0
	BO*	12.8	185.4	30.2	69.8	0.0
	B8 or (C8 or CU) *	12.8	185.3	30.4	69.6	0.0
	CS*	13	185.3	30.4	69.6	0.0
	CC*	16.3	185.4	30.2	69.8	0.0
TOR	Norlin (2012)	20–35	165–182	85–96	1–5	1–7
	AB*	14.7	157.0	95.3	4.7	0.0
	AO*	14.5	156.3	97.1	2.9	0.0
	BB*	23.2	155.8	98.2	1.8	0.0
	BO*	23.7	156.7	96.1	3.9	0.0
	B8 or (C8 or CU) *	23.7	156.7	96.0	4.0	0.0
	CS*	20.9	156.7	96.0	4.0	0.0
	CC*	17.6	156.7	96.0	4.0	0.0
TOP	Norlin (2012)	20–40	20–50	5–13	5–10	40–60
	AB*	14.5	35.3	22.8	0.0	77.2
	AO*	14.5	36.4	19.4	3.2	77.4
	BB*	14.5	35.3	22.8	0.0	77.2
	BO*	14.5	36.4	19.4	3.2	77.4
	B8 or (C8 or CU) *	14.5	36.4	19.4	3.2	77.4
	CS*	26	16.3	7.6	2.3	90.1
	CC*	28.8	12.9	5.7	2.0	92.2

* First letter refers to Process type A or B or C and second letter to base case (B) or optimized (O) or pressure of 8 mbar (8) at tower T-203 for USA CTO (U) or Scandinavian CTO (S) or Canadian CTO (C)
Source: Adapted from Norlin (2012).

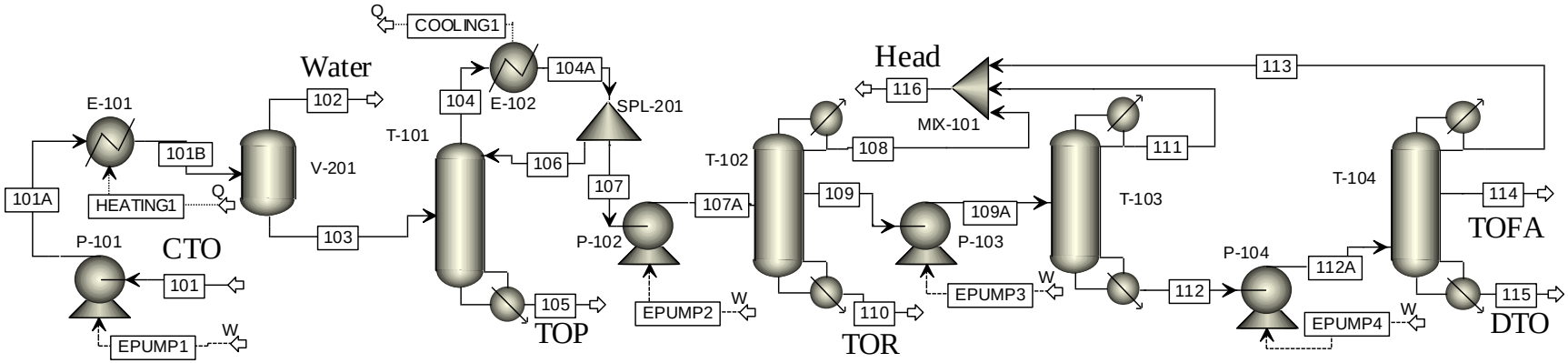

Figure 6.4 – Process A for tall oil purification from CTO producing Head, TOP, TOR, DTO and TOFA
Source: Adapted from Norlin (2012), Rütti (1986) and Wansbrough, Rough and Cooney (1987).

Table 6.4 – Main stream results of Process AO (Process A optimized) for tall oil purification from USA CTO

Variables\Streams	101	102	103	105	107	108	109	110	112	114	115	116
Mass flow (kton/h)	22.82	0.45	22.36	3.24	19.12	2.45	13.9	2.77	8.22	5.57	1.22	9.56
Pressure (kPa)	101.3	2.0	2.0	1.0	0.2	0.4	0.5	1.2	1.1	1.0	1.8	0.4
Temperature (K)	298.2	357.5	357.5	535.6	305.8	283.4	458.6	521.8	490.2	488.5	510.8	408.9
Water (wt)	0.0200	0.9924	0.0003	0.0000	0.0004	0.0030	0.0000	0.0000	0.0000	0.0000	0.0000	0.0008
Palmitic acid (wt)	0.0351	0.0001	0.0358	0.0016	0.0416	0.0413	0.0499	0.0000	0.0219	0.0073	0.0010	0.0788
Stearic acid (wt)	0.0117	0.0000	0.0119	0.0011	0.0138	0.0059	0.0177	0.0010	0.0292	0.0190	0.1098	0.0021
Oleic acid (wt)	0.2338	0.0003	0.2385	0.0175	0.2760	0.1638	0.3494	0.0055	0.5397	0.6573	0.4220	0.1132
Linoleic acid (wt)	0.1519	0.0002	0.1550	0.0095	0.1797	0.1282	0.2243	0.0013	0.2974	0.2768	0.0729	0.1885
Linolenic acid (wt)	0.0117	0.0000	0.0119	0.0008	0.0138	0.0086	0.0174	0.0002	0.0261	0.0314	0.0126	0.0076
Arachidic acid (wt)	0.0058	0.0000	0.0060	0.0015	0.0067	0.0007	0.0048	0.0211	0.0081	0.0000	0.0546	0.0002
Pimaric acid (wt)	0.0323	0.0007	0.0329	0.0012	0.0383	0.0654	0.0412	0.0000	0.0006	0.0001	0.0000	0.0766
Palustric acid (wt)	0.0754	0.0009	0.0769	0.0026	0.0895	0.1404	0.0983	0.0000	0.0020	0.0003	0.0000	0.1788
Isopimaric acid (wt)	0.0431	0.0007	0.0439	0.0017	0.0511	0.0845	0.0554	0.0000	0.0009	0.0001	0.0000	0.1021
Abietic acid (wt)	0.1615	0.0000	0.1648	0.1848	0.1614	0.0015	0.0287	0.9707	0.0485	0.0000	0.3257	0.0004
Dheabietic acid (wt)	0.0431	0.0043	0.0439	0.0002	0.0513	0.2696	0.0230	0.0000	0.0000	0.0000	0.0000	0.1025
Neoabietic acid (wt)	0.0646	0.0005	0.0659	0.0034	0.0765	0.0870	0.0899	0.0001	0.0256	0.0077	0.0012	0.1484
Sitosterol (wt)	0.1100	0.0000	0.1122	0.7740	0.0000	0.0000	0.0000	0.0000	0.0000	0.0000	0.0000	0.0000

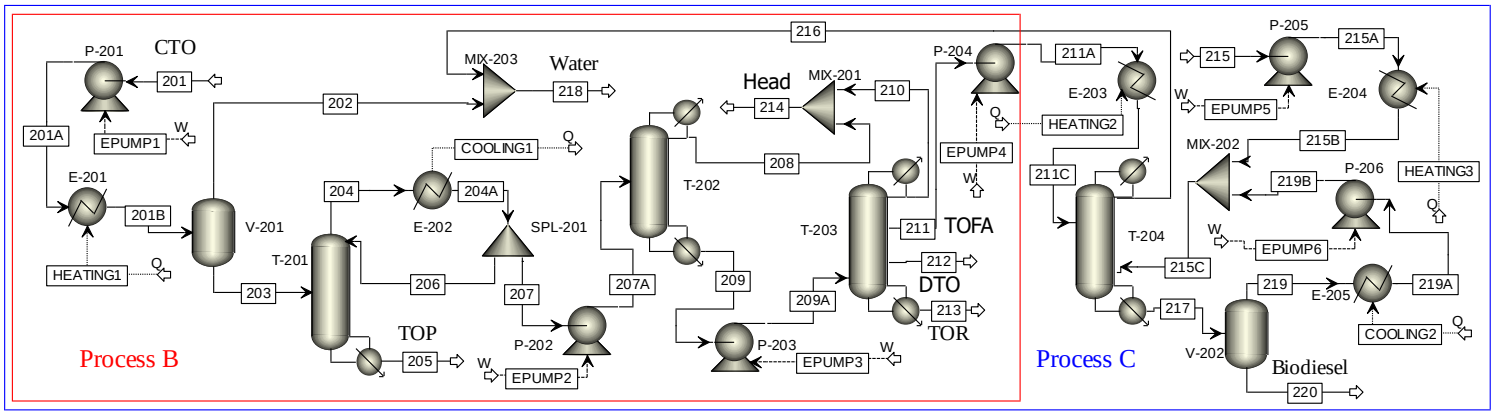

Figure 6.5 – Process B and C for tall oil purification and biodiesel production obtaining Head, TOP, TOR, DTO and biodiesel
Source: Adapted from Norlin (2012), Rütti (1986), Walas (1990) and Wansbrough, Rough and Cooney (1987).

Table 6.5 – Stream results of Process B8 or C8: Process B or C optimized for tall oil purification from USA CTO with T-203 condenser at 8 mbar

Variables\Streams	201	202	203	205	207	208	209	210	211	212	213	214
Mass flow (kton/h)	22.82	0.45	22.36	3.24	19.12	7.53	11.59	1.39	5.97	1.49	2.75	8.92
Pressure (kPa)	101.3	2.0	2.0	1.0	0.2	0.8	2.0	0.4	0.8	1.5	2.3	0.4
Temperature (K)	298.2	357.5	357.5	535.6	305.8	313.6	509.1	467.9	482.9	504.6	534.6	342.1
Water (wt)	0.0200	0.9923	0.0003	0.0000	0.0004	0.0010	0.0000	0.0000	0.0000	0.0000	0.0000	0.0008
Palmitic acid (wt)	0.0351	0.0001	0.0358	0.0016	0.0416	0.1039	0.0011	0.0053	0.0008	0.0006	0.0000	0.0885
Stearic acid (wt)	0.0117	0.0000	0.0119	0.0011	0.0138	0.0003	0.0225	0.0021	0.0349	0.0298	0.0019	0.0006
Oleic acid (wt)	0.2338	0.0003	0.2385	0.0175	0.2760	0.0307	0.4353	0.3845	0.6457	0.4252	0.0093	0.0858
Linoleic acid (wt)	0.1519	0.0002	0.1550	0.0095	0.1797	0.0856	0.2408	0.5727	0.2874	0.1855	0.0016	0.1614
Linolenic acid (wt)	0.0117	0.0000	0.0119	0.0008	0.0138	0.0023	0.0213	0.0274	0.0300	0.0190	0.0003	0.0062
Arachidic acid (wt)	0.0058	0.0000	0.0060	0.0015	0.0067	0.0000	0.0111	0.0000	0.0002	0.0357	0.0270	0.0000
Pimaric acid (wt)	0.0323	0.0007	0.0329	0.0012	0.0383	0.0973	0.0000	0.0000	0.0000	0.0000	0.0000	0.0821
Palustric acid (wt)	0.0754	0.0009	0.0769	0.0026	0.0895	0.2272	0.0000	0.0000	0.0000	0.0000	0.0000	0.1918
Isopimaric acid (wt)	0.0431	0.0007	0.0439	0.0017	0.0511	0.1298	0.0000	0.0000	0.0000	0.0000	0.0000	0.1095
Abietic acid (wt)	0.1615	0.0000	0.1648	0.1848	0.1614	0.0000	0.2663	0.0000	0.0000	0.3033	0.9599	0.0000
Dheabietic acid (wt)	0.0431	0.0043	0.0439	0.0002	0.0513	0.1302	0.0000	0.0000	0.0000	0.0000	0.0000	0.1099
Neoabietic acid (wt)	0.0646	0.0005	0.0659	0.0034	0.0765	0.1919	0.0016	0.0080	0.0010	0.0008	0.0000	0.1632
Sitosterol (wt)	0.1100	0.0000	0.1122	0.7741	0.0000	0.0000	0.0000	0.0000	0.0000	0.0000	0.0000	0.0000

Table 6.6 – Main stream results of Process CO: Process C optimized for tall oil purification from USA CTO and biodiesel production with T-203 condenser at 8 mbar

Variables\Streams	215	216	217	218	219	220
Mole flow (kmol/hr)	21.71	21.32	21.95	46.24	0.38	21.57
Mass flow (kton/h)	0.70	0.39	6.31	0.84	0.02	6.29
Pressure (kPa)	101.3	101.3	102.6	2.0	58.0	58.0
Temperature (K)	298.2	371.6	516.8	290.6	517.0	517.0
Methanol (wt)	1.0000	0.0155	0.0037	0.0072	0.4748	0.0020
Water (wt)	0.0000	0.9845	0.0000	0.9886	0.0000	0.0000
Methyl Oleate (wt)	0.0000	0.0000	0.9940	0.0000	0.5243	0.9957
Oleic acid (wt)	0.0000	0.0000	0.0014	0.0002	0.0004	0.0014
Linoleic acid (wt)	0.0000	0.0000	0.0000	0.0001	0.0000	0.0000
Pimaric acid (wt)	0.0000	0.0000	0.0000	0.0004	0.0000	0.0000
Palustric acid (wt)	0.0000	0.0000	0.0000	0.0005	0.0000	0.0000
Isopimaric acid (wt)	0.0000	0.0000	0.0000	0.0004	0.0000	0.0000
Abietic acid (wt)	0.0000	0.0000	0.0000	0.0000	0.0000	0.0000
Dheabietic acid (wt)	0.0000	0.0000	0.0000	0.0023	0.0000	0.0000
Neoabietic acid (wt)	0.0000	0.0000	0.0009	0.0003	0.0005	0.0009

Unlike Process A, there is no side stream at tower T-202 of Process B and bottom stream 209 was removed composing mainly of FFA and RA. After to be pumped, stream 209A of Process BB fed stage 46 from tower T-203 with 51 stages, where these specifications were basically defined by Walas (1990) for CTO purification based on steam distillation. As a consequence, lower condenser pressure (4 mbar) was adopted here following specification of third distillation column tested by Rütti (1986). Furthermore, $T_{reb}$was kept below 263ºC in order to use high-pressure steam at 900 psig (HHP steam) and to avoid decomposition of RA and FFA (PARKASH, 2003; RÜTTI, 1986).

Outlet streams from T-203 resulted in one distillate stream 210 of heads, two side streams 211 and 212 of TOFA 99.89 wt% and DTO; and a bottom stream 213 of TOR 98.2 wt%. As for Process AB, all products were also compared to Norlin's results as shown in Table 6.3. Moreover, stream results for both CTO purification processes are presented in Table 6.4 and Table 6.5 for optimized cases to be detailed in the next paragraphs.

From these results, both designed processes were evaluated technically based on capacity to produce biodiesel achieving ANP standard, so that 99.8 wt% of FFA at TOFA stream is required to attain it. As a result, Process AB should not be considered for biodiesel production. Until with these results, both processes were mapped, sized and evaluated related to economic feasibility as shown by energy and economic indicators at Figure 6.6a–b. Process BB showed much higher utility cost and TAC despite of slightly lower total capital cost.

Consequently, both processes were optimized in order to improve economic feasibility and to evaluate possible changes for process AB to be technical feasible.

For instance, water separation in adiabatic flash vessel V-101 or V-201 was already optimized in processes AB and BB based on sensitivity analysis for input variables temperature of heat exchanger (T_{E-101}) E-101 or E-201 and pressure (P_{V-101}) of flash vessel; and cost estimation using spreadsheets. The set of variables T_{E-101} = 105 ºC and P_{V-101} = 20 mbar were defined by trade-off of low TAC, high water purity in the vapor stream 102 or 202 and high vapor to feed mass ratio. While for towers T-101 and T-201, feed stage (FS) was the input variable obtaining a FS = 9 as optimal since resulted in lowest TAC, T_{reb}, Q_{reb} and amount of abietic acid keeping drop pressure (ΔP) close to 8 mbar as considered by Rütti (1986).

Further optimization was carried out defining processes AO and BO, where O means optimized, as shown in Figure 6.6. Design specifications were obtained varying N, FS, mole reflux ratio (RR), distillate to feed ratio (D/F) or bottom to feed ratio (B/F) and side to feed ratio (S/F) for columns including a side stream. In this case, an user FORTRAN routine was implemented in sensitivity analysis block to make easier convergence, avoiding $FS > N$ and decreasing number of iterations and, consequently, simulation time.

Optimal design specifications for tower T-102 were obtained for low TAC and T_{reb}; and higher yield of heads and side stream, while low TAC and lowest mass fraction of neoabietic acid at the bottom stream 112 (w_{Neo}^{112}) were decision variables for T-103. It is worth to mention that to keep low values w_{Neo}^{112} were important to obtain higher FFA purity at TOFA stream 114 from T-104, since vapor pressure of neoabetic acid and oleic acid are close. For column T-104, decision was taken based on high yield of heads (η_{head}) and TOFA (η_{TOFA}) in addition to high yield of DTO (η_{DTO}) between $5 \leq \eta_{DTO} \leq 15\%$.

For tower T-202 from Process BO, low TAC and high mass purity of FFA at the bottom stream were the decision variables, while optimal condition of T-203 was obtained from a trade-off between low TAC, high yield of products inside the range defined by Norlin (2012), except to TOFA that was kept above the range; and high purity of FFA and RA at TOFA stream 211 and TOR stream 213, respectively. Product results from both optimized processes were also compared to Norlin's results. Furthermore, main design and operating conditions, equipment sizes and capital costs are shown in Table 6.7. From these results, C_{TC} for Process BO was lower than Process AO because of the additional column T-102 and high RR in column T-104

to achieve FFA purity at TOFA stream 114 of 99.2 wt% (< 99.8 wt%). Consequently, Process B was the unique techno-economic feasible for biodiesel production.

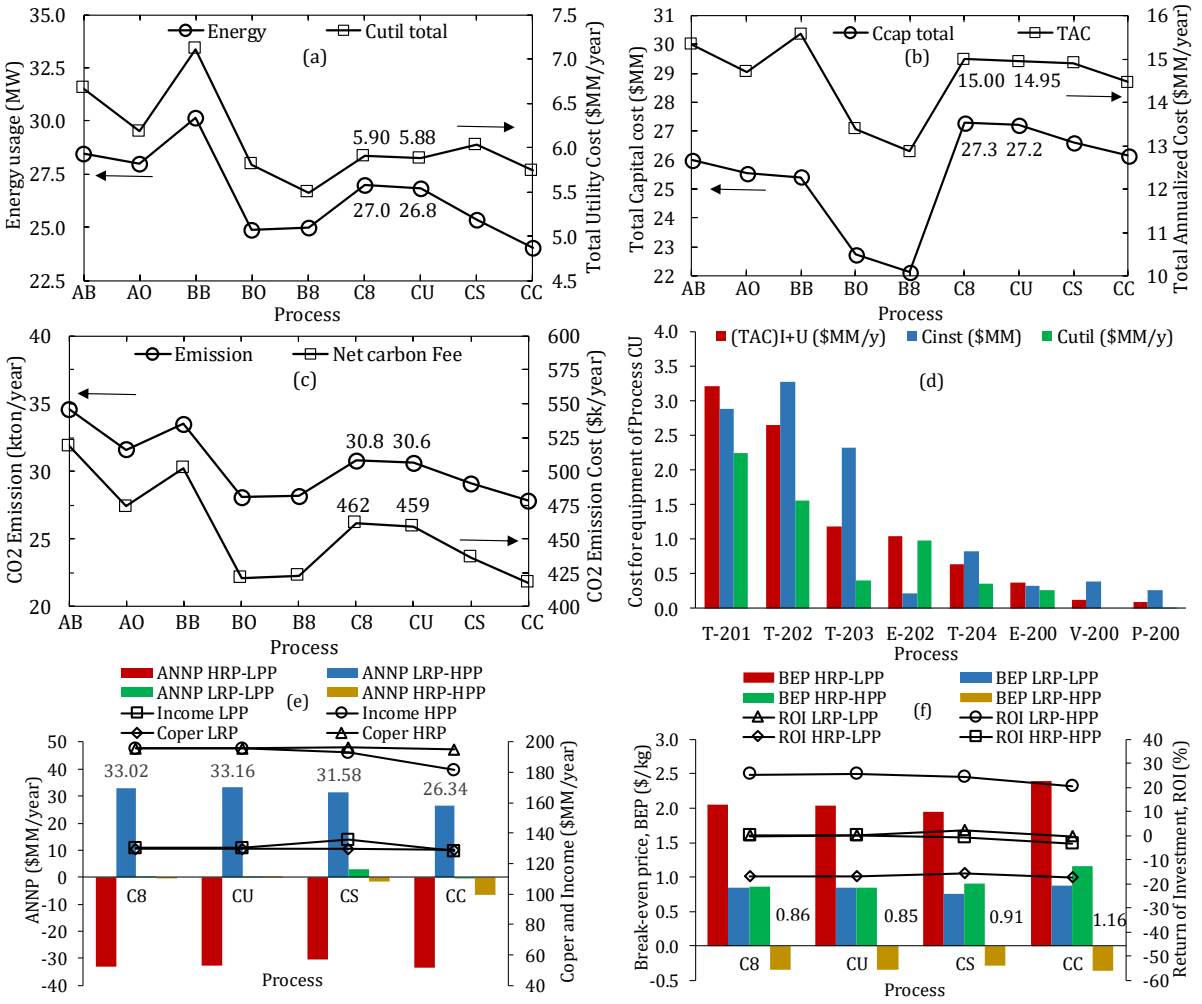

Figure 6.6 – Comparison of (a) energy usage, (b, e, f) economic and (c) environment indicators results for all processes studied; and (d) installed cost of each equipment (or set) for process CU

Table 6.7 – Main operating conditions, equipment sizes and capital costs for processes AO and BO

Block	Description	Process AO	Process BO
V-101/V-201	P (mbar)[a]	20.0	20.0
	T (K)[b]	357.5	357.5
	$D \times L$ (m)[c]	1.37 × 3.96	1.37 × 3.96
	cost ($MM)[d]	0.201	0.201
T-101/T-201	RR[e]	1.0	1.0
	B/F[f]	0.060	0.060
	P (mbar)[a]	2.0/9.7	2.0/9.7
	T (K)[b]	467.8/535.6	467.8/535.6
	Q (MW)[g]	0/6.82	0/6.82
	N/FS[h]	9/9	9/9
	$D \times L$ (m)[c]	5.49 × 7.47	5.49 × 7.47
	cost ($MM)[d]	2.820	2.820
T-102	RR[e]	1	
	B/F[f]	0.138	
	P (mbar)[a]	4.0/12.0	
	T (K)[b]	283.4/521.7	
	Q (MW)[g]	-0.88/2.49	
	$N/FS/SS$[h]	11/6/2	
	$D \times L$ (m)[c]	4.27 × 7.92	
	cost ($MM)[d]	1.846	
T-103/T-202	RR[e]	3.0	1.5
	D/F[f]	0.400	0.392
	P (mbar)[a]	4.0/10.8	4.0/16.0
	T (K)[b]	442.5/490.2	301.0/504.3
	Q (MW)[g]	-2.05/2.18	-3.11/4.55
	N/FS[h]	11/5	23/6
	$D \times L$ (m)[c]	3.66 × 7.92	5.18 × 12.8
	cost ($MM)[d]	1.527	3.250
T-104/T-203	RR[e]	20.0	8.5
	D/F[f]	0.175	0.225
	$(S_1/F)/(S_2/F)$[i]	0.680	0.525/0.127
	P (mbar)[a]	4.0/18.0	4.0/22.6
	T (K)[b]	464.4/510.7	467.9/534.7
	Q (MW)[g]	-2.74/2.72	-1.21/1.14
	$N/FS/S_1S/S_2S$[h]	31/28/14	51/45/11/51
	$D \times L$ (m)[c]	4.42 × 16	2.9 × 23.93
	cost ($MM)[d]	3.026	2.313
	Pumps cost ($MM)[d]	0.202	0.299
	Heat exchangers cost ($MM)[d]	0.301	0.150
	Total installed cost ($MM)[d]	9.923	9.033
	Total capital cost, C_{TC} ($MM)[d]	25.557	22.736

[a]P is pressure; [b]T is temperature; [c]$D \times L$ are diameter and length; [d]$MM means million dollars; [e]RR is reflux mole ratio; [f]B/F and D/F are bottom and distillate to feed mole ratio; [g]Q means condenser duty/reboiler duty; [h]$N/FS/S_1S/S_2S$ means number of stages, feed stage, first side stream stage and second side stream stage; [i]$(S_1/F)/(S_2/F)$ means first side stream and second side stream to feed mole ratio.

Afterwards, a change in condenser pressure (P_{cd}) from 4 mbar to 8 mbar at column T-202 was proposed to Process BO, requiring cooling water instead chilled water. As a result, utility costs and TAC were lower than Process BO according to Figure 6.6a–b. This process from USA CTO was denoted Process B8 since P_{cd} = 8 mbar at column T-202 and was defined as the standard process to design esterification unit. As a consequence, Process C was defined including CTO purification plus esterification reaction in a CDC using Relite CFS and a flash vessel for reactants recycle as shown in Figure 6.5.

6.3.2.2 Biodiesel production from esterification

After CTO purification, esterification reaction was carried out in a CDC to convert TOFA from stream 211 in FAME. For this reason, methanol was fed above stage 33 close to the bottom of tower T-204 of N = 34, while TOFA was fed above stage 14 to be converted in the reactive stages from 14 to 32 using 350 kg/stage of solid catalyst Relite CFS inside structured packing Mellapak® 752Y from Sulzer Chemtech. These conditions were the same applied by Pérez-Cisneros et al. (2016), except for the amount of catalyst (1 ton/stage) since they used a feed flow rate of oleic acid of 100 kmol/h. Furthermore, in order to avoid biodiesel decomposition at T_{reb} > 275 ºC, a MR of methanol to FFA of 1.042 was adopted instead of a stoichiometric ratio as defined by Pérez-Cisneros et al. (2016). Another simplification was to adopt oleic acid and neoabietic acid as pseudocomponents for all FFA and RA from TOFA stream 211, since they were the majored components in this stream. Stream results for process C is shown in Table 6.6.

Oleic acid was almost complete converted at CDC, so that bottom stream 217 showed to attain ANP standard for minimum FAME purity and maximum acidity. However, methanol purity was still above the maximum mass fraction of 0.2% and a flash vessel operating at vacuum (0.58 bar) was required to obtain biodiesel attaining requirements from ANP standard (ANP, 2014). In addition, the vapor product stream 219 was condensed and mixed with methanol fresh fed to CDC in order to avoid additional waste treatment costs. On the other hand, water is also produced from esterification reaction and was removed at the top of CDC through stream 216 with mass fraction (w_{water}^{216}) close to 98.4 wt%. Finally, this stream was mixed with the water-rich stream 202 from CTO purification resulting in the stream 218 with

w_{water}^{218} = 98.9 wt%. Stream 218 was considered as cooling water to be credited in PS according to chemical prices from Table 6.2.

Profiles at CDC T-204 were also evaluated as shown in Figure 6.7. For the temperature profile, a similar behavior to results from Pérez-Cisneros et al. (2016) was observed, except for reboiler stage since higher T was supplied at feed stream (326ºC), so that lower T_{reb} was required. Furthermore, they obtained T > 275 ºC at reactive section that can result in decomposition of biodiesel and is out of T range from the kinetic model. For this reason, a slight excess of methanol was adopted (MR = 1.042) (LIN; ZHU; TAVLARIDES, 2013). Despite this an extrapolation of 10 ºC from the T range of 50 ºC to 120 ºC was considered acceptable.

From other profiles from Figure 6.7, the highest reaction rate was obtained in an intermediate reactive stage as well as found by Pérez-Cisneros et al. (2016). Furthermore, high concentration of water was detected close to the top of tower T-204 and different profiles of mass fractions were obtained to phases I and II, since RADFRAC block was modeled as VLLE. As a result, water concentration at reactive section could be an issue; however, Eley-Rideal kinetic model takes in account reversible kinetic constants and adsorption of water in the catalyst, since CDC removes water continually, so that water stays a short time inside reactive stages of T-204.

Due to the issue of water, a catalytic divided-wall column (CDWC) was studied with similar configuration from reactive divided-wall column (RDWC) defined by Kiss et al. (2012) as shown in Figure 6.2b. However, unlike from Kiss et al. (2012) that used a shorter-chain FFA (lauric acid) with higher volatility, complete conversion of oleic acid required high T (> 300 ºC) inside reactive section, until same for higher MR (= 1.2). For this reason, CDWC was considered to not be technical feasible in order to avoid decomposition of biodiesel and/or of catalyst since thermal stability for Relite CFS is guaranteed until 140 ºC (RESINDION, 2017).

From these results, process C8 based on CDC was considered technically feasible and followed to optimization of esterification unit resulting in process CU, where U is to remember that process C was obtained from USA CTO. Similarly, Processes CS and CC were defined from Scandinavian CTO and Canadian CTO, respectively. Firstly, some input variables affecting tower T-204 were chosen, such as: T of heater E-203 (T_{E-203}), RR, liquid holdup (H_L) as catalyst mass per reactive stage, number of rectification (N_R), reactive (N_{RX}) and stripping stages (N_S). After a stochastic optimization was carried out based on procedure from our previous work using connection between Matlab, VBA and Aspen Plus. Evolution from the

objective function TAC was analyzed according to Figure 6.8, showing a minimum after 5,000 iterations and keeping in this point until 15,000 iterations (ALBUQUERQUE et al., 2019b; KISS et al., 2012; SEGOVIA-HERNÁNDEZ; GÓMEZ-CASTRO, 2017).

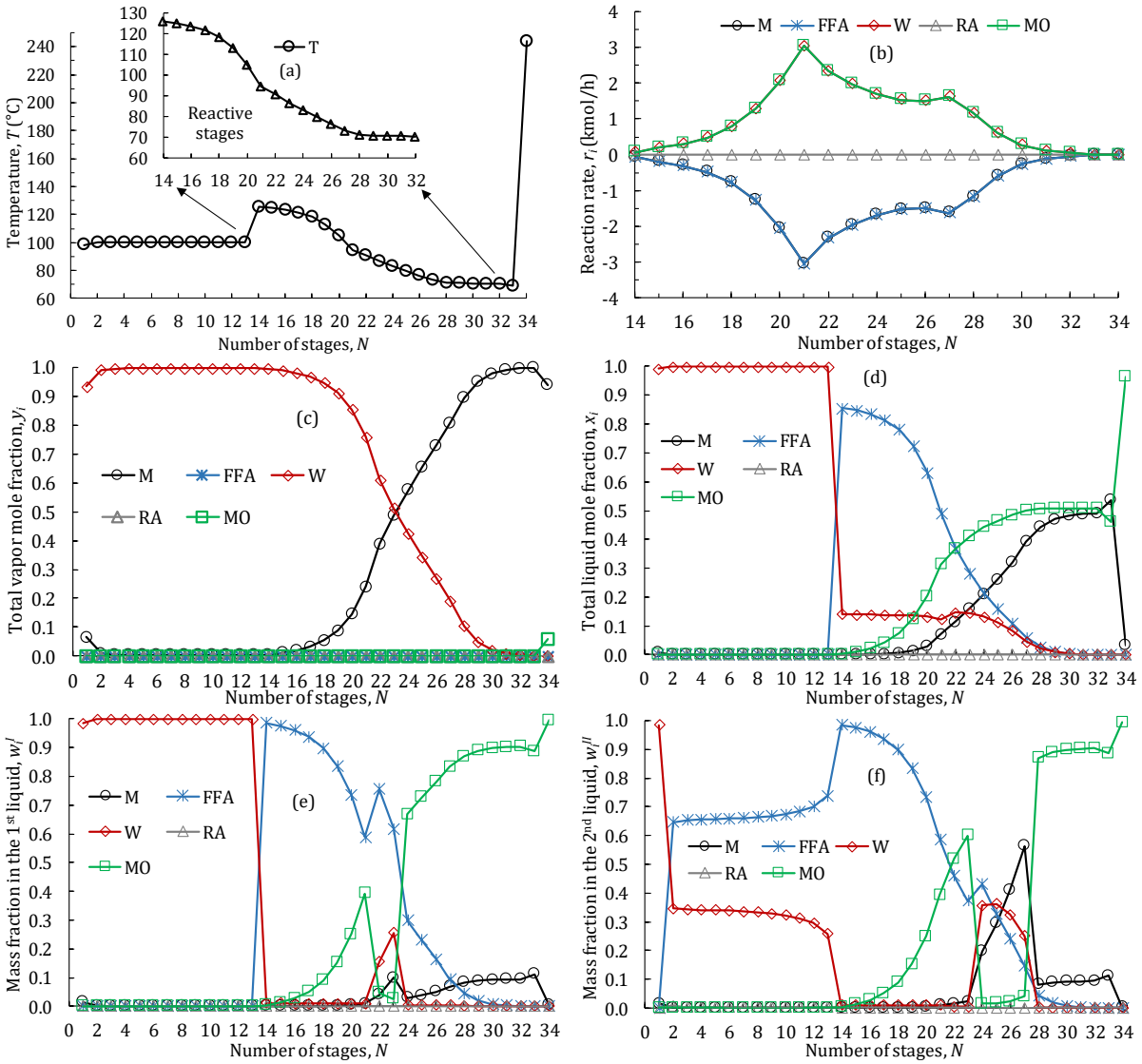

Figure 6.7 – Profiles results from CDC T-204 of process C8 from USA CTO

As a consequence, Process CU was optimized using T_{E-203} = 220 ºC, RR = 1.68, H_L = 233.5 kg/stage, N_R = 12, N_{RX} = 18 and N_s = 2. Moreover, cost evaluation inside Aspen Plus was carried out with these values and confirmed that Process CU showed a slightly lower costs, BEP, energy usage and CO_2 emission than Process C8 as well as slightly higher A_{NNP}, income (or PS) and ROI as shown in Figure 6.6. It is worth to mention, for instance, that an A_{NNP} for LRP-HPP case of 33.16 $MM for process CU compared to 33.02 $MM for process C8

represents an additional A_{NNP} of 140,000 $/year. Furthermore, for processes C8 and CU were adopted a H_L = 350 kg/stage and 233.5 kg/stage for a supposed catalyst lifetime of four weeks. As a result, if the real catalyst lifetime is less than it, higher operational cost is expected for process C8.

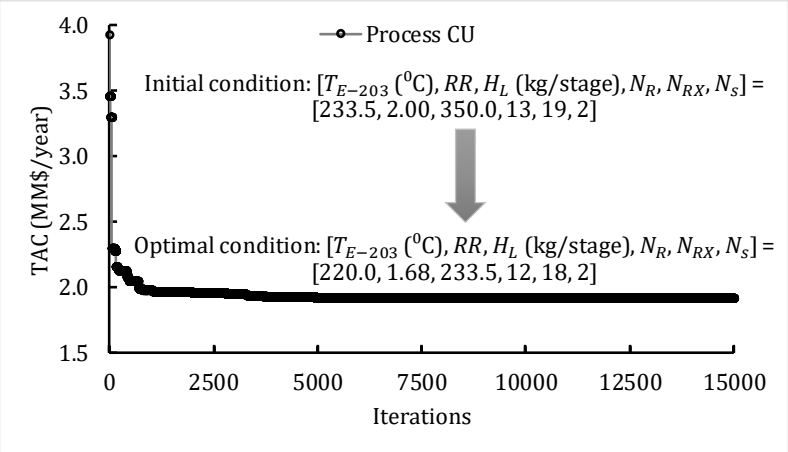

Figure 6.8 – Evolution of TAC cost during the stochastic optimization of Processes A1 and A2
Source: Adapted from Albuquerque et al. (2019b)

Process CU was also evaluated by costs of separated equipment as shown Figure 6.6d. From these results tower T-202 showed the highest installed cost, while T-201 presented the highest utility and total annualized costs based on installed and utility costs (TAC_{I+U}). As a result, further optimization should be carried out for these two distillation columns. However, additional optimization was not performed, since simulations of CTO purification were embedded with experimental results from pilot plant investigated by Rütti (1986).

6.3.2.3 Flexibility study

From optimized design of process CU based on USA CTO, processes CS and CC were designed adopting different CTO composition presented in Table 6.1 for Scandinavian and Canadian CTO. Basically, just few input variables as B/F at T-201 and D/F and S_1/F at T-301 were changed in order to obtain a flexible design valid for a wider CTO composition range. As a result, main operating conditions, equipment sizes and costs for processes CU, CS and CC are shown in Table 6.8 and Table 6.9, where PS and BEP were calculated considering an average price from chemicals presented in Table 6.2. Consequently, results from column Final

can be used as preliminary equipment sizes and costs for a construction of a biodiesel industry with CTO capacity of 200 kton/year considering the CTO composition range studied.

Table 6.8 – Main operating conditions, equipment sizes and costs for CTO purification unit from processes CU, CS and CC

block	description	Process CU	Process CS	Process CC	Final
V-201	P (mbar)[a]	20.0	20.0	20.0	20.0
	T (K)[b]	357.5	357.4	357.3	357.5
	$D \times L$ (m)[c]	1.37 × 3.96	1.37 × 3.96	1.37 × 3.96	1.37 × 3.96
	cost ($MM)[d]	0.201	0.201	0.201	0.201
T-201	RR[e]	1	1	1	1
	B/F[f]	0.06	0.112	0.126	0.06-0.126
	P (mbar)[a]	2.0/9.7	2/9.5	2/9.4	2.0/9.7
	T (K)[b]	467.8/535.6	467.2/549.4	466.2/552.9	466.2/552.9
	Q (MW)[g]	0/6.82	0/6.35	0/6.2	0/6.82
	N/FS[h]	9/9	9/9	9/9	9/9
	$D \times L$ (m)[c]	5.49 × 7.47	5.18 × 7.47	5.18 × 7.47	5.49 × 7.47
	cost ($MM)[d]	2.891	2.394	2.415	2.891
T-202	RR[e]	1.5	1.5	1.5	1.5
	D/F[f]	0.392	0.392	0.392	0.392
	P (mbar)[a]	8/19.6	8/19.1	8/19.2	8/19.6
	T (K)[b]	313.6/509.1	311.9/507.5	311.6/507.3	311.6/509.1
	Q (MW)[g]	-3.13/4.66	-2.81/4.12	-2.66/3.93	-3.13/4.66
	N/FS[h]	23/6	23/6	23/6	23/6
	$D \times L$ (m)[c]	4.88 × 12.8	4.72 × 12.8	4.57 × 12.8	4.88 × 12.8
	cost ($MM)[d]	3.284	3.032	2.798	3.284
T-203	RR[e]	8.5	8.5	8.5	8.5
	D/F[f]	0.225	0.198	0.166	0.166-0.225
	S_1/F[i]	0.525	0.500	0.493	0.493-0.525
	S_2/F [i]	0.128	0.128	0.160	0.128-0.160
	P (mbar)[a]	4/22.5	4/22.9	4/22.9	4/22.9
	T (K)[b]	467.8/534.6	467.5/535.4	467.4/535.4	467.4/535.4
	Q (MW)[g]	-1.21/1.1	-1.5/1.4	-1.49/1.4	-1.5/1.4
	$N/FS/S_1S/S_2S$ [h]	51/45/11/31	51/45/11/31	51/45/11/31	51/45/11/31
	$D \times L$ (m)[c]	2.9 × 23.93	3.35 × 23.93	3.35 × 23.93	3.35 × 23.93
	cost ($MM)[d]	2.332	2.780	2.721	2.780

[a]P is pressure; [b]T is temperature; [c]$D \times L$ are diameter and length; [d]$MM means million dollars; [e]RR is reflux mole ratio; [f]B/F and D/F are bottom and distillate to feed mole ratio; [g]Q means condenser duty/reboiler duty; [h]$N/FS/S_1S/S_2S$ means number of stages, feed stage, first side stream stage and second side stream stage; [i]S_1/F and S_2/F means first side stream and second side stream to feed mole ratio respectively.

Results for these processes related to energy usage, costs and CO_2 emissions are also shown in Figure 6.6a–c, where all these indicators decrease following the order: process CU > process CS > process CC. According to Figure 6.6e–f, A_{NNP} and ROI for LRP-HPP case showed the same pattern despite to be different from the other cases, where until same negative

A_{NNP} values were obtained as a result of operation costs to be higher than income when, for instance, HRP-LLP case was considered. Related to BEP, process CS showed the lowest value for cases including LPP, since Scandinavian CTO combines the highest and lowest concentration of FFA and RA, respectively. On the other hand, process CU for HRP-HPP case showed the lowest BEP since the higher concentration of RA contributed to increase income.

Table 6.9 – Main operating conditions, equipment sizes and costs for esterification unit from processes CU, CS and CC

block	description	Process CU	Process CS	Process CC	Final
T-204	RR[a]	1.68	1.68	1.68	1.68
	B/F[b]	0.507	0.507	0.507	0.507
	P (bar)[c]	1.01/1.03	1.01/1.03	1.01/1.03	1.01/1.03
	T (K)[d]	371.5/516.8	371.5/516.8	371.7/515.5	371.5/516.8
	Q (MW)[e]	-0.65/1.09	-0.65/1.09	-0.51/0.85	-0.51/1.09
	$N/FS_{TOFA}/FS_{\mathrm{MeOH}}$[f]	32/13/31	32/13/31	32/13/31	32/13/31
	$N_{RX}/RX_iS\text{-}RX_fS$[g]	18/13-30	18/13-30	18/13-30	18/13-30
	$D \times L$ (m)[h]	0.76 × 19.35	0.76 × 19.35	0.61 × 19.35	0.76 × 19.35
	cost ($MM)[i]	0.82	0.82	0.733	0.82
V-202	P (bar)[c]	0.58	0.58	0.58	0.58
	T (K)[d]	516.9	516.9	515.7	516.9
	$D \times L$ (m)[e]	1.07 × 3.66	1.07 × 3.66	1.07 × 3.66	1.07 × 3.66
	cost ($MM)[i]	0.194	0.194	0.194	0.194
Pumps cost ($MM)[i]		0.261	0.257	0.256	0.261
Heat exchangers cost ($MM)[i]		0.547	0.534	0.531	0.547
Total installed cost ($MM)[i]		10.53	10.212	9.849	10.978
Total capital cost ($MM)[i]		27.22	26.56	26.15	28.38
Raw materials cost ($MM/year)[i]		142.86	142.86	142.35	
Utility cost ($MM/year)[i]		5.88	6.00	5.74	
Operating cost ($MM/year)[i]		162.64	162.77	161.92	
Product Sales, PS ($MM/year)[i]		163.02	164.32	155.00	
TAC ($MM/year)[i]		171.72	171.62	170.64	
BEP ($/ton)		846.10	824.90	1012.70	

[a]RR is reflux mole ratio; [b]B/F and D/F are bottom and distillate to feed mole ratio; [c]P is pressure; [d]T is temperature; [e]Q means condenser duty/reboiler duty; [h]$N/FS_{TOFA}/FS_{MeOH}$ means number of stages and feed stages of TOFA and methanol; $N_{RX}/RX_iS\text{-}RX_fS$ means number of reactive stages, initial and final reactive stage; [h]$D \times L$ are diameter and length; [i]$MM means million dollars.

6.4 CONCLUSIONS

A new biodiesel production process from USA CTO using SAC by CDC was investigated. As a consequence, a conventional and an alternative CTO purification process based on four and three distillation columns were studied, designed and compared related to techno-economic feasibility. Both processes had some design specification optimized by sensitivity analysis and cost estimated using spreadsheets. Process B from alternative route using three distillation columns was found to be more techno-economic feasible and environment friendly to produce biodiesel achieving all requirements from ANP standard. Esterification reaction was carried out following this process B by CDC and CDWC in presence of Relite CFS. Process C based on CDC was shown to be the unique technical feasible, so that was designed and optimized using a stochastic procedure. TAC from Process C was minimized and an optimum design was found for T_{E-203} = 220 ºC, RR = 1.68, H_L = 233.5 kg/stage, N_r = 12, N_{RX} = 18 and N_s = 2. Finally, a flexibility study was developed including Canadian and Scandinavian CTO, so that a final design was proposed for biodiesel production from CTO. Moreover, the lowest BEP (0.75 $/kg) was obtained for LRP-LPP case from Scandinavian CTO (Process CS), which was related to the highest FFA and lowest RA contents.

ACKNOWLEDGMENTS

The authors acknowledge FACEPE/NUQAAPE, INCTAA, CNPq and FINEP for financial support including Aspen license. A. A. A. is also grateful to Capes for a Ph.D. scholarship.

NOMENCLATURE

A_{NNP}	net annual profit after taxes ($MM/year)
B/F	bottom to feed ratio (mole/mole)

BEP	break-even price ($/kg or $/ton)
C_{inst}	installed cost ($MM)
C_{oper}	operation cost ($MM/year)
C_{TC}	total capital cost ($MM/year)
C_{util}	utility cost ($MM/year)
$D \times L$	diameter × Length (m × m)
D/F	distillate to feed ratio (mole/mole)
FS	feed stage
FS_{MeOH}	methanol feed stage
FS_{TOFA}	tall oil fatty acid feed stage
H_L	liquid holdup or mass of catalyst per stage (kg/stage)
MR	molar ratio methanol to FFA (or oil)
N	number of stages
N_R	number of rectification stages
N_{RX}	number of reactive stages
N_S	number of stripping stages
P	pressure (mbar or bar)
P_{cd}	condenser pressure
PS	product sales or income ($MM/year)
P_{V-101}	pressure on vessel PV-101 (mbar)
Q	heat duty (MW)
Q_{reb}	reboiler duty (MW)
ROI	return of Investment (%)
RR	reflux ratio (mole/mole)
RX_fS	final reactive stage
RX_iS	initial reactive stage
S_1/F	sidestream feed ratio from first side stream stage (mole/mole)
S_2/F	sidestream feed ratio from second side stream stage (mole/mole)
SS	sidestream stage
T	temperature (K)
TAC	total annualized cost ($MM/year)
TAC_{I+U}	total annualized cost from installed cost plus utility cost ($MM/year)
T_{E-101}	temperature on heater E-101 (ºC)
T_{E-203}	temperature on heater E-203 (ºC)

T_{reb}	reboiler temperature (ºC or K)
w_{Neo}^{112}	neobietic acid mass fraction on stream 112
w_{water}^{216}	water mass fraction on stream 216
w_{water}^{218}	water mass fraction on stream 218

Abbreviations

$MM	million dollars
AN	acid number
ANP	National Agency of Petroleum, Natural Gas and Biofuels
CDC	catalytic distillation column
CDWC	catalytic divided-wall column
CSTR	continuous stirred tank reactor
CTO	crude tall oil
DTO	distilled tall oil
EPA	United States Environment Protection Agency
FAME	fatty acid methyl esters
FFA	free fatty acids
GHC	greenhouse gas emissions
HHHP steam	higher than HHP steam (99 bar)
HHP steam	higher than HP steam (61 bar)
HP steam	high pressure steam (42 bar)
HPP	highest Product Price
HRP	highest Raw material Price
LP steam	low pressure steam (6 bar)
LPP	lowest Product Price
LRP	lowest Raw material Price
M	methanol
MO	methyl oleate
MP steam	moderate pressure steam (11 bar)
MR	molar ratio
NRTL	Non-Random Two Liquid
OA	oleic acid
PCC	Pearson correlation coefficient

Process A	CTO purification process using four distillation columns
Process AB	base case from Process A
Process AO	process A optimized
Process B	CTO purification process using three distillation columns
Process B8	process B optimized with P_{cd} = 8 mbar for tower T-202
Process BB	base case from Process B
Process BO	process B optimized with P_{cd} = 4 mbar for tower T-202
Process C	CTO purification by Process B plus an esterification unit using a CDC column
Process C8	process B8 including a esterification unit using a CDC column
Process CC	process C8 with CDC globally optimized using Canadian CTO
Process CS	process C8 with CDC globally optimized using Scadinavian CTO
Process CU	process C8 with CDC globally optimized using USA CTO
RA	resin acids
SAC	solid acid-catalyzed
SS	stainless steel
TAG	triacylgycerol
TOFA	tall oil fatty acids
TOP	tall oil pitch
TOR	tall oil rosin
UN	United Nations
UNIFAC	Universal Functional Group Activity Coefficient
USA	United States of America
VBA	Visual Basic for Applications
VLLE	vapor-liquid-liquid equilibrium
W	water

Greek Symbols

ΔP	pressure drop (mbar)
η_{DTO}	yield of distilled tall oil (%)

REFERENCES

ADEWALE, P. O.; CHRISTOPHER, L. P. Thermal and Rheological Properties of Crude Tall Oil for Use in Biodiesel Production. **Processes**, v. 5, n. 4, p. 59, 2017.

ALBUQUERQUE, A. A.; DANIELSKI, L.; STRAGEVITCH, L. Techno-Economic Assessment of an Alternative Process for Biodiesel Production from Feedstock Containing High Levels of Free Fatty Acids. **Energy & Fuels**, v. 30, n. 11, p. 9409−9418, 2016.

ALBUQUERQUE, A. A.; NG, F. T. T.; DANIELSKI, L.; STRAGEVITCH, L. Phase equilibrium modeling in biodiesel reaction systems (submitted). **Fluid phase equilibria**, 2019a.

_____. Reactive separation processes applied to biodiesel production: Design, optimization and techno-economic assessment of solid acid-catalyzed route from residual oil and fats (submitted). **Applied Energy**, 2019b.

ALIBABA. **Tall Oil**. 2018. Available at: <https://www.alibaba.com/showroom/chemicals-price-list.html>. Accessed on: 2018/06/17.

ALTIPARMAK, D.; KESKIN, A.; KOCA, A.; GÜRÜ, M. Alternative fuel properties of tall oil fatty acid methyl ester–diesel fuel blends. **Bioresource Technol.**, v. 98, n. 2, p. 241−246, 2007.

ARO, T.; FATEHI, P. Tall oil production from black liquor: Challenges and opportunities. **Separation and Purification Technology**, v. 175, p. 469−480, 2017.

ATADASHI, I. M.; AROUA, M. K.; ABDUL AZIZ, A. R.; SULAIMAN, N. M. N. The effects of catalysts in biodiesel production: A review. **Journal of Industrial and Engineering Chemistry**, v. 19, n. 1, p. 14−26, 2013.

AVHAD, M. R.; MARCHETTI, J. M. A review on recent advancement in catalytic materials for biodiesel production. **Renew. Sust. Energ. Rev.**, v. 50, p. 696−718, 2015.

BABCOCK, R. E.; CLAUSEN, E. C.; POPP, M.; SCHULTE, W. B. **Yield Characteristics of Biodiesel Produced from Chicken Fat-Tall Oil Blended Feedstocks**. Washington, DC, United States, p.1−47. 2008

BOKIS, C. P.; CHEN, C.-C.; ORBEY, H. A segment contribution method for the vapor pressure of tall-oil chemicals. **Fluid Phase Equilibria**, v. 155, n. 2, p. 193−203, 1999.

CARDOSO, A. L.; NEVES, S. C. G.; SILVA, M. J. Esterification of Oleic Acid for Biodiesel Production Catalyzed by SnCl2: A Kinetic Investigation. **Energies**, v. 1, n. 2, p. 79, 2008.

CORDERO-RAVELO, V.; SCHALLENBERG-RODRIGUEZ, J. Biodiesel production as a solution to waste cooking oil (WCO) disposal. Will any type of WCO do for a transesterification process? A quality assessment. **Journal of Environmental Management**, v. 228, p. 117−129, 2018.

COVERT, T.; GREENSTONE, M.; KNITTEL, C. R. Will We Ever Stop Using Fossil Fuels? **Journal of Economic Perspectives**, v. 30, n. 1, p. 117−138, 2016.

DEMIRBAS, A. Methylation of wood fatty and resin acids for production of biodiesel. **Fuel**, v. 90, n. 6, p. 2273−2279, 2011.

DRBAL, L. F.; BOSTON, P. G.; WESTRA, K. L. **Power plant engineering**. ed. New York: Springer 1996. 858p.

FARAG, H. A.; EL-MAGHRABY, A.; TAHA, N. A. Optimization of factors affecting esterification of mixed oil with high percentage of free fatty acid. **Fuel Processing Technology**, v. 92, n. 3, p. 507−510, 2011.

GAURAV, A.; NG, F. T. T.; REMPEL, G. L. A new green process for biodiesel production from waste oils via catalytic distillation using a solid acid catalyst – Modeling, economic and environmental analysis. **Green Energy & Environment**, v. 1, n. 1, p. 62−74, 2016.

GNANAPRAKASAM, A.; SIVAKUMAR, V. M.; SURENDHAR, A.; THIRUMARIMURUGAN, M.; KANNADASAN, T. Recent Strategy of Biodiesel Production from Waste Cooking Oil and Process Influencing Parameters: A Review. **Journal of Energy**, v. 2013, p. 10, 2013.

HOLMBOM, B.; ERÄ, V. Composition of tall oil pitch. **Journal of the American Oil Chemists' Society**, v. 55, n. 3, p. 342−344, 1978.

JACOBSON, K.; GOPINATH, R.; MEHER, L. C.; DALAI, A. K. Solid acid catalyzed biodiesel production from waste cooking oil. **Applied Catalysis B: Environmental**, v. 85, n. 1, p. 86−91, 2008.

KESKIN, A.; GÜRÜ, M.; ALTIPARMAK, D. Biodiesel production from tall oil with synthesized Mn and Ni based additives: Effects of the additives on fuel consumption and emissions. **Fuel**, v. 86, n. 7, p. 1139−1143, 2007.

KESKIN, A.; YAŞAR, A.; GÜRÜ, M.; ALTIPARMAK, D. Usage of methyl ester of tall oil fatty acids and resinic acids as alternative diesel fuel. **Energy Conversion and Management**, v. 51, n. 12, p. 2863−2868, 2010.

KIRSCHNER, M. **Chemical Profile: Tall Oil**. ICIS, 2005. Available at: <https://www.icis.com/explore/resources/news/2005/12/22/2010699/chemical-profile-tall-oil/>. Accessed on: 2018/06/10.

KISS, A. A. **Advanced Distillation Technologies**. 1. ed. Chichester, West Sussex, United Kingdom: John Wiley & Sons, Ltd, 2013. 414p.

KISS, A. A.; SEGOVIA-HERNÁNDEZ, J. G.; BILDEA, C. S.; MIRANDA-GALINDO, E. Y.; HERNÁNDEZ, S. Reactive DWC leading the way to FAME and fortune. **Fuel**, v. 95, p. 352−359, 2012.

KRALOVA, I.; SJÖBLOM, J. Biofuels–Renewable Energy Sources: A Review. **Journal of Dispersion Science and Technology**, v. 31, n. 3, p. 409−425, 2010.

LIN, R.; ZHU, Y.; TAVLARIDES, L. L. Mechanism and kinetics of thermal decomposition of biodiesel fuel. **Fuel**, v. 106, p. 593−604, 2013.

LUYBEN, W. L. **Distillation design and control using AspenTM simulation**. 2. ed. Hoboken, New Jersey: Wiley, 2013. 512p.

MANSIR, N.; TAUFIQ-YAP, Y. H.; RASHID, U.; LOKMAN, I. M. Investigation of heterogeneous solid acid catalyst performance on low grade feedstocks for biodiesel production: A review. **Energy Conversion and Management**, v. 141, p. 171−182, 2017.

MECKLING, J.; NAHM, J. The politics of technology bans: Industrial policy competition and green goals for the auto industry. **Energy Policy**, v. 126, p. 470−479, 2019.

NATIONAL AGENCY OF PETROLEUM, NATURAL GAS AND BIOFUELS (ANP). **ANP Resolution No. 45, of 25.8.2014 - DOU 26.8.2014**. 2014.

NIEMELÄINEN, M. **Tall oil depitching in kraft pulp mill**. MSc Dissertation. Espoo, Finland: School of Chemical Engineering, Aalto University, 2018. 74p.

NOGUEIRA, J. M. F. Refining and Separation of Crude Tall-Oil Components. **Separation Science and Technology**, v. 31, n. 17, p. 2307−2316, 1996.

NORLIN, L. H. **Tall Oil**. In: ULLMANN, F. Ullmann's Encyclopedia of Industrial Chemistry. 7 ed. Berlin: Wiley-VCH Verlag GmbH & Co. KGaA, 2012. p. 583−596. v. 35.

PARKASH, S. **Refining Processes Handbook**. ed. Burlington: Elsevier, 2003. 688p.

PÉREZ-CISNEROS, E. S.; MENA-ESPINO, X.; RODRÍGUEZ-LÓPEZ, V.; SALES-CRUZ, M.; VIVEROS-GARCÍA, T.; LOBO-OEHMICHEN, R. An integrated reactive distillation process for biodiesel production. **Computers & Chemical Engineering**, v. 91, p. 233−246, 2016.

RESINDION. **Water treatment**. Ion exchange resins for water treatment, Binasco, Milan, Italy, 2017. Available at: <http://www.rfpconsulting.it/resins/water-treatment.html>. Accessed on: June 20, 2018.

ROHAN. **Pine-Derived Chemicals Market worth 5.27 Billion USD by 2021**. MarketsandMarkets, Magarpatta 2016. Available at: <https://www.marketsandmarkets.com/PressReleases/pine-derived-chemicals.asp>. Accessed on: 2019/01/22.

ROUHANY, M.; MONTGOMERY, H. **Global Biodiesel Production: The State of the Art and Impact on Climate Change**. In: TABATABAEI, M. and AGHBASHLO, M. Biodiesel: From Production to Combustion. 1 ed. Cham, Switzerland: Springer International Publishing, 2019. p. 1−14.

RÜTTI, V. A. Fatty acid separation with Sulzer-Mellapak® columns: Experiments, Design and Industrial Experience (in German: Fettsäuretrennung mit Sulzer-Mellapak®-Kolonnen Versuche, Auslegung und industrielle Erfahrung). **Fats, Soaps, Paints (Fette, Seifen, Anstrichmittel)**, v. 88, n. S1, p. 515−519, 1986.

SEGOVIA-HERNÁNDEZ, J. G.; GÓMEZ-CASTRO, F. I. **Stochastic Process Optimization using Aspen Plus®**. 1. ed. Boca Raton: CRC Press Taylor & Francis Group, 2017. 242p.

SOUZA, S. P.; SEABRA, J. E. A.; NOGUEIRA, L. A. H. Feedstocks for biodiesel production: Brazilian and global perspectives. **Biofuels**, v. 9, n. 4, p. 455−478, 2018.

STEINIGEWEG, S.; GMEHLING, J. Esterification of a Fatty Acid by Reactive Distillation. **Industrial & Engineering Chemistry Research**, v. 42, n. 15, p. 3612−3619, 2003.

TESSER, R.; CASALE, L.; VERDE, D.; DI SERIO, M.; SANTACESARIA, E. Kinetics and modeling of fatty acids esterification on acid exchange resins. **Chemical Engineering Journal**, v. 157, n. 2, p. 539−550, 2010.

TESSER, R.; DI SERIO, M.; GUIDA, M.; NASTASI, M.; SANTACESARIA, E. Kinetics of Oleic Acid Esterification with Methanol in the Presence of Triglycerides. **Industrial & Engineering Chemistry Research**, v. 44, n. 21, p. 7978−7982, 2005.

UNITED NATIONS (UN). Paris Agreement. In: Conference of the Parties 21 (COP 21), 21, 2015, Paris. **Proceedings...** Paris: United Nations, 2015. p. 27.

UNITED STATES ENVIRONMENTAL PROTECTION AGENCY (EPA). **Mandatory Reporting of Greenhouse Gases; Final Rule**. Environmental Protection Agency, Washington, 2009. Available at: <https://www.epa.gov/regulations-emissions-vehicles-and-engines/final-rule-mandatory-reporting-greenhouse-gases>. Accessed on: 2018/07/21.

VAN DE GRAAF, T. Is OPEC dead? Oil exporters, the Paris agreement and the transition to a post-carbon world. **Energy Research & Social Science**, v. 23, p. 182−188, 2017.

VAN DER PLOEG, F. Fossil fuel producers under threat. **Oxford Review of Economic Policy**, v. 32, n. 2, p. 206−222, 2016.

VYAS, A. P.; VERMA, J. L.; SUBRAHMANYAM, N. A review on FAME production processes. **Fuel**, v. 89, n. 1, p. 1−9, 2010.

WALAS, S. M. **Chemical Process Equipment: Selection and Design**. 1. ed. Boston: Butterworth-Heinemann, 1990. 782p.

WANSBROUGH, H.; ROUGH, M.; COONEY, S. **Tall oil production and processing**. In: GRANT, R. and GRANT, C. Grant & Hackh's chemical dictionary. 5 ed. New York: McGraw-Hill Book Company, 1987. p. 641.

ZERVOS, A.; ADIB, R. **Renewables 2018 Global Status Report**. Renewable Energy Policy Network for the 21st Century, Paris, 2018. Available at: <http://www.ren21.net/wp-content/uploads/2018/06/17-8652_GSR2018_FullReport_web_-1.pdf>. Accessed on: 2019/01/22.

ZHANG, Y.; DUBÉ, M. A.; MCLEAN, D. D.; KATES, M. Biodiesel production from waste cooking oil: 2. Economic assessment and sensitivity analysis. **Bioresource Technology**, v. 90, n. 3, p. 229−240, 2003.

7 CONCLUSIONS

Innovative reactive separation processes for biodiesel production from residual oil and fats (ROFs) and crude tall oil (CTO) were investigated, such as: reactive distillation column (RDC), catalytic distillation column (CDC), catalytic absorption column (CAC) and catalytic divided-wall column (CDWC).

Firstly, FFA separation from ROFs by liquid-liquid extraction (LLEx) using methanol was optimized in Chapter 3. RSM and a CCD for two cases involving yellow and brown greases were adopted. Furthermore, the base case and alternative process using a set of reactor/distillation column and a RDC, respectively, were also designed and compared related to techno-economic feasibility. Both processes showed to be technical feasible and presented similar economic assessment based on economic indicators, so that the base case process could be chosen since presented lower net Carbon fee/tax. As result, not always reactive separation processes can be more economical, requiring a further investigation by preliminary techno-economic assessment.

Secondly, a lack of a rigorous phase equilibrium modeling to represent the vapor-liquid-liquid equilibrium in RDC and CDC for biodiesel production from ROF was identified in Chapter 4. As a consequence, thermophysical properties for acylglycerols were evaluated and estimated by group contribution (GC) and constituent fragment (CF) approaches. Calculated results agreed to experimental ones from triacylglycerols (TAGs), edible and non-edible oils. Furthermore, a VLE, LLE and VLLE databanks including 5980, 2411 and 41 data, respectively, were built and used to develop a phase equilibrium modeling using NRTL model. Experimental data were successfully correlated by NRTL model based on low deviations and agreement to calculated phase diagrams and tie lines.

Three set of interaction parameters were obtained for NRTL model, where NRTL1 showed to be the first choice for SAC processes by CDC, since reported experimental results for this process was validated using these parameters and suitable kinetic models. On the other hand, simulated results of HAC process by NRTL2 showed closer results to experimental ones, suggesting to be the most suitable model for alkali-catalyzed process. Finally, NRTL3 was obtained regressing all binary interaction parameters involving experimental data and showed to be also successful to correlate experimental results from SAC process despite of the difficulty

to represent biodiesel yield. As a consequence, NRTL1 can be used in Aspen simulations of SAC process, while NRTL3 can be used in other commercial simulators.

Thirdly, reactive separation processes for biodiesel production from ROFs based on SAC process were investigated comparing two configurations for simultaneous esterification and transesterification reactions based on CDC and CAC using HWSi/Al2O3 as catalyst. These were also designed, local optimized and compared related to techno-economic feasibility to SAC hydro-esterification process based on hydrolysis reaction in a PFR reactor and esterification reaction in a CDC column. Processes based on CDC and CAC showed to be more economical than hydro-esterification route and a heat integration was also proposed for these two processes.

CDC process also showed to be most economical before the heat integration, while CAC was the best process after it. Furthermore, after the heat integration both processes presented similar results for CO_2 emissions and lower waste stream cost for CAC process. However, CDC process was chosen to be optimized since flowsheet was simpler before to be heat integrated and presented lower CO_2 emissions, energy usage and BEP. A stochastic optimization based on connection between Aspen Plus, VBA from Microsoft Excel and Matlab resulted in a global minimum solution (or very close to it) for TAC objective function. Optimal condition was obtained for a total of ten input variables from three distillation columns including CDC: number of stages (N), reflux ratio (RR), distillate to feed ratio (D/F) and molar ratio (MR) of methanol to ROF at the feed stream.

CDC process was also flexibilized through addition of other two designs involving FFA content between 5 to 25%, so that a final design for common range of ROFs including yellow and brown greases was obtained. A BEP between 0.74–0.75 \$/kg for HRP-LPP case from yellow grease was found and showed to be close to reported one of 0.67 \$/kg, since higher cost was obtained due to updated parameters added to the economic model from Aspen Plus.

A biodiesel production plant from SAC process was also developed from CTO in Chapter 6, where two different routes including a base case and an alternative process with four and three distillation columns, respectively, were compared related to techno-economic assessment of CTO purification. The alternative process showed to be more techno-economic feasible for biodiesel production, since produced higher purity of FFA in TOFA stream and presented suitable values of energy usage, economic and environment indicators. Esterification reaction was carried out in a CDC using Relite CFS as catalyst for USA CTO. This process was

also compared to CDWC process removing water as a side stream. However, this latter did not show to be technical feasible since temperature in some reactive stages were above 300 ºC, so that can decompose biodiesel and destabilize the catalyst.

Biodiesel production process from CTO by CDC was also optimized based on the same procedure of stochastic optimization to minimize TAC. Optimal operation was identified varying feed temperature of TOFA, RR, liquid holdup (H_L) in reactive stages (amount of catalyst) and number of reactive, rectification and stripping stages. Finally, a flexibility study was carried out varying CTO composition based on Scandinavian and Canadian CTO. The lowest BEP was identified when FFA and resin acids (RA) contents were the highest and lowest, respectively.

7.1 FUTURE WORKS

From this work is expected some future works based on identification of limitations, opportunities and lack of experimental data, such as:

- ✓ Measurement of vapor-liquid-liquid equilibrium (VLLE) data for biodiesel reaction systems including transesterification and esterification reactions;
- ✓ Experimental study of SAC process from ROF and TOFA by CDC using HWSi/Al2O3 and Relite CFS as catalysts, respectively;
- ✓ Phase equilibrium data for biodiesel reaction systems from ethyl route;
- ✓ Optimization studies based on other genetic algorithms for multi-objective functions minimization including the Pareto front methodology.

REFERENCES

ABRAMS, D. S.; PRAUSNITZ, J. M. Statistical thermodynamics of liquid mixtures: a new expression for the excess Gibbs energy of partly or completely miscible systems. **AIChE Journal**, v. 21, n. 1, p. 116–128, 1975.

ABREU, F. R.; ALVES, M. B.; MACÊDO, C. C. S.; ZARA, L. F.; SUAREZ, P. A. Z. New multi-phase catalytic systems based on tin compounds active for vegetable oil transesterificaton reaction. **Journal of Molecular Catalysis A: chemical**, v. 227, n. 1–2, p. 263–267, 2005.

ADEWALE, P.; DUMONT, M.-J.; NGADI, M. Recent trends of biodiesel production from animal fat wastes and associated production techniques. **Renewable and Sustainable Energy Reviews**, v. 5, n. 4, p. 50, 2015.

ALBUQUERQUE, A. A.; DANIELSKI, L.; STRAGEVITCH, L. Techno-economic assessment of an alternative process for biodiesel production from feedstock containing high levels of free fatty acids. **Energy & Fuels**, v. 30, n. 11, p. 9409–9418, 2016.

ARANDA, D. A. G.; SANTOS, R. T. P.; TAPANES, N. C. O.; RAMOS, A. L. D.; ANTUNES, O. A. C. Acid-Catalyzed Homogeneous Esterification Reaction for Biodiesel Production from Palm Fatty Acids. **Catalysis Letters**, v. 122, n. 1, p. 20–25, 2008.

ARO, T.; FATEHI, P. Tall oil production from black liquor: Challenges and opportunities. **Separation and Purification Technology**, v. 175, p. 469–480, 2017.

ATADASHI, I. M.; AROUA, M. K.; ABDUL AZIZ, A. R.; SULAIMAN, N. M. N. The effects of water on biodiesel production and refining technologies: A review. **Renewable and Sustainable Energy Reviews**, v. 16, n. 5, p. 3456–3470, 2012.

AVHAD, M. R.; MARCHETTI, J. M. A review on recent advancement in catalytic materials for biodiesel production. **Renewable and Sustainable Energy Reviews**, v. 50, p. 696–718, 2015.

BABCOCK, R. E.; CLAUSEN, E. C.; POPP, M.; SCHULTE, W. B. **Yield Characteristics of Biodiesel Produced from Chicken Fat-Tall Oil Blended Feedstocks**. Washington, DC, United States, p.1–47. 2008

BANCHERO, M.; KUSUMANINGTYAS, R. D.; GOZZELINO, G. Reactive distillation in the intensification of oleic acid esterification with methanol – A simulation case-study. **Journal of Industrial and Engineering Chemistry**, v. 20, n. 6, p. 4242–4249, 2014.

BERRIOS, M.; SILES, J.; MARTÍN, M. A.; MARTÍN, A. A kinetic study of the esterification of free fatty acids (FFA) in sunflower oil. **Fuel**, v. 86, n. 15, p. 2383–2388, 2007.

BOON-ANUWAT, N.-N.; KIATKITTIPONG, W.; AIOUACHE, F.; ASSABUMRUNGRAT, S. Process design of continuous biodiesel production by reactive distillation: Comparison between homogeneous and heterogeneous catalysts. **Chemical Engineering and Processing: Process Intensification**, v. 92, p. 33–44, 2015.

BRAZIL. **Law N° 11097 from January 13, 2005**. Presidency of the republic, Brasília, Brazil, 2005.

_____. **Law N° 13263 from March 23, 2016**. Presidency of the republic, Brasília, Brazil, 2016.

_____. **Resolution N° 16 from October 29, 2018**. Presidency of the republic, Brasília, Brazil, 2018.

CAI, Z.-Z.; WANG, Y.; TENG, Y.-L.; CHONG, K.-M.; WANG, J.-W.; ZHANG, J.-W.; YANG, D.-P. A two-step biodiesel production process from waste cooking oil via recycling crude glycerol esterification catalyzed by alkali catalyst. **Fuel Processing Technology**, v. 137, p. 186–193, 2015.

CAMÚS, J. M. G.; LABORDA, J. Á. G. **Liquid biofuels: biodiesel and bioethanol (in Spanish)**. Technological Vigilance Report, Madrid, 2006. Available at: http://www.madrimasd.org/informacionidi/biblioteca/Publicacion/doc/VT/vt4_Biocarburantes_liquidos_biodiesel_y_bioetanol.pdf. Accessed on: 2017/09/05.

CANAKCI, M.; SANLI, H. Biodiesel production from various feedstocks and their effects on the fuel properties. **Journal of industrial microbiology & biotechnology**, v. 35, n. 5, p. 431–441, 2008.

CANAKCI, M.; VAN GERPEN, J. Biodiesel production via acid catalysis. **Transactions of the ASAE-American Society of Agricultural Engineers**, v. 42, n. 5, p. 1203–1210, 1999.

_____. Biodiesel production from oils and fats with high free fatty acids. **Transactions of the American Society of Agricultural and Biological Engineers (ASABE)** v. 44, n. 6, p. 1429–1436, 2001a.

CANAKCI, M.; VAN GERPEN, J. A Pilot Plant to Produce Biodiesel from High Free Fatty Acid Feedstocks. **2001 ASAE Annual Meeting**, v. 46, n. 4, p. 945–954, 2001b.

CARNITI, P.; CORI, L.; RAGAINI, V. A critical analysis of the hand and Othmer-Tobias correlations. **Fluid Phase Equilibria**, v. 2, n. 1, p. 39–47, 1978.

CERIANI, R.; GANI, R.; LIU, Y. Prediction of vapor pressure and heats of vaporization of edible oil/fat compounds by group contribution. **Fluid Phase Equilibria**, v. 337, p. 53–59, 2013.

CERÓN SÁNCHEZ, A. A. **Evaluación experimental de la producción de biodiesel por destilación reactiva**. Universidad Nacional de Colombia-Sede Manizales, 2010. 131p.

ÇETINKAYA, M.; KARAOSMANOĞLU, F. Optimization of Base-Catalyzed Transesterification Reaction of Used Cooking Oil. **Energy & Fuels**, v. 18, n. 6, p. 1888–1895, 2004.

CHAI, M.; TU, Q.; LU, M.; YANG, Y. J. Esterification pretreatment of free fatty acid in biodiesel production, from laboratory to industry. **Fuel Processing Technology**, v. 125, p. 106–113, 2014.

CORDEIRO, C. S.; SILVA, F.; WYPYCH, F.; RAMOS, L. P. Heterogeneous catalysts for production of fatty acid monoesters (biodiesel) (in Portuguese). **New Chemistry**, v. 34, n. 3, p. 477–486, 2011.

COSSIO-VARGAS, E.; HERNANDEZ, S.; SEGOVIA-HERNANDEZ, J. G.; CANO-RODRIGUEZ, M. I. Simulation study of the production of biodiesel using feedstock mixtures of fatty acids in complex reactive distillation columns. **Energy**, v. 36, n. 11, p. 6289–6297, 2011.

COSTA NETO, P. R.; ROSSI, L. F. S.; ZAGONEL, G. F.; RAMOS, L. P. The utilization of used frying oil for the production of biodiesel (in Portuguese). **New Chemistry (Química nova)**, v. 23, n. 4, p. 531–537, 2000.

DARNOKO, D.; CHERYAN, M. Kinetics of palm oil transesterification in a batch reactor. **Journal of the American Oil Chemists' Society**, v. 77, n. 12, p. 1263–1267, 2000.

DAWODU, F. A.; AYODELE, O.; XIN, J.; ZHANG, S.; YAN, D. Effective conversion of non-edible oil with high free fatty acid into biodiesel by sulphonated carbon catalyst. **Applied Energy**, v. 114, n. p. 819–826, 2014.

DEMIRBAS, A. Progress and recent trends in biodiesel fuels. **Energy Conversion and Management**, v. 50, n. 1, p. 14–34, 2009.

DIAZ-FELIX, W.; RILEY, M. R.; ZIMMT, W.; KAZZ, M. Pretreatment of yellow grease for efficient production of fatty acid methyl esters. **Biomass and Bioenergy**, v. 33, n. 4, p. 558–563, 2009.

DIMIAN, A. C.; BILDEA, C. S.; OMOTA, F.; KISS, A. A. Innovative process for fatty acid esters by dual reactive distillation. **Computers & Chemical Engineering**, v. 33, n. 3, p. 743–750, 2009.

FARAG, H. A.; EL-MAGHRABY, A.; TAHA, N. A. Optimization of factors affecting esterification of mixed oil with high percentage of free fatty acid. **Fuel Processing Technology**, v. 92, n. 3, p. 507–510, 2011.

FOGLER, H. S. **Elements of chemical reaction engineering**. 5. ed. United States: Prentice Hall, 2016. 957p.

FOLLEGATTI-ROMERO, L. A.; OLIVEIRA, M. B.; BATISTA, F. R. M.; BATISTA, E. A. C.; COUTINHO, J. A. P.; MEIRELLES, A. J. A. Liquid–liquid equilibria for ternary systems containing ethyl esters, ethanol and glycerol at 323.15 and 353.15K. **Fuel**, v. 94, p. 386–394, 2012.

FREEDMAN, B.; BUTTERFIELD, R. O.; PRYDE, E. H. Transesterification kinetics of soybean oil 1. **Journal of the American Oil Chemists' Society**, v. 63, n. 10, p. 1375–1380, 1986.

FREEDMAN, B.; PRYDE, E. H.; MOUNTS, T. L. Variables affecting the yields of fatty esters from transesterified vegetable oils. **Journal of the American Oil Chemists Society**, v. 61, n. 10, p. 1638–1643, 1984.

GARCIA, C. M.; TEIXEIRA, S.; MARCINIUK, L. L.; SCHUCHARDT, U. Transesterification of soybean oil catalyzed by sulfated zirconia. **Bioresour Technol**, v. 99, n. 14, p. 6608–13, 2008.

GAURAV, A.; NG, F. T.; REMPEL, G. L. A new green process for biodiesel production from waste oils via catalytic distillation using a solid acid catalyst–Modeling, economic and environmental analysis. **Green Energy & Environment**, v. 1, n. 1, p. 62–74, 2016.

GMEHLING, J.; WEIDLICH, U. Results of a modified UNIFAC method for alkane-alcohol systems. **Fluid phase equilibria**, v. 27, p. 171–180, 1986.

GNANAPRAKASAM, A.; SIVAKUMAR, V. M.; SURENDHAR, A.; THIRUMARIMURUGAN, M.; KANNADASAN, T. Recent strategy of biodiesel production from waste cooking oil and process influencing parameters: a review. **Journal of Energy**, v. 2013, p. 1–10, 2013.

GÓMEZ-CASTRO, F. I.; RICO-RAMÍREZ, V.; SEGOVIA-HERNÁNDEZ, J. G.; HERNÁNDEZ-CASTRO, S. Feasibility study of a thermally coupled reactive distillation process for biodiesel production. **Chemical Engineering and Processing: Process Intensification**, v. 49, n. 3, p. 262–269, 2010.

_____. Esterification of fatty acids in a thermally coupled reactive distillation column by the two-step supercritical methanol method. **Chemical Engineering Research and Design**, v. 89, n. 4, p. 480–490, 2011.

GUAN, G.; KUSAKABE, K.; SAKURAI, N.; MORIYAMA, K. Transesterification of vegetable oil to biodiesel fuel using acid catalysts in the presence of dimethyl ether. **Fuel**, v. 88, n. 1, p. 81–86, 2009.

HAND, D. B. Dineric distribution. **The Journal of Physical Chemistry**, v. 34, n. 9, p. 1961–2000, 1930.

HANSEN, H. K.; RASMUSSEN, P.; FREDENSLUND, A.; SCHILLER, M.; GMEHLING, J. Vapor-liquid equilibria by UNIFAC group contribution. 5. Revision and extension. **Industrial & Engineering Chemistry Research**, v. 30, n. 10, p. 2352–2355, 1991.

HASSAN, S. Z.; VINJAMUR, M. Parametric effects on kinetics of esterification for biodiesel production: A Taguchi approach. **Chemical Engineering Science**, v. 110, p. 94–104, 2014.

HE, B.; SINGH, A.; THOMPSON, J. A novel continuous-flow reactor using reactive distillation technique for biodiesel production. **Transactions of the American Society of Agricultural and Biological Engineers (ASABE)**, v. 49, n. 1, p. 107–112, 2006.

HENLEY, E. J.; SEADER, J. D. **Equilibrium-stage separation operations in chemical engineering**. 1. ed. New York: John Wiley & Sons, 1981. 768p.

HERINGTON, E. A thermodynamic test for the internal consistency of experimental data on volatility ratios. **Nature**, v. 160, n. 4070, p. 610-611, 1947.

JANSRI, S.; RATANAWILAI, S. B.; ALLEN, M. L.; PRATEEPCHAIKUL, G. Kinetics of methyl ester production from mixed crude palm oil by using acid-alkali catalyst. **Fuel Processing Technology**, v. 92, n. 8, p. 1543–1548, 2011.

KAUR, M.; ALI, A. Lithium ion impregnated calcium oxide as nano catalyst for the biodiesel production from karanja and jatropha oils. **Renewable Energy**, v. 36, n. 11, p. 2866–2871, 2011.

KAUR, N.; ALI, A. Lithium zirconate as solid catalyst for simultaneous esterification and transesterification of low quality triglycerides. **Applied Catalysis A: General**, v. 489, p. 193–202, 2015.

KISS, A. A. Novel process for biodiesel by reactive absorption. **Separation and Purification Technology**, v. 69, n. 3, p. 280–287, 2009.

_____. **Process Intensification Technologies for Biodiesel Production: Reactive Separation Processes**. 1. ed. Arnhem: Springer, 2014. 103p.

KISS, A. A.; SEGOVIA-HERNÁNDEZ, J. G.; BILDEA, C. S.; MIRANDA-GALINDO, E. Y.; HERNÁNDEZ, S. Reactive DWC leading the way to FAME and fortune. **Fuel**, v. 95, p. 352–359, 2012.

KONWAR, L. J.; WÄRNÅ, J.; MÄKI-ARVELA, P.; KUMAR, N.; MIKKOLA, J.-P. Reaction kinetics with catalyst deactivation in simultaneous esterification and transesterification of acid oils to biodiesel (FAME) over a mesoporous sulphonated carbon catalyst. **Fuel**, v. 166, p. 1–11, 2016.

KULKARNI, M. G.; DALAI, A. K. Waste cooking oil an economical source for biodiesel: a review. **Industrial & engineering chemistry research**, v. 45, n. 9, p. 2901–2913, 2006.

LAM, M. K.; LEE, K. T.; MOHAMED, A. R. Homogeneous, heterogeneous and enzymatic catalysis for transesterification of high free fatty acid oil (waste cooking oil) to biodiesel: A review. **Biotechnology Advances**, v. 28, n. 4, p. 500–518, 2010.

LEE, S.; POSARAC, D.; ELLIS, N. Process simulation and economic analysis of biodiesel production processes using fresh and waste vegetable oil and supercritical methanol. **Chemical Engineering Research and Design**, v. 89, n. 12, p. 2626–2642, 2011.

LI, Y.; ZHANG, X.-D.; SUN, L.; ZHANG, J.; XU, H.-P. Fatty acid methyl ester synthesis catalyzed by solid superacid catalyst /ZrO2–TiO2/La3+. **Applied Energy**, v. 87, n. 1, p. 156–159, 2010.

LIU, Y.; WANG, L. Biodiesel production from rapeseed deodorizer distillate in a packed column reactor. **Chemical Engineering and Processing: Process Intensification**, v. 48, n. 6, p. 1152–1156, 2009.

MA, F.; CLEMENTS, L. D.; HANNA, M. A. The Effects of Catalyst, Free Fatty Acids, and Water on Transecterification of Beef Tallow. **American Society ot Agricultural Engineers**, v. 41, n. 5, p. 1261–1264, 1998.

MA, F.; HANNA, M. A. Biodiesel production: a review. **Bioresource technology**, v. 70, n. 1, p. 1–15, 1999.

MACHADO, G. D.; ARANDA, D. A. G.; CASTIER, M.; CABRAL, V. F.; CARDOZO-FILHO, L. Computer Simulation of Fatty Acid Esterification in Reactive Distillation Columns. **Industrial & Engineering Chemistry Research**, v. 50, n. 17, p. 10176–10184, 2011.

MAGNUSSEN, T.; RASMUSSEN, P.; FREDENSLUND, A. UNIFAC parameter table for prediction of liquid-liquid equilibriums. **Industrial & Engineering Chemistry Process Design and Development**, v. 20, n. 2, p. 331–339, 1981.

MANSIR, N.; TAUFIQ-YAP, Y. H.; RASHID, U.; LOKMAN, I. M. Investigation of heterogeneous solid acid catalyst performance on low grade feedstocks for biodiesel production: A review. **Energy Conversion and Management**, v. 141, p. 171–182, 2017.

MARCHETTI, J. M. **Biodiesel Production Technologies**. 1. ed. New York: Nova Science Publishers, 2010. 166p.

MARDHIAH, H. H.; ONG, H. C.; MASJUKI, H.; LIM, S.; LEE, H. A review on latest developments and future prospects of heterogeneous catalyst in biodiesel production from non-edible oils. **Renewable and Sustainable Energy Reviews**, v. 67, p. 1225–1236, 2017.

MAZUBERT, A.; POUX, M.; AUBIN, J. Intensified processes for FAME production from waste cooking oil: a technological review. **Chemical engineering journal**, v. 233, p. 201–223, 2013.

MEHER, L.; SAGAR, D. V.; NAIK, S. Technical aspects of biodiesel production by transesterification—a review. **Renewable and sustainable energy reviews**, v. 10, n. 3, p. 248–268, 2006.

MOHITE, S.; KUMAR, S.; PAL, A.; MAJI, S. Biodiesel Production from High Free Fatty Acid Feed Stocks through Transesterification. In: International Conference of Advance Research and Innovation (ICARI-2015), 2015, New Delhi, India. **Proceedings...** New Delhi, India: ICARI, 2015. p. 113–115.

MUEANMAS, C.; PRASERTSIT, K.; TONGURAI, C. Transesterification of triolein with methanol in reactive distillation column: simulation studies. **International Journal of Chemical Reactor Engineering**, v. 8, n. 1, p., 2010.

NATIONAL AGENCY OF PETROLEUM, NATURAL GAS AND BIOFUELS (ANP). **Market Information: Montly biodiesel bulletin**. Brazilian National Agency of Petroleum, Natural Gas and Biofuels, Brasília, Brazil, 2019. Available at: <http://www.anp.gov.br/producao-de-biocombustiveis/biodiesel/informacoes-de-mercado>. Accessed on: 2019/01/27.

NOGUEIRA, J. M. F. Refining and Separation of Crude Tall-Oil Components. **Separation Science and Technology**, v. 31, n. 17, p. 2307–2316, 1996.

NORLIN, L. H. **Tall Oil**. In: ULLMANN, F. Ullmann's Encyclopedia of Industrial Chemistry. 7 ed. Berlin: Wiley-VCH Verlag GmbH & Co. KGaA, 2012. p. 583–596. v. 35.

NOSHADI, I.; AMIN, N. A. S.; PARNAS, R. S. Continuous production of biodiesel from waste cooking oil in a reactive distillation column catalyzed by solid heteropolyacid: Optimization using response surface methodology (RSM). **Fuel**, v. 94, p. 156–164, 2012.

NOUREDDINI, H.; ZHU, D. Kinetics of transesterification of soybean oil. **Journal of the American Oil Chemists' Society**, v. 74, n. 11, p. 1457–1463, 1997.

OMOTA, F.; DIMIAN, A. C.; BLIEK, A. Fatty acid esterification by reactive distillation. Part 1: equilibrium-based design. **Chemical Engineering Science**, v. 58, n. 14, p. 3159–3174, 2003a.

_____. Fatty acid esterification by reactive distillation: Part 2—kinetics-based design for sulphated zirconia catalysts. **Chemical Engineering Science**, v. 58, n. 14, p. 3175–3185, 2003b.

OTHMER, D.; TOBIAS, P. Liquid-liquid extraction data-the line correlation. **Industrial & Engineering Chemistry**, v. 34, n. 6, p. 693–696, 1942.

PARK, J.-Y.; WANG, Z.-M.; KIM, D.-K.; LEE, J.-S. Effects of water on the esterification of free fatty acids by acid catalysts. **Renewable Energy**, v. 35, n. 3, p. 614–618, 2010.

PÉREZ-CISNEROS, E. S.; MENA-ESPINO, X.; RODRÍGUEZ-LÓPEZ, V.; SALES-CRUZ, M.; VIVEROS-GARCÍA, T.; LOBO-OEHMICHEN, R. An integrated reactive distillation process for biodiesel production. **Computers & Chemical Engineering**, v. 91, p. 233–246, 2016.

PHAN, A. N.; PHAN, T. M. Biodiesel production from waste cooking oils. **Fuel**, v. 87, n. 17, p. 3490–3496, 2008.

PODDAR, T.; JAGANNATH, A.; ALMANSOORI, A. Use of reactive distillation in biodiesel production: A simulation-based comparison of energy requirements and profitability indicators. **Applied Energy**, v. 185, p. 985–997, 2017.

PRASERTSIT, K.; MUEANMAS, C.; TONGURAI, C. Transesterification of palm oil with methanol in a reactive distillation column. **Chemical Engineering and Processing: Process Intensification**, v. 70, p. 21–26, 2013.

PRAUSNITZ, J.; LICHTENTHALER, R. N.; AZEVEDO, E. G. D. **Molecular thermodynamics of fluid-phase equilibria**. 3. ed. New Jersey: Prentice Hall, 1999. 886p.

RAIMUNDO, R. C. **Evaluation of thermodynamic models for application in biodiesel production processes (in Portuguese)**. MSc dissertation. Curitiba, Paraná: Federal University of Paraná, 2013. 122p.

RAMOS, L. P.; DA SILVA, F. R.; MANGRICH, A. S.; CORDEIRO, C. S. Biodiesel production technologies. **Virtual Journal of Chemistry**, v. 3, n. 5, p. 385–405, 2011.

RASHTIZADEH, E.; FARZANEH, F.; TALEBPOUR, Z. Synthesis and characterization of Sr3Al2O6 nanocomposite as catalyst for biodiesel production. **Bioresour Technol**, v. 154, p. 32–7, 2014.

REDLICH, O.; KISTER, A. Algebraic representation of thermodynamic properties and the classification of solutions. **Industrial & Engineering Chemistry**, v. 40, n. 2, p. 345–348, 1948.

REFAAT, A. A. Different techniques for the production of biodiesel from waste vegetable oil. **International Journal of Environmental Science & Technology**, v. 7, n. 1, p. 183–213, 2010.

RENON, H.; PRAUSNITZ, J. M. Local compositions in thermodynamic excess functions for liquid mixtures. **AIChE journal**, v. 14, n. 1, p. 135–144, 1968.

REZAEI, R.; MOHADESI, M.; MORADI, G. R. Optimization of biodiesel production using waste mussel shell catalyst. **Fuel**, v. 109, p. 534–541, 2013.

ROHAN. **Pine-Derived Chemicals Market worth 5.27 Billion USD by 2021**. MarketsandMarkets, Magarpatta 2016. Available at: <https://www.marketsandmarkets.com/PressReleases/pine-derived-chemicals.asp>. Accessed on: 2019/01/22.

SANDLER, S. I. **Chemical, Biochemical, and Engineering Thermodynamics**. 5. ed. Hoboken, New Jersey: John Wiley & Sons, 2017. 1032p.

SANI, Y. M.; DAUD, W. M. A. W.; ABDUL AZIZ, A. R. Activity of solid acid catalysts for biodiesel production: A critical review. **Applied Catalysis A: General**, v. 470, p. 140–161, 2014.

SANTANDER, C. M. G. **Modeling and simulation of a reactive distillation plant for biodiesel production (in Portuguese)**. MSc dissertation. Campinas: State University of Campinas, 2010. 197p.

SANTIAGO-TORRES, N.; ROMERO-IBARRA, I. C.; PFEIFFER, H. Sodium zirconate (Na2ZrO3) as a catalyst in a soybean oil transesterification reaction for biodiesel production. **Fuel Processing Technology**, v. 120, p. 34–39, 2014.

SANTOS, G. R. **Liquid-liquid equilibrium in aqueous electrolytic systems (In Portuguese)**. MSc dissertation. Campinas: State University of Campinas, 1999. 169p.

SÉ, R. A. G. **Liquid-liquid equilibrium in polymeric aqueous biphasic systems containing electrolytes**. MSc dissertation. Campinas: Campinas State University, 2001. 112p.

SEADER, J. D.; HENLEY, E. J.; ROPER, D. K. **Separation process principles: Chemical and Biochemical Operations**. 3. ed. New York: John Wiley & Sons, 2011. 849p.

SENDZIKIENE, E.; MAKAREVICIENE, V.; JANULIS, P.; KITRYS, S. Kinetics of free fatty acids esterification with methanol in the production of biodiesel fuel. **European Journal of Lipid Science and Technology**, v. 106, n. 12, p. 831–836, 2004.

SHU, Q.; GAO, J.; LIAO, Y.; WANG, J. Reaction Kinetics of Biodiesel Synthesis from Waste Oil Using a Carbon-based Solid Acid Catalyst. **Chinese Journal of Chemical Engineering**, v. 19, n. 1, p. 163–168, 2011.

SILVA, J. P. D. **Evaluation by factorial design of biodiesel production via reactive distillation**. MSc dissertation. Recife: Federal University of Pernambuco, 2013. 118p.

SIMASATITKUL, L.; SIRICHARNSAKUNCHAI, P.; PATCHARAVORACHOT, Y.; ASSABUMRUNGRAT, S.; ARPORNWICHANOP, A. Reactive distillation for biodiesel production from soybean oil. **Korean Journal of Chemical Engineering**, v. 28, n. 3, p. 649–655, 2011.

SMITH, J. M.; VAN NESS, H. C.; ABBOTT, M. M. **Introduction to Chemical Engineering Thermodynamics (In Portuguese)**. 7. ed. LTC, 2007. 466p.

SOUZA, T. P. C.; STRAGEVITCH, L.; KNOECHELMANN, A.; PACHECO, J. G. A.; SILVA, J. M. F. Simulation and preliminary economic assessment of a biodiesel plant and comparison with reactive distillation. **Fuel Processing Technology**, v. 123, p. 75–81, 2014.

STAMENKOVIĆ, O. S.; TODOROVIĆ, Z. B.; LAZIĆ, M. L.; VELJKOVIĆ, V. B.; SKALA, D. U. Kinetics of sunflower oil methanolysis at low temperatures. **Bioresource Technology**, v. 99, n. 5, p. 1131–1140, 2008.

STATISTA. **Leading biodiesel producers worldwide in 2017, by country (in billion liters)**. Global biodiesel production by country 2017, New York, USA, 2019. Available at: <https://www.statista.com/statistics/271472/biodiesel-production-in-selected-countries/>. Accessed on: 2019/01/27.

STEINIGEWEG, S.; GMEHLING, J. Esterification of a fatty acid by reactive distillation. **Industrial & engineering chemistry research**, v. 42, n. 15, p. 3612–3619, 2003.

SU, Y.-C.; LIU, Y. A.; DIAZ TOVAR, C. A.; GANI, R. Selection of Prediction Methods for Thermophysical Properties for Process Modeling and Product Design of Biodiesel Manufacturing. **Industrial & Engineering Chemistry Research**, v. 50, n. 11, p. 6809–6836, 2011.

TALEBIAN-KIAKALAIEH, A.; AMIN, N. A. S.; ZAREI, A.; JALILIANNOSRATI, H. Biodiesel Production from High Free Fatty Acid Waste Cooking Oil by Solid Acid Catalyst. In: International Conference on Process Systems Engineering (PSE ASIA), 6, 2013, Kuala Lumpur. **Proceedings ...** Kuala Lumpur: PSE ASIA, 2013. p. 1–5.

TESSER, R.; CASALE, L.; VERDE, D.; DI SERIO, M.; SANTACESARIA, E. Kinetics and modeling of fatty acids esterification on acid exchange resins. **Chemical Engineering Journal**, v. 157, n. 2, p. 539–550, 2010.

THIRUVENGADARAVI, K. V.; NANDAGOPAL, J.; BALA, V. S. S.; KIRUPHA, S. D.; VIJAYALAKSHMI, P.; SIVANESAN, S. Kinetic study of the esterification of free fatty acids in non-edible Pongamia pinnata oil using acid catalyst. **Indian Journal of Science and Technology**, v. 2, n. 12, p. 20–24, 2009.

TREYBAL, R. E. **Liquid extraction**. 2. ed. New York: McGraw-Hill, 1963. 621p.

TUCHLENSKI, A.; BECKMANN, A.; REUSCH, D.; DÜSSEL, R.; WEIDLICH, U.; JANOWSKY, R. Reactive distillation—industrial applications, process design & scale-up. **Chemical Engineering Science**, v. 56, n. 2, p. 387–394, 2001.

U.S. ENERGY INFORMATION ADMINISTRATION (EIA). **Monthly Biodiesel Production Report with data for December 2018**. U.S. Energy Information Administration, Washington,

2019. Available at: <https://www.eia.gov/biofuels/biodiesel/production/biodiesel.pdf>. Accessed on: 2019/03/18.

UNNITHAN, U. R.; TIWARI, K. K. Kinetics of Esterification of Oleic Acid and Mixtures of Fatty Acids with Methanol Using Sulphuric Acid and p-Toluenesulphonic Acid as Catalysts. **Indian Journal of Technology**, v. 25, p. 477–479, 1987.

VAN GERPEN, J. Biodiesel processing and production. **Fuel processing technology**, v. 86, n. 10, p. 1097–1107, 2005.

VICENTE, G.; MARTÍNEZ, M.; ARACIL, J.; ESTEBAN, A. Kinetics of Sunflower Oil Methanolysis. **Industrial & Engineering Chemistry Research**, v. 44, n. 15, p. 5447–5454, 2005.

VYAS, A. P.; VERMA, J. L.; SUBRAHMANYAM, N. A review on FAME production processes. **Fuel**, v. 89, n. 1, p. 1–9, 2010.

WALAS, S. M. **Phase equilibria in chemical engineering**. 1. ed. Boston: Butterworth-Heinemann, 1985. 688p.

WEST, A. H.; POSARAC, D.; ELLIS, N. Assessment of four biodiesel production processes using HYSYS.Plant. **Bioresour Technol**, v. 99, n. 14, p. 6587–601, 2008.

XIAO, Y.; LI, H.; XIAO, G.; GAO, L.; PAN, X. Simulation of the catalytic reactive distillation process for biodiesel production via transesterification. In: Materials for Renewable Energy and Environment (ICMREE), 2013, Chengdou, China, **Proceedings...** Chengdou, China: IEEE, 2014. p. 196–199.

YAN, S.; SALLEY, S. O.; NG, K. Y. S. Simultaneous transesterification and esterification of unrefined or waste oils over ZnO-La2O3 catalysts. **Applied Catalysis A: General**, v. 353, n. 2, p. 203–212, 2009.

ZADRA, R. Improving process efficiency by the usage of alcoholates in the biodiesel production. In: Brazil-Germany Forum on Biodiesel, 4, 2006, Aracatuba. **Proceedings ...** Aracatuba: FeiBio, 2006. p. 3456–3470.

ZHANG, Y.; DUBÉ, M. A.; MCLEAN, D. D.; KATES, M. Biodiesel production from waste cooking oil: 1. Process design and technological assessment. **Bioresource Technology**, v. 89, n. 1, p. 1–16, 2003a.

_____. Biodiesel production from waste cooking oil: 2. Economic assessment and sensitivity analysis. **Bioresource Technology**, v. 90, n. 3, p. 229–240, 2003b.

ZONG, L.; RAMANATHAN, S.; CHEN, C.-C. Fragment-based approach for estimating thermophysical properties of fats and vegetable oils for modeling biodiesel production processes. **Industrial & engineering chemistry research**, v. 49, n. 2, p. 876–886, 2009.

_____. Predicting Thermophysical Properties of Mono- and Diglycerides with the Chemical Constituent Fragment Approach. **Industrial & Engineering Chemistry Research**, v. 49, n. 11, p. 5479–5484, 2010.

APPENDIX A – KINETIC MODELS FOR TRANSESTERIFICATION AND ESTERIFICATION REACTIONS

Kinetic models for simultaneous transesterification and esterification reactions in the CDC or CAC column using HWSi/Al_2O_3 from Chapter 5 were given by Gaurav, Ng and Rempel (2016) as a pseudo-first-order rate law,

$$\frac{dC_{TAG}}{dt} = -k'_{trans} \cdot C_{TAG} \tag{A.1}$$

$$\frac{dC_{FFA}}{dt} = -k'_{ester} \cdot C_{FFA} \tag{A.2}$$

where C_{TAG} and C_{FFA} are molarity of TAG and FFA components at mol·L^{-1}; k'_{trans} and k'_{ester} are pseudo-kinetic constants (high molar ratio of methanol to oil) for the transesterification and esterification reactions at sec^{-1}; and t is the reaction time. In addition, the kinetic constants for both reactions can be obtained from Arrhenius equation given by Equation A.3,

$$k'_r = k_0 \cdot exp\left(\frac{-E_a}{RT}\right) \tag{A.3}$$

where k_0 is the pre-exponential (Arrhenius) factor at sec^{-1}, E_a is the activation energy at kJ·(mol·K)$^{-1}$, T is temperature at K and k'_r are pseudo-kinetic constant for some reaction r.

Kinetic parameters for both esterification and transesterification reaction are shown in Table A.1.

Table A.1 – Kinetic parameters

Parameter	k_0	E_a
Unit	sec^{-1}	kJ·mol^{-1}
Transesterification	10.100	58.32
Esterification	0.128	34.06

Source: Gaurav, Ng and Rempel (2016).

APPENDIX B – ESTERIFICATION REACTION USING RELITE CFS

Esterification reaction in the CDC column using Relite CFS from Chapter 6 was modeled by the kinetic model proposed by Tesser et al. (2010) based on uncatalyzed (r_{uc}) and catalyzed (r_{cat}) terms of reaction rate given by Equations B.1 to B.9.

$$r_{uc} = k_1 C_A^2 C_M \tag{B.1}$$

$$k_1 = k^{ref} exp\left[\frac{E_a}{R}\left(\frac{1}{T_{ref}} - \frac{1}{T}\right)\right] \tag{B.2}$$

$$r_{cat} = \frac{k_{cat} H_A C_A^R - k_{-cat} \frac{H_E C_E^R C_W^R}{C_M^R}}{1 + \frac{H_A C_A^R}{C_M^R} + \frac{H_E C_E^R}{C_M^R} + \frac{H_W C_W^R}{C_M^R}} \tag{B.3}$$

$$C_i^R = \frac{K_i^{eff} C_i^B}{\sum_j K_j C_j^B} \tag{B.4}$$

$$K_i^{eff} = \frac{K_i \rho_i}{M_i} \tag{B.5}$$

Table B.1 – Parameters from partition model

Component	K_i/mL·mol^{-1}	K_i^{eff}
Water	1.000	0.05420
Methanol	0.317	0.00690
Fatty acid	1.000	0.00300
Methyl ester	0.317	0.00088

Source: Tesser et al. (2010).

Table B.2 – Kinetic and ion exchange parameters

Parameter	k_{cat}^{ref}	$E_{a,cat}$	H_A	H_W	H_E
Unit	cm^3·g$_{cat}^{-1}$·min^{-1}	kcal·mol^{-1}			
Forward	13.07	12.77	0.31	1.55	0.17
Backward	3.85	7.96			

Source: Tesser et al. (2010).

$$\frac{dn_i}{dt} = \nu(r_{uc}V_L + r_{cat}W_{cat}) \quad \text{(B.6)}$$

$$n_i^R + n_i^B = n_i \quad \text{(B.7)}$$

$$n_i^R = C_i^R V^{abs} W_{cat} \quad \text{(B.8)}$$

$$C_i^B = \frac{n_i^B}{V_L} \quad \text{(B.9)}$$

From these equations r_{uc} and r_{cat} from Equation B.1 and B.3 are added in Equation B.6 to compose the real reaction rate solved simultaneously by a material balance from Equations B.6 to B.9. In addition, W_{cat} is the weight of catalyst loaded per stage, ν is the total stoichiometric factor, V_L and V^{abs}(=0.790 $cm^3 \cdot g_{res}^{-1}$ of relite CFS) are liquid volume and specific volume adsorbed in the case of pure methanol (less than 10 wt% of water).

For all these equations C_i^B (n_i^B) and C_i^R (n_i^R) are concentrations (moles) of the ith component in bulk phase and inside the resin; respectively. C_i and n_i are overall concentration and mole number of the ith species. Moreover, H_i is the ionic exchange equilibrium for the reactions of protonated methanol with ith component; K_i or K_j is the partition constant of pure ith component; K_i^{eff} means the effective partition constant taking in account the molecular size of pure ith component; ρ_i and M_i is molar density and molecular mass of the ith component, where subscripts A, W and E refers to acid (FFA), water and ester, respectively.

Furthermore, k_1 and k_{cat} (k_{-cat}) are kinetic constants for uncatalized and catalyzed reaction for forward (backward); E_a (16.28 $kcal \cdot mol^{-1}$) and $E_{a,cat}$ ($E_{a,-cat}$) are activation energy for uncatalyzed and forward (backward) catalyzed step; k^{ref} (65.78 $cm^6 \cdot mol^{-2} \cdot min^{-1}$) and k_{cat}^{ref} (k_{-cat}^{ref}) are reference kinetic constants for uncatalyzed and forward (backward) catalyzed step; and T and T_{ref} (=373.16 K) are temperature and reference temperature. Parameters from partition and kinetic models are presented in Table B.1 and Table B.2.